



260-IN.-DIA MOTOR FEASIBILITY
DEMONSTRATION PROGRAM (u)

STATIC TEST FIRING OF MOTOR 260-SL-2
FINAL REPORT

Prepared for
NATIONAL AERONAUTICS AND SPACE ADMINISTRATION
CONTRACT NO. NAS3-6284

(NASA-CR-54982) THE 260-IN.-DIA MOTOR
FEASIBILITY DEMONSTRATION PROGRAM. STATIC
TEST FIRING OF MOTOR 260-SL-2 Final
Report (Aerojet-General Corp., Sacramento,
Calif.) 189 p

N74-71133

Unclas
00/99 31179

(PAGES)
00/99
(CATEGORY)
28
NASA CR OR TMX OR AD NUMBER

CLASSIFIED BY
UNCLASSIFIED
By authority of E.G. No. 11652
Changed by O. N. W. [signature] Date 9/12/93

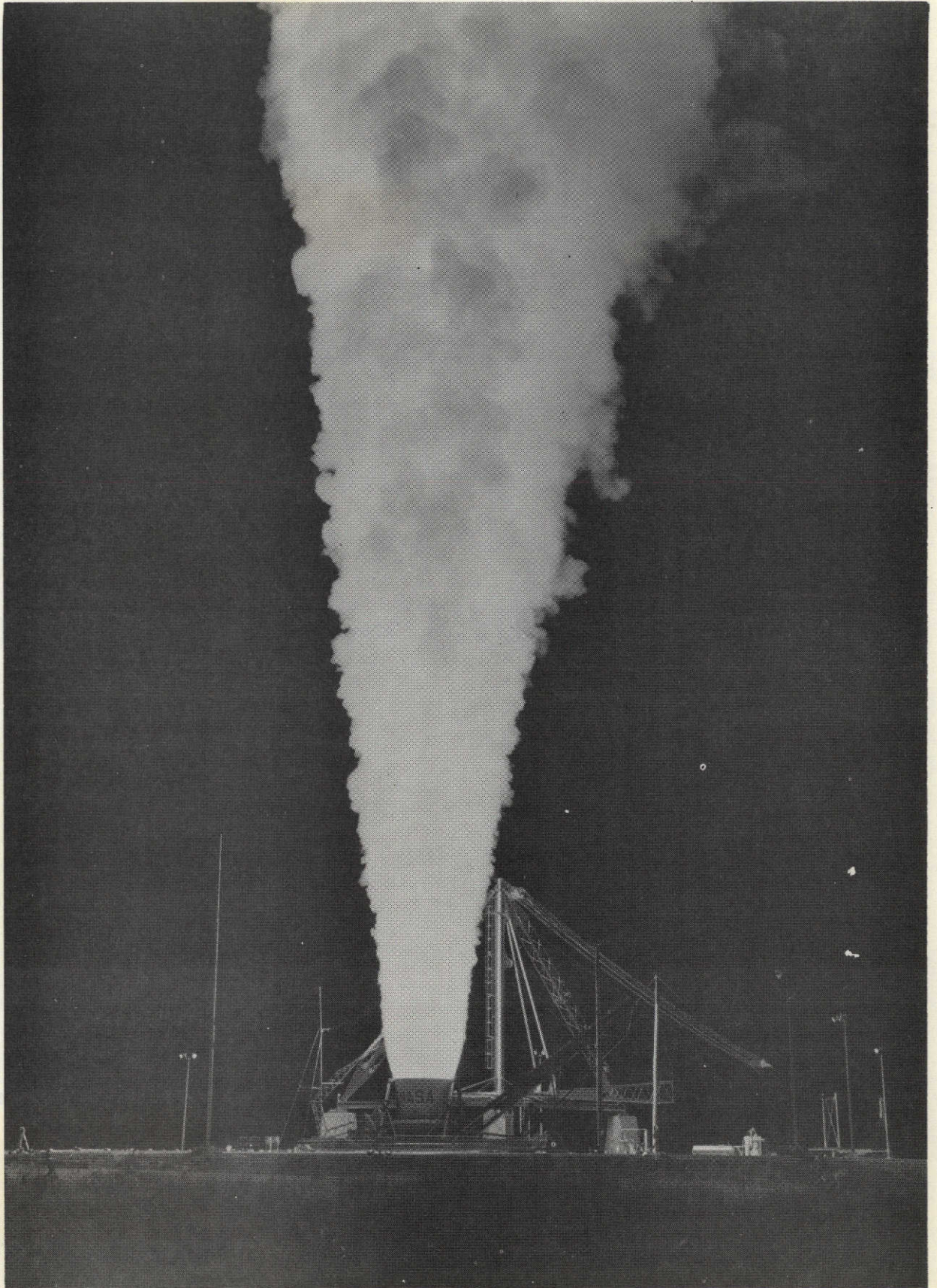


AEROJET-GENERAL CORPORATION

0771

REPRODUCED BY
NATIONAL TECHNICAL
INFORMATION SERVICE
U.S. DEPARTMENT OF COMMERCE
SPRINGFIELD, VA. 22161

SACRAMENTO, CALIFORNIA



C66-8890

NASA CR-54982

FINAL REPORT

260-IN.-DIA MOTOR FEASIBILITY
DEMONSTRATION PROGRAM (u)

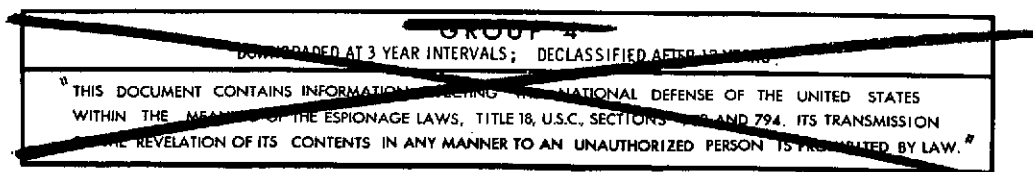
STATIC TEST FIRING OF MOTOR 260-SL-2

Prepared for
NATIONAL AERONAUTICS AND SPACE ADMINISTRATION

25 MARCH 1966

Contract No. NAS3-6284

Technical Management
NASA Lewis Research Center
Cleveland, Ohio
James J. Kramer



AEROJET-GENERAL CORPORATION
A SUBSIDIARY OF THE GENERAL TIRE & RUBBER COMPANY

TABLE OF CONTENTS

	<u>Page</u>
I. Summary and Conclusions	1
II. Objectives	3
III. Design and Fabrication	4
A. Chamber	4
B. Nozzle	6
C. Chamber Insulation	18
D. Ignition Motor Assembly	19
E. Propellant Grain	23
IV. Motor Processing	25
A. Chamber Insulation	25
B. Chamber Lining	25
C. Propellant Processing and Motor Casting	26
D. Postcast Operations	28
E. Motor Final Assembly	30
V. Testing	34
A. Test Plan	34
B. Special Test Equipment	35
C. Instrumentation	38
D. Test Preparations	39
VI. Test Results	41
A. Data Processing	41
B. Data Analysis	41
C. Ignition System Performance	48
D. Ballistic Performance Analysis	52
E. Component Evaluation	54
F. Special Test Equipment Performance	62
G. Environmental Effects on Facilities and STE	64
References	66
Instrumentation Plan, Motor 260-SL-2 (Static Test)	Appendix

FIGURE LIST

	<u>Figure</u>
260-SL-2 Motor Assembly	1
260-SL-2 Motor Chamber	2
Motor Weight Summary	3
260-SL-2 Motor Nozzle	4
260-SL-2 Motor Exit Cone	5
260-SL-2 Nozzle Shell	6
Comparison of 260-SL-1 and -2 Nozzle Insulation Thickness	7
Component Properties of 260-SL-2 Nozzle Entrance Insert	8
Component Properties of 260-SL-2 Nozzle Throat Insert	9
Component Properties of 260-SL-2 Nozzle Throat Extension Insert	10
Component Properties of 260-SL-2 Exit Cone Liner	11
Exit Cone Bonding Process Summary	12
260-SL-2 Ignition Motor Assembly	13
260-SL-2 Ignition Motor Booster	14
Ballistic Performance Requirements	15
260-SL-2 Grain Configuration	16
260-SL-2 Propellant Formulation	17
260-SL-2 Liner Formulation	18
Acceptance Analysis of SD-850-2 Liner Batches Prepared for Lining Motor 260-SL-2	19
Propellant Casting Setup for Motor 260-SL-2	20
Submix and Premix Analysis	21
Liquid Strand Burning Rate of ANB-3105 Propellant Processed for Motors 260-SL-1 and -2	22
Uncured Density of ANB-3105 Propellant Processed for Motors 260-SL-1 and -2	23
DER-332 Content of ANB-3105 Propellant Processed for Motors 260-SL-1 and -2	24
Ammonium Perchlorate Content of Continuous Mixed ANB-3105 Propellant for Motors 260-SL-1 and -2	25
Mechanical Properties of Propellant vs Cure Time	26
Mechanical Properties of Propellant after Cure	27
Propellant Constant Strain Properties	28

FIGURE LIST (cont.)

	<u>Figure</u>
Internal View of Grain Bore	29
Grain Bore Deflection Comparison for Motors 260-SL-1 and -2	30
Motor Installation in Test Facility	31
Motion Picture Placement	32
Overall View of Test Setup	33
Pretest View of Quench System	34
Pretest View of Ignition Tower Retraction System	35
Pretest View of Horizontal Stabilizers and Retention Rods	36
A-DD Instrumentation Capability	37
A-DD Test Facility Electrical Control Schematic	38
Motor 260-SL-2 Instrumentation Summary	39
Motor 260-SL-2 Instrumentation Locations	40
A-DD Special Test Instrumentation Installation	41
Pretest View of Motor 260-SL-2	42
Time-Event Summary	43
Acceleration Data Summary	44
Chamber Strain, Locations S-3 and S-4	45
Chamber Strain, Locations S-5 and S-6	46
Chamber Strain, Locations S-7 and S-8	47
Chamber Strain, Locations S-15, S-16, and S-17	48
Motor 260-SL-2 Ignition Transient	49
260-SL Motor Ignition Sequence	50
Posttest View of Ignition Motor and Sled Assembly	51
Summary of 260-SL Ignition Motor and Booster Assembly Ballistic Performance Data	52
Flow Conditions in Motor Nozzle Prior to Propellant Ignition	53
Analysis of 260-SL Motor Pressure Rise	54
Ballistic Performance Summary	55
Actual 260-SL-2 Ballistic Performance Curve	56
Predicted 260-SL-2 Ballistic Performance Curve	57
Burning Rate Variation as a Function of Temperature Gradient	58
Burning Rate Correction as a Function of Web Action Time	59

FIGURE LIST (cont.)

	<u>Figure</u>
Burning Rate Adjustment as a Function of Grain Length	60
Comparison of Ballistic Performance of Motors 260-SL-1 and -2	61
Posttest Condition of Forward Head Insulation	62
Posttest View of Forward Head Insulation	63
Posttest View of Forward Insulation	64
Posttest View of Aft Head Insulation	65
Posttest View of Aft Head Insulation with FMC-200 Potting Compound Removed	66
Predicted and Actual Aft Head Insulation Erosion	67
Posttest Condition of Insulation Seams	68
Posttest View of Firing Cap Insulation	69
Surface Recession of Motor Nozzle	70
Nozzle Surface Recession Profile, Motor 260-SL-2	71
Nozzle Surface Recession Profiles, Motor 260-SL-1 and -2	72
Nozzle Insulation Erosion Profile	73
Nozzle Erosion Contour	74
Posttest View of Nozzle Entrance Insert	75
Posttest View of Nozzle Throat Insert	76
Posttest View of Nozzle Throat Insert Surface	77
Posttest View of Nozzle Throat Extension Insert	78
Posttest View of Exit Cone	79
Posttest View of Exit Cone Ablation Surface	80
Posttest View of Exit Cone Exterior	81
Vertical Distance vs Time for Ignition Motor and Support Fixture	82
Terminal Velocity of Ignition Motor and Support Fixture at 100 ft	83
Tower Position-vs-Time Curve	84
Posttest View of Ignition Motor Track Assembly	85
Location of Temperature Indication Paint Panels	86

I. SUMMARY AND CONCLUSIONS

Motor 260-SL-2, the second 260-in.-dia motor fabricated by Aerojet-General Corporation under contract to the National Aeronautics and Space Administration, was test fired at the Aerojet-Dade Division facility at 7:00 p.m., 23 February 1966. Ballistic performance of the motor was essentially as predicted and the performance of all subsystems closely duplicated the performance previously obtained in test firing of motor 260-SL-1.

Motor ignition was smooth and stable with an ignition interval of 0.336 sec. The initial steady-state chamber pressure of 466 psia was attained at 0.62 sec after fireswitch. When forward-end chamber pressure reached 125 psia, the command signal to actuate the explosive bolts retaining the ignition motor in position was initiated; the ignition motor and retaining structure assembly were then ejected with the sled proceeding up the track normally. The cables restraining the sled failed and the ignition motor assembly followed a trajectory similar to that occurring in the firing of motor 260-SL-1, with impact in the planned area approximately 50 yards beyond the end of the canal to the east of the cast cure, and test facility. Retraction of the igniter support tower was initiated when the assembly cleared the end of the tower. The tower retraction cycle was initiated at 0.570 sec, and the tower was fully retracted at 4.8 sec.

Propellant burning was normal with maximum pressure and thrust of 601 psia and 3,564,000 lbf, respectively, recorded at 40.5 sec. During the action time of 129.8 sec, the motor operated at an average chamber pressure of 489 psia and delivered an average thrust of 2,865,000 lbf. The total impulse during motor action time was 371,900,000 lbf-sec, yielding a specific impulse of 228.9 lbf-sec/lbm at motor conditions, which is equivalent to a specific impulse of 246.1 lbf-sec/lbm at standard conditions.

I, Summary and Conclusions (cont.)

Measured chamber pressure versus time was within 1% of predicted values during 80% of motor action time and closely duplicated performance obtained during the firing of motor 260-SL-1. Results obtained verify the adequacy of improved propellant grain processing techniques used for this motor. The confidence level in the capability to produce the selected propellant formulation with consistent properties was further increased by use of PBAN terpolymer from a lot that was manufactured by a supplier different from that of the material previously used in this program.

The structural integrity of the pressure vessel was maintained throughout the firing. There is no evidence that any gas leakage occurred or that abnormal loads were applied to any component. The internal insulation afforded adequate thermal protection. Structural integrity of the nozzle and exit cone was also maintained for the firing duration. Erosion performance of the nozzle rubber insulation and all ablative plastic liner components was very similar to that obtained in the firing of motor 260-SL-1. The average measured postfiring throat diameter was 1.25 in. greater than the prefiring diameter, which yields an average throat erosion rate of 4.8 mils/sec during motor action time.

The previous test firing of motor 260-SL-1 demonstrated that fabrication, handling, and processing of all components required for large unitized-chamber solid propellant rocket motors is feasible. The complete success of motor 260-SL-2 further confirms this demonstration, and also increases the confidence level in the materials, component designs, fabrication methods, and processing operations used for these motors.

II. OBJECTIVES

The primary objectives of the static test firing of motor 260-SL-2 were:

A. To demonstrate that high reproducibility of performance is obtainable for all components of a very large solid rocket motor.

B. To demonstrate predictability of ballistic performance of large solid rocket motors and show that a reproducible correlation exists between propellant burning rate as determined in laboratory tests and that occurring in actual motor firing.

C. To further confirm the suitability, and thereby increase the confidence level in use of materials, component designs, fabrication methods, and processing operations selected for application to very large solid rocket motors.

D. To verify the adequacy of improved propellant grain processing techniques and demonstrate performance of propellant formulated from a lot of terpolymer that was manufactured by a different supplier than material previously used in this program.

Secondary test objectives included obtaining data to define the effect of the motor firing on test facility and equipment items, and environmental effects in the area of motor firing to confirm data obtained during the firing of motor 260-SL-1.

III. DESIGN AND FABRICATION

The 260-in.-dia short-length rocket motor (260-SL-2) consists of a monolithic steel chamber with a 260-in. nominal inside diameter, a single, fixed nozzle with plastic ablative insulation, and a composite propellant cast in an internal-star monolithic grain. Ignition is by an externally mounted ignition motor, firing through the nozzle of the motor. The motor assembly is defined in Figure 1.

The Contract Work Statement required that all components designs use existing and proven materials and processes to as large an extent as possible; this requirement has been met in motor 260-SL-2. Except for minor changes in the chamber insulation, the motor is identical in design to motor 260-SL-1, which was successfully test fired on 25 September 1965.

Fabrication of the major motor components was conducted by subcontractors, in compliance with designs prepared by Aerojet. Propellant manufacturing and motor processing operations were conducted by Aerojet at the Aerojet-Dade Division (A-DD), Dade County, Florida.

A. CHAMBER

1. Design

The chamber is of monolithic construction with a nominal 260-in. ID, is fabricated of 18%-nickel maraging steel with a yield strength of 200,000 to 235,000 psi at 0.2% offset (200 class), and has a minimum design factor of safety of 1.3 based on the original maximum expected operating pressure (MEOP) of 670 psia. A reduction in minimum yield strength of 5% throughout the pressure vessel is allowed for weld efficiency when combined with weld mismatch, resulting in 190,000 psi as the minimum design allowable yield strength.

III, A, Chamber (cont.)

The 260-SL-2 chamber is defined in Figure 2. The design may be used in the full-length configuration by incorporating additional center-section lengths.

The 260-SL-2 chamber design consists of a 260-in.-ID cylindrical section that is 510 in. long between the forward and aft equators, a hemispherical forward head with a 5.2-in.-dia polar flange, and a hemispherical aft head with a 183-in.-dia nozzle attachment flange. The overall chamber length is 735.11 in. A skirt is provided at each end of the chamber.

The minimum design thickness of each section of the chamber and the stress conditions which were the determining design criteria, are listed below:

<u>Component</u>	<u>Minimum, Thickness, in.</u>	<u>Design Criteria</u>
Cylindrical Section	0.600	Pressure-vessel membrane stress
Forward Head	0.340	Membrane stress plus head-to-cylinder discontinuity loading
Aft Head	0.600	Membrane stress plus nozzle attachment flange discontinuity loads
Forward Skirt	0.700	Full-length motor weight and thrust times 1.2 plus 4-degree TVC loads; all times 1.25 dynamic load factor
Aft Skirt	0.500	Horizontal handling loads of 1.3 g axially and 3.0 g radially

The nozzle attachment flange incorporates a shear lip design which minimizes the joint cross section required and eliminates the possibility of developing shear loads in the bolts. There are 220 drilled and tapped bolt holes in the aft face of the flange for installation of the nozzle assembly.

A 5.2-in.-ID flange is incorporated in the forward head of the chamber to facilitate fabrication, processing, and hydrostatic test. Essentially, the joint is designed for a pressure-only loading condition with a cap for the

III, A, Chamber (cont.)

test firing. The firing cap has three 1/4-in.-dia instrumentation pressure taps and a shear lip to carry the high shear component of membrane load.

2. Fabrication

The chamber was fabricated by Sun Shipbuilding & Dry Dock Co., Chester, Penn., using identical materials and fabrication techniques that were used on the 260-SL-1 motor chamber. A detailed description of fabrication procedures used for both chambers is presented in the final test report of motor 260-SL-1, Reference 1.

All manufacturing deviations are documented in the Motor Log Book and were accepted by Engineering Review Board action prior to the chamber hydrostatic test. All such deviations were considered to be minor and did not affect the structural integrity of the chamber assembly. The hydrostatic proof test subjected the chamber and nozzle-shell assembly to a pressure of 1.2 MEOP. Basic membrane stresses recorded during the hydrostatic proof test at the more significant areas of fabrication deviation were below the minimum stress of 190,000 psi.

The actual weight of the completed chamber was 122,085 lb (Figure 3).

B. NOZZLE

1. Design

a. Configuration

Motor 260-SL-2 has a single, fixed, on-center nozzle with a 71.000-in. initial throat diameter; the nozzle design is shown in Figure 4. The throat diameter was selected on the basis of motor performance requirements established from interior ballistic design and performance parameters.

III, B, Nozzle (cont.)

The nozzle configuration consists of an entrance section with a radius of curvature equal to the throat radius, a throat extension, and an exit cone with a divergence half-angle of 17.5 degrees. The exit cone expansion ratio is 6.0:1, which is the optimum sea-level expansion for a chamber pressure of 600 psia; the exit cone configuration is shown in Figure 5.

b. Components

(1) Nozzle Shell

The nozzle shell (Figure 6) is designed to provide aft-end closure for the pressure vessel and structural support for the ablative plastic inserts; the minimum design thickness of the shell is 0.75 in. The entrance configuration of the nozzle shell has a double conical angle. The steep initial angle was designed for compatibility with the chamber joint, and the shallower conical angle forward of the throat section was designed to minimize the entrance-liner insert thickness and to permit inclusion of a mechanical stop for the throat insert. A seven-degree angle was selected for the throat section so that the throat insert would restrain against ejection loads.

The forward attachment flange has the structural capacity for a 4-degree jet-deflection bending moment. The flange has 220 1.310-in.-dia holes, which are match-drilled to the corresponding tapped holes on the chamber aft flange. The ID of the nozzle-flange shear lip is machined to within a total range of 0.015 in. of the OD of the chamber aft flange.

One-hundred and seventy-six 0.931-in.-dia holes are drilled and counterbored through the aft flange for installation of the exit cone assembly.

(2) Ablative Plastic Components

The nozzle has three ablative plastic inserts bonded to the structural shell. Each insert contains an ablative surface material selected

III, B, Nozzle (cont.)

for erosion-resistance characteristics and an overwrap material selected for insulating and structural properties. Carbon cloth and phenolic, MX-4926, was selected as the ablation surface material between the upstream area ratio of 2.0:1 and the downstream area ratio of 3.0:1, where high resistance to erosive effects of motor exhaust gases is required. The less costly, less erosion-resistant silica-cloth and phenolics were selected for the high-area ratio regions; MX-2646 was used upstream of the throat between the area ratios of 3.25:1 and 2.0:1, and FM-5131 was used downstream for area ratios greater than 3.0:1. The overwrap material for the entrance insert is MX-2646; all other inserts of the nozzle were overwrapped with FM-5131.

Each insert is designed so that the tape laminations are oriented at a particular angle with respect to the ablation surface. The entrance insert has a laminate orientation of 80 degrees (nominal) with respect to the nozzle center line for both the silica-cloth-and-phenolic and the carbon-cloth-and-phenolic ablation surface materials. The entrance insert is located between the upstream area ratios of 3.25:1 and 1.10:1. The throat insert has a laminate orientation of 67 degrees (nominal) and is located from the 1.10:1 upstream area ratio to the 1.05:1 downstream area ratio. The throat extension insert has a laminate orientation of 30 degrees (nominal) and is located between the downstream area ratios of 1.05:1 and 2.0:1. The laminate orientation of the overwrap material is parallel to surface for all three inserts in order to provide maximum insulation protection for the structural shell.

The exit-cone liner extends between the downstream area ratios of 2.01:1 and 6.0:1. Both the MX-4926 and FM-5131 ablation surface materials have laminates oriented parallel to the nozzle center line. The two materials are overwrapped parallel to the surface of the part with FM-5131.

The insert-thickness design is based on the predicted temperature profile through the insert and the structural requirement due to thermal stresses. The designed insert thickness is determined to be adequate for twice the predicted ablation depth and to have sufficient thickness below the heat-affected zone for structural requirements.

III, B, Nozzle (cont.)

The plastic inserts and rubber insulation are bonded to the structural shell with epoxy adhesive. Buna N rubber O-rings are used to prevent gas flow at the interface between the inserts and structural shell.

(3) Rubber Insulation

The nozzle rubber entrance section is designed to provide insulation in the nozzle shell from the step joint to the nozzle plastic entrance insert. The Gen-Gard V-44 rubber nozzle insulation is 176.2 in. in diameter at the step joint and 92.1 in. in diameter where the rubber blends into the nozzle silica cloth and phenolic liner. The maximum rubber thickness is 12.7 in. at the 130-in. diameter. The design thickness was determined as a function of exposure time, thickness-loss rate of V-44 observed in 100-in.-dia motor tests as a function of Mach numbers, and a 2.0 safety factor.

The rubber insulation thickness specified for the 260-SL-2 component is less than that used on 260-SL-1. As shown in Figure 7, the 260-SL-2 nozzle insulation was thinner than the nozzle insulation in motor SL-1.

(4) Exit Cone Structural Shell

The exit cone structural shell is a honeycomb sandwich structure with forward- and aft-end flange rings and is bonded to the exit-cone plastic liner with Epon 913 adhesive. The honeycomb sandwich consists of 17-7 PH stainless-steel facings with a minimum 0.2% offset yield strength of 150,000 psi and a 0.72-in.-thick aluminum honeycomb core. Two 0.026-in.-thick sheets are used for the inner facing and one 0.026-in.-thick sheet is used for the outer facing, with doubler sheets at the splice joints.

The stainless-steel facings are bonded to the aluminum core and forward- and aft-end rings with Epon 955 adhesive film. The bond-line thickness is from 0.005 to 0.011 in. The forward- and aft-end rings are designed for

III, B, Nozzle (cont.)

attachment and handling and are made of normalized AISI 4131 steel and AISI 4340 steel, respectively. An aluminum segmented ring is provided at the exit plane to retain and minimize movement between the liner and structural shell.

To provide protection against radiant heating from the exhaust gas, Gen-Gard V-61 trowelable insulation is applied around the exit cone aft ring, and cork sheet insulation is bonded on the aft 4 ft of the exit-cone exterior surface.

2. Fabrication

a. Nozzle Shell

The 260-SL-2 nozzle shell was fabricated by Sun Shipbuilding, using essentially the same techniques and materials as were used on the 260-SL-1 nozzle shell, except that all final machining of the 260-SL-2 shell was completed prior to hydrostatic test. A description of the fabrication of the nozzle shell is reported in Reference 1.

b. Plastic Components

The fabrication plans for the entrance, throat, and throat extension inserts of the nozzle were similar. The ablative surface liner was tape-wrapped on a mandrel at the specified laminate orientation angle, vacuum bagged, and preformed liner was then machined on the outside diameter and overwrapped parallel to the surface with silica cloth and phenolic tape to the required thickness. The composite insert was vacuum-bagged and final-cured in an autoclave cycle at 300°F and 300-psi pressure. The cured insert was machined on the outside diameter and ends to mate with the nozzle shell and adjacent components.

Deviations from the above fabrication procedures and discrepancies from the design requirements for each plastic component are delineated below.

III, B, Nozzle (cont.)

(1) Entrance Insert

The entrance cap liner was preformed at approximately 180°F for approximately 3 hr longer than the cycle specified. In subsequent test values for the fully cured part the physical properties were verified to be within specification limits.

After machining the outside diameter of the preformed liner, undersized discrepant areas were observed in three circumferential regions. One discrepancy (0.030 to 0.200 in. deep by 0.125 to 1.00 in. wide) was located in the silica cloth and phenolic material adjacent to the forward end. The other two regions were in the carbon cloth and phenolic material; one was located near the silica cloth to carbon cloth interface, and the other approximately 10 in. aft of the interface. The discrepancies in the two carbon cloth regions were 0.005 to 0.140 in. deep by 0.200 to 0.450 in. wide. These grooves were sanded to roughen the glazed surfaces, and each side of the groove was feathered to an angle of 15 degrees to the main surface. The grooves were subsequently filled with silica cloth and phenolic overwrap material during overwrapping of the liner.

The surface at the 128.13-in. diameter of the final cured insert was undersize by a maximum of 0.25 in. The undersized area was filled with additional Epon 913 adhesive during bonding of the insert to the nozzle shell.

A series of radiographic and ultrasonic inspections showed one delamination and five resin defect indications. The delamination was located midway axially in the silica cloth and phenolic liner and adjacent to the overwrap interface. One resin defect was in the silica cloth and phenolic liner near the interface to the carbon cloth and phenolic. Nondestructive test data indicated that these defects were all of less severity than the delamination indications observed in the 260-SL-1 nozzle throat insert. Physical properties data from test specimens of this component are shown in Figure 8.

III, B, Nozzle (cont.)

(2) Throat Insert

No discrepancies were observed in the final-cured throat insert. Physical properties data from test specimens of this component are shown in Figure 9.

(3) Throat Extension Insert

The depth of the O-ring groove was 0.177 to 0.193 in. for approximately 90 degrees of the circumferential length; this depth was 0.007 in. over maximum dimensions. Compression of the O-ring is still within design limits, and areas forward and aft of the O-ring were sealed with Epon 913 adhesive.

No silica cloth and phenolic material was available for property determinations from the aft test ring, because the as-wrapped liner was held to the maximum possible length to assure sufficient bagging surface during preform and cure without blocking the vacuum ports on the mandrel. The mechanical and physical properties of the silica cloth and phenolic were determined from the forward test ring and are presented in Figure 10.

All results were within specification limits except for volatile content of the silica-cloth overwrap. The average volatile content was 3.29%, as compared with the specification limit of 3% maximum. This discrepancy was acceptable because the overwrap is used primarily as an insulator. Components with volatile contents of 3.0 to 3.5% were used in the 120-SS-1 and 260-SL-1 motor nozzles with no apparent effect on performance.

(4) Exit Cone Liner

The fabrication sequence for the plastic liner was to tape both the MX-4926 and FM-5131 innerwrap materials parallel to the nozzle center line, machine the outside diameter, and overwrap FM-5131 tape parallel to the surface

III, B, Nozzle (cont.)

The composite part was then wrapped with a sandwich of nylon tape in tension. Longitudinal metal strips were used to prevent axial slippage of the nylon tape. The composite part was then vacuum-bagged and cured at 300°F.

Mechanical and physical property determinations were conducted on the cured liner. The forward and aft test rings of the liner were sectioned into test specimens and tested in accordance with specification requirements. There was insufficient material in the silica overwrap of the aft test ring for interlaminar shear and microtensile test specimens; therefore, properties were determined from the forward test ring. Test results of the exit cone liner are shown in Figure 11. All test values met the specification requirements with the exception of the volatile percentage, which was 3.29% maximum, exceeding the specified 3.0% maximum. This deviation was accepted since previous components from the 120-SS-1 and 260-SL-1 motor nozzles performed as designed with comparable volatile content.

Ultrasonic inspections were performed on the liner to check for flaws, delaminations, and inclusions. No indications were obtained.

c. Rubber Insulation

The nozzle insulation was fabricated by Goodyear Tire & Rubber Co., using 0.250-in.-thick plies of Gen-Gard V-44 rubber. Layup and cure of the insulation was accomplished to the design contour using a segmented steel mandrel. The assembly was vacuum sealed and cured in an autoclave. A test block equivalent to the thickest section of the nozzle rubber insulation was cured with the component to permit determination of vulcanization temperature by means of imbedded thermocouples. These sample blocks were subsequently sectioned and tested to verify that acceptable cure was obtained. After cure, the nozzle insulation interior surface was ground to the design contour.

III, B, Nozzle (cont.)

d. Nozzle Assembly

The plastic inserts were bonded to the nozzle shell in the following sequence: throat extension, throat, and entrance insert. Each insert was dry-fitted to the nozzle shell; shim thickness gages were used to determine the bond-line thickness. O-rings were lubricated with MIL-L-4343 and installed in the O-ring grooves. PR-1910 silicone rubber sealant was applied to the tapered interface gap between inserts. The mating surfaces of the insert and shell were coated with Epon 913 adhesive, assembled, and positioned in accordance with the dry fit. The assembly was cured at room temperature for a minimum of 72 hr. After the inserts were bonded, the interior surfaces of the entrance and throat inserts were machined to the specified contour.

The V-44 rubber insulation was then bonded in place with Epon 948 adhesive and vacuum-bag cured at ambient temperature. The forward face of the V-44 insulation was final-machined to the designed configuration.

The bond-line thicknesses, which were determined during assembly, are tabulated in Figure 12 (the thicknesses were within the specified limits). Adhesive bond strength was determined from test panels of representative bond-line thickness for each bonding cycle. Each panel was processed simultaneously with the assembly and was sectioned into specimens, which were tested for lap tensile shear strength. The bond strengths for the nozzle assembly components (Figure 12) met the minimum requirements, with the exception of the insulation bond strength. However, the values obtained were greater than those obtained on the 120-SS-1 and 260-SL-1 motor nozzles, and were acceptable.

Axial gaps between inserts were measured after the inserts were in place in the shell. A summary of the gaps is shown in Figure 12. The slight deviations from specification tolerances in the gap dimensions, which occurred between the throat insert and nozzle shell and between the entrance and throat inserts, were minor and were acceptable. Also, a gap deviation occurred between the rubber

III, B, Nozzle (cont.)

insulation and entrance insert. However, a greater disparity occurred in the 260-SL-1 nozzle without degrading performance; therefore, the deviation in the 260-SL-2 nozzle was accepted.

Ultrasonic inspection of the liner bond was performed with complete surface scanning. The inspection included a wet sonic inspection directly after bonding and a dry sonic inspection after adhesive cure. Another inspection was conducted after the entire assembly was completed. A summary of the ultrasonic inspection results is shown in Figure 12. No defects exceeded the specification requirement.

A leak test of the bonded nozzle assembly was conducted as a final inspection of the bond between the steel shell and the inserts to assure that no gas flow path existed at the bond line. The leak detection media was Freon pressurized to 50 psi with nitrogen. The detection media was introduced sequentially at the forward and aft interfaces of the throat insert. All other plastic-insert interface joints and the plastic-to-steel bond interfaces were checked for leakage; no leakage was detected in the nozzle assembly.

The internal surface of the nozzle plastic inserts was coated with Skydrol 162-Y-22 primer and a trial assembly of the nozzle with the exit cone was completed.

e. Exit Cone Assembly

The exit-cone honeycomb structure was assembled in three bond cycles that successively built up the structural shell on the liner. In each case, the assembly was vacuum-bagged and cured at $185^{\circ} \pm 10^{\circ}\text{F}$ for 4 hr with a vacuum of 20 to 25 in. of Hg.

In the first cycle the inner layer of stainless steel was bonded to the plastic liner with Epon 913 epoxy adhesive. In the second cycle the

III, B, Nozzle (cont.)

second stainless steel layer, aft flange, and honeycomb were bonded to the inner steel layer. Epon 913 adhesive was used for bonding the aft flange to the liner, while Epon 955 film adhesive was used for bonding the inner facings and honeycomb core.

In the third cycle the forward flange, outer facing, and outer doublers were bonded in place. The O-ring was installed in the groove of the liner. Epon 913 adhesive was used for bonding the forward flange to the liner, and Epon 955 film adhesive was used for bonding the outer facing and outer doublers. After bonding, screws were installed to attach the outer doublers to the forward and aft flanges.

The thickness of the forward flange was changed from the specified dimension of 0.500 to 0.520 in. to a dimension of 0.486 to 0.509 in. and the aft-flange thickness was also changed from 0.250 to .280 in. to a dimension of 0.279 to 0.297 in. to compensate for variation in the inner doubler material and bond-line thickness. Bond-line thicknesses for each component of the honeycomb structure during assembly are tabulated in Figure 12.

Adhesive bond strength was determined either from test panels of representative bond line thickness for each component or from trepan test data. The bond strengths of the exit-cone assembly components are shown in Figure 12. The tensile shear strengths of test specimens were less than the specified minimum; however, the values are in excess of the functional design requirements. The trepan test results on the actual assembly were above requirements and are a truer representation of the bond strengths.

The results of the ultrasonic inspection of bonds are summarized in Figure 12. Ultrasonic inspection of the exit cone liner ID after assembly revealed intermittent delaminations at the forward end extending up to 50% of the circumference and 1/8 to 1/4 in. beneath the ID. The delaminations were injected with Epon 913 and cured at room temperature.

III, B, Nozzle (cont.)

The completed exit-cone assembly was leak tested to assure the lack of gas flow in the bond line between the plastic liner and honeycomb structure and within the bond lines of the honeycomb structure. No leakage was detected in the exit-cone assembly.

The five segments of the retainer ring were bonded to the aft flange ring with Epon 913 adhesive. The 190 retaining bolts and nuts were installed.

Sheet-cork insulation was bonded to the aft 4 ft of the exit-cone external surface with epoxy adhesive. A vacuum-bag cure at ambient temperature was used. Vinyl primer was sprayed on the cork sheet. The internal surface of the exit-cone plastic liner was sprayed with Skydrol 162Y22 primer and cured at ambient temperature.

A sling failure caused the leak test fixture to drop onto the exit cone assembly during posttest disassembly operations. The resulting damage consisted of three 0.5-in.-square by 0.050-in.-deep gouges in the front face of the forward flange; five indentations (up to 0.125 in. deep) on the outer doublers; and two 5-in.-square gouged areas in the cork insulation. The forward flange gouges were blended and dye penetrant inspection indicated that the flange was acceptable. The damaged areas of the doublers were ultrasonically inspected, and unbonding was indicated between the outer doubler and the facing. The unbonded and damaged portions of the doublers were removed and replaced with new doubler pieces which were bonded with Epon 913. Subsequent ultrasonic inspection indicated no unbonding in the repaired areas. The damaged areas of the cork were removed and replaced with new cork.

The boom of a lift truck came in contact with the exit cone, causing minor indentations to two outer facings which were 0.045 to 0.070 in. deep and created an unbonded area of approximately 1 sq in. in a doubler scallop. The areas surrounding the indentations were ultrasonically inspected, found to be sound, and accepted for use in motor 260-SL-2.

III, Design and Fabrication (cont.)

C. CHAMBER INSULATION

1. Design

Motor 260-SL-2 was insulated with vulcanized Gen-Gard V-44 butadiene acrylonitrile rubber segments bonded into the motor chamber. Insulation thickness was determined from observed material loss rates, exposure time, and a 2.0 safety factor.

The forward head insulation thickness ranged from 1.25 in. at the access boss in the forward dome to 0.20 in. (minimum) at the cylindrical section joint.

The cylindrical section insulation consisted of three plies of 0.100-in.-thick (minimum) V-44 rubber. Addition of the third ply was based on the 260-SL-1 test firing data, as a result of the higher-than-expected loss rate of the cylindrical section insulation during the extended posttest after-burn, which occurred prior to quench actuation.

The aft insulation thickness varied from 2.76 in. at the nozzle step joint (vs 4.26 in. on Motor 260-SL-1) to 0.20 in. at the center-section joint.

The area around the 5.2-in.-dia boss in the forward dome and the forward cap was insulated with 1.25-in.-thick V-44 rubber. A female step joint was incorporated in the 24-in.-OD forward insulation disk to mate with the male step joint on the forward cap assembly.

The 0.25-in.-thick Gen-Gard V-45 rubber forward and aft propellant boots are designed to protect the propellant for 220 sec, which originally incorporated a 2.0 safety factor based on a 110-sec web action time.

III, C, Chamber Insulation (cont.)

2. Fabrication

The forward and aft insulation and boot segments were laid up on auxiliary tooling conforming to the dimensions of the chamber heads. After layup, the components were cured in an autoclave. Sample blocks of unvulcanized V-44 rubber, equivalent to the thickest portion of the insulation component, were cured with each component to provide vulcanization temperature by means of imbedded thermocouples. After cure, the sample blocks were sectioned and tested to verify acceptable cure hardness.

Sheets of 33-in.-wide unvulcanized V-44 rubber were rolled on drums for cylindrical-section insulation. The drum was then vacuum-sealed and cured in an autoclave. After vulcanization, the sheets were visually inspected and spark tested.

The forward firing-cap insulation and forward boss insulation were compression molded in a 1020-ton press and autoclave cured.

D. IGNITION MOTOR ASSEMBLY

1. Design

The aft-end ignition motor assembly for the 260-SL motors, shown in Figure 13, consists of four major subassemblies: ignition motor, ignition motor booster, booster initiator, and safety-arming device.

a. Ignition Motor

The Ladish D-6aC forged steel pressure vessel was designed to meet the following operating requirements:

III, D, Ignition Motor Assembly (cont.)

Nominal operating pressure, psia	1000
MEOP (nominal pressure x 1.5), psia	1500
Proof pressure (MEOP x 1.33), psia	2000
Design pressure (MEOP x 2.0), psia	3000

The required tensile yield strength of the Ladish D-6aC forged steel is 200,000 to 220,000 psi.

The internal surfaces of the ignition motor are insulated with 0.50-in.-thick V-44 rubber.

The ignition motor exit cone consists of AISI-4130 steel forgings and plate with an ultimate tensile strength of 160,000 to 180,000 psi. To reduce the heat-flux into the exit cone steel during ignition motor operation, the interior surface is coated with zirconium oxide. A phenolic-impregnated silica-cloth throat insert is bonded into the aft closure with Epon 913 adhesive.

The grain configuration is an inverted, 30-point gear with a 0.50-in. web thickness. The propellant is ANP-2758, a polyurethane formulation with a 0.8 in./sec burning rate at 1000 psia, developed and fully qualified for use in the Wing II second-stage Minuteman igniter.

b. Ignition Motor Booster

The ignition motor booster, shown in Figure 14, is a modified first-stage Polaris B-3 Alclo grain, contained in an AISI 4130 steel chamber. A 78-gm, 1.0-in.-dia by 1.0-in.-thick, solid Alclo grain is the primary booster charge and is contained in a smaller AISI 4130 steel chamber. The secondary booster charge is a 2.0-gm mixture of Alclo pyrotechnic powder and boron-barium chromate ignition powder and is contained in a small cavity in the booster mounting adapter.

III, D, Ignition Motor Assembly (cont.)

c. Booster Initiator

The 2.0-gm, 2A boron-potassium nitrate booster initiator is a modification of the Minuteman second-stage igniter initiator. The initiator is the connecting pyrotechnic link between the two ES-003 squibs (U.S. Flare 207 D-1) in the safety and arming device and the ignition motor booster. The 2.0-gm charge is installed in a small aluminum capsule, located in the booster mounting adapter.

2. Component Fabrication

The components for ignition motor assembly 260-IM-07 were fabricated by subcontractors and shipped to Aerojet, Sacramento, for inspection and final assembly. No tolerance or processing deviations occurred during the fabrication and assembly of the 260-SL-2 ignition motor.

The ignition-motor chamber was fabricated by the Oakland Machine Works, Oakland, California. The forward closure, chamber, and aft closure were machined from Ladish D-6aC steel forgings after welding. The measured yield tensile strength of the Ladish D-6aC specimens ranged from 201,000 to 214,000 psi.

The Holz Rubber Co., Lodi, California, installed the V-4 $\frac{1}{2}$ rubber insulation into the chamber. The final-cure Shore "A" hardness ranged from 78 to 82, which is within the design tolerances.

The exit cone was also manufactured by the Oakland Machine Works. The average measured ultimate tensile strength of the AISI 4130 steel specimens was 174,500 psi. Zirconium oxide was applied to the interior surface by a plasma-arc spray process.

The throat insert was fabricated by Elder Industries, Los Angeles, Calif., from FM-5131 silica cloth and phenolic supplied by U.S. Polymeric Chemical Co.

III, D, Ignition Motor Assembly (cont.)

The KR 80000-07 safety and arming device was obtained from the Minuteman Wing VI second-stage program. The device is currently in use on all three stages of the Wing VI missile. The ES-003 squibs, which are housed in the safety and arming device, contain 90 milligrams of pyrotechnic material.

3. Processing and Final Assembly

a. Propellant Processing

Propellant installation was accomplished by a mold-casting and secondary bonding technique. The propellant was mixed in 1800- to 2000-lb batches and cast into molds. After cure, the exposed propellant in the mold was restricted by bonding 0.100-in.-thick Gen-Gard V-45 rubber sheets to the propellant surface with SD-850-2 liner. The restricted propellant slabs were removed from the molds and bonded into the insulated chamber with Epon 948 adhesive. Ten propellant slabs were required.

Two ANP-2758 propellant batches were mixed; 575 lb of each batch were used in ignition motor 260-IM-07. Propellant from these batches was also used in the ignition motor for motor 260-SL-1. The cured propellant properties met the design requirements, and the ballistic performance of this propellant used in the 260-SL-1 ignition motor firing was satisfactory.

b. Final Assembly

Ignition motor 260-IM-07 was assembled at A-DD. Samples from each batch of the propellant, SD-850-2 liner, and Epon 948 adhesive used in 260-IM-07 were taken during propellant installation. The SD-850-2 liner bond strength between the ANP-2758 propellant and cured V-45 rubber met the design requirement, as shown below.

III, D, Ignition Motor Assembly (cont.)

<u>Propellant Batch</u>	<u>Double-Plate Tensile Tests</u> <u>Liner Bond Tensile Strength, psi</u>	
	<u>Measured</u>	<u>Required</u>
4-MM1-14	107, 115, 117	60 minimum
4-MM1-15	121, 115, 115	

The Epon 948 adhesive peel strength between cured V-44 and V-45 rubber ranged from 16 to 33 lb/in. for 20 samples; the minimum design requirement is 8.0 lb/in.

E. PROPELLANT GRAIN

1. Design Description

a. Grain Configuration

The grain configuration for motor 260-SL-2 is identical to that of motor 260-SL-1 and was designed to meet the performance requirements of the work statement, which are summarized in Figure 15. As shown in Figure 16, the perforation is a three-point star resembling a cloverleaf. A partial web is used in the forward head to reduce ballistic curve regressivity in the short-length motor. The 4.0-in. radii of the star-point fillets are a compromise between sliver loss and stress concentration. All surfaces have fore-to-aft tapers to facilitate core removal.

The propellant-to-chamber bond is partially released at the ends of the chamber to reduce peak stresses resulting from thermal shrinkage and acceleration loads. The released ends of the grain are bonded to release boots, as shown in Figure 16.

b. Propellant

The propellant tailored for the 260-SL motors is a conventional ammonium perchlorate and aluminum composite with a binder based on a terpolymer of polybutadiene, acrylonitrile, and acrylic acid (PBAN). The specific formulation

III, E, Propellant Grain (cont.)

(Figure 17) is adjustable for raw material lot-to-lot variabilities. The diepoxide curative content is adjusted to achieve target mechanical properties, and the ferric oxide content is varied to achieve desired burning rate.

c. Liner

The SD-850-2 liner used for bonding ANB-3105 propellant to the chamber insulation is a PBAN-based formulation, similar to the propellant binder, with appropriate fillers and curing agents for satisfactory application properties. The liner is applied to a thickness of 0.035 ± 0.010 in. and is cured at elevated temperature. The specific liner formulation developed for the 260-SL motors is shown in Figure 18.

IV. MOTOR PROCESSING

A. CHAMBER INSULATION

In preparation for insulation, the interior surface of the chamber was cleaned with methyl chloroform until the surface showed no visible oil or residue and then sandblasted with No. 50 aluminum oxide grit. After final cleaning, Fuller 162-Y-22 epoxy primer was sprayed on the chamber interior.

Motor insulation was installed by Goodyear at the A-DD facility. The aft, forward and sidewall insulation components were bonded to the 260-SL-2 chamber with Epon 948 adhesive. The V-groove joints in the forward and aft insulation were seamed with Gen-Gard V-61 potting insulation. The step joint at the forward and aft flanges were machined to final dimensional configuration after insulation components were bonded in the chamber. The joints in the forward and aft boots were seamed with Germax-accelerated V-45 rubber and cured.

B. CHAMBER LINING

Following completion of insulation installation, the insulation surface was prepared for lining. The surface was abraded by grit blasting, and then cleaned by wiping with methyl chloroform solvent. Dry air at 160°F was then circulated through the chamber for 5 days to remove all moisture and volatiles from the insulation surface. After this period, the surface was again solvent-wiped and given a final 8-hr drying period with circulating air at 135°F.

The insulated chamber was lined with SD-850-2 liner; the liner was spread on the insulation surface using trowels having thickness-control spacer wires. The liner was then brushed with stiff-bristle brushes, and troweled a second time to remove any excess material. Finally, the liner was brushed to a smooth surface. Three 450-lb batches of SD-850-2 liner were used, all of which had satisfactory acceptance properties, as shown in Figure 19. The net weight of liner applied to the chamber was 908 lb, and the average installed liner thickness, based on liner weight and application area, was 33 mils, which lies within the design thickness range of 35 ± 10 mils.

IV, B, Chamber Lining (cont.)

The liner was cured for two days at 80°F, followed by two days at 135°F. The ambient temperature precure allowed the liner to gel sufficiently to prevent running or sagging during the high temperature cure period.

Liner-to-propellant bond test specimens were prepared from each the three SD-850-2 liner batches, using ANB-3105 propellant from 25 of the batches cast into 260-SL-2; the bond tensile and shear strengths of these specimens average 161 and 121 psi, respectively. The specimens failed randomly in the propellant. The high bond-strength levels and the type of specimen failure are typical of the SD-850-2 to ANB-3105 bonding system, and indicated that the 260-SL-2 liner preparation and application were satisfactory.

C. PROPELLANT PROCESSING AND MOTOR CASTING

The insulated and lined chamber was removed from the General Process Building and installed in the Cast, Cure, and Test Facility. The casting core, which had previously been assembled and coated with the release agent, was then installed in the chamber. The movable casting building was positioned over the caisson, and the chamber and core were preheated to the casting temperature of 135°F with dry circulating air. After preheating, the propellant casting tooling was assembled. The casting setup is shown in Figure 20.

As a result of the technical data and experience obtained during the casting of motor 260-SL-1, several modifications to the propellant casting technique were made. A Propellant Pot Processing Building was constructed adjacent to the movable Casting Building. The full propellant transfer pots were routed through this building and processed for casting, including the installation of the diaphragm and the pressure head. The transfer pots were then moved to the Casting Building and positioned for casting.

The adjustable casting stands used for casting motor 260-SL-1 were replaced by a transfer-pot rail system, which consists of a rigid platform constructed over the

IV, C, Propellant Processing and Motor Casting (cont.)

caisson with a set of guide rails to transport and position each transfer pot over the respective casting tube. The basic casting-tube system procedures were not changed, with the exception of the allowable casting-tube immersion depth. During the first half of the casting, the maximum allowable casting-tube immersion depth was 8 ft; this depth was reduced to 4 ft for the remainder of the casting. The shallower immersion depth was selected to further improve the propellant-to-liner bond. Modifications were made in the casting-tube withdrawal, cleaning, and cutting operations, which substantially reduced the operational times for these procedures.

Casting of motor 260-SL-2 was initiated on 29 November and completed on 9 December. A total of 1,677,837 lb of ANB-3105 propellant was cast into the motor. A total of 276 pots of propellant was produced, consisting of 193 pots of vertical batch mixed propellant (5500 lb each) and 83 continuous mixed pots (8500 lb each). Five vertical batches and one continuous mix pot were scrapped. Two vertical mixed batches failed to meet the density specification, two batches exhibited small oxidizer agglomerates, and one batch was scrapped because of equipment malfunction. The continuous mixed pot was scrapped for burning rate deviation.

A total of 47 12,000-lb batches of premix were prepared, of which one batch was scrapped because of dispensing errors. All other batches were well within specification limits (Figure 21).

The uncured-propellant qualification data (Figures 22 through 25) indicate that good reproducibility of propellant properties was obtained and that the mean values were very close to theoretical and target requirements. For purposes of comparison, the uncured-propellant qualification data from motor 260-SL-1 are also presented in these figures.

The liquid strand burning rates (Figure 22) showed no statistical difference between the two motors, with overall average rates (continuous plus batch mixed propellant) of 0.4445 and 0.4439 in./sec for motors 260-SL-1 and -2, respectively.

IV, C, Propellant Processing and Motor Casting (cont.)

The continuous mixed propellant appeared to be more variable for motor 260-SL-2, exhibiting a sample-to-sample standard deviation of 0.0124 in./sec as compared to a value of 0.0092 in./sec for motor 260-SL-1.

The liquid density for the propellant cast into the two motors is very close to the theoretical values, as shown in Figure 23. Because of the higher curing agent concentration required for motor 260-SL-2, the theoretical density is higher (1.751 vs 1.752 gm/cc). All pot-to-pot and sample-to-sample standard deviations are approximately 0.002 gm/cc.

The averaged measured DER-332 curing agent content (Figure 24) agreed with the theoretical values to within 0.7% for both processes. The standard deviations for the results appear to be higher for motor 260-SL-2 than for the motor 260-SL-1 propellant.

The measured wt% oxidizer (continuous mixed propellant only) was almost identical for the two motors with respect to both mean values and standard deviations (Figure 25).

Upon completion of casting, the casting rails and associated equipment were removed, and the motor was sealed. Warm air was circulated around the chamber to maintain the grain temperature at 135°F during the propellant cure period.

D. POSTCAST OPERATIONS

Samples of propellant from every sixth batch cast into motor 260-SL-2 were tested for mechanical properties; testing was initiated after 16 days of cure at 135°F. The data, shown in Figure 26, indicate that propellant cure stabilizes after about 28 to 32 days of cure. On the basis of these data, together with Shore "A" hardness measurements made on samples from all batches, cure was considered to be complete after the last batch cast had cured for 28 days. Motor cool-down was initiated on 6 January 1966.

IV, D, Postcast Operations (cont.)

Samples from each of the batches of propellant cast into motor 260-SL-2 were tested for mechanical properties at the start of motor cool-down (28 to 38 days of cure at 135°F). The data (Figure 27) indicate an overall average initial modulus of 453 psi, which is well within the target range of 400 to 600 psi.

Additional samples from every sixth pot were tested to determine the propellant constant strain tolerance. The data, shown in Figure 28, indicate that samples from all batches withstood 15% strain for one week at 77°F, and nearly 95% of the samples held when tested at the maximum strain level of 20%. These results indicate that the 260-SL-2 propellant constant strain tolerance is greater than that measured for the 260-SL-1 propellant.

The grain was cooled from the 135°F cure temperature to the desired operating range of 60 to 100°F by circulating 62°F air outside the chamber and inside the casting core. Heat-transfer calculations showed that 14 days of cooling would produce a temperature distribution in the 260-SL-2 grain which would stabilize at about 80°F after an additional four-week period of ambient temperature exposure during final assembly operations. Cooling was therefore terminated on 20 January 1966.

The core was removed from the grain on 21 January 1966; the net extraction force at core breakaway was 46,000 lb. Visual inspection of the grain bore surface showed that several small voids and blemishes were present; however, the surface appearance was satisfactory, with no evidence of structural deficiency. Figure 29 shows the grain bore after core removal.

Radial measurements of the propellant-grain bore were taken after core removal to determine the grain deformation resulting from thermal shrinkage and slump. Measurements were obtained just after core removal, and again 7 days and 15 days later. The measured radial deformations for 260-SL-2 as shown in Figure 30, agree well with analytical predictions and are similar to those obtained on 260-SL-1. The 260-SL-2 grain bore profile showed more shrinkage effects at 7 and 15 days than that observed in the 260-SL-1 grain. This was apparently a result of the lower average grain temperature existing in 260-SL-2 as a result of low ambient temperature exposure.

IV, D, Postcast Operations (cont.)

After core removal, the aft surface of the grain was trimmed to the required dimensions. The final net propellant weight was 1,673,000 lb.

Prior to nozzle installation, the gap between the aft boot and the aft chamber insulation was filled with ambient curing polysulphide rubber potting compound (FMC-200). A total of 6,488 lb of material was required to fill the gap. Cure samples, taken from each 55-gal drum of potting compound after mixing showed that all the material cured to the required physical properties.

E. MOTOR FINAL ASSEMBLY

1. Nozzle and Exit Cone Receiving

After the nozzle and exit cone assemblies arrived at A-DD from TRW, Cleveland, Ohio, a visual inspection was made of both interior and exterior surfaces of the components. No damage during shipment was noted. Inside contour measurements of both the nozzle and exit cone were obtained at six equiangularly spaced locations.

Ultrasonic inspection was performed on the interior surfaces of both the nozzle and exit cone to check for structural damage to plastic components during shipment. Ultrasonic inspection of the nozzle-shell exterior surface was performed to determine whether the integrity of bonds between the nozzle shell and plastic inserts had been impaired by shipment. Results obtained indicated that no significant changes had occurred during shipment.

A dimensional check disclosed that local areas of the aft face of the throat extension plastic insert extended from 0.001 to 0.010 in. above the aft face of the nozzle shell flange. These areas were reworked to drawing tolerance by handsanding.

Visual inspection of the nozzle assembly revealed minor variations from drawing requirements as described below.

IV, E, Motor Final Assembly (cont.)

a. Primer had been applied on the machined nozzle-exit cone flange OD and on the spotface and counterbore of the flange holes. The material was removed by wire brushing prior to assembly.

b. Voids existed in the PR-1913 potting material at the interface between the nozzle entrance insert and the throat insert. These voids were filled with silicone rubber PR-1913-24 potting material.

c. Voids were apparent in the bonding of the throat extension insert to the steel shell at the nozzle-exit cone flange. These voids were filled with Epon 828 epoxy resin.

After inspection of the exit cone was completed, an additional 24-in. section of cork insulation was applied to the exit cone external surface, just forward of, and adjacent to, the existing cork layers.

2. Nozzle and Forward Cap Installation

The nozzle was fitted with the leak test closure and weighed with two 20,000-lbf load cells. The actual weight of the nozzle assembly was 26,126 lb. To check the gap between the insulation joint during trial assembly, strips of putty enclosed in cellophane were placed around the perimeter of the joint. The nozzle was then lowered into position, leveled, and placed on the chamber flange. Inspection disclosed that the gap between the rubber insulation faces was sufficient to ensure that the potting compound would fill and provide a seal at all step joint surfaces.

The nozzle was then removed from the chamber and PR-1913 silicone-rubber potting compound was applied to the mating surfaces of the chamber-insulation step joint to the approximate thicknesses measured during trial assembly. The O-ring was positioned in the groove and lubricant applied. The nozzle was lowered onto the guiding tapered pins, leveled, and lowered into position. MIL-T-5544 thread lubrication was applied to the threads and under the heads of all bolts prior to hand-tight installation. One bolt at the 114-degree location could not be installed due to a

IV, E, Motor Final Assembly (cont.)

mismatched hole. No explanation for this problem has been established. Three bolts in each quadrant were then torqued to 250 ft-lb: reinspection disclosed no measurable gap between the two mating flanges. The specified maximum torque of 800 ft-lb was then applied to all remaining bolts.

The forward cap was installed on the motor, using procedures for measurement of insulation step joint clearance similar to those described for nozzle installation. The 15 bolts retaining the cap were torqued to 90 ft-lb.

3. Motor Leak Test

Pressure transducers were assembled to the forward cap and secured for the leak test. A 12-hr elapsed time was required for cure of the PR-1913 joint sealant prior to conducting the leak test.

The motor interior was initially pressurized to 45 psig with dry nitrogen and then increased to 50 psig with helium. A helium leak-detection system was used to check for leakage at the aft-closure nozzle-attachment flange, the forward cap-to-chamber interface, and at each pressure seal on the three transducers. No leakage was detected.

After leak testing was completed, the misalignment bolt hole in the nozzle shell was enlarged sufficiently to permit installation of the final bolt.

4. Exit Cone Installation

The leak-test cover was removed and the surface of the nozzle shell flange was prepared for a trial assembly of the exit cone. Step-joint gap determinations, again using putty, indicated an insufficient gap. The forward end face of the exit cone plastic liner was subsequently ground and handsanded until the final gap was within drawing tolerance. The surfaces were cleaned and the O-ring lubricated and placed in the groove in the nozzle shell. PR-1913 silicone-rubber potting compound

IV, E, Motor Final Assembly (cont.)

was applied to all mating surfaces of the nozzle and exit cone liner prior to final assembly of the two components. The exit cone was then lowered into position and retained with 176 nuts and bolts torqued to 250 ft-lb.

Gen-Gard V-61 rubber compound was prepared and troweled onto the end and outer diameter of the exit cone aft flange to provide radiant heat insulation for the flange. The nozzle weather cover was then installed.

V. TESTING

A. TEST PLAN

The test firing of 260-SL-2 was conducted in accordance with Project Directive 34. The test requirements were essentially the same as were specified for the 260-SL-1 static test firing.

Motor positioning in the Cast, Cure, and Test Facility is controlled by installation of the thrust takeout assembly. This operation was the first item of the test plan to be performed and was accomplished prior to installation of the chamber in the Cast, Cure and Test Facility. The forward skirt of the motor rests on a thrust takeout ring which is supported by three 5,000,000-lb capacity load cells during the firing and by three hydraulic jacks during motor processing operations. This ring was installed with the aid of optical alignment instruments to within 0.050 in. of a true level plane and 0.50 in. of the true axial center line of the thrust takeout assembly. This precise base-ring alignment assures that the maximum misalignment of the motor thrust axis, when combined with the maximum buildup of chamber and nozzle fabrication tolerances, will not exceed 0.20 degree. Figure 31 shows the motor installation in the test facility.

Instrumentation to measure motor thrust, chamber pressure, acceleration, temperatures, strain, and chamber growth were installed in accordance with the requirements of Project Directive 34. This instrumentation plan is presented in the appendix. Data defining the operation of the ignition and quench systems and the environmental effects of the firing on adjacent tooling and facilities were also recorded. Nine motion picture cameras documented the test firing, as shown in Figure 32.

Datacraft Inc., Gardena, California, under a separate contract to NASA, Marshall Space Flight Center, recorded sound pressure level, motor acceleration, and exhaust infrared-radiation data.

The ignition of the motor 260-SL-2 was initiated by a firing command to the safety-arming device on the Mod 260 ignition motor. When the 260-SL-2 grain

V, A, Test Plan (cont.)

ignited and the fore-end pressure reached a preset level of 125 psia, a command was given by either of the two ignition motor release control-units to fire the 28 explosive bolts securing the ignition motor and sled assembly to the supporting fixtures. A secondary timing system in each control unit would fire the bolts at approximately 0.500 sec in the event of a failure in the pressure-sensing system.

When the ignition motor and sled assembly traveled 26.8 ft to the top of the track, a breakwire was fractured. This event initiated tower retraction.

A carbon-dioxide quench system was used for extinguishing the post-firing burning of insulation components in the chamber interior. The quench system was programmed for actuation as the chamber pressure approached 0 psig. The water-fog nozzle quench system used on the 260-SL-1 test was not specified for use on this test in an effort to prevent the cracking or delamination of the plastic inserts encountered in the previous test. Approximately 12,000 lb of liquid CO₂ were introduced into the chamber interior at a pressure of 300 psig.

Following the test, all recorded data were returned to Solid Rocket Operations, Sacramento, for reduction and analysis. Posttest evaluation of chamber insulation and nozzle liner component performance was accomplished in accordance with Project Directive 31.

B. SPECIAL TEST EQUIPMENT

The major items of special test equipment required for the static test firing of the 260-SL motors are shown in Figures 33 through 36. The design criteria, component description, and function of each system was discussed in detail in Reference 1. A listing of these items, with a brief description of the major function of each tool or subsystem, is presented below.

V, B, Special Test Equipment (cont.)

1. Thrust Measurement System

- a. Spacer: Reduces the effective depth of the caisson to that required for the 260-SL motors.
- b. Load Cells: Three 5,000,000-lbf load cells measure the thrust generated by the rocket motor.
- c. Thrust Transfer Ring: Supports the motor at the forward skirt and transmits the thrust to the load cells.
- d. Horizontal Stabilizers: Restrict transverse movement of the motor, while allowing axial freedom of movement.
- e. Hydraulic Jacks: Support motor weight during all processing and test preparation operations.

2. Flight Retention System

- a. Torodial Collar: Surrounds the nozzle, preventing aft movement of the motor in the event of a malfunction.
- b. Tension Rods: Connect collar to anchors in caisson wall and act as the primary load-carrying members.
- c. Beams: Support collar assembly, quench, and ignition-motor retention and release systems.

3. Quench System

Directs CO₂ to the chamber interior for extinguishing posttest burning and charring of insulation components.

V, B, Special Test Equipment (cont.)

4. Ignition Motor Retention-and-Release System

This system secures the ignition motor in the required position in the 260-SL nozzle until 260-SL motor ignition is assured, and then provides the controlled release and direction of the ignition motor and sled assembly to a pre-determined impact area.

Several modifications were made in various components of this system after the static test of motor 260-SL-1. These modifications were designed to increase the eastward impulse of the igniter motor-and-sled assembly imparted by the retention cables. These changes were:

- a. The top 15.2 ft of the tower was removed to allow shortening of the retention cables and supporting poles, thus reducing cable acceleration loads.
- b. The cable length was reduced from 326.5 to 305 ft.
- c. The near-pole length was shortened from 82.5 to 55.4 ft; the far-pole length was reduced from 46.5 to 18.9 ft.
- d. A fairing was installed on the primary gas impingement areas of the sled assembly to reduce the drag load and, consequently, the upward velocity. This increases the time the cable force is applied to the unit, thereby increasing the eastward impulse.

5. Data Acquisition System

The data acquisition system at the A-DD test facilities has been designed to incorporate the features that have been installed and utilized successfully in the facilities at Aerojet, Sacramento. The capability of the system was designed to meet the criteria established in the Work Statement and is summarized in Figure 37.

V, B, Special Test Equipment (cont.)

All data processing, instrumentation equipment calibration, and repair are accomplished at Aerojet, Sacramento. The system is capable of (but not limited to) measuring force, pressure, strain, temperature, acceleration, event occurrences, and photographic recordings. The instrumentation system is described in detail in Reference 1.

6. Control System

An electric supply, distribution, and monitoring system is installed to perform such functions as igniter arming and firing explosive-bolt initiation, tower retraction, and quench system operation. The primary source of power is a 28-vdc motor generator unit. A schematic of the system logic is shown in Figure 38.

C. INSTRUMENTATION

To thoroughly define the ballistic performance and physical response of the 260-SL-2 motor and ignition system during the static test firing, 91 channels of data were recorded. These are summarized as follows:

<u>Parameter</u>	<u>No. of Channels</u>
Chamber pressure:	
260-SL-2	3
Ignition Motor	2
Thrust	6
Chamber and nozzle temperature	34
Vibration and shock	12
Chamber and nozzle strain	15
Chamber growth	2
Event sequence	17
	<hr/>
	91

V, C, Instrumentation (cont.)

A listing of the instruments used to measure and record these data is shown in Figure 39. The location of each sensing gage on the motor is defined by Figure 40.

An additional 23 channels of data were recorded to define the operation of various STE components and the environment created by the 260-SL motor firing on adjacent facilities and equipment. Figure 41 shows the location of these instruments or sensors.

D. TEST PREPARATIONS

Test preparation began with the installation of the thrust measurement system at the -59-ft platform of the Cast, Cure, and Test Facility. The final inspection of the thrust-ring alignment showed a maximum deviation at any location on the top face of 0.031 in. from a true level plane and that the center was displaced 0.25 in. southeast of the longitudinal center line of the spacer assembly. These deviations are well within the tolerances specified.

When the chamber was installed on the thrust ring, and with the ring being supported by the three cells, a maximum out-of-level condition of 0.188 in. was measured on the nozzle attachment flange.

Prior to nozzle assembly, the nozzle and exit cone were instrumented with thermocouples, strain gages, and accelerometers. The three aft horizontal stabilizers were installed; this operation completed the thrust takeout-system assembly.

After installation of the nozzle on the motor, the antifiight retention system was installed. Three Taber Model 206 pressure transducers were connected to the forward cap after its assembly on the forward boss flange. All pressure fittings were torqued to prescribed values and marked with torque paint.

V, D, Test Preparations (cont.)

The quench system was positioned and functionally checked out after exit cone installation. Operation of all components of the system was normal.

The igniter motor was assembled and leak tested prior to installation on the sled assembly. The safety and arming device and Mod 260 ignition motor booster were installed on ignition motor 260-IM-07. Two pressure transducers were mounted on the booster adapter. A leak-detection solution was used to indicate any leakage at the motor or transducer pressure seals with the igniter interior pressurized to 35 psig with dry nitrogen. No leaks were detected.

Concurrently with the mechanical test preparations, the installation of the various instrumentation sensors on the motor and the setup of the recording equipment in the control room was being accomplished.

The igniter motor and sled assembly was secured to the support fixtures with 28 explosive bolts, and attachment of the four retention cables was accomplished. The completed setup for the 260-SL-2 motor static test is shown in Figure 42.

VI. TEST RESULTS

A. DATA PROCESSING

The magnetic tape recording of analog pressure and thrust data, recorded on the Ampex FR1200 tape recorder, was replayed through a voltage sampling system and recorded on magnetic tape in a digital format. The digitized tape served as the input, via an appropriate extending program, to the CDC 3100 computer which provided a tabulation in engineering units of pressure and thrust (uncorrected for propellant weight loss) and an input tape for the IBM 7094 computer analysis. This data was reviewed for validity prior to final processing on the IBM 7094.

The computer input tape recording of digital performance data, along with ballistic constants (propellant weight, pretest and posttest throat area, atmospheric pressure, etc.), was programed into an IBM 7094 computer. The output of this program provided instantaneous values of pressure and thrust (corrected for propellant weight loss), integration of pressure and thrust, delivered specific impulse, specific impulse at standard conditions, and a computed throat area vs time at two efficiency levels.

Determination of ignition interval, web action time, action time, and all sequential event data was made from oscillographic recordings. All other data recorded on oscillographs, i.e., motor temperatures and strains, were reduced by manual measurements of analog deflections and application of factors obtained from calibration records, with manual tabulation or graphical plotting of resulting data. Vibration data originally recorded on magnetic tape were played back on an oscillograph at a 50-in./sec chart speed and then manually reduced in the same manner as indicated for data originally recorded on oscillographs.

B. DATA ANALYSIS

Of the 114 channels of recorded data specified by the instrumentation plan, all channels were operable at the start of the test, and valid readout of 108 channels was obtained. A sequential time-event summary of the firing, including all

VI, B, Data Analysis (cont.)

recorded event functions, is presented in Figure 43. Motion picture coverage produced excellent documentation of events and verified the absence of abnormal performance. An evaluation of each major category of recorded data is listed below.

1. Chamber Pressure

Valid recordings of the three installed chamber pressure transducers were obtained for the entire firing duration, with variation of 1% or less between values from each transducer. No abrupt or unusual perturbations in pressure traces and no indication of oscillations of pressure occurred.

Instantaneous pressure values were obtained by averaging tabulated digital values of P_{c1} and P_{c2} readouts obtained after reduction of data, and then adding ambient pressure. The P_{c1} and P_{c2} readouts generally did not differ by greater than 4 psi and the respective $P_c dt$ integrals differed by approximately 0.9%. The most accurate instantaneous values of chamber pressure were thus obtained by using the average of the two readouts.

2. Thrust

Six thrust readouts, obtained from two redundant sensing elements in each of three installed load cells, were the values of thrust vs time used for ballistic analysis. Instantaneous thrust values were obtained by summation of all six tabulated digital values of thrust readouts recorded after reduction of data, by dividing this summation by 2, and by subtracting the calculated instantaneous value of motor weight. Calculated weight at each time point was obtained by subtracting the weight of propellant expended at that time from the original measured motor weight.

The weight loss in firing measured by the load cells varied less than 1% from the calculated weight of propellant and inert materials expended. The distribution of force applied to the three load cells was within $\pm 1\%$ of the mean value during the firing duration.

VI, B, Data Analysis (cont.)

3. Acceleration

Motor 260-SL-2 instrumented with crystal accelerometers to determine the vibration environment produced by the motor and to detect any abnormal behavior of the motor or components. The data were recorded on magnetic tape during the firing and played back on oscillographs for data analysis.

The vibration response of motor 260-SL-2 was almost identical to that of 260-SL-1. The maximum vibration response occurred during the ignition interval and only very low level oscillations were observed during the steady-state operation. No significant increase in vibration response was observed during the tailoff period. There were no observable transients or perturbations during the entire firing. The maximum vibration responses and associated frequencies recorded during the firing are listed in Figure 44.

4. Case and Nozzle Temperatures

Thirty-two of the 34 thermocouples on the motor recorded surface temperatures until 350 sec after fire switch. The other two thermocouples (T31 and T33) monitored the ambient air temperature adjacent to the exit cone skin. Thermocouples on the motor skin were insulated from the effects of the ambient air temperature.

The primary objectives of thermocouple placement were to verify the adequacy of the chamber and nozzle insulation by monitoring the temperature at those areas expected to receive the greatest thermal inputs and to aid in determination of the source of any component malfunction. The instrumentation plan in the appendix gives the location and selection criteria for each temperature measurement.

The recorded data demonstrate that the outer surface temperatures barely exceeded the ambient level during the 350-sec recording period. Temperature measurements made at locations identical to the 260-SL-1 test show excellent correlation.

VI, B, Data Analysis (cont.)

The highest temperature recorded on the surface of the chamber was 147°F. This occurred at a mid-chamber location (T6) where maximum exposure of the cylinder wall insulation to hot gas was expected. Temperature at this location was still slowly rising at the end of the 350-sec recording time. The other thermocouples on the cylindrical section of the chamber sensed temperature increases of 30 to 65°F during this period.

There was no measured temperature increase on the forward and aft heads, although it is recognized that maximum temperatures were reached some hours after the firing. The forward head could be touched three hours after the test, but sustained pressure by the hand was impossible, indicative of a temperature somewhat less than 200°F.

There was no significant temperature rise at any location on the nozzle shell. A maximum increase of 10°F recorded opposite the throat insert forward joint was a result of external heating.

Exit-cone skin temperatures increased up to 30°F and were still slowly rising at the end of the data recording period. Low-pressure flame, which billowed around the exit cone during tailoff, accounted for this temperature rise. The ambient air temperature adjacent to the exit cone surface, 72 in. forward of the exit plane, increased 64°F to a maximum of 132°F. A temperature of 137°F was reached 10 in. forward of the exit plane.

5. Chamber and Nozzle Strain

A limited amount of strain data were obtained since stress distribution in the chamber and nozzle shell was analyzed at the higher loading conditions existing during the hydrostatic test.

VI, B, Data Analysis (cont.)

Three locations were instrumented in the hoop and meridional axes at the locations which were the highest stressed during the hydrostatic test and were the result of fabrication deviations. The primary purpose of these gages was to detect any evidence of yielding or excessive stress in the event of any overpressurization during the test.

The recorded data from these locations reflect the smooth pressure-vs-time curve. The calculated membrane hoop stress (127,000 psi) at the location of prime concern on the chamber (S-3, S-4--porosity in the weld) based on measured strain data,* agree very well with the theoretical stress of $\gamma_h = \frac{pr}{t}$ (125,000 psi). A plot of strain vs pressure is shown in Figure 45 for this area, along with a comparison plot of strain data recorded during the hydrostatic test. Good correlation is shown between the two sets of data, with the small differences being due to data-system accuracies and the grain load-carrying ability.

Strain data recorded from biaxial gages (S-5, S-6, S-7, and S-8) adjacent to the weld between the forward boss flange and the dollar plate at the point of maximum discontinuity correlate very well with values obtained during hydrostatic test. This relationship is shown below.

260-SL-2 Static Test

$$\epsilon_h = 4900 \text{ microin./in.}$$

$$\epsilon_m = 2500 \text{ microin./in.}$$

260-SL-2 Hydrostatic Test

$$\epsilon_h = 4700 \text{ microin./in.}$$

$$\epsilon_m = 2580 \text{ microin./in.}$$

The relatively high meridional stress (195,000 psi) calculated from the biaxial strain data reflects the bending stresses from the contour deviation between the dollar plate and the forward flange forging. The pressure strain plots for gage locations S-5, S-6, S-7, and S-8 are nonlinear (Figures 46 and 47), and reflect

$$* \sigma_h = \frac{E}{1 - \mu^2} \left[\epsilon_h + \mu \epsilon_m \right]$$

VI, B, Data Analysis (cont.)

the local change of radius from a flatter surface to a generally spherical shape as the pressure increases. Interior strain measurements taken at this area during hydrostatic proof test show that bending accounts for approximately 56,000 psi of the total stress, leaving 139,000 psi as the true net tensile stress, which is well below the minimum yield strength of the material.

A maximum hoop strain of 1675 microin./in. was recorded at location S-2 on the nozzle shell, which corresponds to the location of maximum stress on the plastic entrance section insert. A strain of 2,200 microin./in. was measured at this location in the hydrostatic test of the 260-SL-2 chamber assembly, which suggests that 20 to 25% of the loading from pressurization may be carried by the plastic insert. The measured strain compares well with the 1860 microin./in. measured at this location on the 260-SL-1 static test.

Four uniaxial strain gages were installed on the aft flange of the exit cone in the hoop direction at the 0-, 90-, 180-, and 270-degree orientations. The purpose of these gages was to determine the amount, if any, of nonsymmetrical loading of the exit cone as a result of igniter-motor misalignment or to abnormal removal of the igniter from the motor nozzle. At 0.27 sec, a peak of -153 microin./in. was recorded at the 0-degree position, and 132 and 209 microin./in. at the 90- and 270-degree positions, respectively. This corresponds to a decrease in radius of less than 0.175 in. at the 0-degree position and an increase of a like amount at the 90- and 270-degree positions. Data from the strain gage at the 180-degree station was lost at ignition. This ellipsoidal deformation of the exit plane was of a transient nature, and the magnitude of the resulting stress is well within allowable values. An uneven distribution of pressure in the exit cone, due to the unsymmetrical reflective configuration of the igniter support assembly, is believed to be the cause of this deformation.

Three uniaxial strain gages (S-15, S-16, and S-17) were oriented in the meridional axis of the forward skirt, spaced 120-degrees apart and above the three load cells. The primary purpose of these gages was to detect any unsymmetrical

VI, B, Data Analysis (cont.)

thrust transfer to the load cells or abnormal loading of the skirt due to motor misalignment or nozzle failure. A plot of the output of these three gages (Figure 48) shows excellent symmetry of load distribution in the skirt.

6. Chamber Growth

Data to determine circumferential and axial chamber growth at the center of the cylindrical section (S-13 and S-14) were lost at ignition due to polarity reversal which caused the traces to go off of the oscillograph record.

VI, Test Results (cont.)

C. IGNITION SYSTEM PERFORMANCE

Aft-end ignition of motor 260-SL-2 was accomplished as designed; the performance further verified the Aerojet aft-end ignition analytical model, the design criteria, and the conclusions reached during the 260-SL motor ignition system development program, which are described in detail in Reference (2). The 260-SL-2 motor ignition transient is presented in Figure 49, and includes the significant ignition sequence events; the 260-SL-1 motor ignition transient is also included in Figure 49 for comparison. A summary of the ignition sequence for both 260-SL motors is shown in Figure 56.

The aft-end ignition performance achieved in the 260-in.-dia motor demonstration program verified the design approach. The ignition intervals for the three 44-SS motors test-fired were 0.165, 0.160, and 0.162 sec; the ignition intervals for the two 260-SL motors were 0.340 and 0.336 sec. The primary requirement of the 260-SL motor ignition system development effort, as specified in the original Work Statement, was to demonstrate ignition performance reproducibility in large solid-propellant motors. The excellent motor ignition performance reproducibility achieved in this program (Figures 49 and 50) clearly fulfilled the Work Statement requirement.

As shown in Figure 49, first motor propellant ignition occurred between 0.17 and 0.18 sec after fire switch. The final relay closure to the explosive bolt capacitor bank was recorded at 0.289 sec; approximately 3 to 5 millisecc later (approximately 0.304 sec), the explosive bolts fired. The ignition motor and support fixture assembly ascended the shortened channel track and the upper wheels on the support fixture reached the top of the tower at 0.546 sec, actuating the tower

VI, C, Ignition System Performance (cont.)

retraction-command breakwire. First motion of the tower retraction linkage was recorded at 0.570 sec. Once again, the retention cables failed as the cable loop between the forward and aft poles was being accelerated. However, the cables imparted sufficient horizontal impulse to the vehicle to direct its trajectory in an easterly direction. The ejected ignition motor and support fixture assembly impacted approximately 150 ft due east of the target canal. The tower was fully retracted 4.8 sec after fire switch. The ignition motor and support fixture were destroyed on impact (Figure 51).

The performance of ignition motor 260-IM-07 met the design requirements; the flame propagation time, ignition interval, and mass flow rate were within the desired range. The ignition motor ballistic data are summarized in Figure 52; included in Figure 52 are ballistic data from 260-SL boosters and ignition motor previously test fired.

The flow conditions that existed in the motor nozzle during ignition of motor 260-SL-1 and 260-SL-2 were similar to the conditions described for the free-volume simulator tests, Reference (2), except that igniter inlet jet plume blockage of the motor throat terminated as the motor bore pressure approached 300 psia. The initial rate of pressure rise in the 260-SL motors was approximately 2700 psi/sec. Approximately 0.3 sec after fire switch and coincident with first motion of the ignition motor, the rate of pressure rise leveled off to a value between 450 and 550 psi/sec (Figure 49); this value was the pressure rise rate that would be expected in the 260-SL motors between 350 and 550 psia, assuming that all the propellant surface was ignited and the igniter jet stream was not affecting flow in the motor nozzle.

VI, C, Ignition System Performance (cont.)

The igniter jet plume exhausted into an adverse pressure gradient environment, i.e., atmospheric pressure at the exit plane and more than twice atmospheric pressure at the 260-SL effective throat plane. The initial flow expansion angle at the igniter exit plane was relatively large and the plume tended to reduce in size as the environmental pressure increased. The result was a flow picture as schematically depicted in Figure 53. The exhaust plume was substantially larger than would be predicted from one-dimensional analysis (Reference 2) because the flow was actually three-dimensional and an adverse pressure gradient existed. A check was made of the flow conditions measured during igniter operation prior to motor propellant ignition, assuming that the actual igniter jet plume occupied 30% of the motor throat area and that the effect of over-expansion from the pressure gradient was approximately 15% of the motor throat area (essentially 45% motor throat blockage). Under these conditions, the calculated motor bore pressure was 65 psia; the measured bore pressures prior to propellant ignition were 62 and 66 psia. The close correlation between the calculated and measured motor bore pressure prior to propellant ignition verified this method of flow analysis. This flow condition was maintained until motor propellant ignition was accomplished.

The various slopes of the measured motor bore pressure rise were readily analyzed. The rate of motor pressure rise at ignition was approximated by differentiating the equation of state for ideal gas:

$$\frac{d P_2}{dt} = \frac{\bar{R}T}{V_1 M} \frac{d \dot{w}}{dt}$$

where P_2 = motor bore pressure, psia

\bar{R} = gas constant, in.-lb/mole-°R (18,528)

T = chamber temperature, °R (~6000)

V_1 = motor free-volume, in³. (8.5×10^6)

M = propellant gas molecular weight, lb/lb-mole (28.1)

VI, C, Ignition System Performance (cont.)

$$\frac{d\dot{w}}{dt} = \dot{w}_{\text{prop}} - \dot{w}_e + \dot{w}_i$$

where \dot{w}_{prop} is given as a function of pressure from the burning rate equation, density, and burning surface area.

$$\dot{w}_{\text{prop}} = 940 P_2^{.41}$$

$$\dot{w}_e = \text{mass-flow rate of the exit gas stream, } C_w P_2 A_e$$

$$A_e = \text{area of motor throat occupied by the motor exit gas stream, in}^2.$$

$$\dot{w}_i = \text{igniter mass flow rate, lb/sec}$$

The slope of the 260-SL motor pressure rise was calculated at 200, 300, and 350 psia; the results were as follows:

<u>Bore Pressure, P_2, psia</u>	<u>Calculated Rate of Motor Pressure Rise, psi/sec</u>
200	2480
300	2170
350	1330

In Figure 54, the calculated slopes were superimposed on the measured 260-SL motor pressure rise curve. An excellent correlation was obtained, except for the condition at 350 psia; the solution to the equation obviously did not represent the true flow conditions at this pressure level. The measured rate of pressure rise at 350 psia was approximately 750 psi/sec; the calculated effective motor throat area necessary to obtain this rate of pressure rise was approximately 3960 sq in., or the full 260-SL motor throat area. Extending the analysis to 400 psia, the calculated rate of pressure rise was 460 psi; these values were in close agreement with both the measured and predicted motor pressure rise rates (500 psi/sec average between 300 and 500 psia).

VI, C, Ignition System Performance (cont.)

This analysis showed that the measured pressure rise characteristics were entirely reasonable. The "knee" in the ignition transient curve was difficult to predict in advance, for it was indicative of the effect of the bow shock between the inlet jet plume and the exit gas stream forming downstream of the 260-SL motor throat plane. Because the bow shock formed aft of the motor throat plane before the igniter moved an appreciable distance away from the motor nozzle after explosive bolt actuation, pressurization of the 260-SL motor bore was independent of igniter ejection.

D. BALLISTIC PERFORMANCE ANALYSIS

1. General

The ballistic performance characteristics of motor 260-SL-2 were in close agreement with those predicted and all design objectives were met. A summary of predicted and actual performance characteristics is presented in Figure 55. The measured 260-SL-2 chamber pressure- and thrust-vs-time curves are shown in Figure 56.

2. Prefiring Performance Prediction

The predicted 260-SL-2 ballistic performance, shown in Figures 55 and 57, was computed with a modified version of Interior Ballistic Computer Program No. 1103, Reference 3. The program calculates propellant burning peripheries based on initial grain geometry and chamber dimensions. Then a step-wise calculation of pressure, burning rates, mass addition, gas velocities, and thrust is carried out for the entire motor duration. The program input for the 260-SL-2 motor prediction included the demonstrated propellant ballistic properties, measured propellant weight, calculated grain temperature, predicted nozzle throat ablation rates, and empirical adjustments based on motor 260-SL-1 performance.

VI, D, Ballistic Performance Analysis (cont.)

A mass flow coefficient of 0.00629 sec^{-1} was used, representing a propellant specific impulse of $244.5 \text{ lbf-sec/lbm}$ at standard conditions.* The propellant specific impulse was accurately characterized in 10KS-2500 size motor firings and was substantiated by the 44-SS motor firings.

Nozzle throat area change was based on the surface recession rates determined for motor 260-SL-1.

No correction was made for changes in grain geometry due to thermal shrinkage or imperfections in the propellant, since the effects were considered to be negligible. The calculation of performance was based on the as-cast configuration, using the liquid density of the propellant at the initial cure temperature, which was approximately 140°F . A final empirical correction in density was made to adjust for the measured propellant weight, which was computed from pre- and postcast chamber weights.

An allowance for the temperature gradient in the grain was made by adjusting the burning rate as a function of burning time. The grain temperature gradient, shown in Figure 58, was calculated from the grain environmental temperatures during cure, cooldown, and final assembly. Because of low ambient air temperatures during final assembly of motor 260-SL-2, the calculated average grain temperature was about 8°F lower than that of motor 260-SL-1.

The predicted propellant burning rate for motor 260-SL-2 was based on 3KS-500 size batch-test motor burning rates, which had an average propellant burning rate of 0.434 in./sec at 600 psia. A 6% scale-up factor, as occurred in the 260-SL-1 motor firing, was applied to the batch-test motor rate, resulting in a predicted basic propellant burning rate for motor 260-SL-2 of 0.460 in./sec at 600 psia. As in the 260-SL-1 motor performance prediction, the burning rate was

*1000 psia chamber pressure exhausting to an ambient pressure of 14.7 psia through a 15-degree half-angle nozzle of optimum expansion ratio.

VI, D, Ballistic Performance Analysis (cont.)

adjusted radially, based on an empirical correlation developed from the ballistic performance of the 44-SS and 120-SS-1 motors. However, the adjustment used in the 260-SL-2 prediction was revised on the basis of the actual 260-SL-1 motor performance. The revised burning rate correction-vs-percent of web action time characteristic is shown in Figure 59. In addition, an axial burning rate adjustment, shown in Figure 60, was applied to simulate the effect of batch-to-batch burning rate variation on the shape of the curve during tailoff.

3. Actual Performance

The pressure-vs-time performance of motor 260-SL-2 closely matches the predicted curve, as shown in Figure 57. The small difference between actual and predicted pressure early in the firing is probably due to a lower-than-expected grain surface temperature. The motor 260-SL-2 pressure-vs-time performance is compared with that of motor 260-SL-1 in Figure 61, demonstrating the excellent reproducibility of the ballistic characteristics of the 260-SL motors. There was no evidence of any pressure perturbations in the 260-SL-2 motor firing, indicating that the modified casting technique used on 260-SL-2 was successful in eliminating pressure peaks of the type that occurred just prior to tailoff in motor 260-SL-1.

E. COMPONENT EVALUATION

1. Chamber and Nozzle Shell

Visual inspections of the chamber and nozzle shell motor components did not show any evidence of excessive heating or paint discoloration during firing or the extended postfiring heat-soak period. Specimen heating tests were conducted

VI, E, Component Evaluation (cont.)

following the 260-SL-1 motor firing to determine the correlation between paint discoloration and temperature. These test results showed that initial paint discoloration occurred at temperatures ranging from 200 to 320°F.

Strain levels measured on the chamber and nozzle shell during firing were low and well within expected values. Strain plots were linear, except for the two locations on the forward head as discussed in section VI,B,5.

2. Chamber Insulation

a. Forward Head Insulation

As discussed in section VI,F, the initial attempts to insert the quench boom were unsuccessful. As a result, posttest burning continued for approximately 10 to 15 min before CO₂ quenching was accomplished. The entire forward head was filled with char debris, and several pieces of smoldering char were discovered as late as 36 hr after the test. Although there was no paint discoloration on the forward head, the metal was still hot to the touch some 6 hr after quench. The motor was washed down and the debris was cleaned out of the forward head. A map of the posttest forward-head insulation condition is shown in Figure 62.

From the 180-in. dia to the forward boss, the insulation was completely charred (Figure 63) and the epoxy had been degraded to the extent that the rubber was no longer bonded to the chamber (Figure 64). The seams were cracked longitudinally between the V-61 and V-44 rubber; the metal primer under the V-61 seams was brown and hard, indicating these areas had been heat-affected. The rubber insulation aft of the 180 in. dia was heavily charred (approximately 0.5-in.-deep), but showed no evidence of excessive erosion or unbondedness.

VI, E, Component Evaluation (cont.)

The rubber insulation forward of the 180 in. dia obviously was subjected to an extremely long heat-soak time. This area was covered by the hot char debris, which acted like an insulator and retained the heat; this area was most likely subjected to temperatures between 300 and 400°F, which was sufficient to degrade the epoxy bond and allow the material to deform. The condition of the rubber and epoxy was indicative of a long heat-soak period at temperatures approaching 300°F. The rubber aft of 180 in. dia exhibited normal erosion, with the thicker char layer resulting from the extended afterburn.

As a result of the long afterburn and heat-soak time, meaningful thickness loss measurements were not possible. However, the thickness of the rubber around the forward boss that was pulled loose ranged from 0.8 to 1.0 in. These values were close to the rubber thicknesses measured after the 260-SL-1 motor test (0.98 to 1.24). Measurements taken at the 228 in. dia indicated a rubber thickness of 1.43 in., as compared to thicknesses from 1.38 to 1.51 in. for 260-SL-1 motor forward insulation at the same diameter. Apparently, the rubber thickness loss rate in motor 260-SL-2 was equivalent to that experienced in motor 260-SL-1.

b. Chamber Cylindrical-Section Insulation

The postfired condition of the cylindrical-section insulation was very similar to the condition of the cylindrical-section insulation after the 260-SL-1 motor test. The main difference was the additional 0.100-in.-thick ply of rubber in 260-SL-2, which was adequate in protecting the motor case from heat during the long afterburn.

The top or third ply was completely eroded away, except in the three longitudinal bands that had been protected by propellant sliver. The second ply in the areas of initial web burnout was completely charred and blistered.

VI, E, Component Evaluation (cont.)

Some of the blistered portions had been burned away, exposing the epoxy bond between the second and first ply. Only in a few isolated places was the first ply exposed, and these areas showed the tan discoloration of heat-affected V-44 rubber. The rubber under the propellant sliver was partially charred only in the third ply; in some areas, charred SD-850-2 liner was still evident.

c. Aft-Head Insulation

The aft-head insulation posttest measurements are shown in Figure 65. The FMC-200 potting compound between the aft boot and insulation was not totally burned away and was effective in protecting the insulation from approximately 6 to 8 in. forward of the nozzle step-joint to the boot bond areas, as shown in Figure 66. The maximum rubber erosion occurred in the 190-degree area. Again, meaningful rubber thickness loss rate data was affected by the potting material. However, the observed maximum rubber thickness loss in motor 260-SL-2 was similar to the thickness loss in 260-SL-1. As shown in Figure 67, the expected material thickness loss for 260-SL-2 aft insulation was 1.28 in.*, based on the measured maximum thickness loss in 260-SL-1. The maximum measured thickness loss in 260-SL-2 was 1.4 in.* (Figure 67).

d. Insulation Seams

The thickness loss of the V-61 seam material was equivalent to the material thickness loss in the adjacent V-44 rubber (Figure 68). As observed after the 260-SL-1 test, the char depth in the V-61 was approximately 0.10 in. deeper than the V-44 char depth. A very thin layer of heat-affected material was located below the char layer in the V-61. The char depth and heat-affected V-61 material again was caused by the long heat-soak period, and was not due to excessive erosion.

*Measured as the distance at the step-joint face from the edge of the initial design thickness to the edge of the posttest thickness on a line perpendicular to the motor case flange.

VI, E, Component Evaluation (cont.)

e. Firing Cap Insulation

A posttest photograph of the firing cap insulation is shown in Figure 69. There was no evidence of gas penetration into the step-joint and the pressure tap holes through the insulation were clear. The exposed face of the cap insulation was eroded flush with the forward insulation disk.

3. Nozzle and Exit Cone

Posttest erosion profiles of the nozzle assembly were taken at 60-degree intervals starting at the 0-degree radial location. The loose char on the V-44 insulation surface was removed prior to profile measurement.

A summary of erosion depths obtained from profile measurements is tabulated in Figure 70. The average erosion profile of the nozzle assembly is shown in Figure 71. The average nozzle throat erosion is 0.624 in. and agrees with the average of six posttest throat diameter measurements taken. Figure 72 compares nozzle insert erosion of motors 260-SL-1 and -2.

The nozzle erosion profile showed a step at the downstream 1.32 area ratio and reflected contraction of the aft 16 in. of the throat extension insert. Further visual inspection of the end of the throat extension insert indicated gaps up to 0.12 in. at the bond line between the plastic insert and steel shell and within the overwrap material. The unbonding and subsequent contraction during cool-down of this portion of the throat extension insert are apparently due to the bond strength being exceeded by thermal expansion stresses and are the result of additional heating of the nozzle inserts from the quench system malfunction after motor burnout. Contraction of the insert renders the erosion values unrealistic and inaccurate within this area; however, the average erosion appeared to be less than that for the 260-SL-1 nozzle.

VI, E, Component Evaluation (cont.)

The exit-cone erosion data were unobtainable as a result of excessive heating caused by the quench system malfunction. Visual inspection showed separation of bonds between the liner and honeycomb facings and within the honeycomb sandwich structure. Dimensional inspection indicated apparent contraction of the plastic liner after excessive heating and subsequent cool-down. The appearance of the surface is similar to that of the 260-SL-1 exit cone, and the erosion depths are not anticipated to have exceeded the 260-SL-1 values.

a. Nozzle Insulation

The performance of the V-44 nozzle rubber insulation was within design limits and was comparable to the nozzle insulation performance in motors 120-SS-1 and 260-SL-1. The 260-SL-2 nozzle insulation maximum surface recession profile is shown in Figure 73; the initial surface contour for both the 260-SL-1 and -2 nozzle insulation, and the maximum surface recession profile for 260-SL-1 nozzle insulation are included in Figure 73 for comparison.

As shown in Figure 74, the erosion contour at the downstream edge of the nozzle insulation, spanning the -2.04:1 area ratio station, was considerably smoother than the 260-SL-1 posttest contour. Apparently, the effort expended to control the nozzle insulation shrinkage in the mandrel during and after cure produced a closer fit with the nozzle plastic components. As a result, a thinner bond line was formed between the rubber and plastic at the blend area, and the irregular erosion experienced in 260-SL-1 from degradation of the rubber-to-plastic bond was averted.

b. Entrance Insert

The erosion characteristics of the entrance insert is similar to that of the 260-SL-1 nozzle. Maximum surface erosion occurred in the silica cloth and phenolic portion of the insert, which was initially fully

VI, E, Component Evaluation (cont.)

covered by V-44 insulation. There is no evidence that variability in erosion of the plastic resulted from any cause other than variation in protection afforded by the V-44 insulation.

The carbon cloth and phenolic portion of the insert, which interfaced with the silica at the -2.0:1 area ratio station, was more uniformly eroded, with small variability near the silica interface reflecting the variation in V-44 insulation erosion. The average erosion contour was similar to 260-SL-1 in this portion of the entrance insert. The average measured depth of erosion at the -1.6:1 area ratio station was 0.27 in., as compared to 0.37 in. for motor 260-SL-1. Moving from the -1.60:1 area ratio station toward the throat, measured erosion exceeded 260-SL-1 erosion by a maximum of 30% at the 1.41 area ratio and then progressively decreased. At the -1.06:1 area ratio station, the average measured erosion was 0.81 in., as compared with 0.84 for motor 260-SL-1.

Figure 75 shows the posttest surface condition of the entrance insert adjacent to the V-44 insulation. No delaminations were observed in the surface of the silica cloth; numerous short circumferential delaminations existed in the surface of the carbon cloth.

c. Throat Insert

The nozzle throat insert was eroded uniformly around its circumference except for a local deep erosion at the 140-degree location. The local erosion shown in Figure 76 is 0.20 in. deeper than the adjacent surface and is an extension of the irregular V-44 insulation erosion pattern into the nozzle throat. At the throat station, the erosion depth obtained in contour measurements was 0.56 to 0.71 in., with an average of 0.61 in., as compared to 0.70 in. for motor 260-SL-1. Average erosion at the throat obtained from the differences between pretest and posttest diameter measurements taken at six angular locations was 0.624 in. The action time throat recession rate is 4.8 mils/sec. The total erosion was greatest at the entrance end of the insert (-1.06:1 area ratio station) and decreased progressively over the length of the insert.

VI, E, Component Evaluation (cont.)

The physical appearance of the surface of the throat is shown in Figure 77. Numerous circumferential delaminations were apparent. The area downstream from the throat showed surface roughness similar in appearance to that observed at this location in the 260-SL-1 nozzle throat insert.

d. Throat Extension Insert

The measured depth of erosion of the throat extension insert was less than the 260-SL-1 erosion over the entire length of the insert. At the upstream end of the insert (1.10:1 area ratio station), the average measured erosion was 0.28 in. as compared to 0.42 in. for 260-SL-1; near the downstream end (1.9:1 area ratio station), the average measured erosion was 0.15-in. as compared to 0.22 for the 260-SL-1 nozzle.

The surface appearance of the throat extension insert is shown in Figure 78. Numerous surface pits were observed, and erosion was uniform. Short circumferential delaminations were apparent with two long circumferential delaminations near the aft end of the insert. These two delaminations are shown in Figure 78. By insertion of steel scales, it was determined that the depth of these delaminations extend approximately to the overwrap material interface.

e. Exit Cone

The ablation surface of the carbon cloth and phenolic portion of the exit cone was smooth, with long circumferential delaminations as shown in Figure 79. Numerous radial cracks were also observed. These delaminations and cracks were similar in appearance to those observed in the exit cone of the motor 260-SL-1, except that more radial cracks were apparent. The interface layer between carbon cloth and silica cloth was delaminated and inspection indicated that the delamination extended to the overwrap material interface.

VI, E, Component Evaluation (cont.)

The ablation surface of the silica cloth and phenolic is also shown in Figure 80. An oxide deposit similar to that observed on the 260-SL-1 exit cone covered the entire surface of the silica cloth. Previous analysis of samples of this deposit by emission spectrograph and X-ray diffraction showed the oxide to be basically mullite ($3\text{Al}_2\text{O}_3 \cdot 2\text{SiO}_2$) with additional silicon present as SiO_2 . This oxide was apparently produced as a melt of SiO_2 from the silica cloth of the liner and Al_2O_3 from the aluminum of the propellant.

Circumferential delaminations were observed over the entire surface of the silica-cloth portion of the liner. Longitudinal depressions were also observed, being most pronounced at the upstream end of the silica-cloth section. The pattern of these depressions correlates with locations of steel strips used to retain the nylon tension wrap during liner cure and appear to result from small fiber reorientation occurring between each of the first layer of these strips.

The V-61 potting compound applied to the exit-cone aft flange afforded adequate thermal protection. The external surface of the exit cone showed evidence of heating, in that the cork-sheet insulation placed over the outer skin of the honeycomb structure was charred or blackened over approximately three-quarters of its circumference (Figure 81) and extended 2 ft further below the exit plane than observed on motor 260-SL-1. Unbonding of the edge of the outer doublers and two repair panels was observed. Inspection by tapping showed that large areas of the bond between the outer facings and honeycomb core were separated. Although no discoloration of the honeycomb external surface was observed, overheating and subsequent degradation of the bond line was evident.

F. SPECIAL TEST EQUIPMENT PERFORMANCE

1. Ignition Motor Retention-and-Release System

Operation of all retention-and-release mechanical and electrical systems was normal. The retention cables accomplished the primary design function,

VI, F, Special Test Equipment Performance (cont.)

imparting sufficient horizontal eastward impulse to the ignition motor and support fixture assembly to assure a trajectory and impact in an area well clear of the motor and nearby plant facilities. Analysis of motion picture coverage, ignition motor trajectory, and breakwire data indicate that cable breakage occurred before the cables were pulled taut, and, as was concluded for the 260-SL-1 motor test, breakage was caused by cable accelerations in excess of 200 g.

Tower breakwire data recorded during the test were used to determine the velocity and acceleration of the ignition motor and support fixture assembly. The distance-vs-time data is shown in Figure 82, and the expression, $x = ct^n$, was used to relate vertical distance traveled as an exponential function of time. A plot of terminal velocity at 100 ft is shown in Figure 83. Included in Figure 83 is a summary of distance, time, velocity, and acceleration of the ignition motor and support fixture assembly in both motor tests. This summary shows that there was no significant decrease in measured vehicle velocity gained by streamlining the flat impingement surface of the ignition motor and support fixture assembly.

Tower retraction was normal and the assembly was not damaged by exhaust gas impingement. First movement of the tower retraction linkage was recorded at 0.57 sec; 1.43 sec later the tower was retracted 5 degrees and was free of the exhaust plume. The tower was fully retarded at 4.8 sec. Figure 84 shows tower position vs time during the retraction and retarding cycle. The posttest condition of the igniter track assembly is shown in Figure 85.

2. Quench System

Quench-boom insertion was initiated 176 sec after fire switch. The measured chamber pressure at this time was approximately 7 psig, and the resultant aerodynamic drag and thermal lifting force was sufficient to prevent completion of the insertion cycle and subsequent CO₂ quench-media discharge at the desired time.

VI, F, Special Test Equipment Performance (cont.)

The hydraulic drive unit continued unsuccessfully in its efforts to drive the boom into the locked position until $T+245$ sec, at which time the boom end began to burn away and the unit was violently retracted by actuation of the CO_2 quench valve. Damage to the boom structure by this action prevented subsequent re-insertion attempts. After the boom was positioned with the aid of a mobile crane, CO_2 was discharged into the motor at approximately 12 min after the firing.

G. ENVIRONMENTAL EFFECTS ON FACILITIES AND STE

A limited amount of data was recorded to define the dynamic and thermal environment existing in the immediate vicinity of the motor.

Measurements made on the 260-SL-1 static test demonstrated that the temperature, vibration, and sound levels in the area of concern are well within the limits that test systems and the facility can tolerate. Data taken at similar locations on the 260-SL-2 static test confirm this conclusion.

1. Temperature

Thermocouples and temperature-sensitive paint were used to measure the thermal effects upon various hardware components adjacent to the motor. The location of thermocouples is presented in Figure 41. An increase of $30^\circ F$ was recorded on the quench system components until boom insertion, at which time data was lost from the thermocouple near the boom tip. The igniter track reached a temperature of $153^\circ F$ (T-T-270-15) at the end of the recording period. Temperatures around the edge of the caisson peaked out at 130 to $190^\circ F$ at $T + 175$ sec.

Temperature-sensitive paint was applied to boards set at four locations around the motor as shown in Figure 86. Each board was painted with 20 paint strips, ranging from 119 to $600^\circ F$, in approximately 25-degree increments. The maximum temperature indicated at each station is also shown in Figure 86.

VI, G, Environmental Effects on Facilities and STE (cont.)

2. Vibration

Valid acceleration data was recorded on magnetic tape at the thrust takeout ring (G_T -TTR-y), the igniter track (G_T -2), and on a relay in the instrumentation terminal room (G_{TR} -1, G_{TR} -2). Vibration measurement from the igniter motor was lost at 0.120 sec due to an undetermined failure in the data channel.

The vibration data on the thrust takeout ring indicates no significant response. There is some evidence of the 200 cps oscillation which was observed on motor 260-SL-1; however, the signal response is in the range of the noise level on this channel, and no useful data can be determined. Vibration data measured on the tower is dominated by a high frequency vibration (2-4 Kc) with an amplitude of 200 to 300 g; this type of vibration has no particular significance. The vibration decreases to a very low level after the tower is retracted out of the jet boundary. Vibration response of the relays is very low. Peak amplitudes of 6 to 7 g at 70 cps were recorded for a short period after motor ignition. The peak amplitude appears to occur during the ignition motor sled travel. Steady-state vibrations are less than 1 g and are down in the noise level of the two channels. These data will be used to determine the advisability of providing a shock mounting system for the relay junction box in the terminal room.

Acceleration data indicates, and visual examination confirms, that the test hardware suffered no adverse effects during the test, and that no abnormal dynamic events occurred.

LIST OF REFERENCES

1. Static Test Firing of Motor 260-SL-1, Aerojet-General Corp., Report No. NAS3-6284 FT-5, 25 October 1965.
2. 260-SL Motor Aft-End Ignition System Development, Aerojet-General Corp., Report No. NASA CR 54454, Final Phase Report, Volume I, 20 August 1965.
3. The Integrated Design Computer Program and the ACP-1103 Interior Ballistics Program, Aerojet-General Corp., Report No. STM-180, 1 December 1964.

Report NASA CR-54982

CONFIDENTIAL

This document contains information which may affect national defense or other matters relating to the internal security of the United States.

(S) This document contains information which may affect national defense or other matters relating to the internal security of the United States.

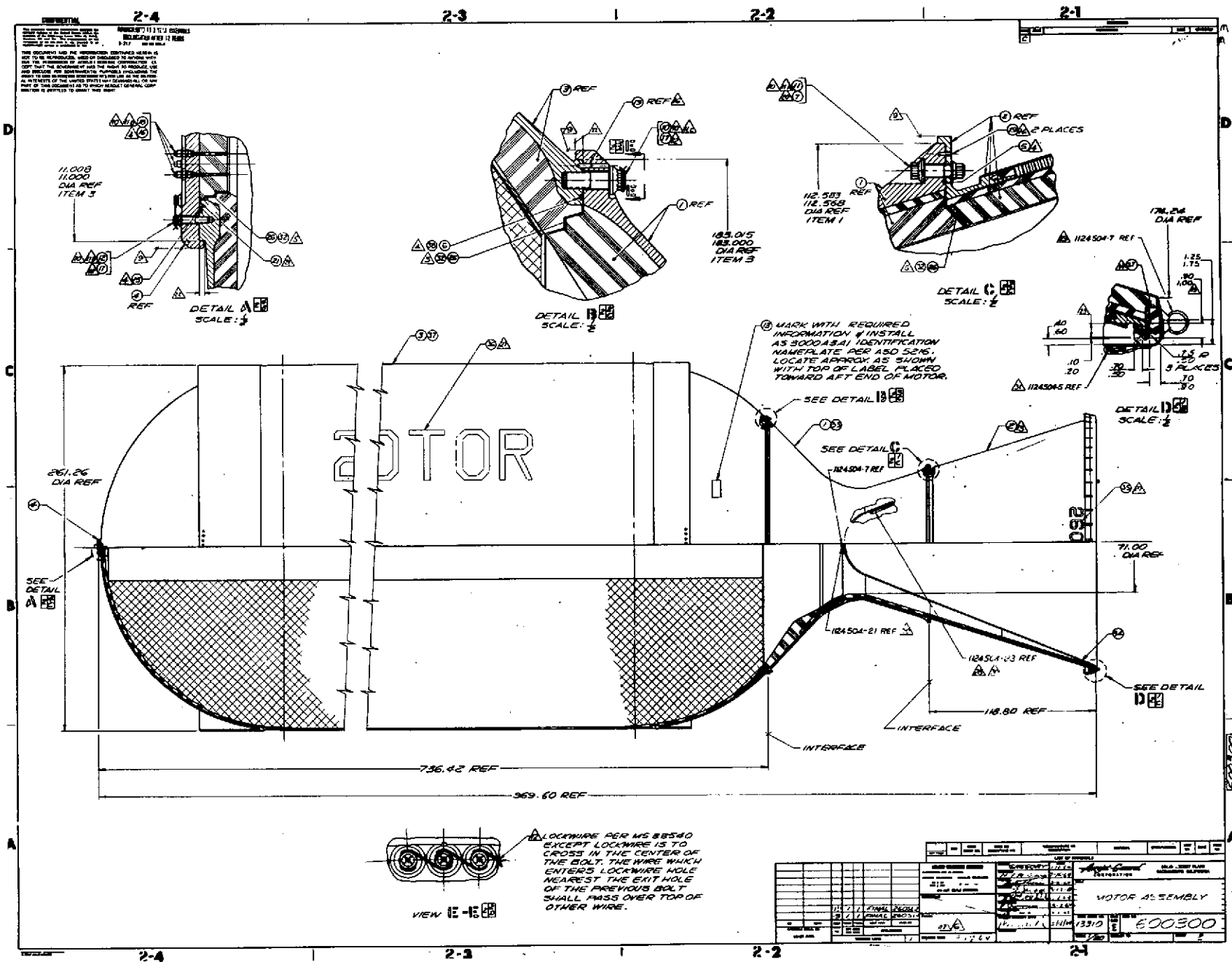
REPRODUCTION OF THIS DOCUMENT IS PROHIBITED WITHOUT THE WRITTEN PERMISSION OF THE AUTHORITY ISSUING IT.

EXCLUDED FROM AUTOMATIC DOWNGRADING AND DECLASSIFICATION SCHEDULE

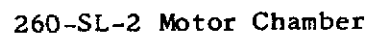
DATE 12-15-98 BY SP-10 JTB/KJS

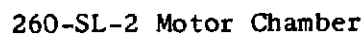
NOTES:

- INTERPRET DRAWING PER STANDARDS PRESCRIBED IN MIL-D-70927.
- REMOVED.
- REMOVED.
- LUBRICATE WITH LUBRICATING GREASE PER MIL-L-4343.
- FILL GAP WITH NJEC MATERIAL PER APPROVED AGC PROCESS.
- TOUGH UP ANY EXPOSED EXTERIOR METALLIC SURFACES PER AGO-38072 USING PRIMER PER MIL-P-8585 COLOR "I". PRIOR TO NOTES B AND C.
- LEAK TEST ITEM 3 AND ITEM 1 ASSEMBLED, USING A FULL END COVER AT ITEM 1 AFF FLANGE, IN ACCORDANCE WITH AGO-38428. NO LEAK TEST COMPOUND PERMITTED ON EXPOSED END OF NOZZLE THROAT EXTENSION INSERT.
- HOLDING FIXTURE SHALL NOT BE REMOVED FROM ITEM 1 UNTIL IT IS ASSEMBLED TO ITEM 2.
- FLAMELESS, EVEN HEATING UP TO 180°F PERMITTED ON NOTED SURFACES TO FACILITATE ASSEMBLY.
- LUBRICATE THREADS AND UNDER BOLT HEADS WITH ANTI-BEIZE COMPOUND PER MIL-T-325A.
- TORQUE PER AGO-5226 10:
A. 250 LBS FT-LB.
B. 90 LBS FT-LB.
C. 800 LBS FT-LB.
D. 100 LBS FT-LB.
- LOCKWIRE PER M533540 EXCEPT AS SHOWN IN VIEW E-E.
- AFTER LEAK TEST INSTALL ITEM 2 AND RELATED ATTACHING PARTS.
- APPLY INSULATION AGO-34235 PER PROCESS APPROVED BY AGC.
- METHOD OF PRESERVATION PER MIL-P-116, METHOD 11.
- INSERT DOREL PINS IN ITEM 1 PRIOR TO ASSEMBLY OF ITEM 1 TO 3, AND 2 TO 1, TO INSURE PROPER ORIENTATION OF COMPONENTS.
- FOLLOWING NOTE:
A. ALLOW AN ADDITIONAL 2 HOURS CURING TIME AT AMBIENT CONDITIONS
B. CLEAN ALL EXTERIOR SURFACES OF 600280-S AND 600280-1P WITH TOLUENE PER FEDERAL SPEC 15-1-148
C. APPLY AVIATION WHITE LAQUER PER MIL-L-7518 COLOR NO. 17875 TO A THICKNESS OF 1.0 - 2.0 MILS. THE DRYING INTERVAL SHALL BE 45 MINUTES BETWEEN COATS. AIR DRY FINAL COAT AT ROOM TEMPERATURE FOR 18 HOURS.
- ASSEMBLY PROCEDURES SHALL HAVE PRIOR ENGINEERING APPROVAL.
VENDOR ITEM SEE SPECIFICATION CONTROL DRAWING FOR PROCEDURE.
- ENVIRONMENTAL LIMITS:
A. PROPPELLANT SURFACE ENVIRONMENTAL LIMITS/EQUILIBRIUM STORAGE CONDITIONS:
1. RELATIVE HUMIDITY - 30% MAXIMUM
2. TEMPERATURE - 80°F ± 20° F
3. DURING PERIODS WHEN PROPPELLANT SURFACE IS EXPOSED, THE MOTOR SHALL BE PURGED WITH AIR OR NITROGEN HAVING A RELATIVE HUMIDITY AND TEMPERATURE WITHIN THE LIMITS OBTAINED IN (1) AND (2) ABOVE.
4. PURGING MAY BE INTERRUPTED FOR 0.5 HOUR PERIODS DURING INTERIMATIONS; THE MOTOR SHALL BE PROTECTED AGAINST MOISTURE.
B. CHAMBER EXTERNAL ENVIRONMENTAL LIMITS:
1. TEMPERATURE - 80°F ± 20° F
- BOND GASKET IN PLACE WITH MIL-A-1154 ADHESIVE AT FOUR (4) EQUALLY SPACED PLACES.
- MIL-L-2539P LUBRICANT MAY BE APPLIED TO NOTED MATING SURFACES TO A DRY FILM THICKNESS OF 0.0002 TO 0.0003 INCHES. APPLY IN ACCORDANCE WITH MANUFACTURER'S INSTRUCTIONS.
- AGO-34335 INSULATION MAY BE RELEASED FROM STEEL SURFACE AND BOLT WITHIN NOTED AREA.
- REMOVED
- REMOVED
- REMOVED
- IDENTIFICATION AND MARKING ON 200-SL MOTOR IS APPLIED IN ACCORDANCE WITH AGO DRAWINGS 1124046 AND 1124508, RESPECTIVELY.
- THE WEATHER COVER ASSEMBLY ROPE 1124504-23 SHALL BE LOCATED AT ZERO DEGREE POSITION WITH RESPECT TO THE MOTOR.
- RINGS 1124504-7 SHALL BE USED DURING LIFTING AND HANDLING OF 1124504-8 COVER
- ROPES 1124504-21 AND 1124504-22 SHALL BE BROUGHT OVER THE EXIT PLANE AND TAIED TO THE INTERNAL SURFACE OF THE EXIT CONE.
- AFTER INSTALLATION, THE SNAP ASSEMBLY 1124504-5 SHALL BE GRAB SHOULD AGAINST THE FORWARD FACE OF THE EXIT PLANE FLANGE.



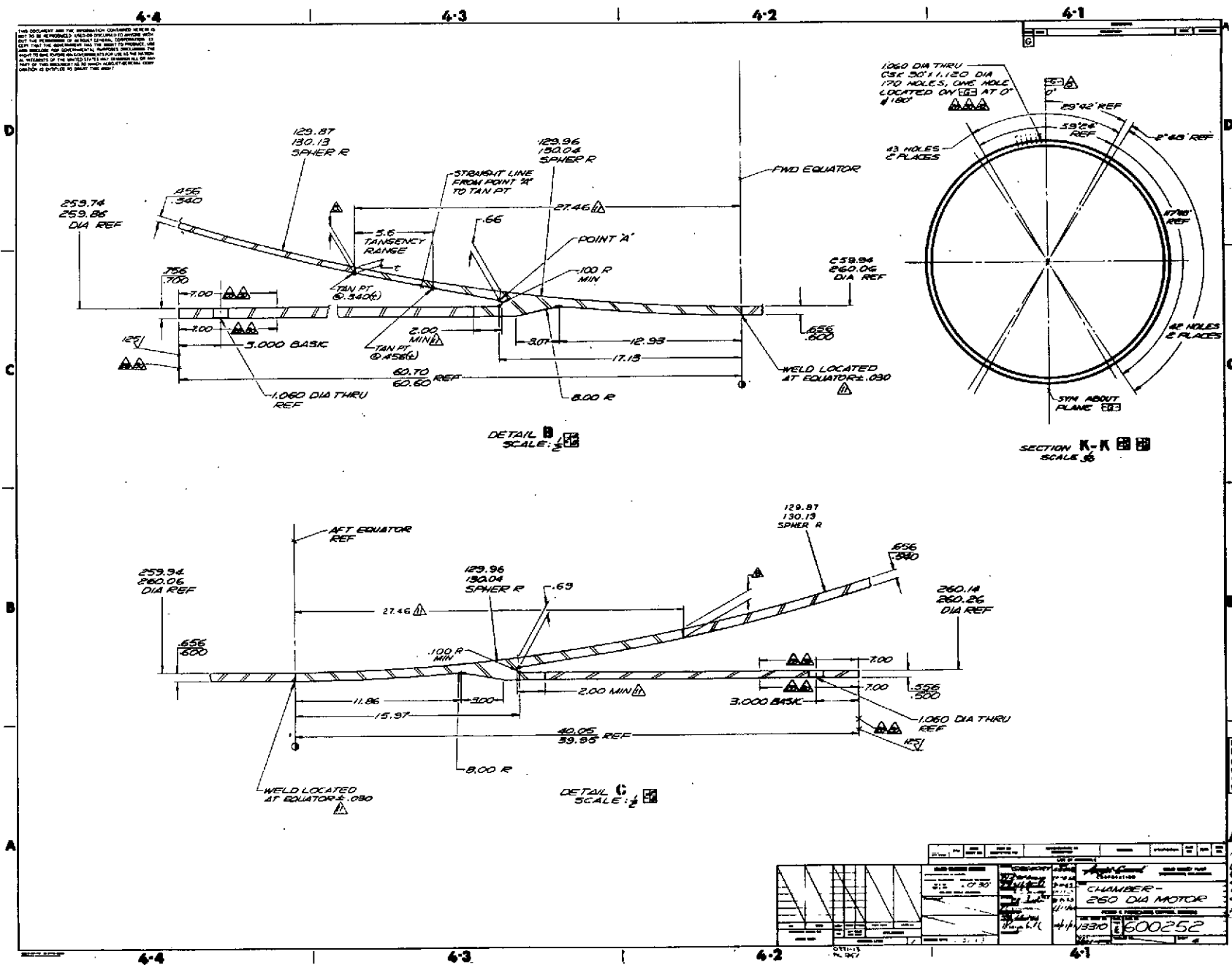
260-SL-2 Motor Assembly (u)





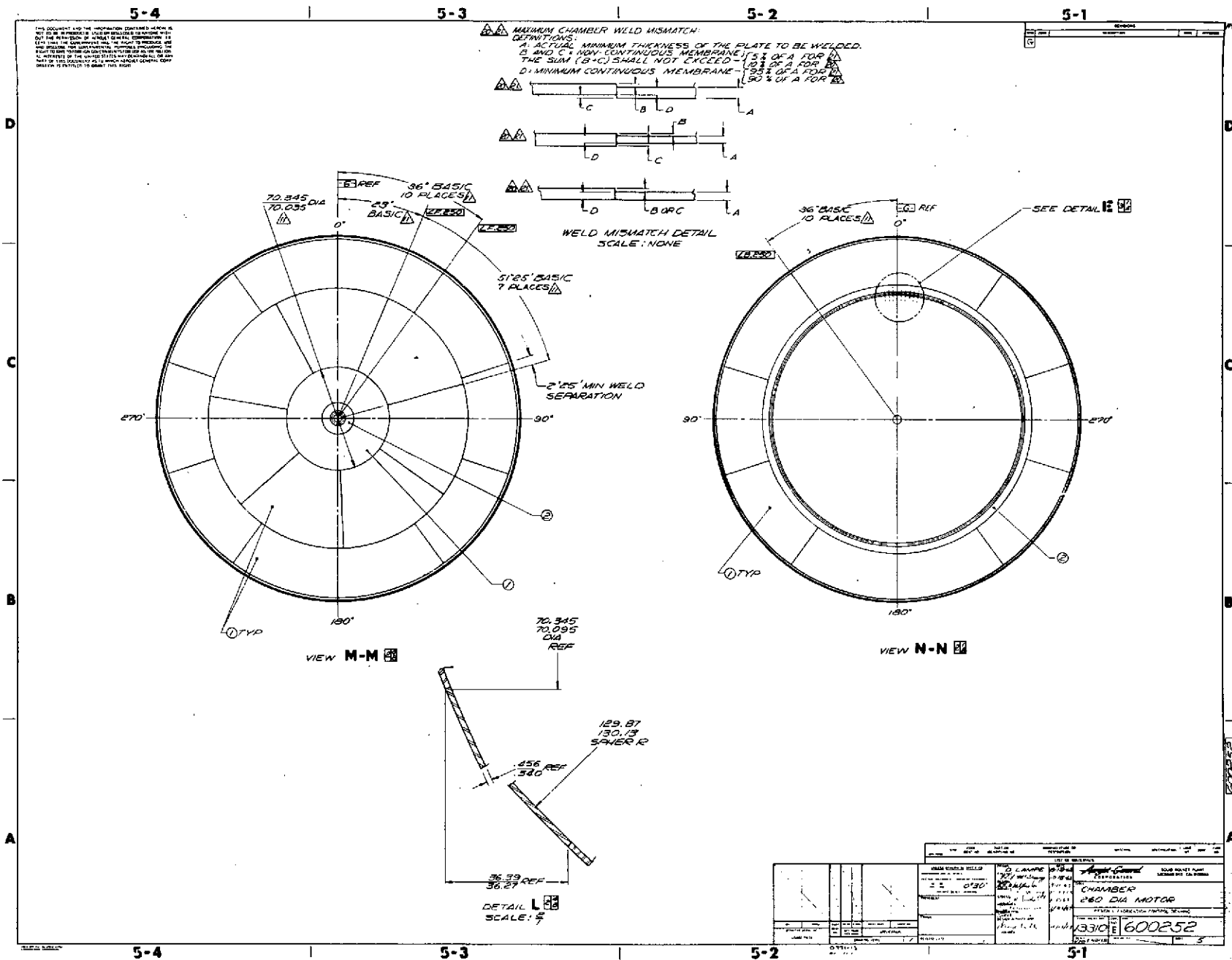
72

Figure 2, Sheet 4 of 5

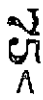


260-SL-2 Motor Chamber

Figure 2, Sheet 5 of 5



<u>Pretest Component</u>	<u>Actual Weight, lb</u>	
Chamber	122,085	
Forward Cap Assembly	42	
Liner	908	
Insulation	<u>18,712</u>	
Insulated Chamber Assembly		141,747
Propellant		1,673,000
Nozzle Shell	12,725	
Nozzle Liner and Insulation	<u>13,401</u>	
Nozzle Assembly		26,126
Exit Cone		9,014
Forward Cap Bolts, Fittings, and O-Rings	2.5	
Nozzle Bolts and O-Ring	362.5	
Exit Cone Bolts, Nuts, and O-Ring	161.5	
Boot Potting Materials (FMC-200)	6487.5	
V-61 Insulation	<u>67.0</u>	
Miscellaneous Assembly Hardware		7,081
Total Pretest Motor Weight		1,856,968
Propellant Mass Fraction		0.901
<u>Posttest Component</u>		
Chamber	140,000 (est.)	
Forward Cap	42	
Nozzle	21,587	
Exit Cone	<u>7,594</u>	
Total Posttest Motor Weight		169,223



260-SL-2 Motor Nozzle

260-SL-2 Motor Nozzle

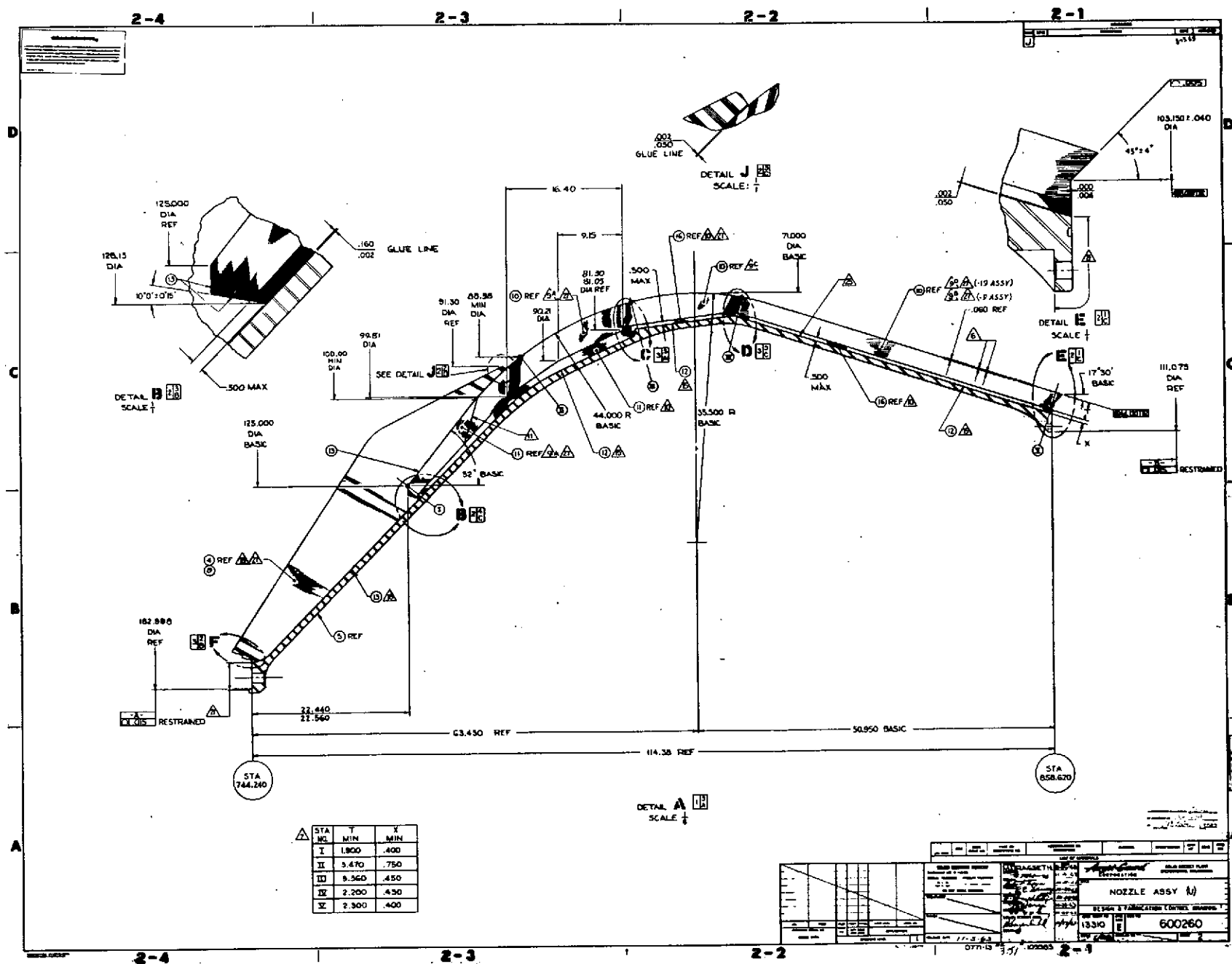
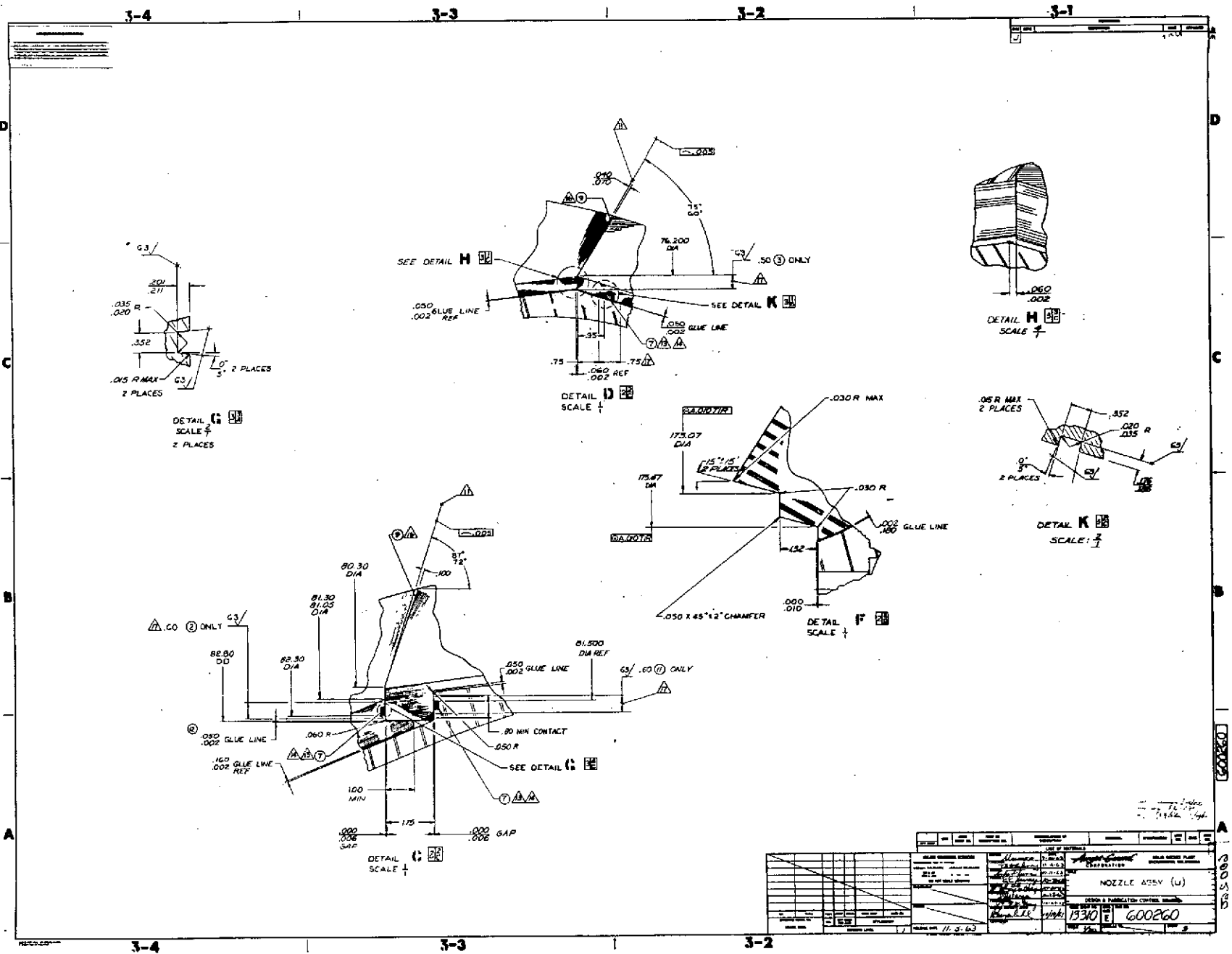


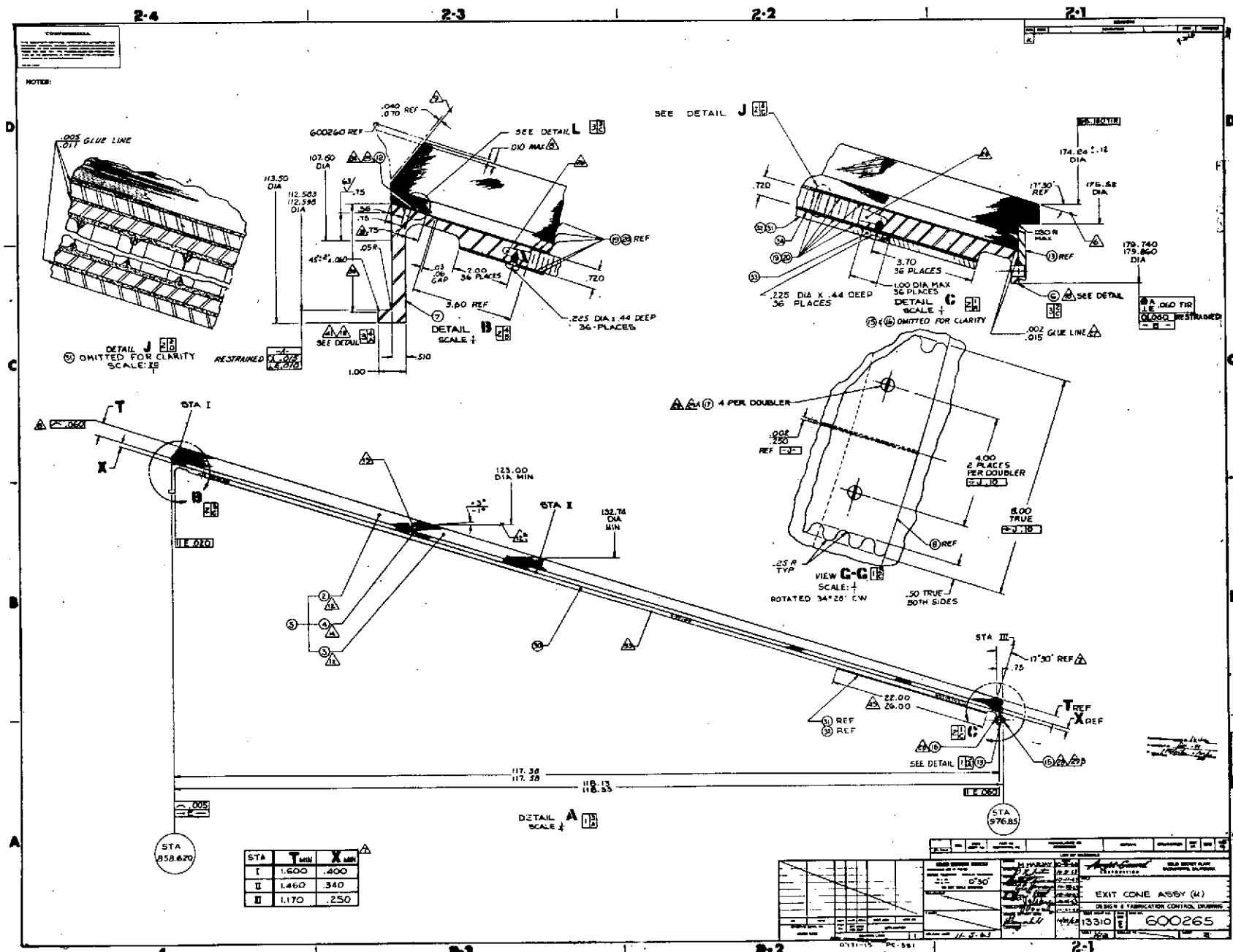
Figure 4, Sheet 3 of 3



260-SL-2 Motor Nozzle

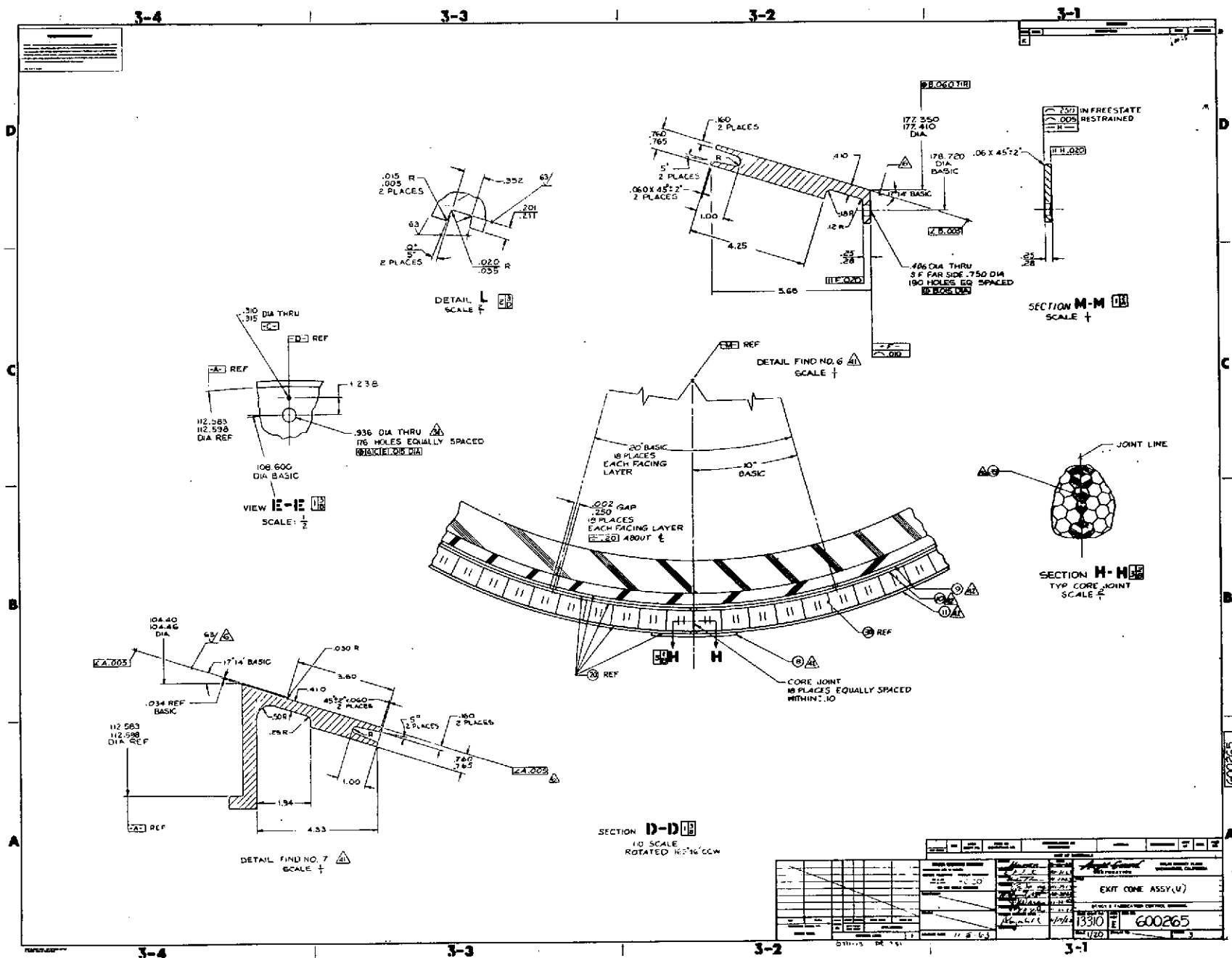
Figure 5, Sheet 2 of 3

79<

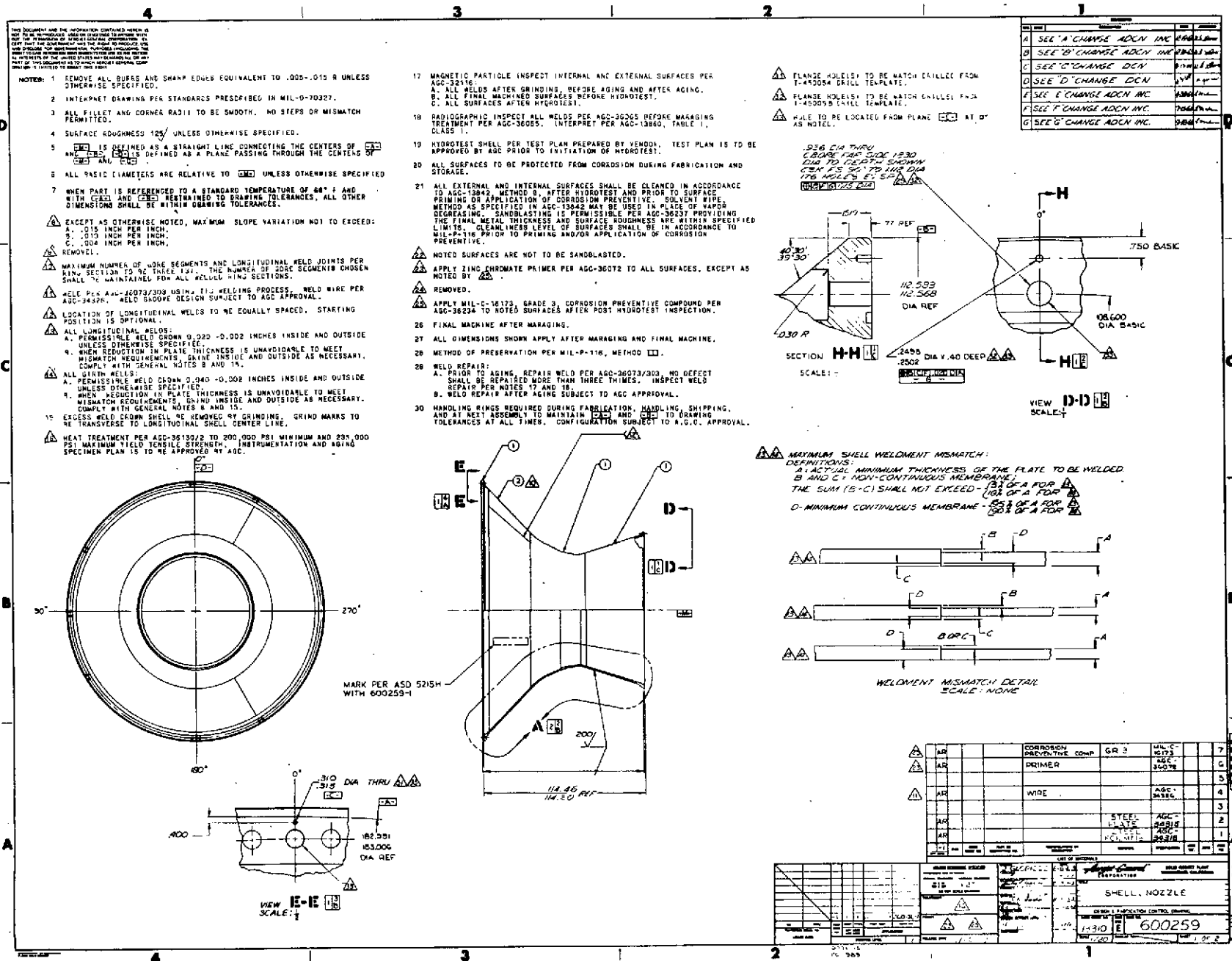


260-SL-2 Motor Exit Cone

Figure 5, Sheet 3 of 3

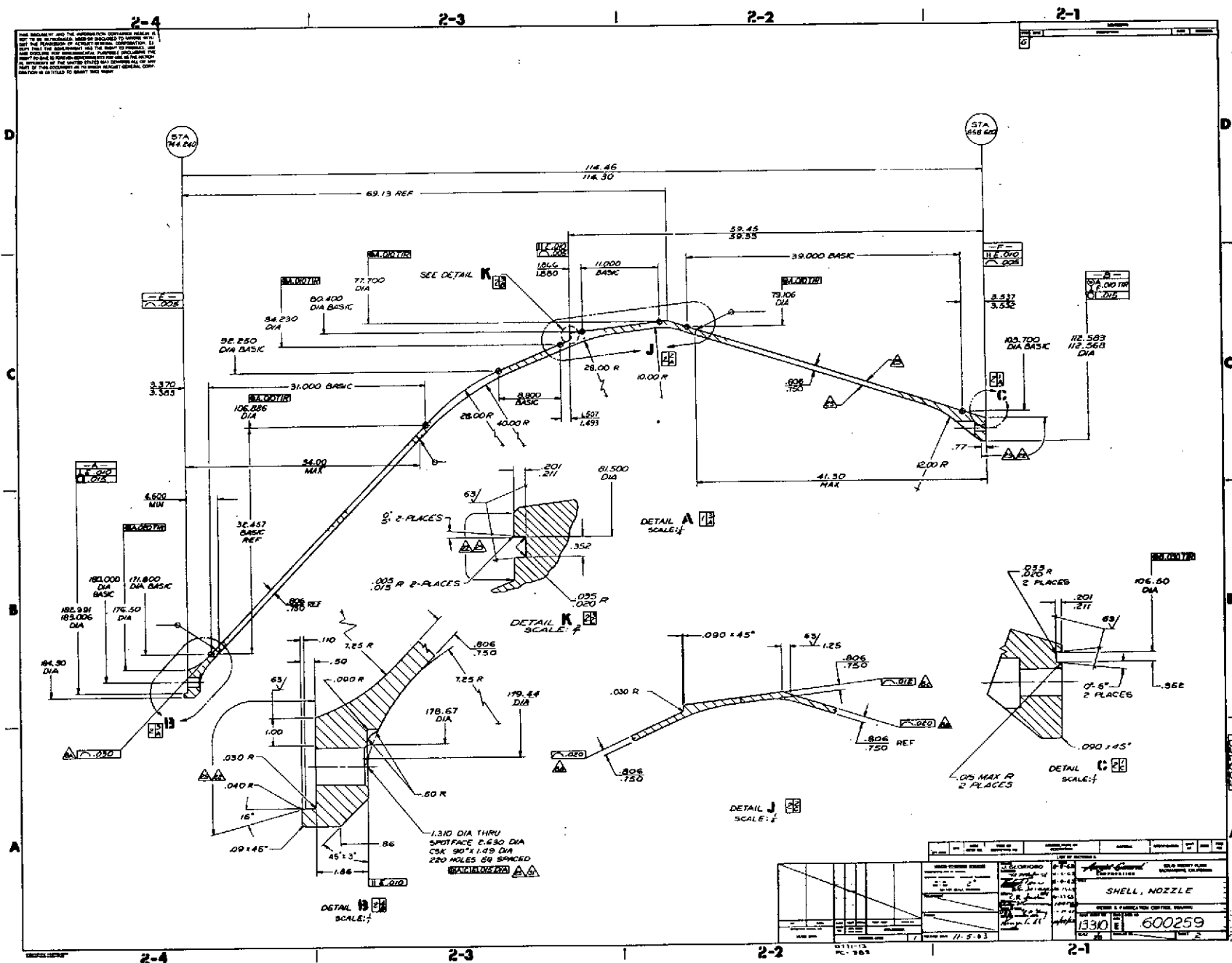


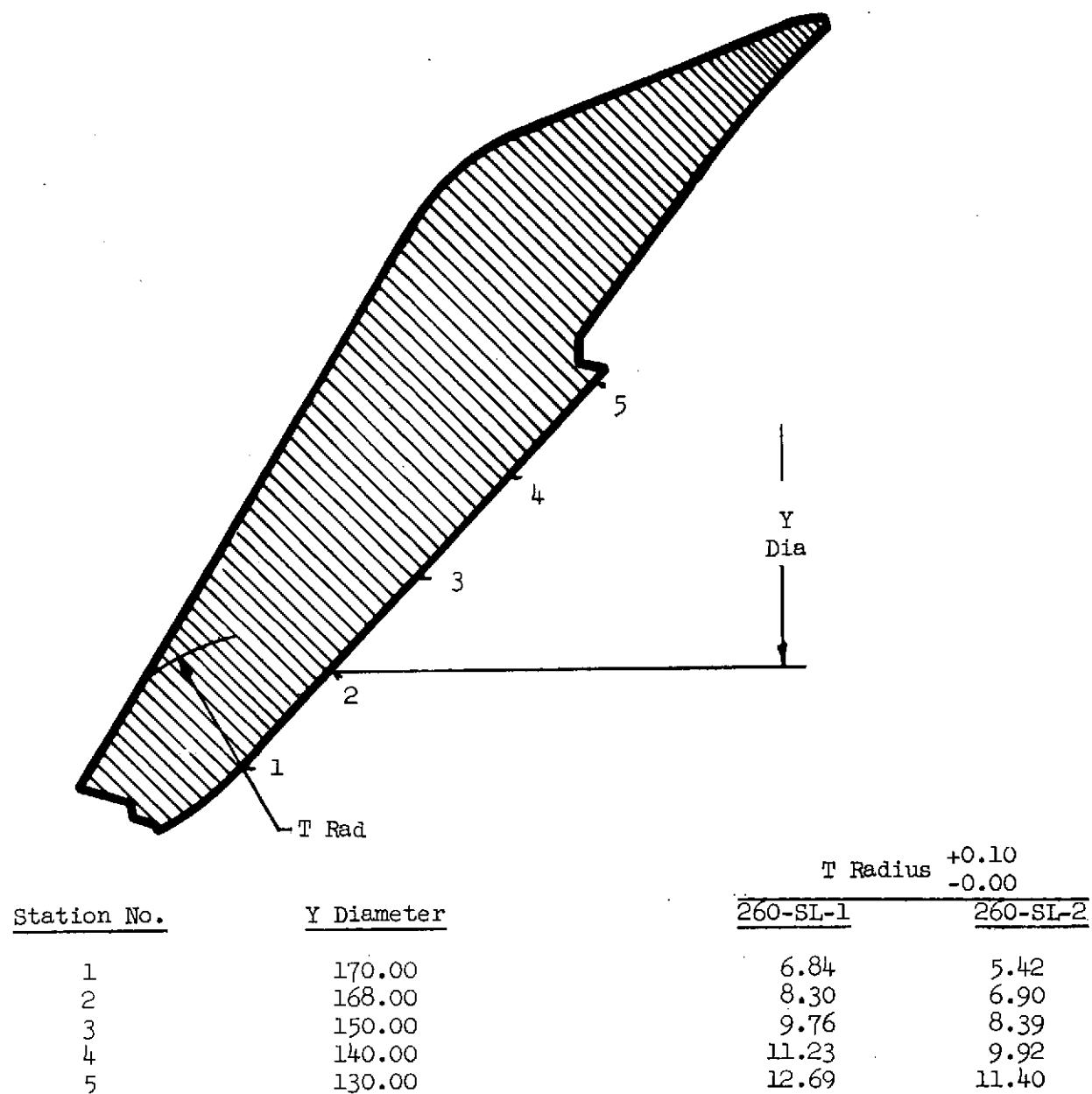
260-SL-2 Motor Exit Cone



260-SL-2 Nozzle Shell

Figure 6, Sheet 2 of 2





Comparison of 260-SL-1 and -2 Nozzle Insulation Thickness

Report NAS3-6284 FT-6

Component Properties after Final Cure from Test Specimens

Test Conducted	Specification Limits	Aft Test Ring		Fwd Test Ring
		Inner Wrap MX-4926	Over Wrap MX-2646	Inner Wrap MX-2646
Specific Gravity per Fed. Test Method Std. 406, Method 5011	1.38 min for MX-4926; 1.75 min. for MX-2646	1.45	1.78	1.80
		1.45	1.80	1.81
		1.45	1.79	1.81
Acetone Extractables per ASTM-D-494-46, %	1% max	0.08	0.07	0.16
		0.11	0.06	0.08
		0.08	0.06	0.05
Interlaminar Shear (208489) per Fed. Test Method Std. 406, psi	1000 psi min	2,980	2,700	--
		2,550	3,100	3,300
		2,810	3,300	3,100
Interlaminar Shear (208489) per Fed. Test Method Std. 406, psi	1000 psi min	Interface Between Inner Wrap and Over Wrap		
		2,100		
		2,400		
		2,600		
Volatile (208491) per TAP-DAP-122, %	3% max	2.71	1.38	1.72
		2.68	1.70	1.67
		2.48	1.51	1.70
Microtensile (208488) per ASTM-D-1708, psi	Report only	17,700	17,600	12,700
		13,400	14,200	19,600
			18,100	17,100
			18,200	

Component Properties of 260-SL-2 Nozzle Entrance Insert

Component Properties after Final Cure from Test Specimens

Test Conducted	Specification Limits	Aft Test Ring		Fwd Test Ring	
		Inner Wrap	Over Wrap	Inner Wrap	Over Wrap
		MX-4926	FM-5131	MX-4926	FM-5131
Specific Gravity per Fed. Test Method Std. 406, Method 5011	1.38 min for MX-4926 1.68 min for FM-5131	1.45 1.45 1.45	1.74 1.74 1.74	1.45 1.44 1.45	1.75 1.75 1.75
Acetone Extractables per ASTM-D-494-46, %	1% max	0.19 0.16 0.16	0.11 0.07 0.11	0.09 0.17 0.11	0.19 0.13 0.12
Interlaminar Shear (208489) per Fed. Test Method Std. 406, Method 1042, psi	1000 psi min	2,500 1,500 5,900	1,600 1,500 1,800	5,020 1,310 5,600	1,410 1,240 1,380
Interlaminar Shear (208489) per Fed. Test Method Std. 406, Method 1042, psi	1000 psi min	Interface Between Inner Wrap and Over Wrap 2,000 1,700 1,500		Interface Between Inner Wrap and Over Wrap 1,480 1,830 1,660	
Volatiles (208491) per TAP-DAP-122, %	3% max	2.20 2.07 2.20	2.83 2.87 2.84	2.14 2.04 2.03	2.84 2.79 2.80
Microtensile (208488) per ASTM-D-1708, psi	Report only	16,300 15,500 14,000	9,300 4,300 4,600	17,100 12,700 14,900	9,900 8,900 10,900

Component Properties of 260-SL-2 Nozzle Throat Insert

Component Properties after Final Cure from Test Specimens

Test Conducted	Specification Limits	Aft Test Ring	Fwd Test Ring	
		Inner Wrap MX-4926	Inner Wrap MX-4926	Over Wrap FM-5131
Specific Gravity per Fed. Test Method Std. 406, Method 5011	1.38 min	1.44	1.45	1.73
	for MX-4926	1.44	1.45	1.73
	1.68 min for FM-5131	1.44	1.45	1.73
Acetone Extractables per ASTM-D-494-46, %	1% max	0.24	0.12	0.25
		0.19	0.11	0.25
		0.20	0.18	0.14
Interlaminar Shear (208489) per Fed. Test Method Std. 406, Method 1042, psi	1000 psi	3,300	2,720	1,410
	min	3,500	2,360	1,470
			2,570	2,040
Interlaminar Shear (208489) per Fed. Test Method Std. 406, Method 1042, psi	1000 psi		Interface Between	
	min		Inner Wrap and	
			Over Wrap	
			2,400	
			2,510	
			2,400	
Volatiles (208491) per TAP-DAP-122, %	3% max	1.93	1.93	3.28
		1.94	2.10	3.31
		1.94	2.02	3.30
Microtensile (208488) per ASTM-D-1708, psi	Report	13,600	15,500	10,200
	only	13,500	15,900	10,400
		12,100	15,600	10,700

Component Properties of 260-SL-2 Nozzle Throat Extension Insert

Component Properties after Final Cure from Test Specimens

Test Conducted	Specification Limits	Aft Test Ring		Fwd Test Ring	
		Inner Wrap	Over Wrap	Inner Wrap	Over Wrap
		FM-5131	FM-5131	MX-4926	FM-5131
Specific Gravity per Fed. Test Method Std. 406, Method 5011	1.38 min for MX-4926 1.68 min for FM-5131	1.71 1.71 1.70	1.71 1.70 1.72	1.42 1.41 1.42	1.71 1.72 1.71
Acetone Extractables per ASTM-D-494-46, %	1% max	0.12 0.14 0.15	0.10 0.11 0.10	0.02 0.11 0.09	0.06 0.07 0.09
Interlaminar Shear (208489) per Fed. Test Method Std. 406, Method 1042, psi	1000 psi min	1,230 1,280 1,140		2,620 1,510 2,200	1,270 1,290 970
Interlaminar Shear (208489) per Fed. Test Method Std. 406, Method 1042, psi	1000 psi min	Interface Between Inner Wrap and Over Wrap 1,020 1,320		Interface Between Inner Wrap and Over Wrap 1,700 2,000 1,960	
Volatiles (208491) per TAP-DAP-122, %	3% max	3.36 3.24 3.26	3.13 3.26 3.13	2.60 2.53 2.62	3.11 3.06 3.06
Microtensile (208488) per ASTM-D-1708, psi	Report only	8,300 7,900 7,500		21,400 18,800 23,100	10,100 7,400 9,000

Component Properties of 260-SL-2 Exit-Cone Liner

Report NASA CR-54982

<u>Bond Joint</u>	<u>Bondline Thickness, in.</u>	<u>Average Bond Shear Strength, psi</u>	<u>Ultrasonic Inspection</u>
Inner Doublers to Plastic	0.017 - 0.027	1540, 1829 (first cure) 1500, 2000 (third cure)	Doubler No. 3: One indication at 7-3/4 in. from edge and 52-1/2 in. from aft end 1/2 in. wide x 1-1/2 in. long. One indication at 19 in. from edge and 33-3/8 in. from aft end 1/2 in. wide x 2 in. long.
Aft Flange to Inner Doublers (Epon 913)	0.022 - 0.062	3240 (first cure) 1928 (second cure)	From 0° (TDC) to 90° CCW (looking aft) signal above optimum bond by maximum of 20% over 3-1/4 in. bond at thickest cross-sectional area of ring.
Inner Facing to Inner Doublers (Epon 955)	0.007 - 0.013	851, 1664 (first cure) 1574, 1843 (second cure)	Not Applicable.
Honeycomb Core to Inner	0.007 - 0.013	851, 1664 (first cure) 1574, 1843 (second cure) Trepan - 715 Flatwise Tensile: 657 (first cure) 717 (second cure)	Not Applicable.
Outer Facing to Honeycomb Core (Epon 955)	0.007 - 0.013	1006, 1388 Trepan - 729 Flatwise Tensile: 798	Nonstandard Areas: Panel No. 2: 14 in. from fwd flange 3 in. from left doubler area 2-1/2 in. x 1/2 in., 46.5 in. from fwd flange 3 in. from left doubler area 1 in. x 2 in., 57.5 in. from fwd flange 3 in. from left doubler area 1 in. x 2-1/2 in. Panel No. 3: 70 in. from fwd flange 3 in. from left doubler area 24 in. x 1/2 in. intermittent. Panel No. 11: 5 in. from flange 2 in. from left doubler area 3 in. x 1/2 in. Panel No. 14: 40.5 in. from flange 3 in. from left doubler. Area 8 in. x 1/2 intermittent.
Forward Flange to Inner Doubler (Epon 913)	0.008 - 0.030	2397	No Indication.
Forward Flange to Plastic Liner (Epon 913)	0.012 - 0.040	2397	No Indication.
Outer Facings to Forward Flange (Epon 955)	0.007 - 0.013	1006, 1388	No Indication.
Outer Facings to Aft Flanges (Epon 955)	0.007 - 0.013	1006, 1388	No Indication.
Outer Doublers to Outer Facings (Epon 955)	0.007 - 0.013	1006, 1388	Nonstandard Areas: Doubler No. 2: 27.5 in. from flange 1 in. from left end of doubler 2-1/4 in. x 1/2 in. area. Doubler No. 3: 19 in. from flange 1 in. from left end of doubler 1 in. x 1/2 in. area. 21.5 in. from flange 1 in. from left end of doubler 2-1/2 in. x 1/2 in. area. 43 in. from flange 1 in. from left end of doubler 1 x 1/2 in. area. Doubler No. 5: 44.5 in. from flange 2 in. from left end of doubler 2 in. x 2-1/2 in. area.

Exit-Cone Bonding Process Summary

88<

Figure 12

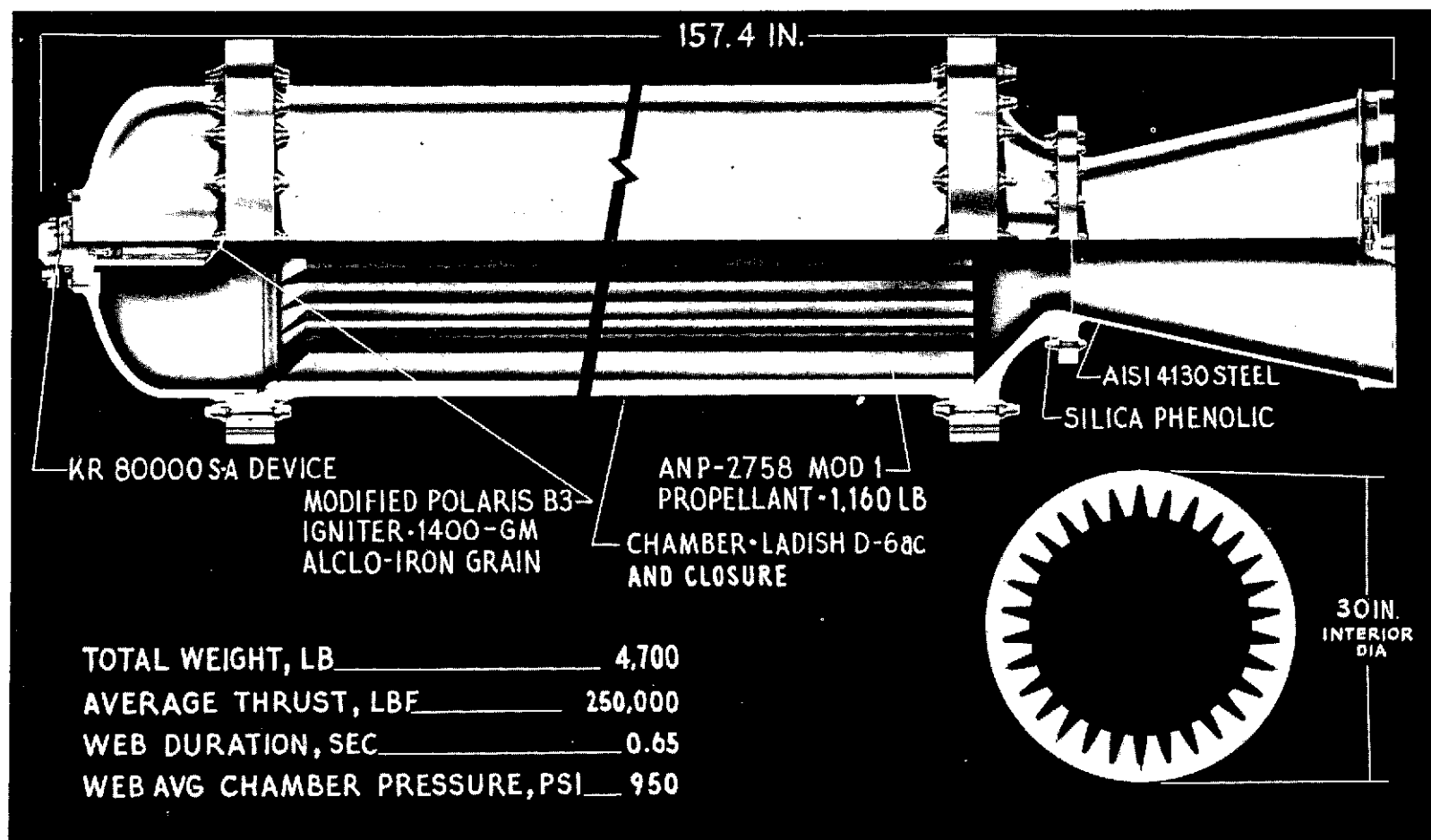
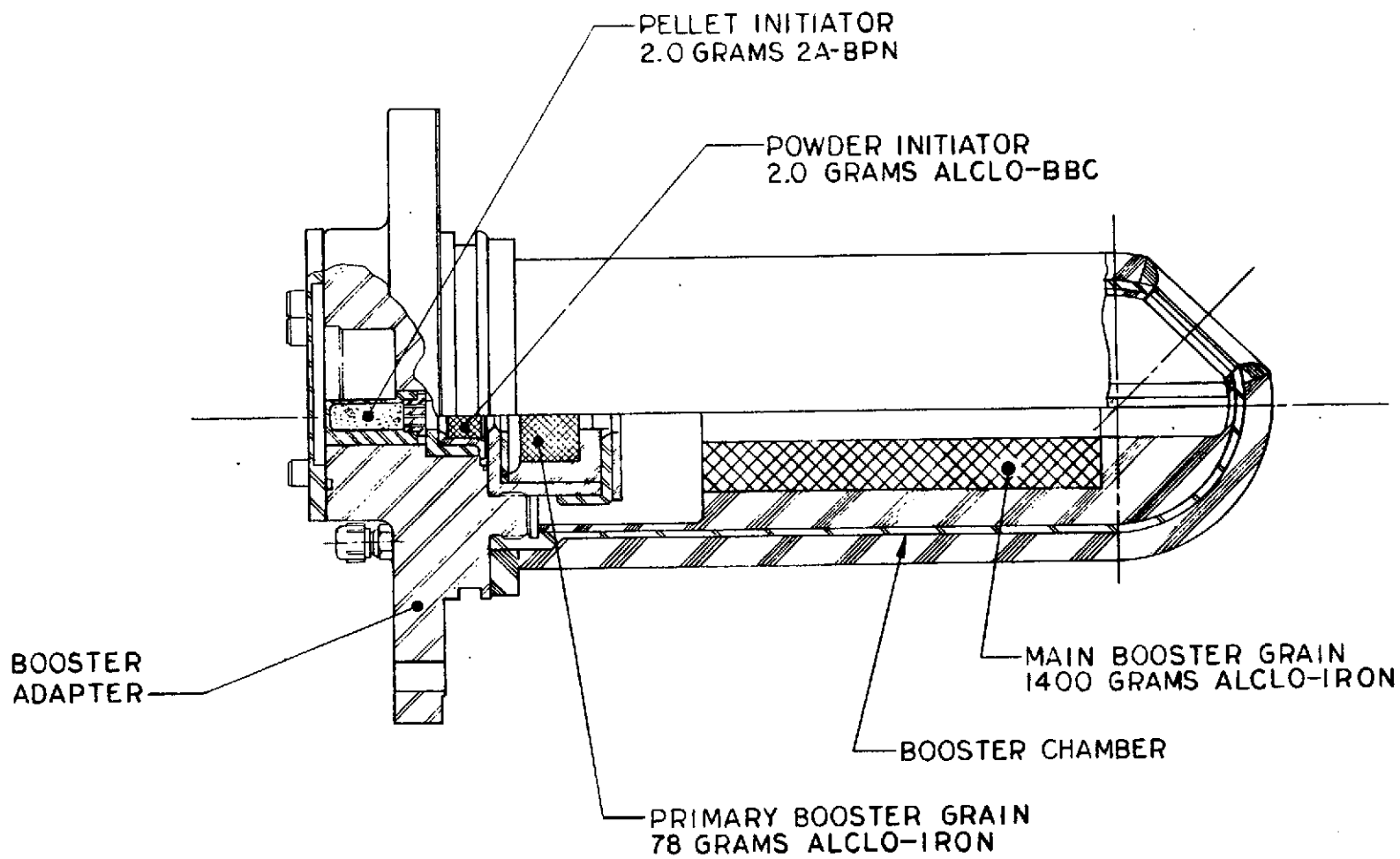


Figure 13

89

260-SL-2 Ignition Motor Assembly

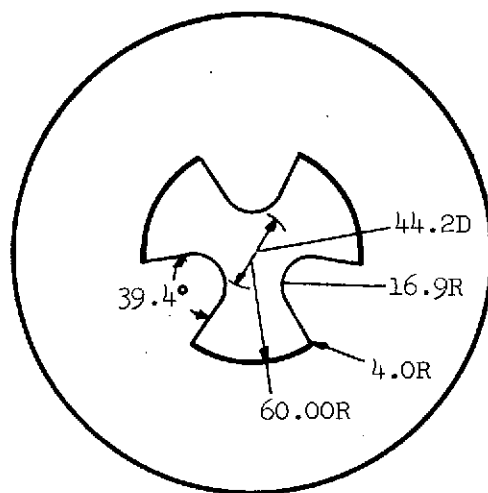
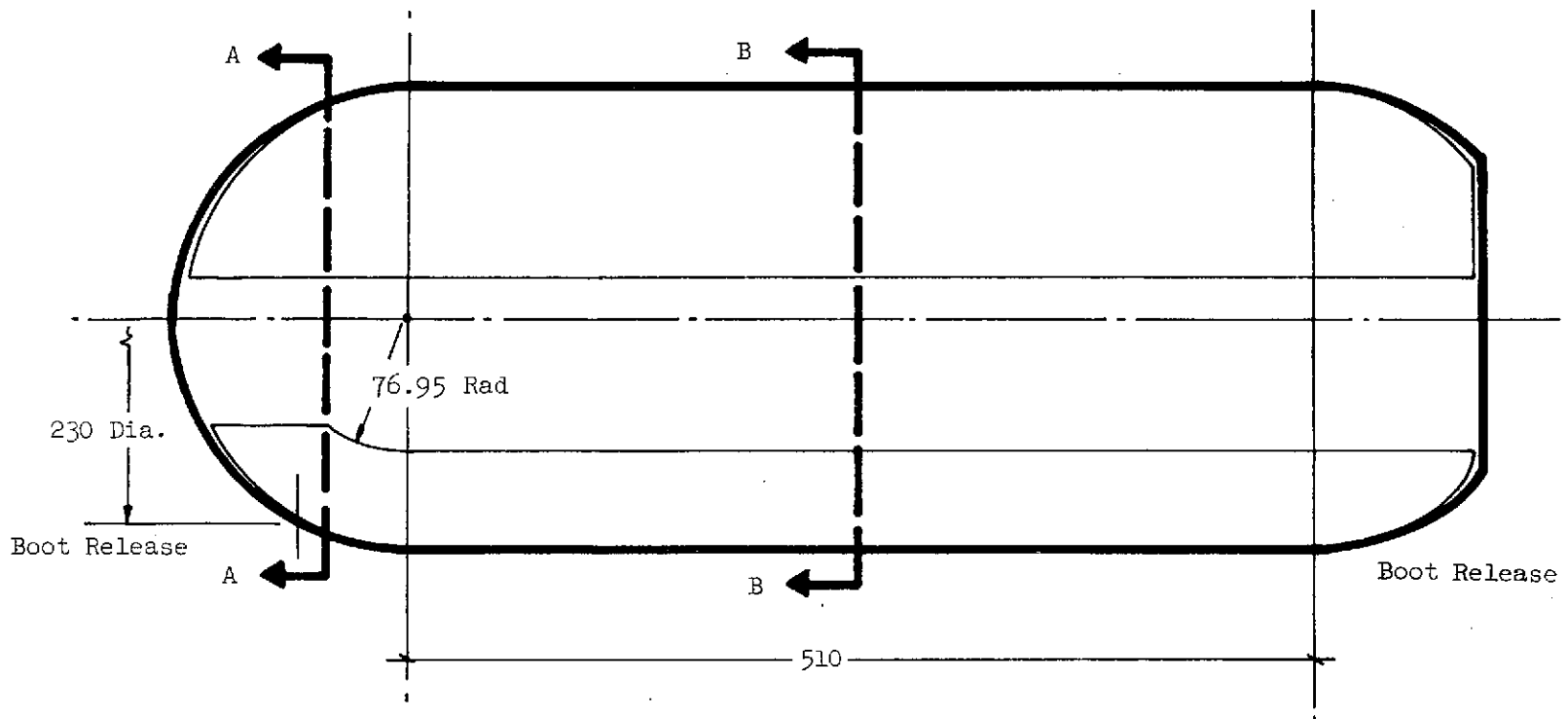


260-SL-2 Ignition Motor Booster

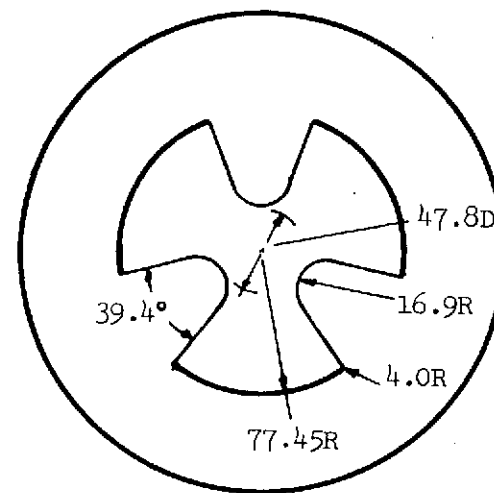
Figure 14

<u>Parameter</u>	<u>Requirement</u>
Average thrust (nominal), lbf	2,750,000
Maximum thrust (nominal), lbf	3,500,000
Average chamber pressure (minimum), psia	450
Web action time (nominal), sec	120
Standard specific impulse (minimum), lbf-sec/lbm	242
Total impulse (minimum), lbf-sec	350,000,000
Pressure-vs-time trace	Neutral \pm 10%
Impulse between web action time and action time (maximum), %	6
Impulse after action time (maximum), %	1
Time between web action time and action time (maximum), sec	20

Ballistic Performance Requirements



A - A



B - B

260-SL-2 Grain Configuration

Figure 16

92

<u>Material</u>	<u>Wt%</u>
Ammonium perchlorate	69.000
Aluminum	15.000
Ferric oxide	0.750
PBAN-A terpolymer (50 equivalents)	8.723
Dodecenylsuccinic anhydride (50 equivalents)	0.696
Di (2-Ethylhexyl) adipate	3.811
Diepoxide (110 equivalents)	2.015
Silicone fluid	<u>0.005</u>
	100.000

260-SL-2 Propellant Formulation (u)

93<

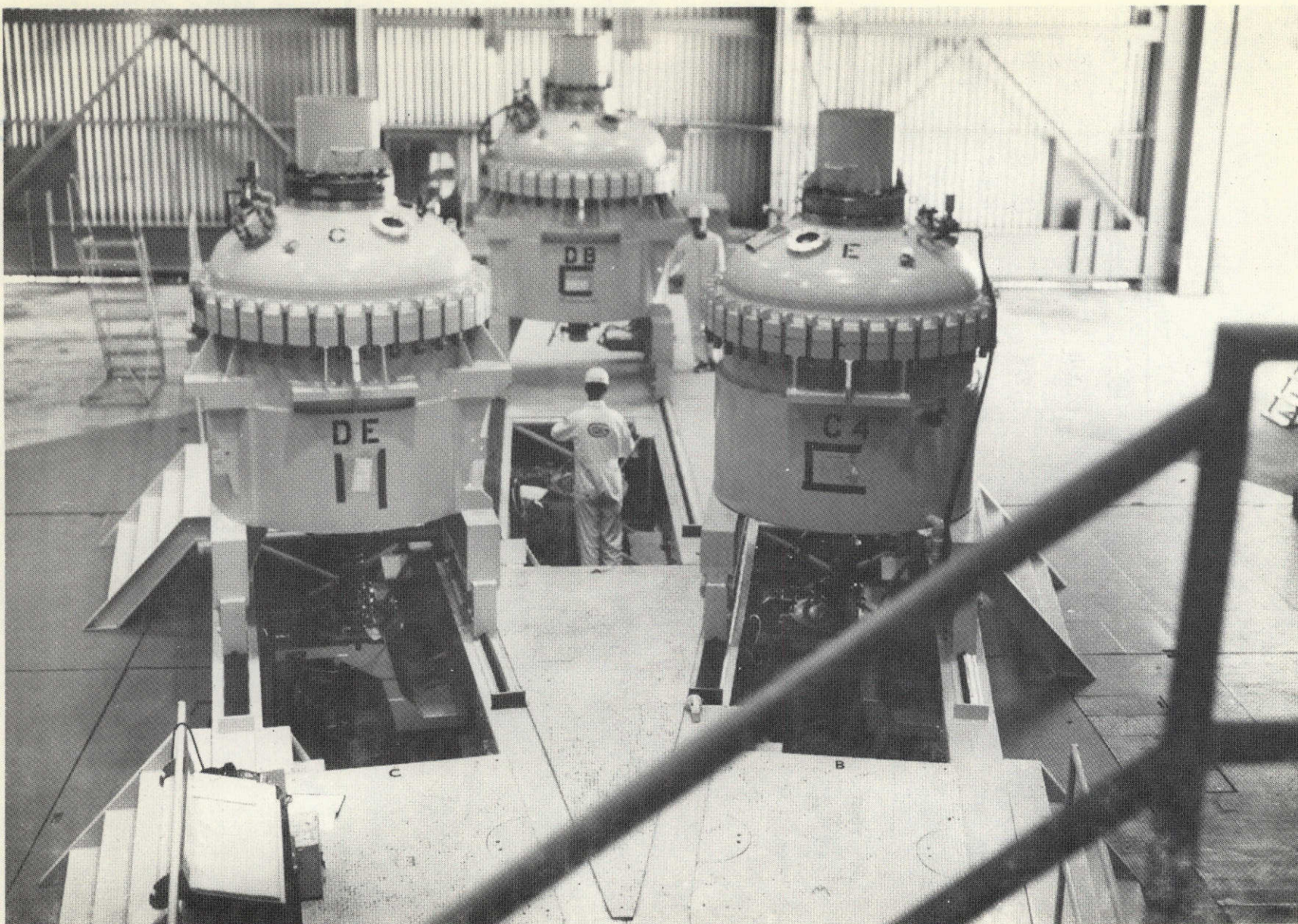
Figure 17

<u>Material</u>	<u>Wt%</u>
PBAN-A terpolymer (7.4 equivalents)	26.99
Methylnadic anhydride (85.5 equivalents)	16.64
Poly (1,4-butylene) glycol (7.1 equivalents)	7.77
Diepoxide (107 equivalents)	40.98
Ferric acetylacetonate	1.00
Ferric oxide	1.86
Silicon dioxide	<u>4.76</u>
	100.00

260-SL-2 Liner Formulation

<u>Submix</u>	<u>Specification Limits</u>	<u>Liner Batch</u>		
		<u>L011</u>	<u>L012</u>	<u>L013</u>
H ₂ O, wt%	0.3 maximum	0.024	0.025	0.027
PBAN, wt%	52.5 \pm 10	53.7	54.8	54.6
MNA, wt%	32.4 \pm 8	29.8	31.0	29.3
<u>Premix</u>				
Density, g/cc	1.054 \pm 0.005	1.057	1.052	1.057
Ash, wt%	3.61 \pm 0.5	3.76	3.71	3.77
FeAA, wt%	1.84 \pm 0.5	1.88	1.82	1.90
<u>Liner</u>				
PBAN, wt%	27.0 \pm 10	27.3	28.6	27.5
DER-332, wt%	41.0 \pm 8	39.7	42.2	39.3

Acceptance Analysis of SD-850-2 Liner Batches Prepared for
Lining of Motor 260-SL-2



96 >

Figure 20

Propellant Casting Setup for Motor 260-SL-2

<u>Submix</u>	<u>Average</u>	<u>Standard Deviation</u>
H ₂ O, wt%	0.0283	0.00676
Total Acid, eq/100g	0.07916	0.000888
DDS, wt%	5.410	0.1372
Density, g/ml	0.9331	0.00098
Refractive Index	1.49197	0.000155
Ash, wt%	0.316*	0.0862

Premix I

Density, g/ml	0.9757	0.00111
Fe ₂ O ₃ , wt%	5.357	0.0977

Premix II

Density, g/ml	1.4536	0.00083
H ₂ O, wt%	0.0104	0.00511
Gas cc/g	0.0236	0.00890

*Three very low values excluded (first, second and fifth batches).

Note: Forty-six submixes and premixes were analyzed.

Submix and Premix Analysis

97<

<u>Process</u>	<u>Motor</u>	<u>Mean</u>	<u>Pot-to-Pot Standard Deviation</u>	<u>No. of Pots</u>	<u>Sample-to-Sample Standard Deviation</u>	<u>No. of Samples</u>
Continuous	260-SL-2	0.4483	0.0093	82	0.0124	164
	260-SL-1	0.4453	0.0070	86	0.0092	172
Batch	260-SL-2	0.4410	0.0043	188		
	260-SL-1	0.4440	0.0043	189		
Continuous	260-SL-2	0.4439	0.0071	270		
Plus Batch	260-SL-1	0.4445	0.0053	275		

Note: Standard deviations include test precision.

Liquid Strand Burning Rate of ANB-3105 Propellant Processed for
Motors 260-SL-1 and 260-SL-2

<u>Process</u>	<u>Motor</u>	<u>Mean</u>	<u>Theoretical Value</u>	<u>Pot-to-Pot Standard Deviation</u>	<u>No. of Pots</u>	<u>Sample-to-Sample Standard Deviation</u>	<u>No. of Samples</u>
Continuous	260-SL-2	1.7515	1.752	0.0019	82	0.0025	164
	260-SL-1	1.7507	1.751	0.0018	86	0.0022	172
Batch	260-SL-2	1.7521	1.752	0.0010	188		
	260-SL-1	1.7514	1.751	0.0011	189		
Continuous Plus Batch	260-SL-2	1.7519	1.752	0.0014	270		
	260-SL-1	1.7511	1.751	0.0018	275		

Note: Standard deviations include test precision.

Uncured Density of ANB-3105 Propellant Processed for Motors 260-SL-1 and -2

Report NASA CR-54982

<u>Process</u>	<u>Motor</u>	<u>Mean</u>	<u>Theoretical Value</u>	<u>Pot-to-Pot Standard Deviation</u>	<u>No. of Pots</u>	<u>Sample-to-Sample Standard Deviation</u>	<u>No. of Samples</u>
Continuous	260-SL-2	2.000	2.015	0.0313	82	0.0394	164
	260-SL-1	1.871	1.872	0.0247	86	0.0303	172
Batch	260-SL-2	2.010	2.015	0.0276	188		
	260-SL-1	1.872	1.872	0.0232	189		
Continuous Plus Batch	260-SL-2	2.008	2.015	0.0291	270		
	260-SL-1	1.872	1.872	0.0237	275		

Note: Standard deviations include test precision.

DER-332 Content of ANB-3105 Propellant Processed for Motors
260-SL-1 and 260-SL-2

	<u>260-SL-1</u>	<u>260-SL-2</u>
Mean AP Content	69.14	69.14
Pot-to-Pot Standard Deviation	0.392	0.362
No. of Pots	86	82
Sample-to-Sample Standard Deviation	0.442	0.427
No. of Samples	172	164

Note: Standard deviations include test precision.

Ammonium Perchlorate Content of Continuous Mixed ANB-3105
 Propellant for Motors 260-SL-1 and 260-SL-2

<u>Mechanical Properties at 77°F</u>	<u>Cure Time at 135°F, Days</u>						
	<u>16</u>	<u>20</u>	<u>24</u>	<u>28</u>	<u>32</u>	<u>36</u>	<u>40</u>
Maximum Tensile Strength, S_m , psi							
Mean	87	93	97	101	103	103	104
Standard Deviation	6.5	8.3	7.5	6.1	8.2	7.3	6.3
Elongation at Maximum Stress, ϵ_m , %							
Mean	32	31	30	30	30	29	29
Standard Deviation	2.4	2.9	2.8	2.0	2.3	2.1	2.2
Elongation at Break, ϵ_b , %							
Mean	41	39	38	38	37	36	35
Standard Deviation	5.1	5.4	4.5	4.0	4.3	4.6	3.7
Initial Modulus, E_0 , psi							
Mean	355	393	422	444	458	460	465
Standard Deviation	31.8	40.8	36.2	34.3	43.7	44.0	37.4

Samples from every sixth pot; total of 32 vertical batch mixed pots and 15 continuous mixed pots

Mechanical Properties of Propellant vs Cure Time

Mechanical Properties at 77°F*				
	<u>S_{rm}, psi</u>	<u>m, %</u>	<u>b, %</u>	<u>E_o, psi</u>
Vertical Batch Mix (n = 188)				
Mean	98	27	32	454
Standard Deviation	8.0	2.8	4.7	33.5
Continuous Mix (n = 81)				
Mean	106	30	38	452
Standard Deviation	5.3	1.8	3.2	33.2
Vertical + Continuous Mix (n = 269)				
Mean	101	28	33	453
Standard Deviation	7.9	2.9	5.1	33.3

* Samples taken from each of 269 pots cast into the motor and tested at the start of motor cooldown -- cure times ranging from 28 to 37 days at 135°F.

Mechanical Properties of Propellant after Cure

<u>Batch</u>	<u>Max. Strain Level Held*</u>	<u>Batch</u>	<u>Max. Strain Level Held*</u>	<u>Batch</u>	<u>Max. Strain Level Held*</u>
C135	20	B254	20	B386	20
C141	20	B260	20	B392	20
C147	20	B266	20	B398	20**
C153	20	B272	20	B410	20
C159	20	B278	20**	B416	20
C165	20	B284	20	B428	20
C171	20	B290	20	B434	20
C177	20	B296	20	B439	20
C183	20	B308	20	B314	15**, 20**
C189	20	B320	20	B332	20
C195	20	B326	20	B344	20
C213	20	B338	20	B362	15**, 20**
C207	20	B350	20	B356	20
C217	20	B368	20	B380	20
B249	20	B374	20	B404	20**

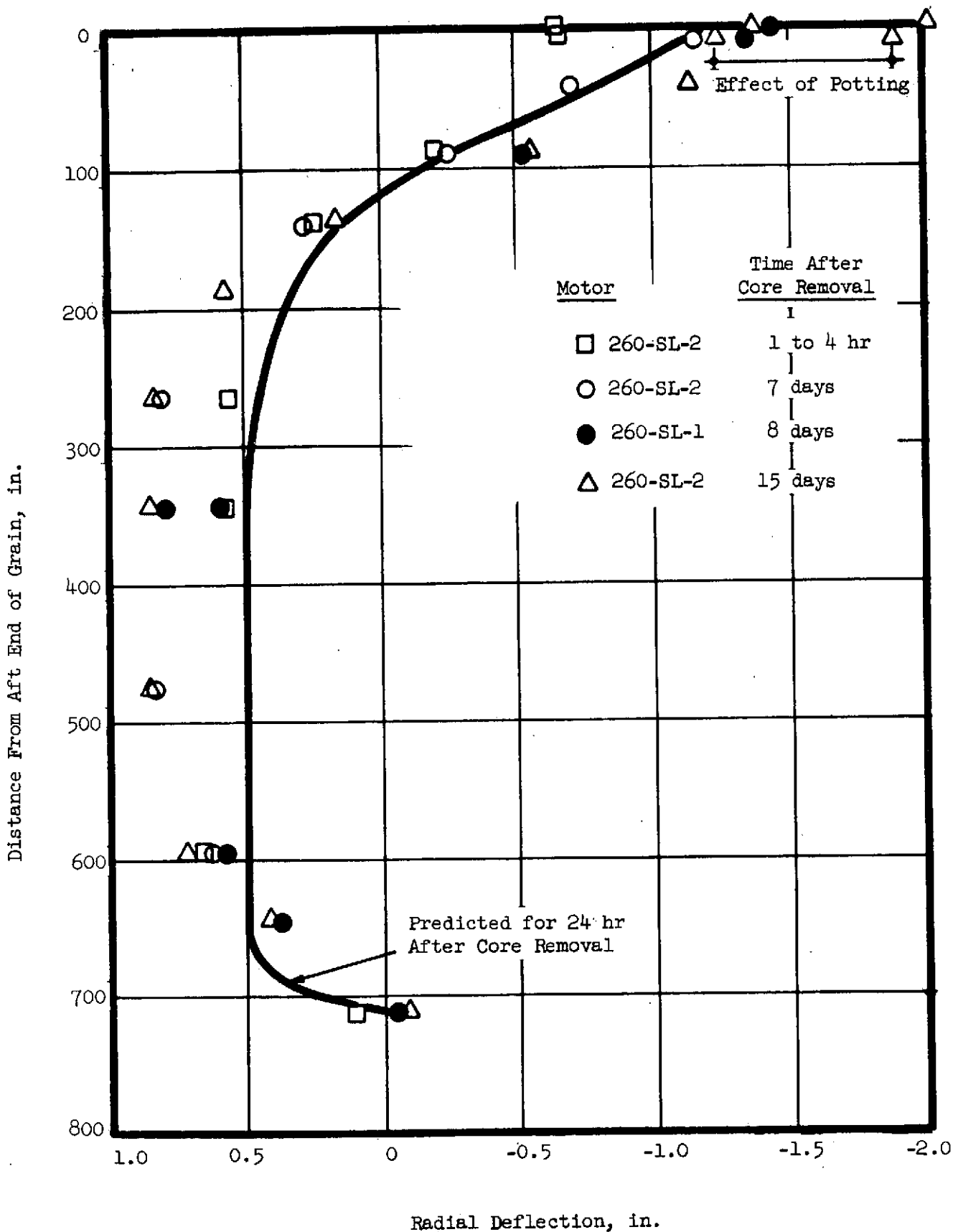
* Maximum strain level tested - 20%

** One bar of two tested

Propellant Constant Strain Properties



Internal View of Grain Bore



Reproduced from
best available copy.



- NOTES:
1. HATCHED DET. DRAWING PER STANDARDS DESCRIBED IN MIL-D-70327.
 2. [A] IS DEFINED AS THE THROAT DIA OF THE MOTOR NOZZLE ASSY.
 3. [B] IS DEFINED AS THE EXIT DIA OF THE MOTOR EXIT CONE ASSY.
 4. [C] IS DEFINED AS A STRAIGHT LINE PASSING THRU [A] & [B].
 5. [D] IS DEFINED AS THE THROAT DIA OF THE IGNITION MOTOR NOZZLE ASSY.
 6. [E] IS DEFINED AS THE EXIT DIA OF THE IGNITION MOTOR NOZZLE ASSY.
 7. [F] IS DEFINED AS A STRAIGHT LINE PASSING THRU [C] & [D].
 8. MISALIGNMENT OF [A] WITH [C] IS TO BE WITHIN THE ENVELOPE DEFINED IN VIEW B.
 9. THE FOLLOWING PROCEDURE SHALL BE USED FOR REMOVAL OF THE H24504-9 WEATHER COVER:
 - a. THE COVER SHALL BE SUPPORTED BY THREE H24504-11 ROPES WHICH ARE ON H24504-7 RINGS.
 - b. LOOSEN AND UNBUCKLE THE FOUR H24504-5 STRAP ASSEMBLIES.
 - c. DETACH THE H24504-13 SEAL ASSEMBLY BY PULLING ON THE H24504-23 ROPE.
 - d. GATHER THE COVER ALONG THE EXIT PLANE FLANGE SO THAT THE COVER IS ON ONE SIDE OF THE IGNITION MOTOR SUPPORT BLANK.
 - e. PULL ON THE H24504-21 ROPE UNTIL THE EXIT PLANE OF THE IGNITION MOTOR IS EXPOSED FROM THE WEATHER COVER.
 - f. LIFT UP BY THE H24504-11 ROPES UNTIL THE WEATHER COVER IS CLEARED OF THE NOZZLE EXIT CONE.

T-450001 REF
THRUST TAKEOUT
SYSTEM

ELEV
512.68

ELEV
500.28

T-45001A REF
HANDLING RING
CHAMBER

600,500.9
MOTOR ASSY

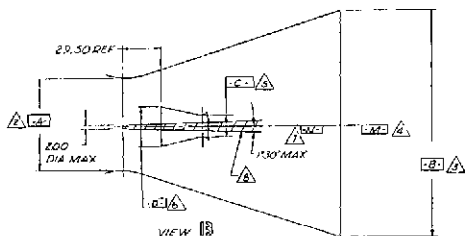
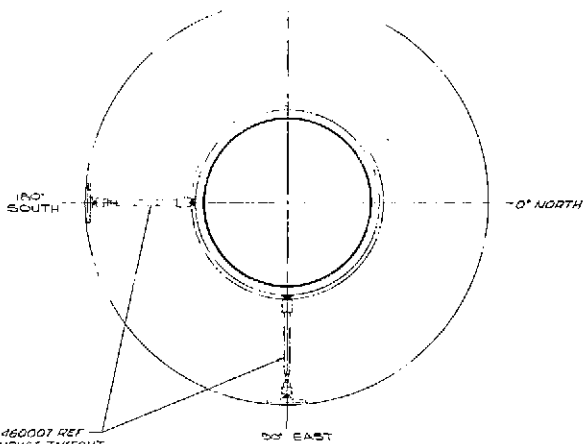
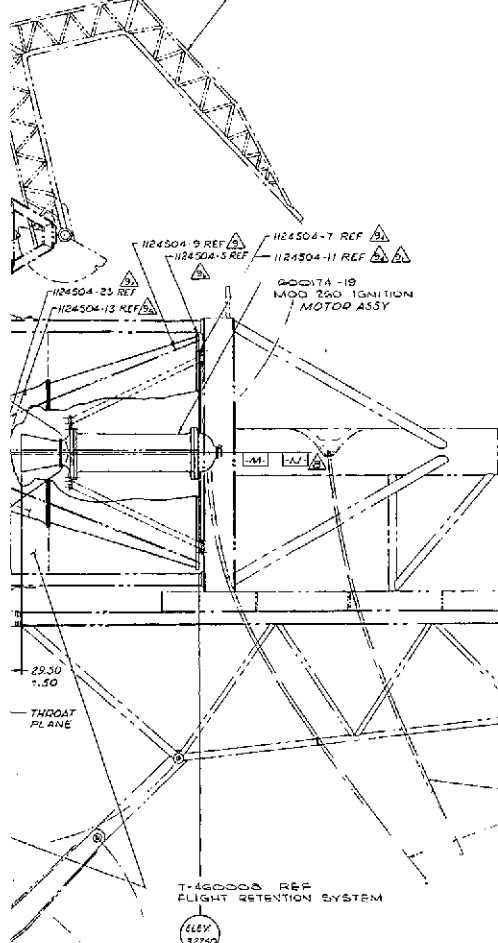
ELEV
291.04

T-45001B REF
HANDLING RING CHAMBER

ELEV
0.00

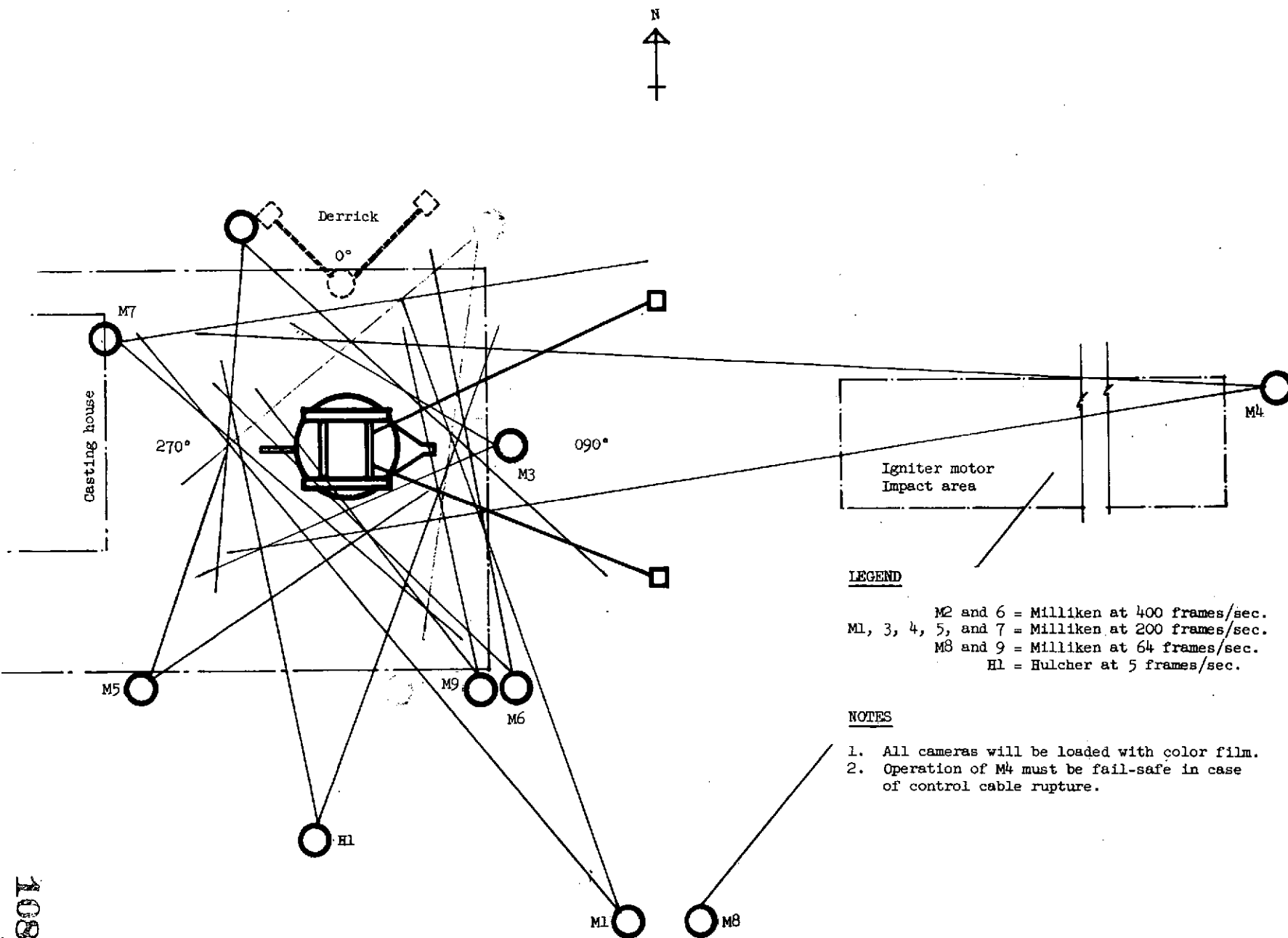
MEAN SEA
LEVEL

T-460011 REF
MOTOR QUENCH SYSTEM



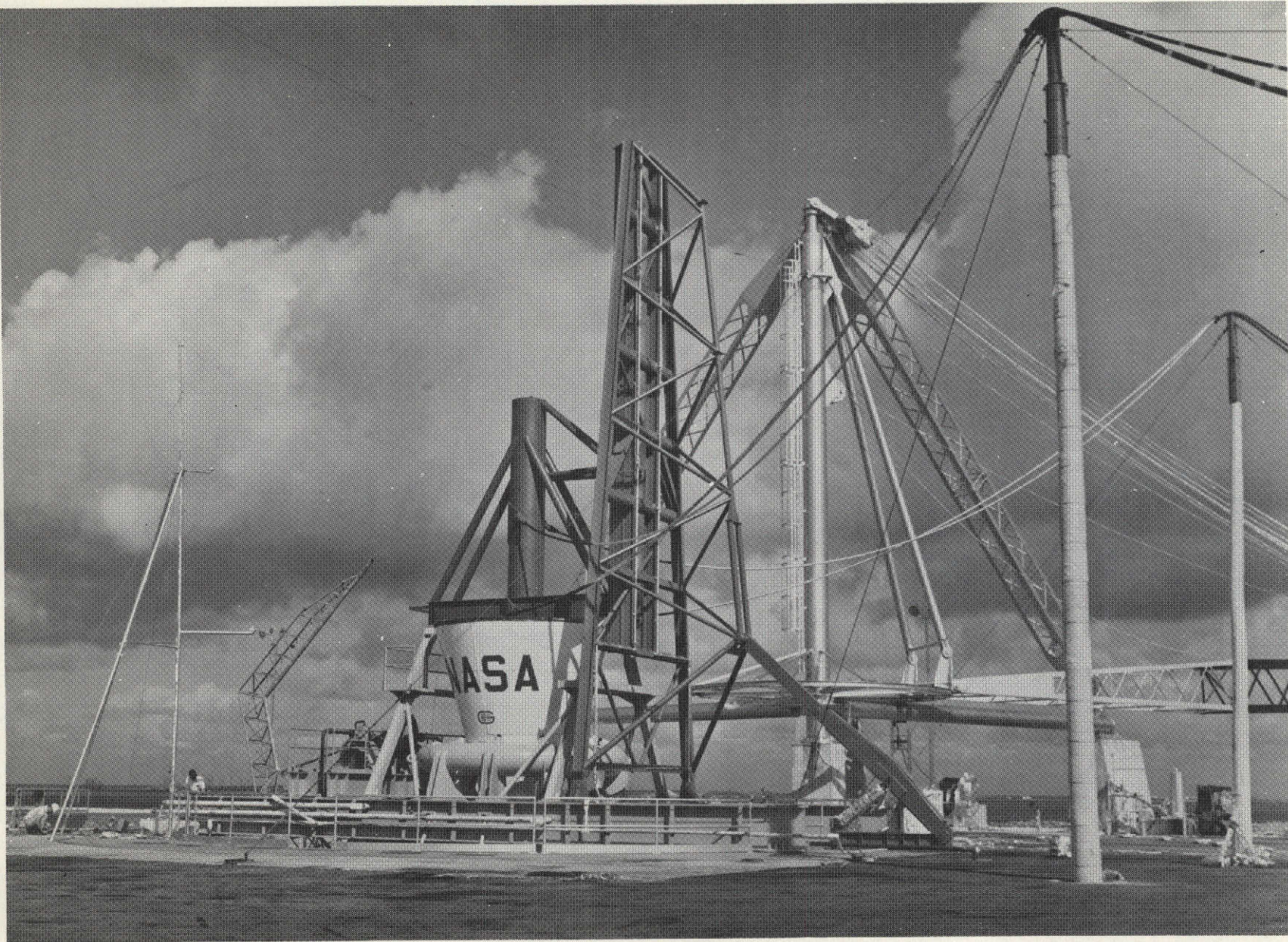
180° 50

T-46
FLK

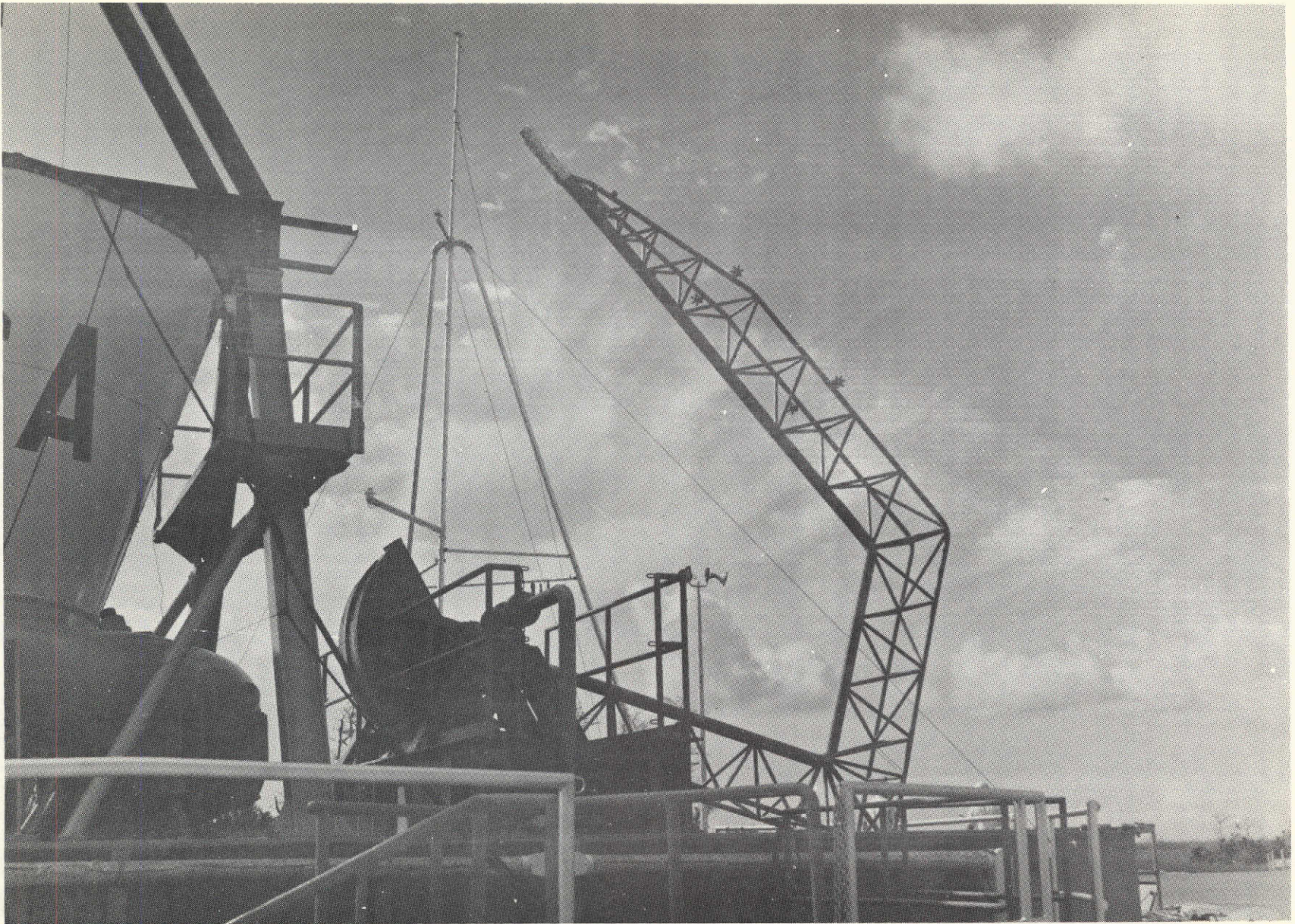


Motion Picture Placement

Figure 32



Overall View of Test Setup



Pretest View of Quench System



Pretest View of Ignition Tower Retraction System



Pretest View of Horizontal Stabilizers and Retention Rods

Acquisition Channels

Pressure, force, and strain	36*
Temperature	24**
Linear motion	12
High frequency	12
Photo instrumentation	9***

Recording Instruments

Oscillographs	7
Strip charts	2
Tape recorder	1
Television monitor	1

* Twelve amplified channels.

** Temperature sampling techniques can increase the number of temperature parameters by 15 per channel.

*** Camera capabilities can be increased through the use of parallel patching circuits and remote motor-generator sets. However, the cameras powered by the motor-generator sets will not have timing and fire-switch indication.



A-DD Test Facility Electrical Control Schematic

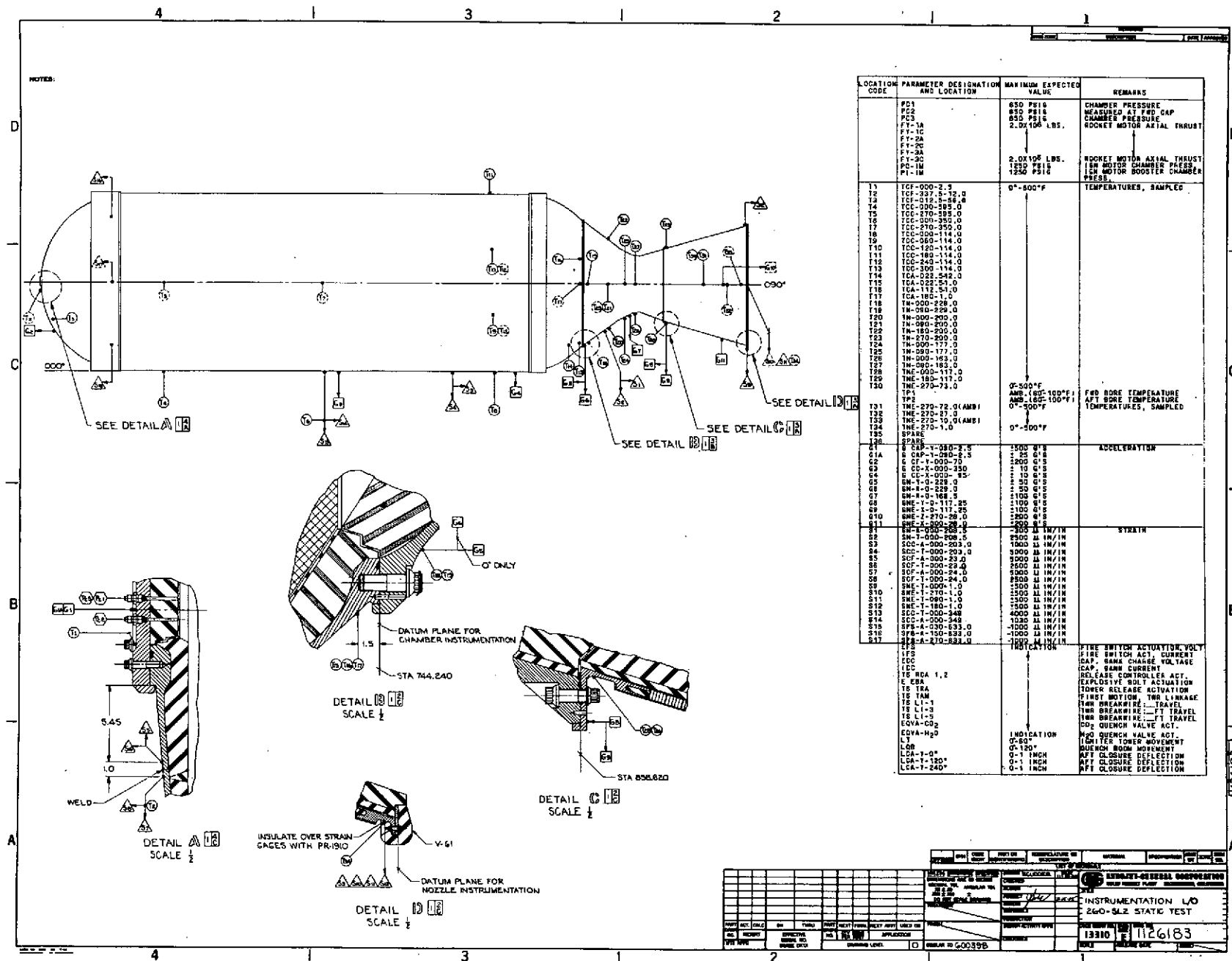
Report NASA CR-54982

A. <u>Sensing Instruments</u>		<u>Type</u>	<u>Channel</u>	<u>Model</u>	<u>Range</u>	
1. Chamber Pressure	Pressure Transducer		Pc1	Taber 206	0 to 750 psig	
			Pc2	Taber 206	0 to 750 psig	
			Pc3	Taber 206	0 to 750 psig	
			Pc1M	Standard Controls, Inc., 900-27	0 to 2000 psig	
			P1M		0 to 2000 psig	
	2. Thrust	Load Cell		Fy1A	Baldwin-Lima-Hamilton Type C1AS, S/N 37000	0 to 5,000,000 lb
				Fy1C		
				Fy2A	Baldwin-Lima-Hamilton Type C1AS, S/N 36353	0 to 5,000,000 lb
				Fy2C		
				Fy3A	Baldwin-Lima-Hamilton Type C1AS, S/N 37001	0 to 5,000,000 lb
		Fy3C				
3. Vibration/Shock	Accelerometer		G1	Endevco 2240	+ 200 g	
			G1A		+ 25 g	
			G2		+ 200 g	
			G3		+ 25 g	
			G4		+ 25 g	
			G5		+ 50 g	
			G6		+ 50 g	
			G7		+ 50 g	
			G8		+ 150 g	
			G9		+ 150 g	
			G10		+ 200 g	
			G11		+ 50 g	
4. Temperature	Thermocouples		T1 through T36	Chromel-Alumel	0 to 500°F	
5. Strain	Strain Gages		S1 through S10	Baldwin-Lima-Hamilton Type FAP-2512	N/A	
6. Growth	Strain Gages (Circumferential)		S11 through S14	Baldwin-Lima-Hamilton Type PA-18	N/A	
B. <u>Amplifiers</u>						
Kintell, Model 112A Model 114AJ						
Dana, Model 2211						
C. <u>Recording Instruments</u>						
Oscillographs						
R1 Honeywell Visicorder, Model 1612						
R2 Consolidated Electrodynamics Corp., Model 5-119						
R3 Consolidated Electrodynamics Corp., Model 5-119						
R4 Consolidated Electrodynamics Corp., Model 5-119						
R5 Consolidated Electrodynamics Corp., Model 5-119						
Tape Recorder						
Amplex, Model FR1200						
Recording Speed						
R1 40 and 4 in/sec						
R2 10 in/sec						
R3 10 in/sec						
R4 10 in/sec						
R5 10 in/sec						
Ampex 60 in/sec						
D. Galvanometers						
Pressure and thrust channels, CEC Type 316 or 320						
Temperature and Strain channels, CEC Type 315						

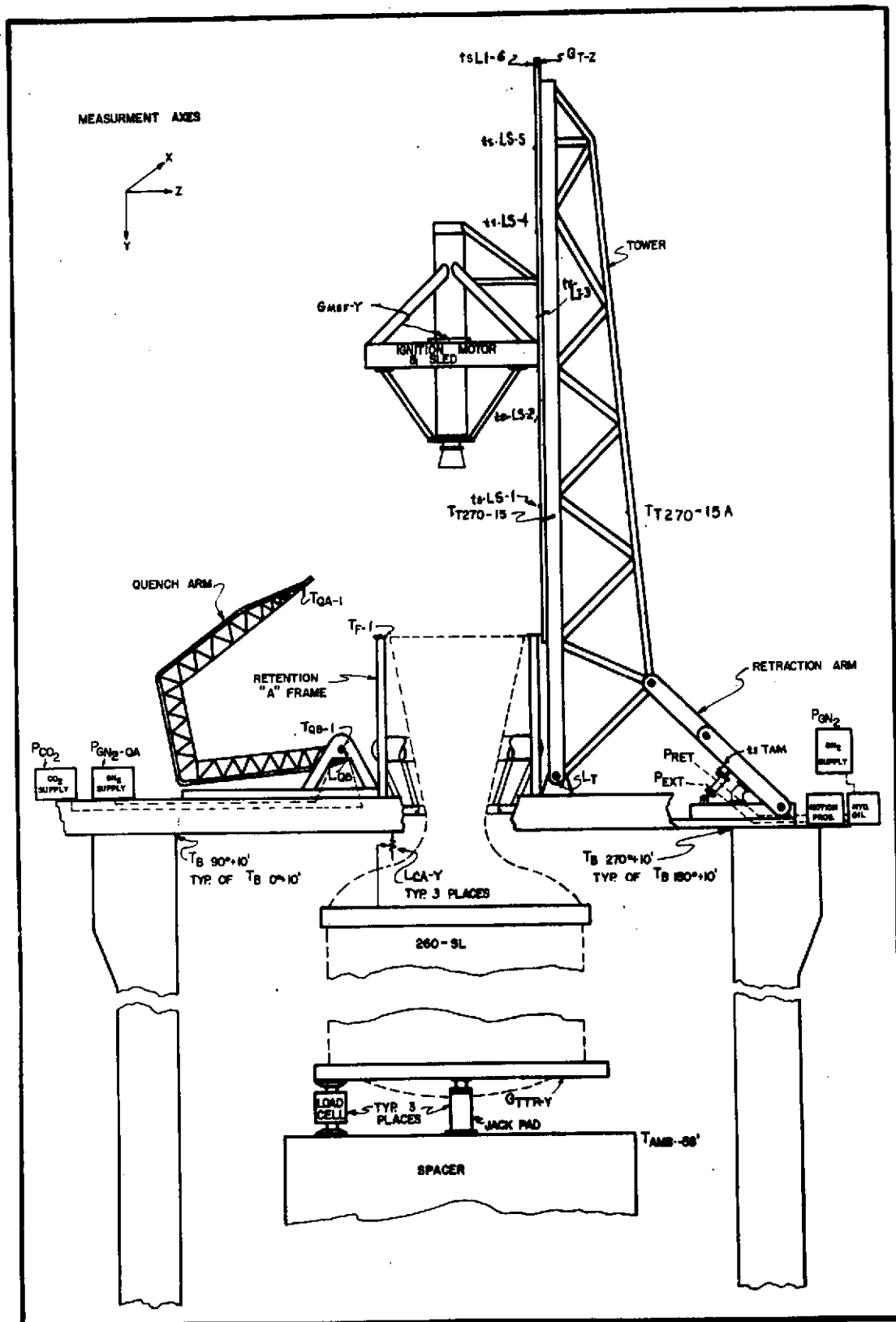
Motor 260-SL-2 Instrumentation Summary

Figure 40

116



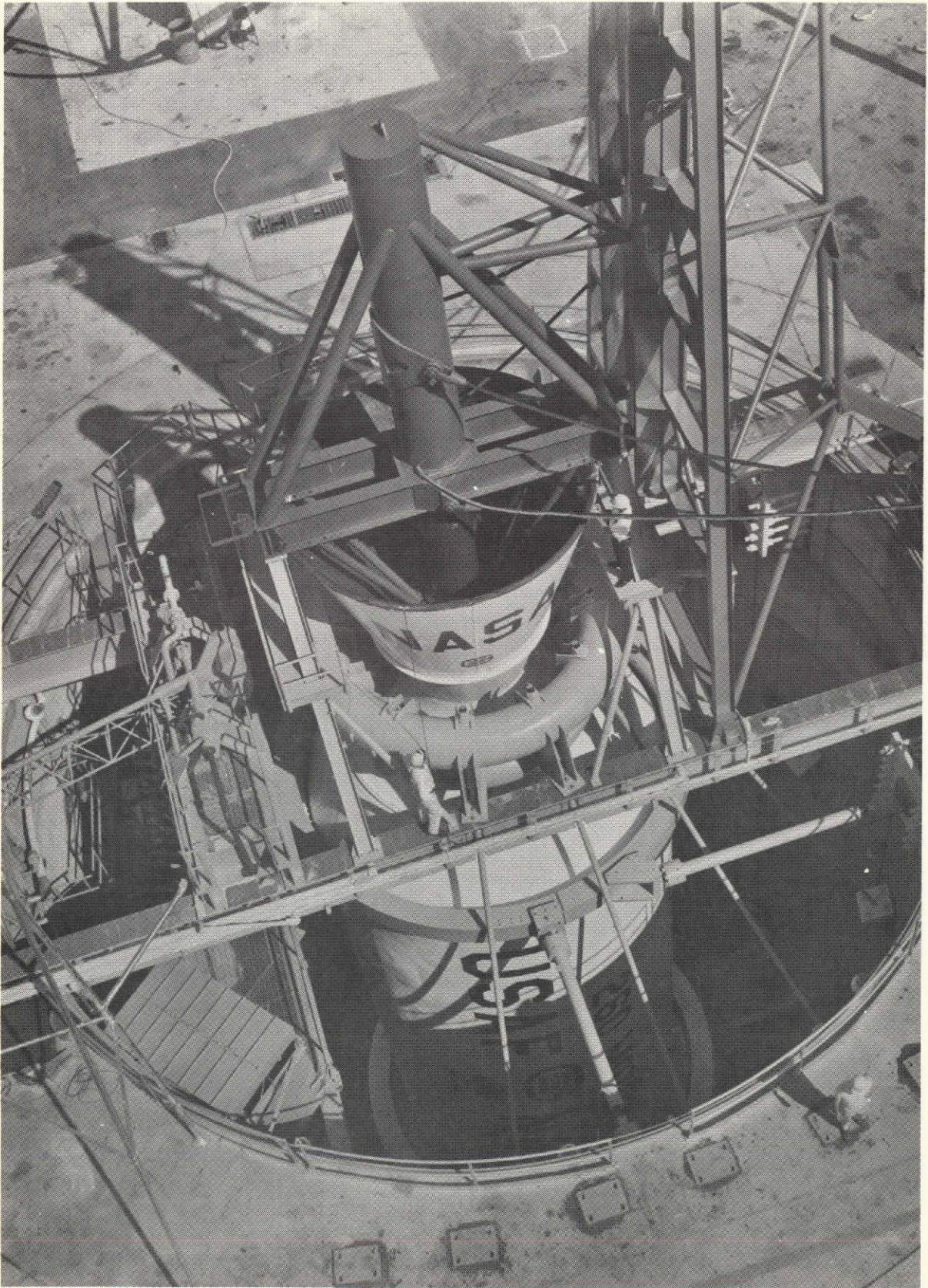
Motor 260-SL-2 Instrumentation Locations



A-DD Special Test Instrumentation Installation

117<

Figure 41



Pretest View of Motor 260-SL-2

Figure 42

260-SL-2

T + 0.000 sec	Fireswitch actuation (1900 hr., 23 Feb. 1966)
T + 0.138 sec	Ignition interval, ignition motor
T + 0.220 sec	260-SL-2 chamber pressure reaches 125 psia
T + 0.255 sec	Release control unit No. 2 logic satisfied, explosive bolt command triggered
T + 0.304 sec	Explosive bolts fire
T + 0.336 sec	Ignition interval, motor 260-SL-2
T + 0.340 sec	Ignition motor pressure data lost
T + 0.545 sec	Ignition motor and sled reach top of track. Tower retraction command initiated
T + 0.570 sec	First movement of tower
T + 4.800 sec	Tower retraction completed
T + 40.085 sec	Maximum chamber pressure reached (601 psia)
T + 114.3 sec	End of web action time
T + 130.1 sec	End of action time
T + 176.0 sec	Quench boom insertion initiated
T + 12 min (approx.)	CO ₂ quench accomplished

Time-Event Summary

PEAK VIBRATION ACCELERATION AMPLITUDE AND PREDOMINANT FREQUENCY

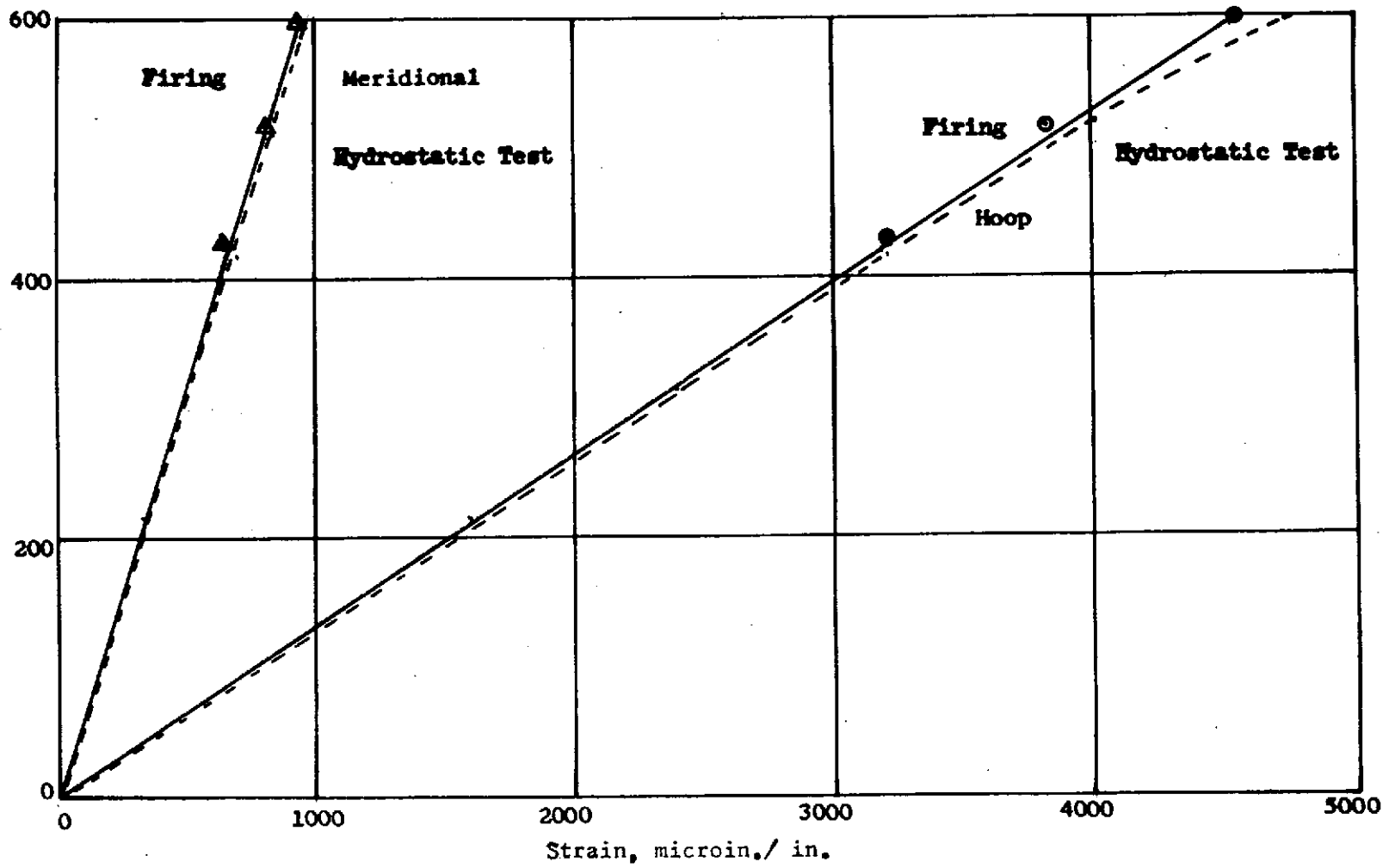
LOCATION	260-SL-1 STATIC FIRING				260-SL-2 STATIC FIRING			
	START TRANSIENT		STEADY OPERATION		START TRANSIENT		STEADY OPERATION	
	Ampl. g's	Freq. - CPS	Ampl. g's	Freq. - CPS	Ampl. g's	Freq. - CPS	Ampl. g's	Freq. - CPS
GCAP-Y-090-2.5 Fwd. Dome, Longitudinal	587	140	12	160	450	120	10	160
GCF-Y-000-70 Fwd. Dome, Longitudinal	TRANSDUCER MALFUNCTIONED AT IGNITION				231	200	8	160
GCC-X-000-350 Case Center, Lateral	3.5 5.0	40 1000	INSIGNIFICANT		4 5.0	50 1000	OUT	
GCC-X-000-95 Y Joint, Lateral	4.2 8	40 1000	INSIGNIFICANT		27 6	300 1000	5 INSIGNIFICANT	250
GN-Y-000-229 Aft. Closure, Longitudinal	50	160	3.5	160	63	160	4	160
GN-X-000-229 Aft. Closure, Lateral	55	160	3.5	160	53	160	10	100-160
GN-X-000-168-5 Nozzle Throat, Lateral	77	2000	6 10	160 1000	90	2000	6 10	160 2000
GN-Y-000-117.25 Exit Cone Joint, Longitudinal	62	1-2000	INSIGNIFICANT		80-100	1-2000	INSIGNIFICANT	
GN-X-000-117.25 Exit Cone Joint, Lateral	94	1-2000	INSIGNIFICANT		210	1-2000	INSIGNIFICANT	
GN-Z-270-28 Exit Cone, Lateral	214 90	2000 300	26	1-2000	190 90	2000 300	25-30	1-2000
GN-X-000-28 Exit Cone, Lateral	NOT RECORDED				210 100	2000 200	25-30	1-2000

Acceleration Data Summary

Figure 44

120

Report NASA CR-54982

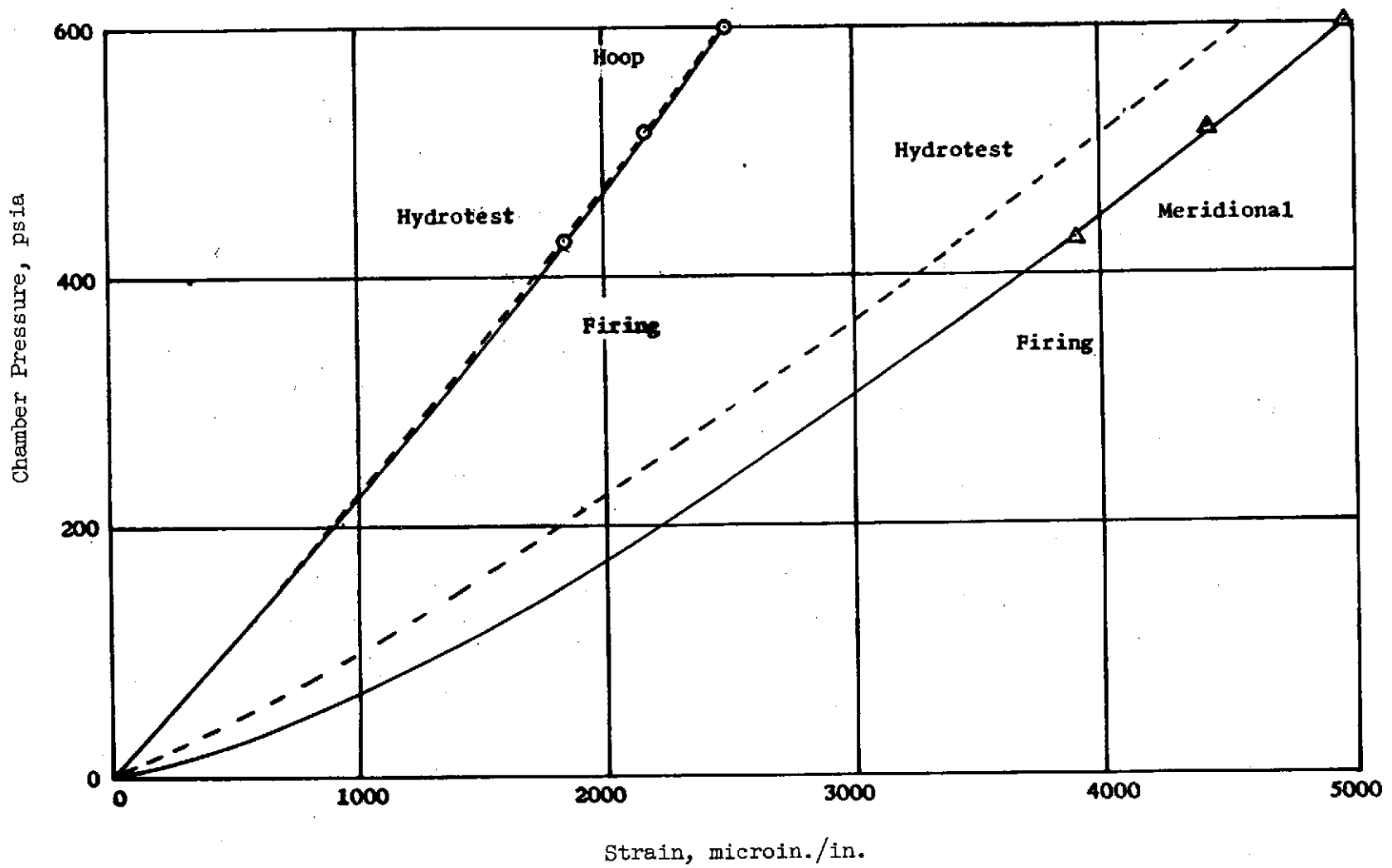


Chamber Strain, Locations S-3 and S-4

Figure 45

Chamber Pressure, psia

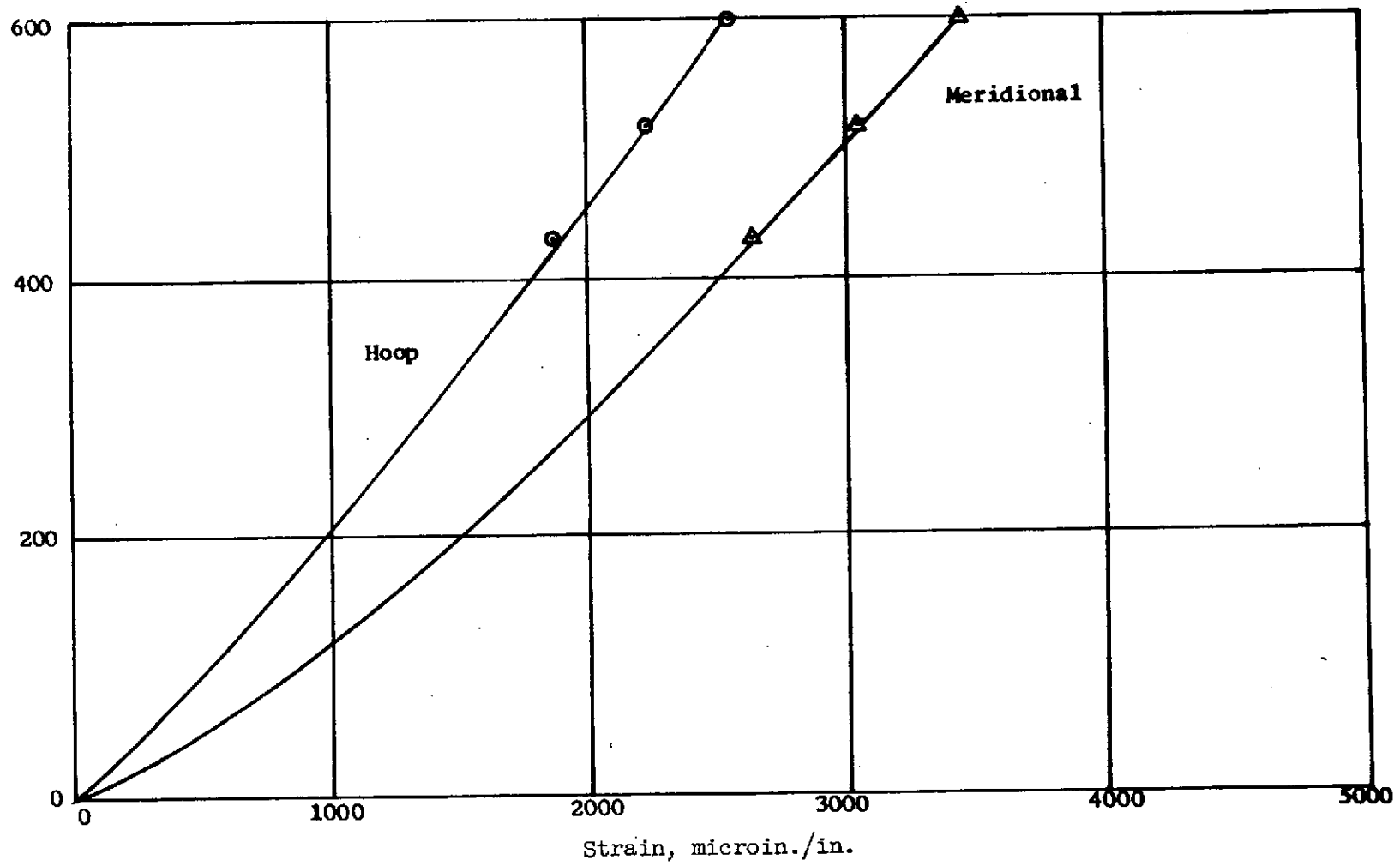
121



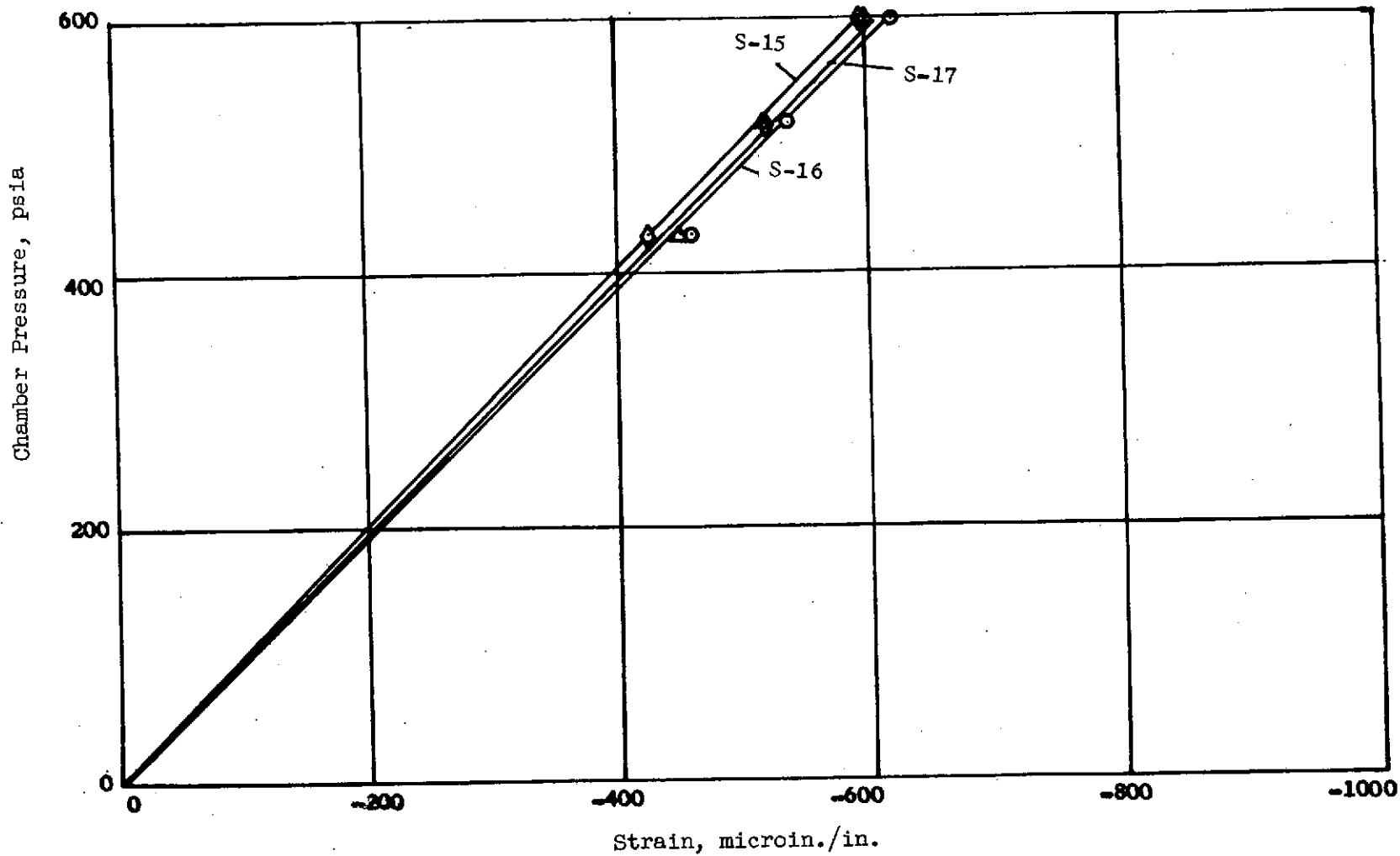
Chamber Strain, Locations S-5 and S-6

Figure 46

Chamber Pressure, psia



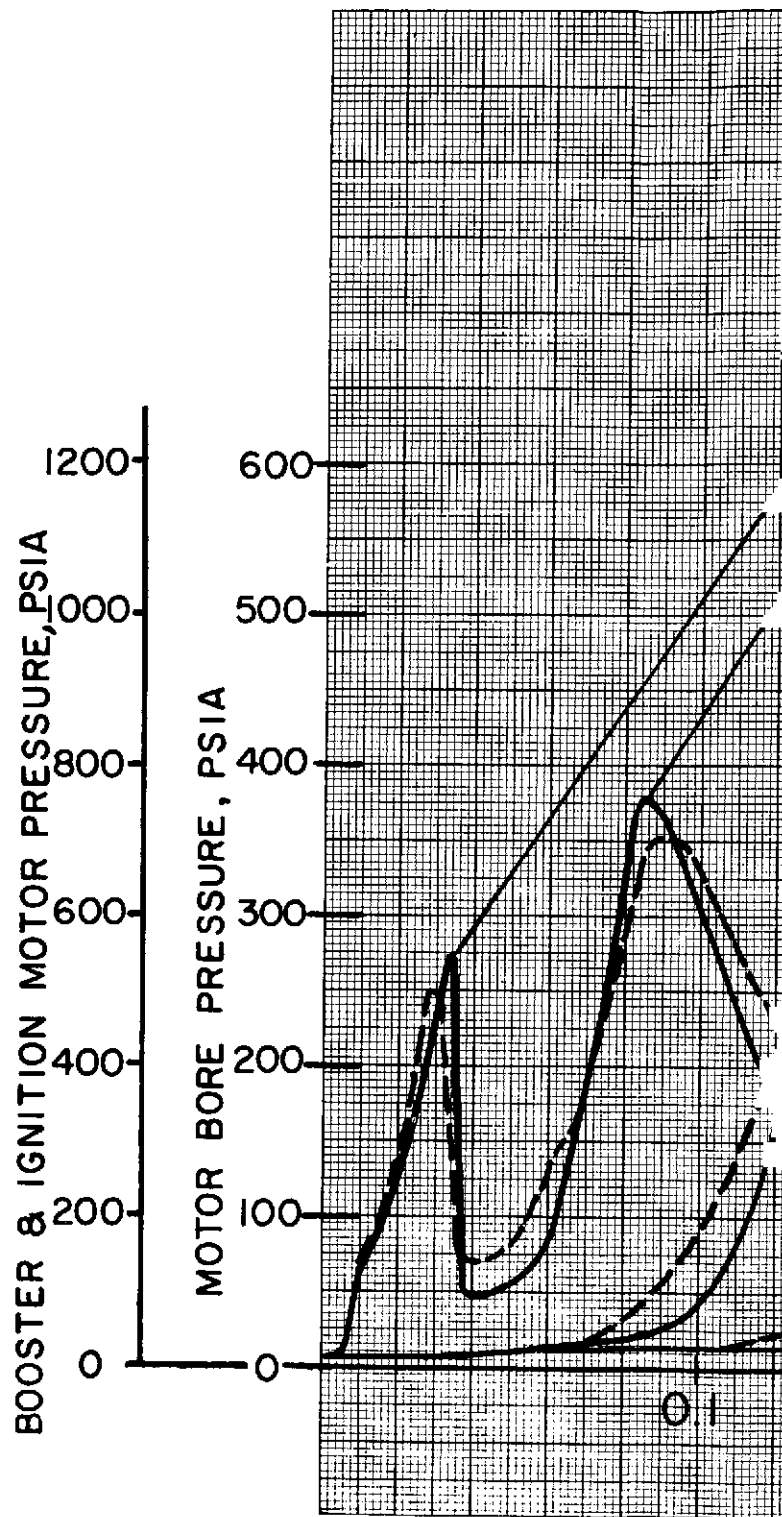
Chamber Strain, Locations S-7 and S-8



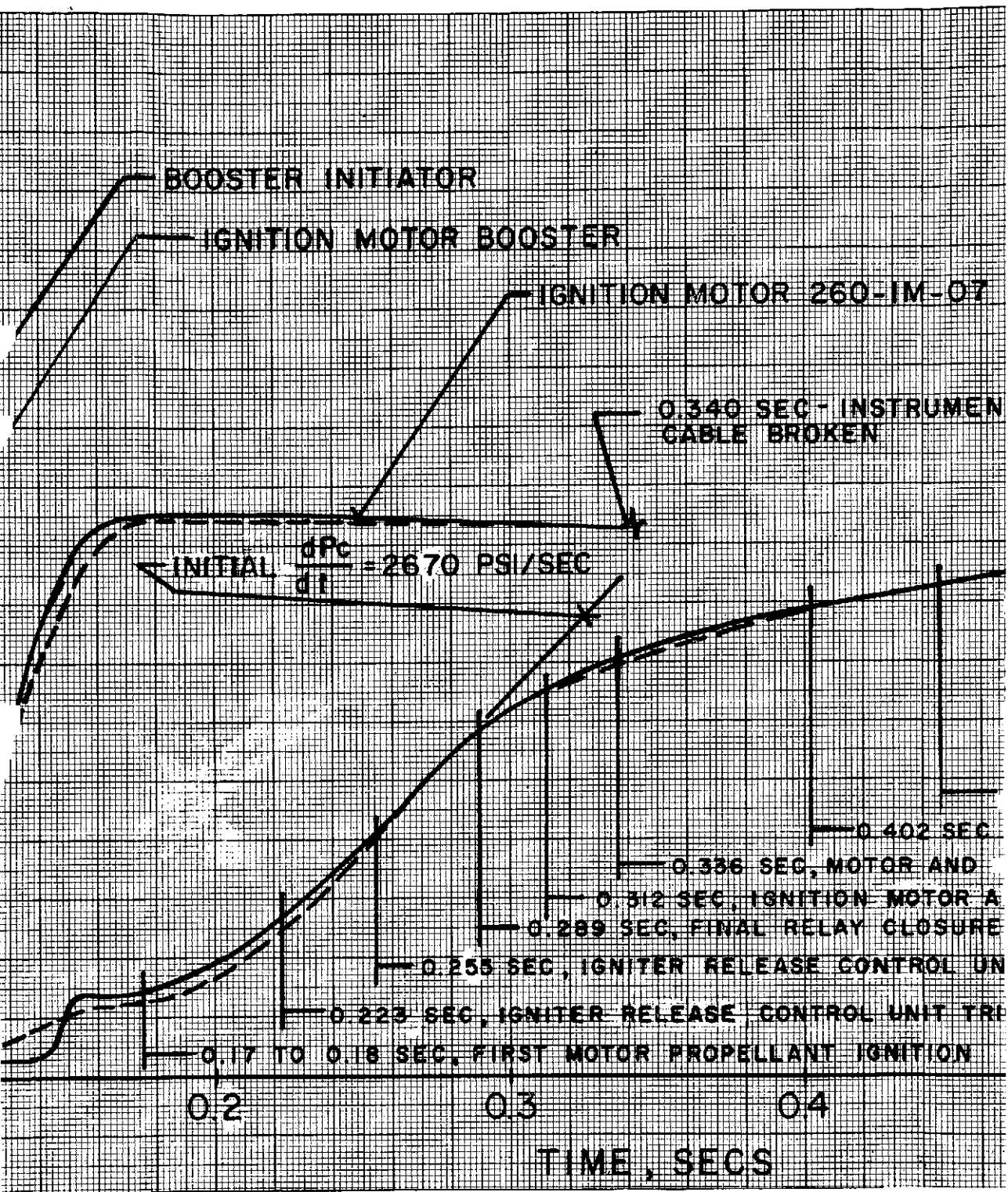
Chamber Strain, Locations S-15, S-16 and S-17

Figure 48

1234



I , meas.	lb-sec	Web duration	INST
I , corr	lb-sec	Web av. press	
I_s	lb-sec/lb	Burning rate	CABLE
I_{s-std}	lb-sec/lb	$\int P_{sn} dt$	
I , vac	lb-sec	$\int P_{sn} A_t dt$	BROKE
I_{s-vac}	lb-sec/lb	$\int_0^F P_{sn} dt$	
I_{s-std}	lb-sec/lb	$A_t av$	
C_w 0.00665	lb/lb-sec	C_f interval	

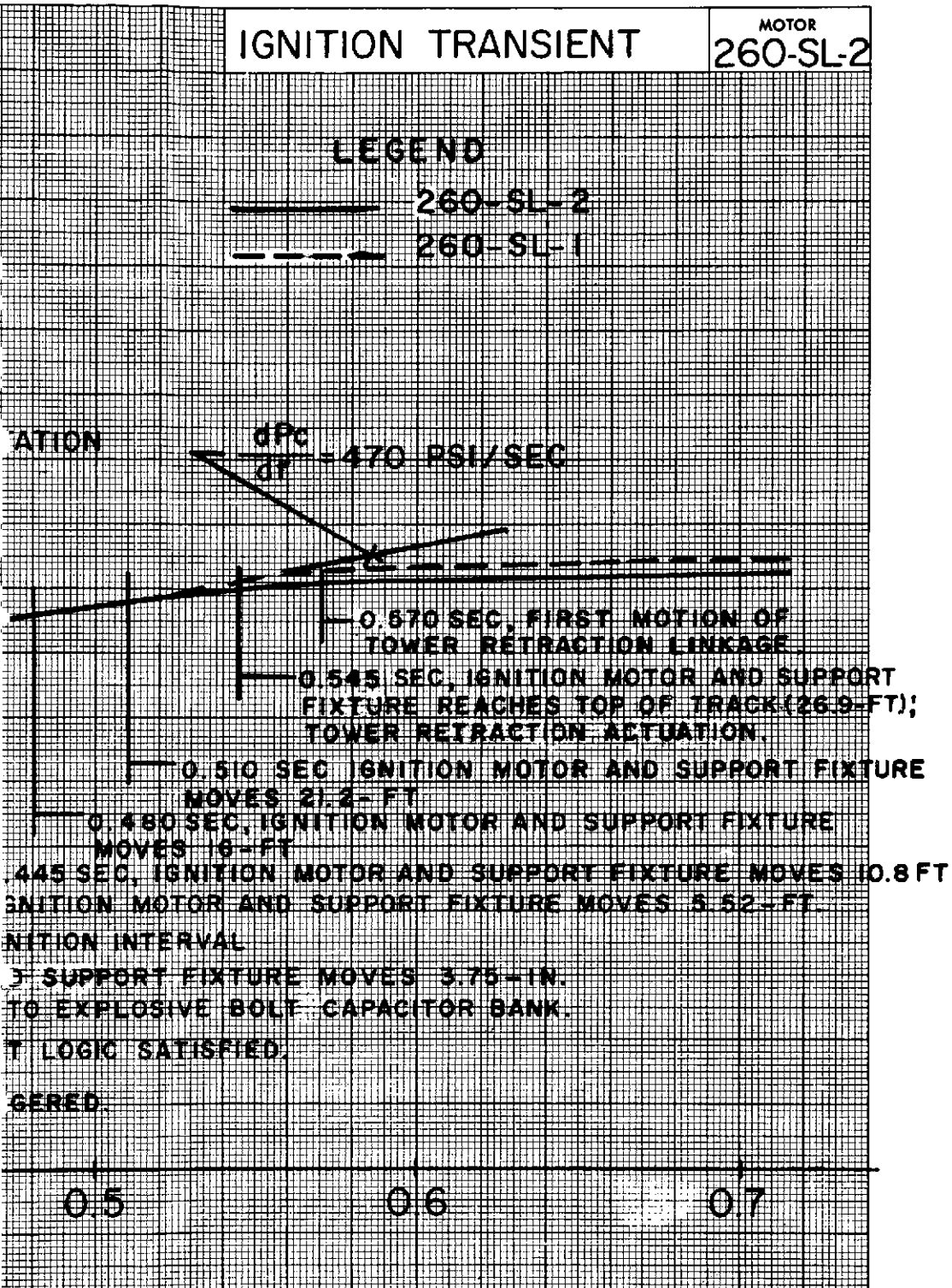


Time, Seconds

sec	Dt (initial) in	¹ 14.488	² 14.492	³ 14.491	⁴ 14.490	Propellant ANP 2758 MOD I	Port area (aft) 462.
psia	Dt (final) in					Weight 1150 lb	Af/At (aft) 2.8 K I
in/sec	De in	29.0				Density 0.0648 lb/in ³	Liner SD-850-2
psia-sec	Ae/At (Initial)	4.0				Batch No. 4-MMI-14815	Total motor wt 47.0
lb-sec	At (initial) 164.82 in ²	At (final)				Configuration 50 POINT INVERT GEAR	Length 157.0 in Dia.
psia-sec	Div half angle 12° 30'					Grain length 90.0 in	Cond temp 60-100
in ²	Throat matl FM 5131 SILICA CLOTH					Grain O. D. 29.0 in	Ign prim. charge 78
	Kf 0.975	Ign interval 138 ms				Web thickness 0.50 in	Main charge 1400

Motor 260-SL-2 Ignition Trans

49-2



in ²	Remarks:	Program 260 DEMONSTRATION
8		Contract NAS3-6284
lb		Test No. LM-DA-03S-BV-1
0 in		Assy Dwg No. 600174
°F		Date fired 23 FEB 1966
g		Prep. By D.L. NACHBAR
g		AEROJET-GENERAL CORPORATION SACRAMENTO CALIFORNIA

Figure 49 -3

<u>Event</u>	<u>Time, sec</u>	
	<u>260-SL-1</u>	<u>260-SL-2</u>
Fire Switch		
Initial Initiator Pressure	0.005	0.005
Peak Initiator Pressure	0.030	0.034
Peak Booster Pressure	0.090	0.085
Ignition Motor Ignition Interval	0.142	0.138
First Motor Propellant Ignition	0.180	0.175
Igniter Release Control Unit Triggered	0.225	0.223
Igniter Release Control Unit Logic Satisfied	0.257	0.255
Final Relay Closure to Explosive Bolt Capacitor Bank	0.287	0.289
Ignition Motor and Support Fixture Moves 3 in.	0.311	0.312
Motor Ignition Interval	0.340	0.336
Ignition Motor and Support Fixture Moves 10.4 ft	0.438	0.445
Ignition Motor and Support Fixture Reaches Top of Track; Tower Retraction Actuated	0.604	0.545*
First Motion of Tower Retraction Linkage	0.614	0.570*
Tower Retraction and Retard Complete	5.2	4.8*

*The tower assembly channel-track was shortened 15 ft for the 260-SL-2 motor test as a result, the vehicle actuated the retraction-command breakwire at the top of the track at an earlier time.

260-SL Motor Ignition Sequence



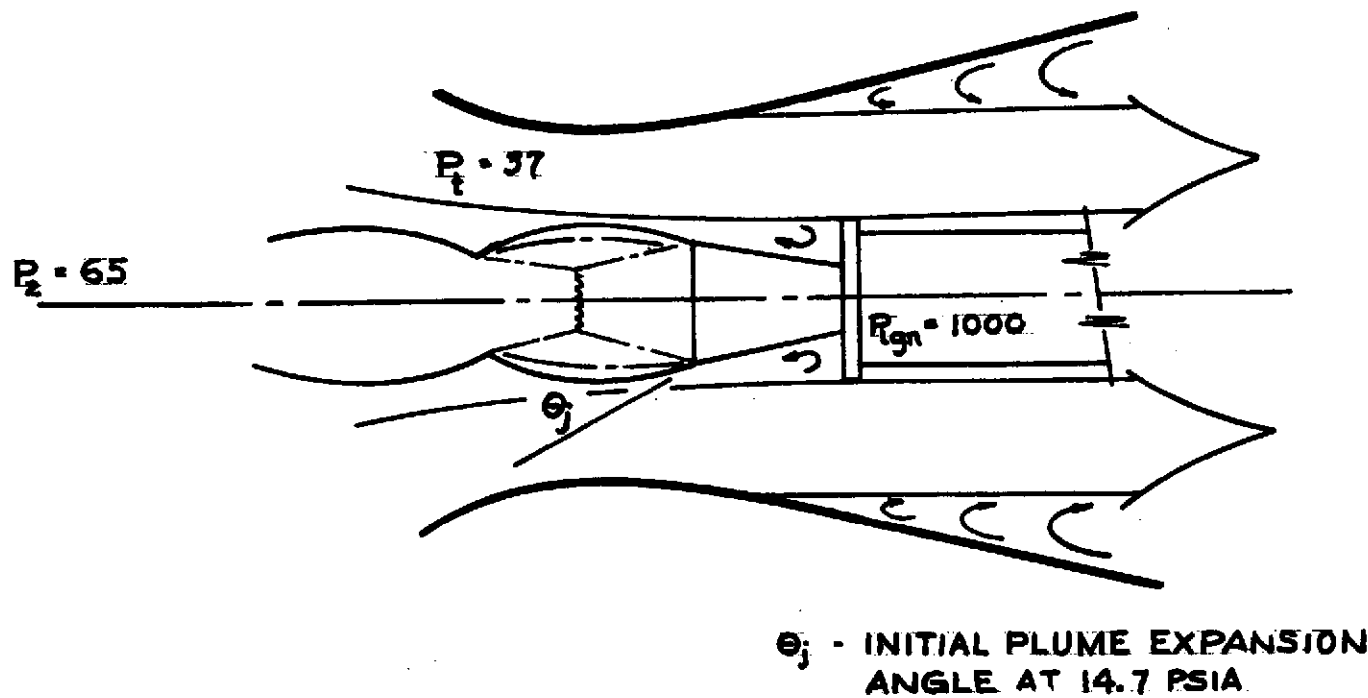
Posttest View of Ignition Motor and Sled Assembly

SUMMARY OF 260-SL IGNITION MOTOR AND BOOSTER ASSEMBLY BALLISTIC PERFORMANCE DATA

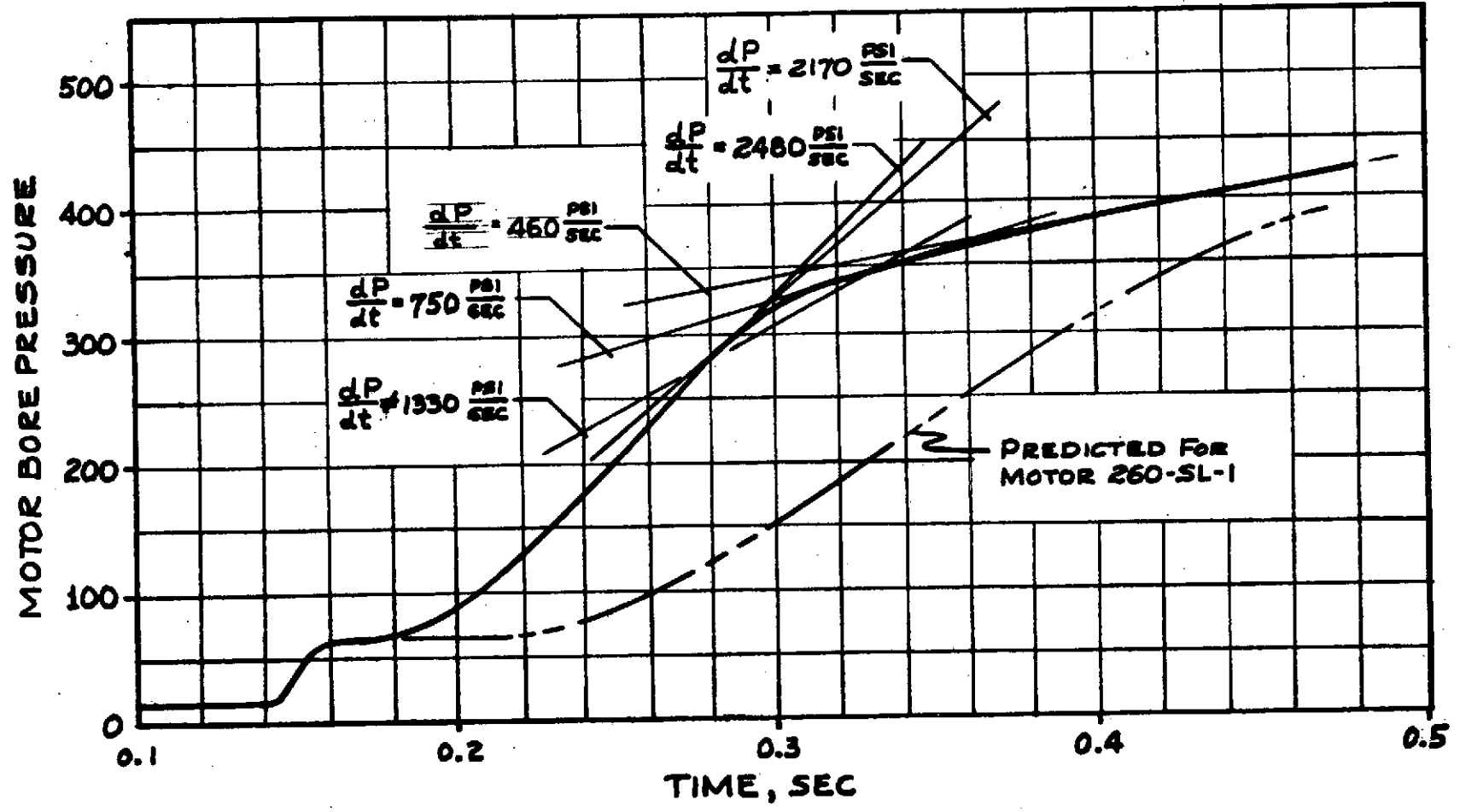
Booster	260-IMB-03	260-IMB-04	260-IMB-05	260-IMB-06	260-IMB-10	260-IMB-11	260-IMB-12	260-IMB-08	260-IMB-13	260-IMB-09
Maximum Initiator Pressure, psia	404	429	464	480	564	465	471	503	539	551
Time to Maximum Initiator Pressure, psia	0.027	0.028	0.028	0.028	0.040	0.034	0.027	0.030	0.033	0.034
Maximum Operating Pressure, psia	530	1041	1038	1023	636	660	660	715	893	703
Time to Maximum Operating Pressure, sec	0.086	0.070	0.071	0.072	0.100	0.094	0.080	0.090	0.073	0.085
Ignition Motor	N/A	260-IM-01	260-IM-02	260-IM-03	260-IM-05	260-IM-04	N/A	260-IM-06	N/A	260-IM-07
Propellant Weight, lb	Booster Test Only	1155	1156	1170	1179	1178	Booster Test Only	1175	Booster Test Only	1175
Maximum Pressure, psia		1103	1128(1)	1002	960	960		950		957
Web Average Pressure, psia		998	(2)	924	900	(4)		(5)		(6)
Web Duration, psia		0.0655	(2)	0.730	0.710	(4)		(5)		(6)
Maximum Thrust, lb		272,000	278,000	250,000	237,000	237,000		232,000		234,000
Maximum Mass Flow Rate, lb/sec		1216	1245	1107	1058	1058		1040		1048
Ignition Interval(3), sec		0.125	0.125	0.115	0.135	0.140		0.142		0.138
Type of Test	Open Air	Open Air	Free Volume	Free Volume	Ignition System Open Air	Ignition System Open Air	Open Air	260-SL-1 Motor Firing	Open Air	260-SL-2 Motor Firing
Test Purpose	Booster Performance Verification	Ignition Motor Assembly Performance Verification	Ignition Capability	Ignition Capability	Ignition Motor Assembly/Retention-and-Release System Demonstration	Ignition Motor Assembly/Retention-and-Release System Demonstration	Verify Condition of Booster Pyrotechnics for 260-SL-1	Aft-End Ignition Demonstration	Verify Condition of Booster Pyrotechnics for 260-SL-2	Aft-End Ignition Demonstration
Date Fired	12 May 1964	18 June 1964	22 July 1964	31 July 1964	29 Oct 1964	17 Feb 1965	15 June 1965	25 Sept 1965	23 Nov 1965	23 Feb 1966

- (1) Measured pressure data lost at 0.110 sec; pressure calculated from thrust data.
 (2) Thrust data lost at 0.390 sec.
 (3) Time from fire switch to 75% of the ignition motor web average pressure.
 (4) Instrumentation cable lost at 0.58 sec.
 (5) Instrumentation cable lost at 0.330 sec.
 (6) Instrumentation cable lost at 0.360 sec.

Summary of 260-SL Ignition Motor and Booster Assembly Ballistic Performance Data



Flow Conditions in Motor Nozzle Prior to Propellant Ignition

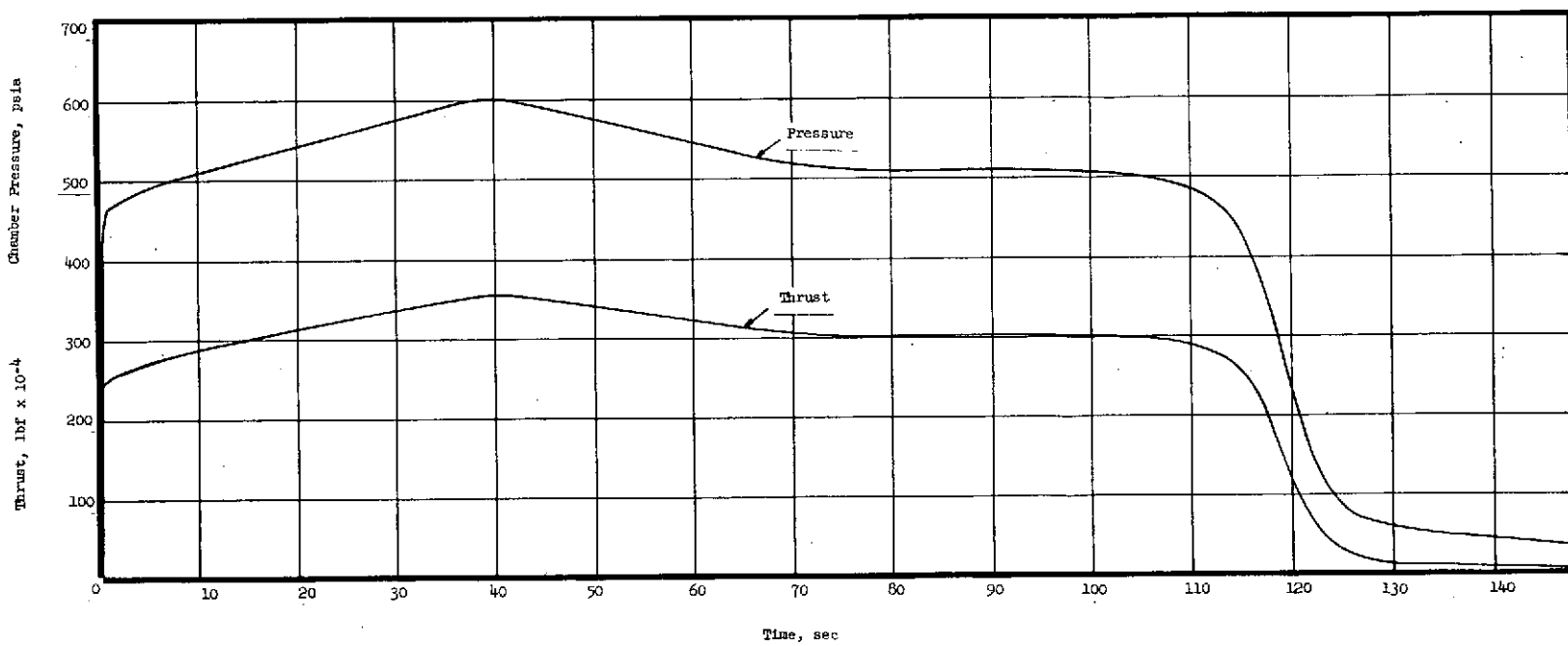


Analysis of 260-SL Motor Pressure Rise

Figure 54

130<

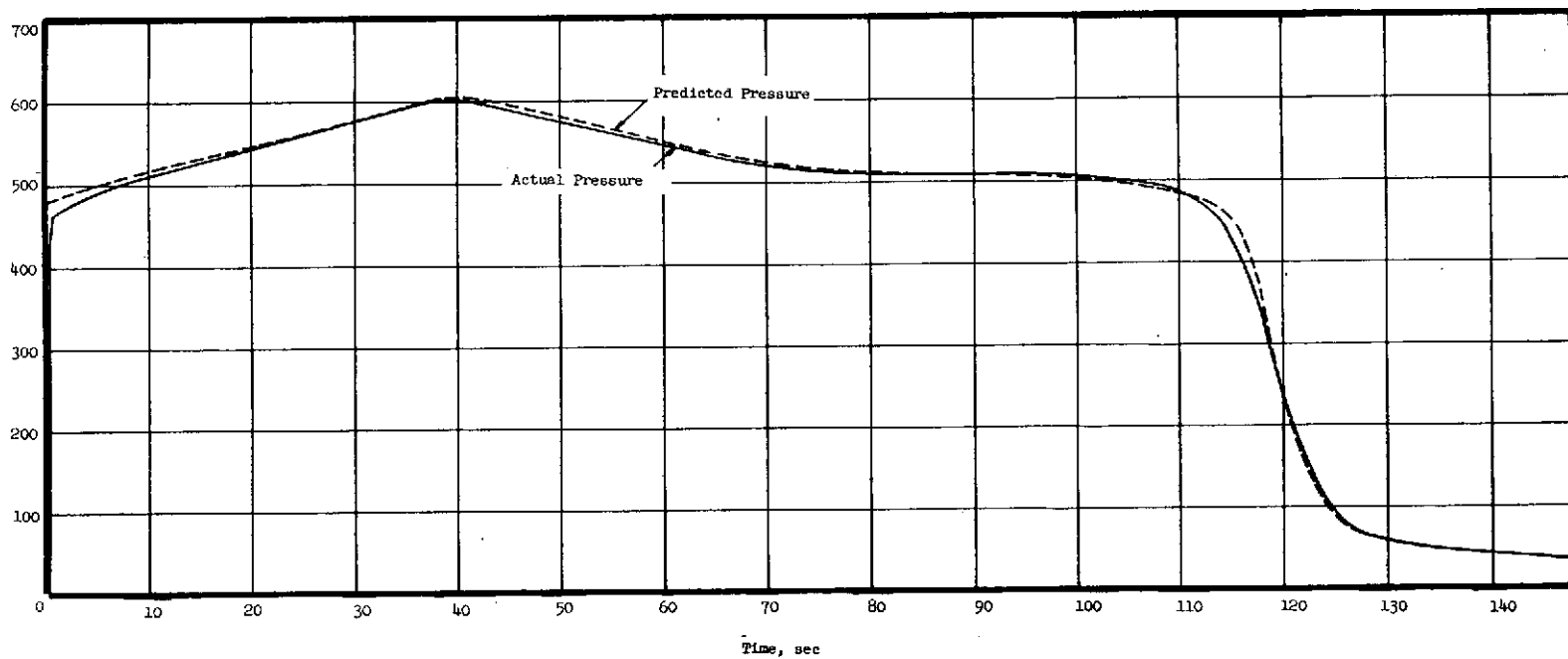
	<u>Predicted</u>	<u>Actual</u>
Total impulse (action time), lbf-sec	369,700,000	371,900,000
Delivered specific impulse, lbf-sec/lbm	227.5	228.9
Standard specific impulse, lbf-sec/lbm	244.6	246.1
Propellant weight, lbm	1,673,000	1,673,000
Web action time, sec	114.9	114.0
Action time, sec	129.8	129.8
Maximum pressure, psia	604	601
Average pressure (web action time), psia	531	530
Average pressure (action time), psia	493	489
Maximum thrust, lbf	3,519,000	3,564,000
Average thrust (web action time), lbf	3,089,000	3,141,000
Average thrust (action time), lbf	2,848,000	2,865,000
Web thickness (average), in.	52.15	52.15
Propellant burning rate at 600 psia, in./sec	0.460	0.460
Nozzle throat diameter, initial/final, in.	71.00/72.46	71.00/72.25
Nozzle throat area, initial/final, sq. in.	3959/4123	3959/4100
Nozzle expansion ratio, initial	6.0	6.0
Nozzle exit cone half-angle, degrees	17.5	17.5



Actual 260-SL-2 Ballistic Performance Curve (u)

Figure 56

132



Predicted 260-SL-2 Ballistic Performance Curve

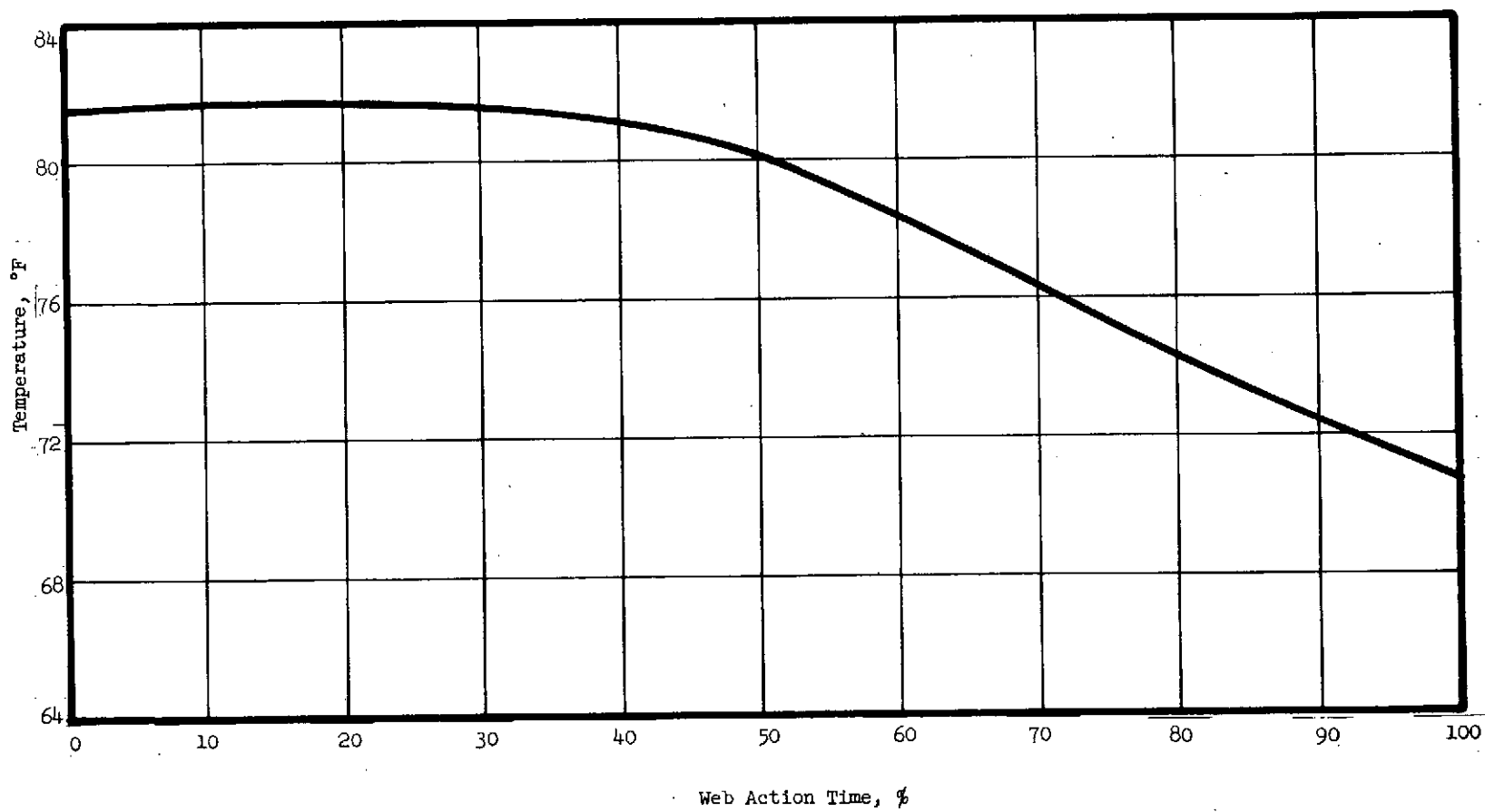
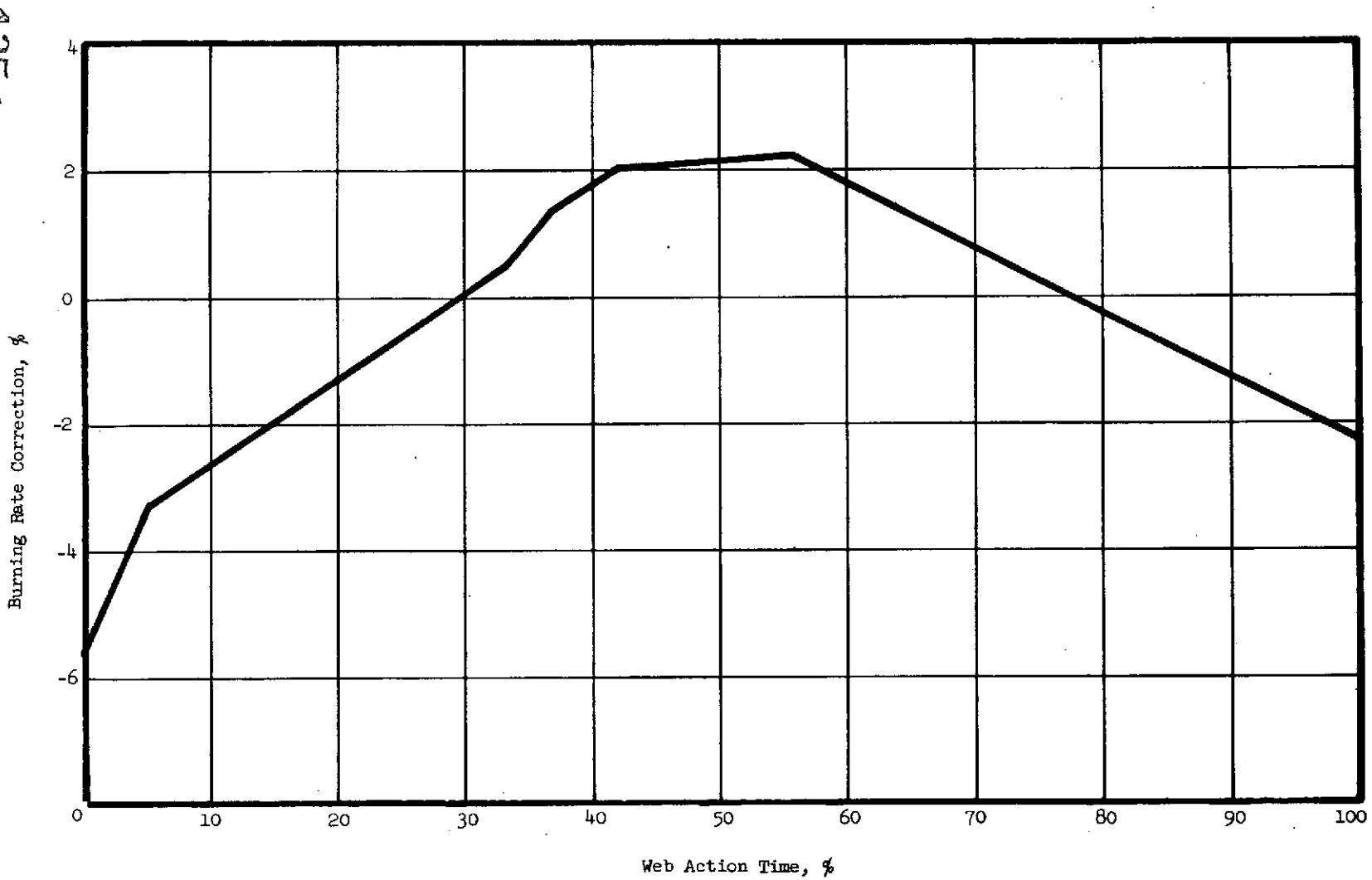


Figure 58

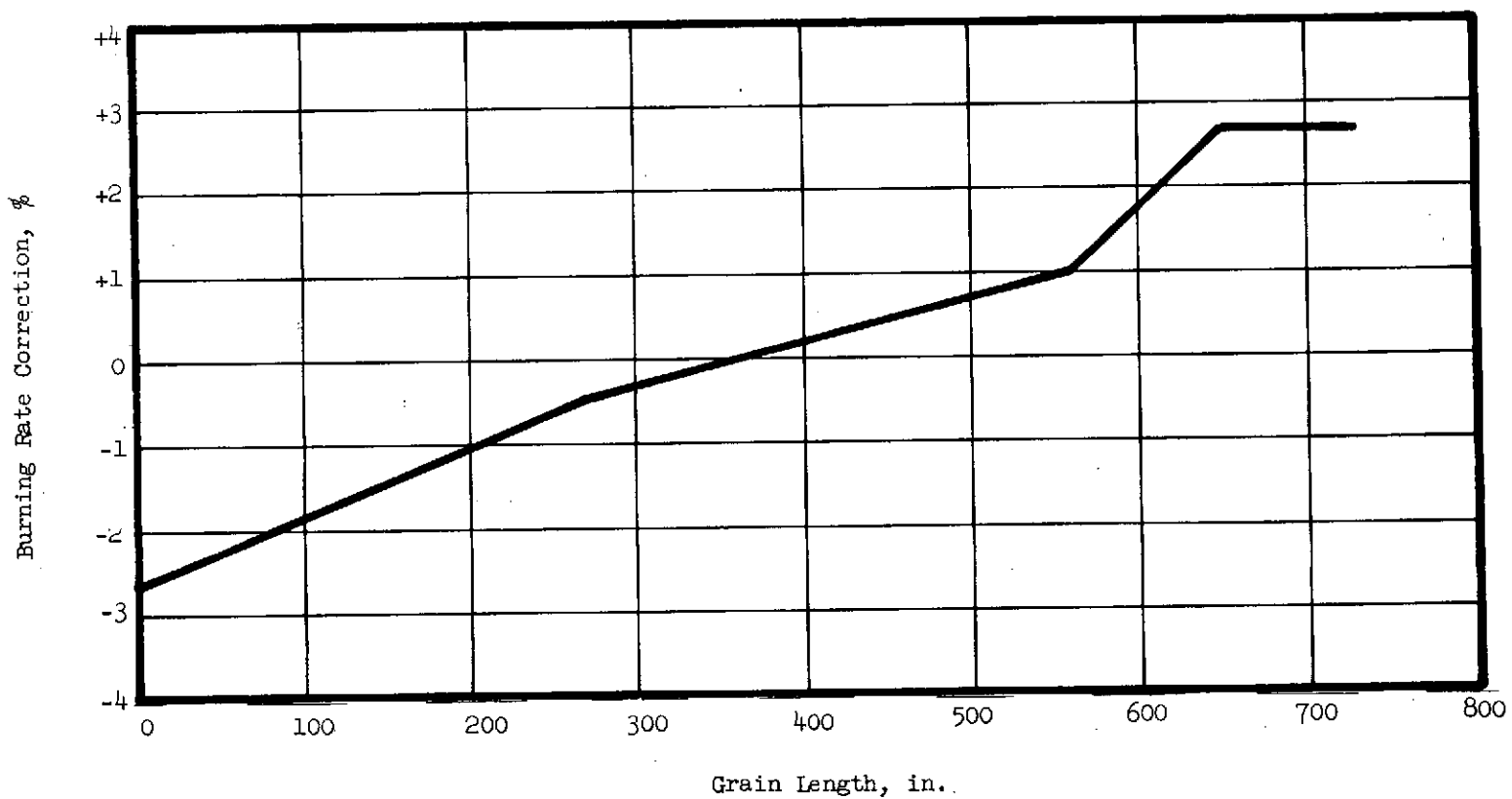
134



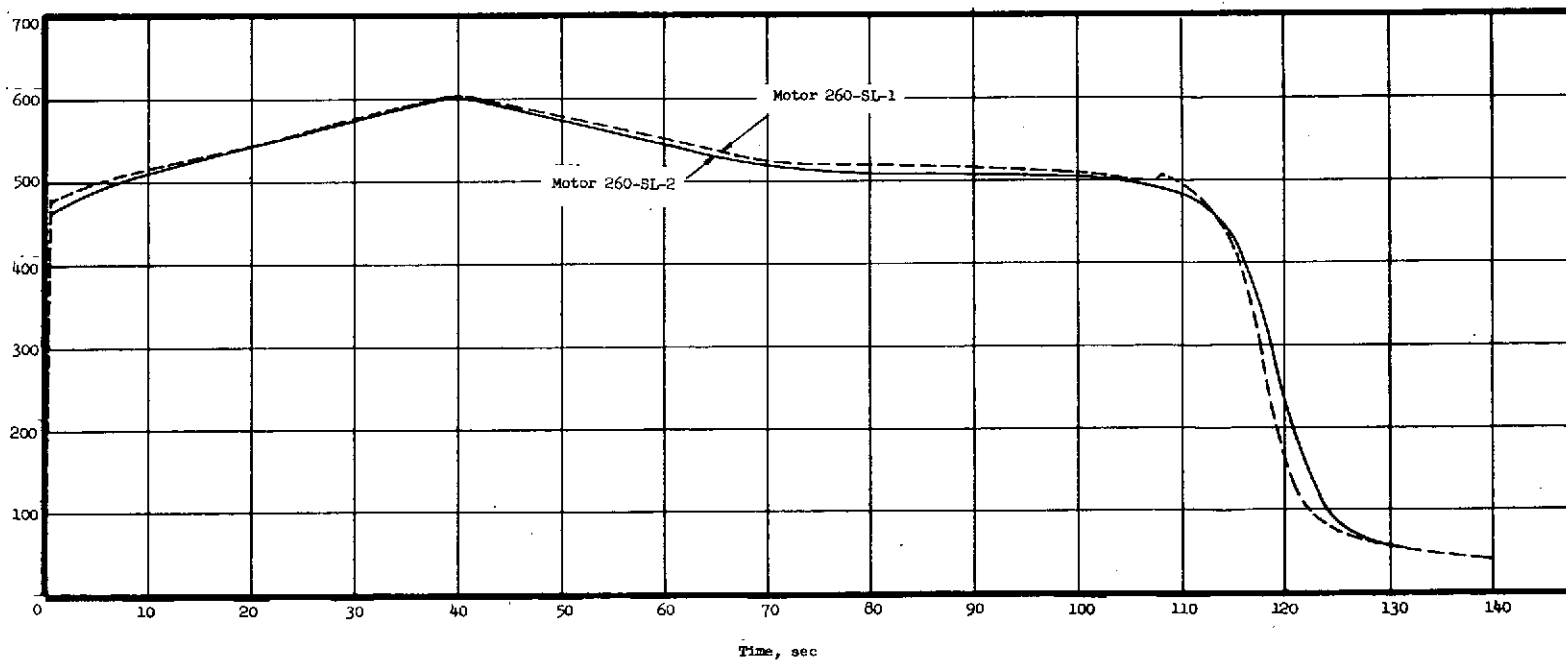
Burning Rate Correction as a Function of Web Action Time

Figure 59

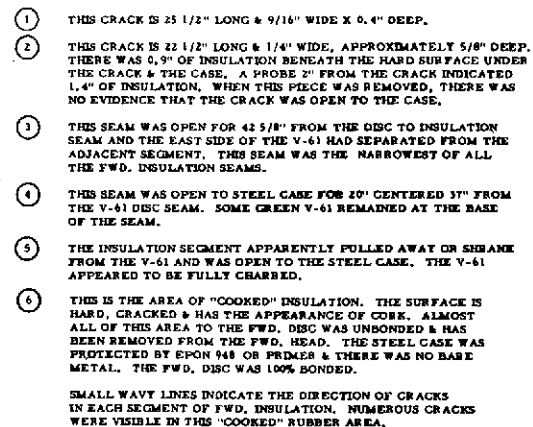
135 ✓



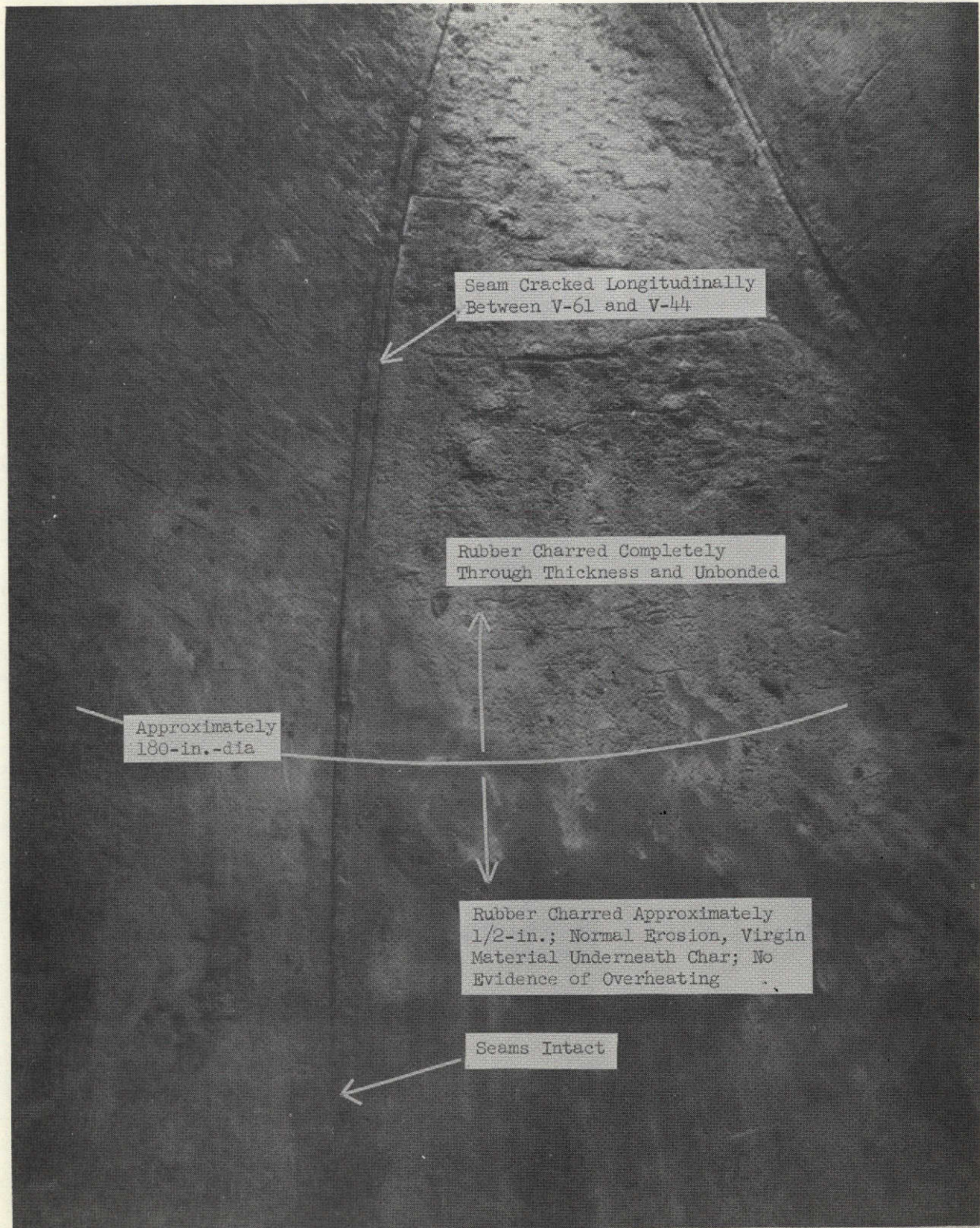
Burning Rate Adjustment as a Function of Grain Length



Comparison of Ballistic Performance of Motors 260-SL-1 and -2



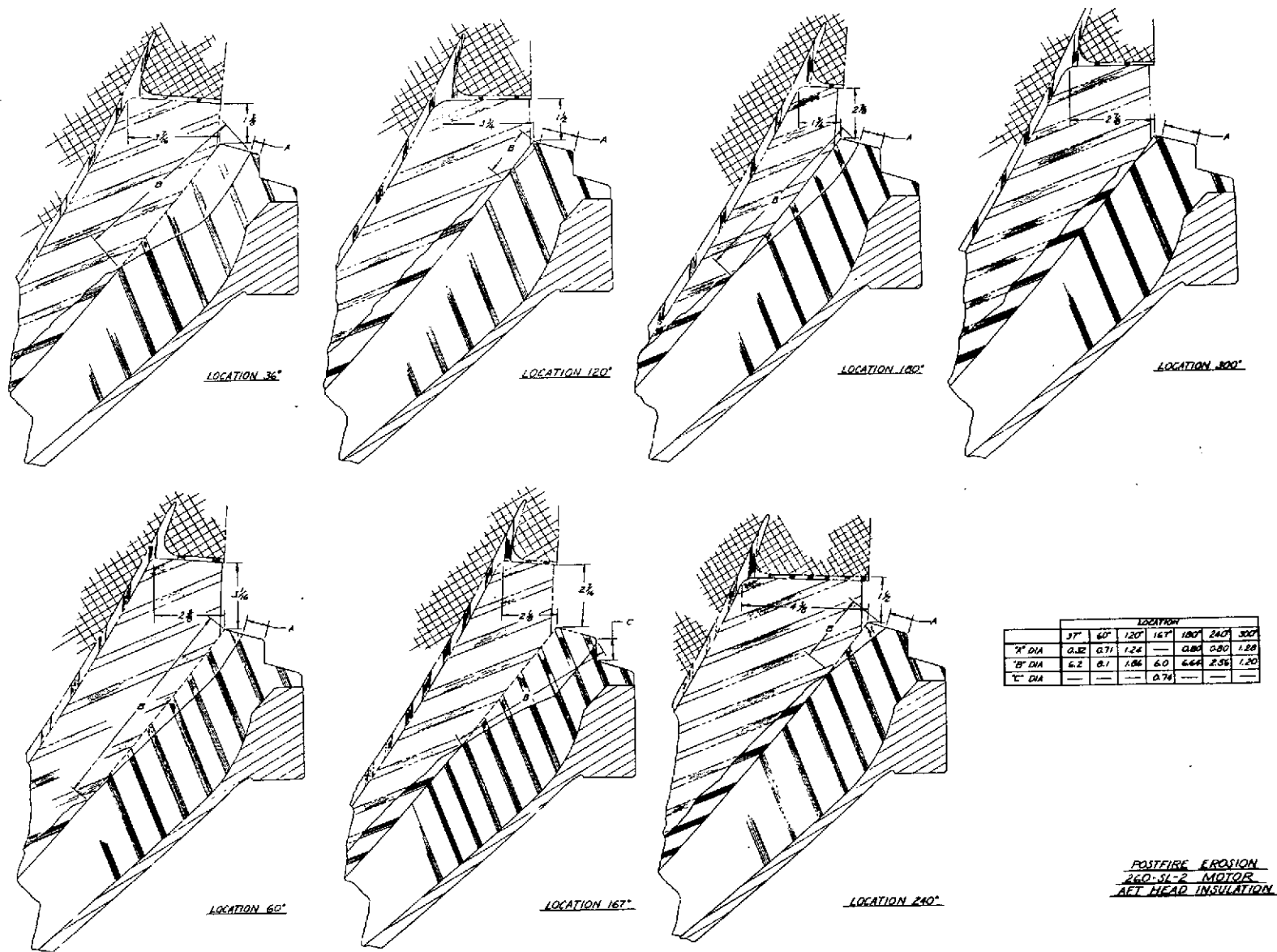
Posttest Condition of Forward Head Insulation





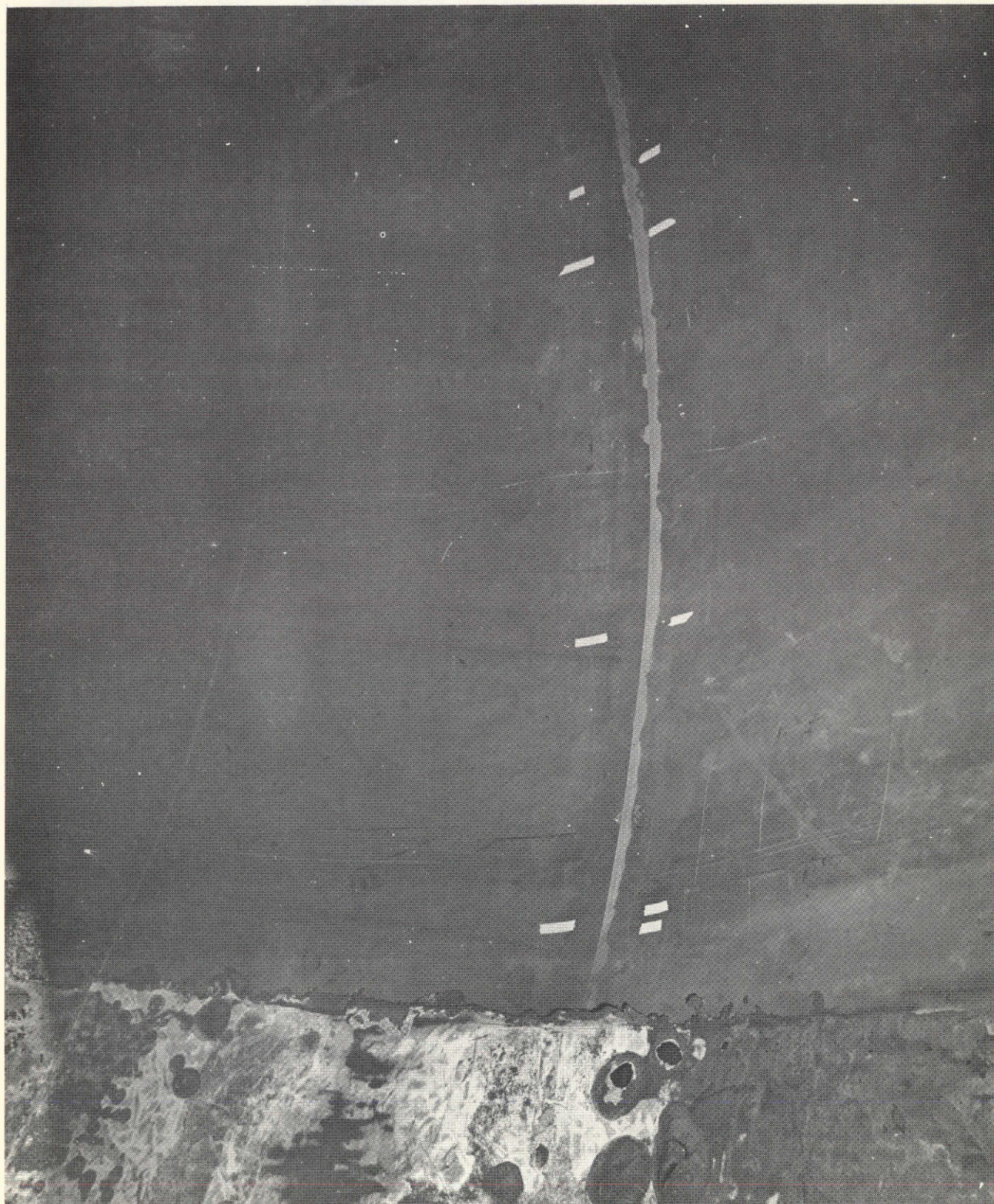
Posttest View of Forward Insulation

Figure 64

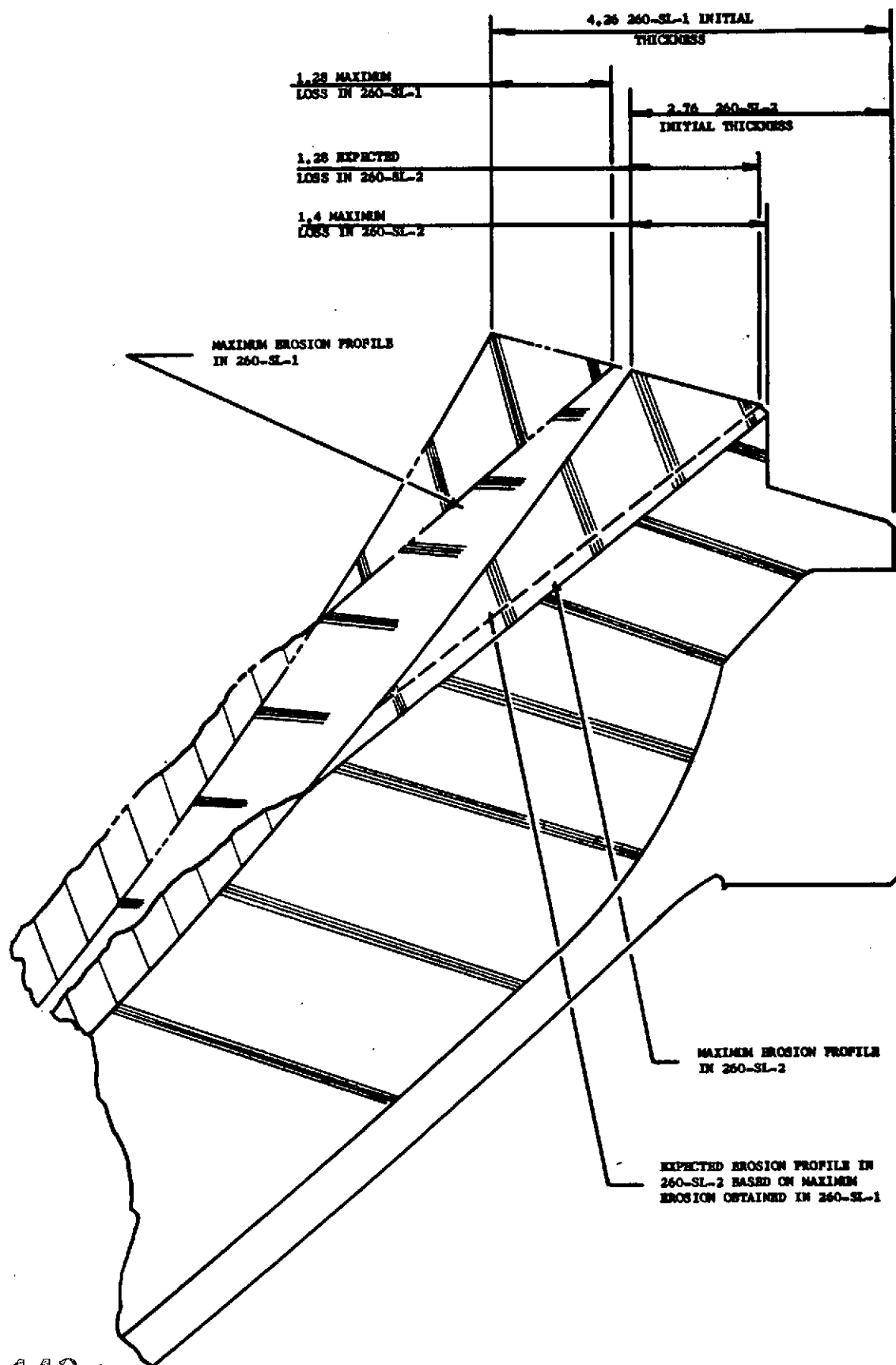


Posttest View of Aft Head Insulation

Figure 65



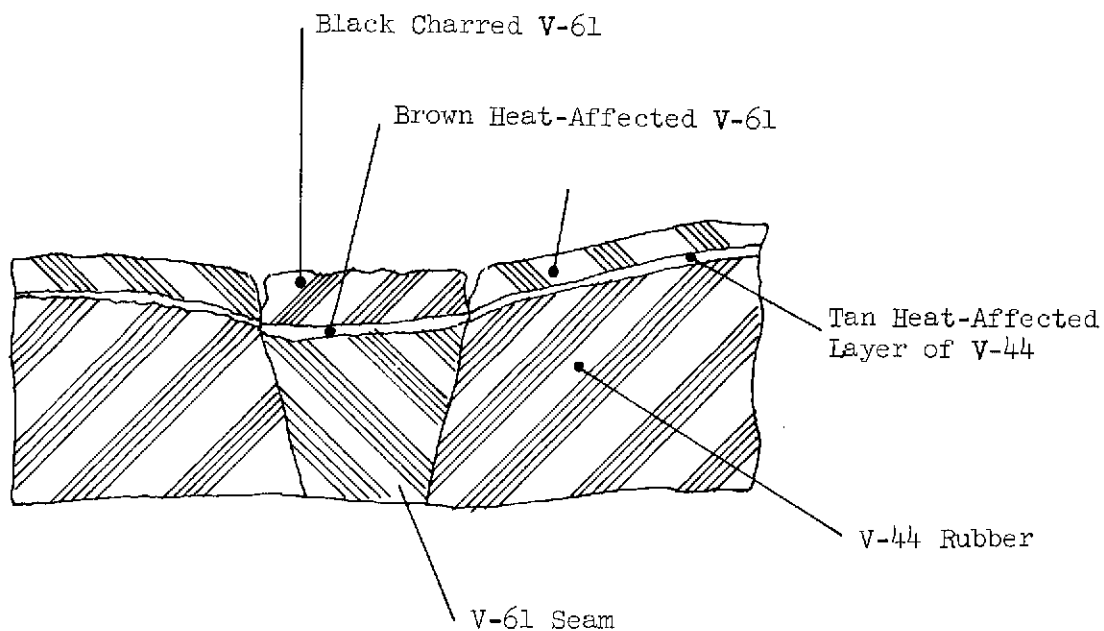
Posttest View of Aft Head Insulation with FMC-200 Potting Compound Removed .



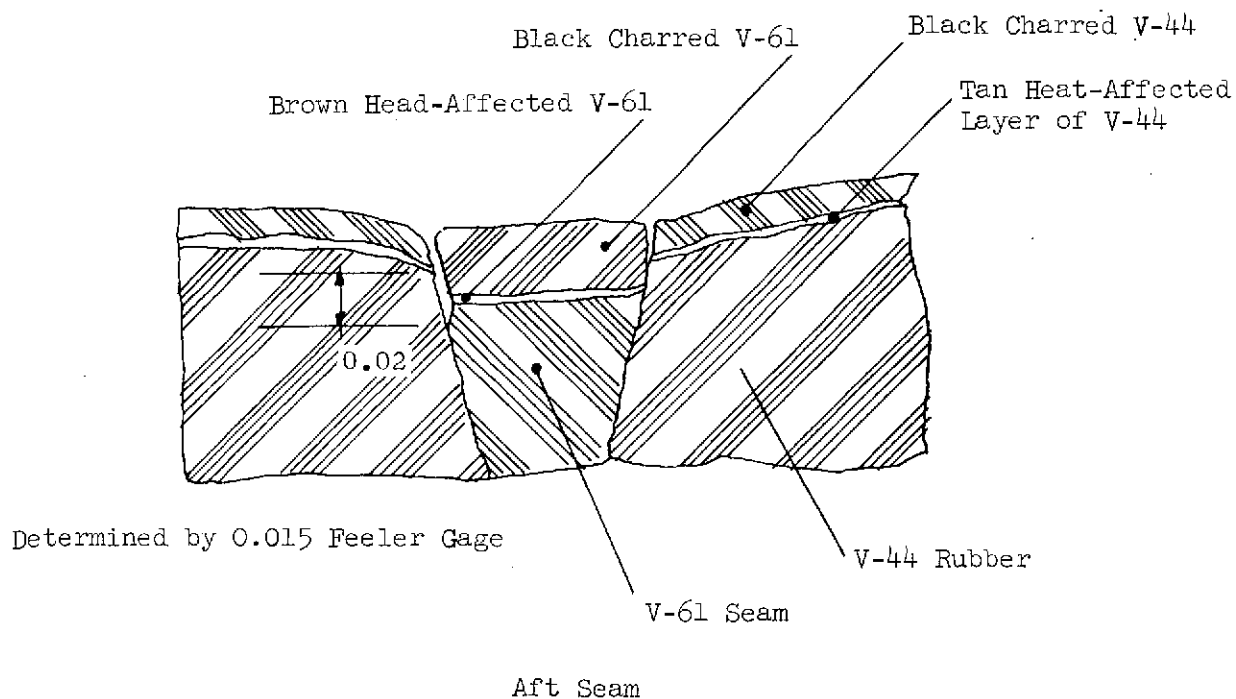
143

Predicted and Actual Aft Head Insulation Erosion

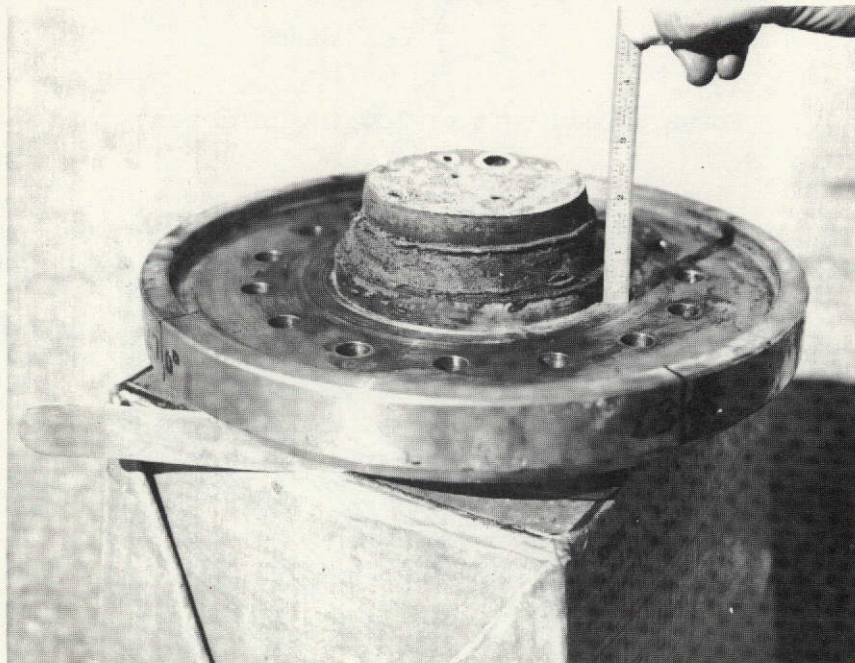
Figure 67



Forward Seam (Aft of 180 in. Diameter)



Posttest Condition of Motor 260-SL-2 Insulation Seams



Posttest View of Firing Cap Insulation

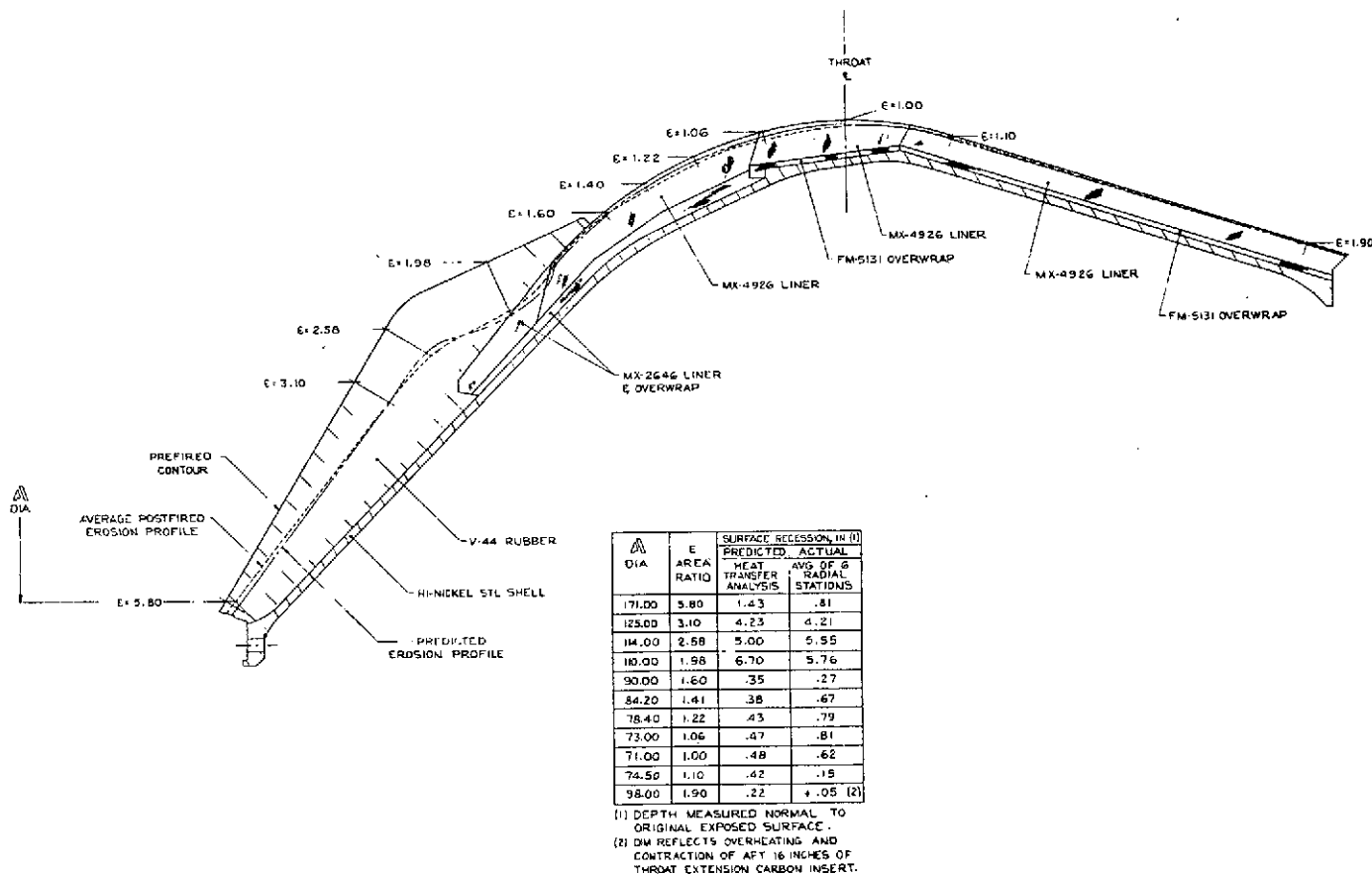
Area Ratio	Material	Predicted Surface Recession, in.*		Actual Surface Recession, in.*								
		Based on Heat Transfer Analysis	Based on Avg 260-SL-1 Data	Radial Location, degrees								
				0	60	120	180	240	300	Avg	Min	Max
-5.80	V-44	1.43**	0.65	0.79	0.83	0.85	0.92	0.85	0.63	0.81	0.63	0.92
-3.10	V-44	4.23**	4.46	4.14	3.87	4.14	4.40	4.20	4.55	4.22	3.87	4.55
-2.58	V-44	5.00**	6.18	5.98	4.94	5.30	5.63	5.44	5.98	5.55	4.94	5.98
-1.98	V-44 and MX-2646	6.70**	6.73	6.50	5.22	5.40	5.73	5.58	6.12	5.76	5.22	6.50
-1.60	MX-4926	0.35	0.37	0.33	0.27	0.36	0.20	0.14	0.32	0.27	0.14	0.36
-1.41	MX-4926	0.38	0.51	0.74	0.67	0.72	0.55	0.59	0.77	0.67	0.55	0.77
-1.22	MX-4926	0.43	0.67	0.85	0.76	0.88	0.68	0.67	0.87	0.79	0.67	0.88
-1.06	MX-4926	0.47	0.84	0.81	0.81	0.81	0.80	0.75	0.91	0.82	0.75	0.91
1.00	MX-4926	0.48	0.70	0.56	0.59	0.56	0.67	0.59	0.71	0.61	0.56	0.71
1.10	MX-4926	0.42	0.28	0.17	0.13	0.09	0.11	0.25	0.17	0.15	0.09	0.25

* Depth measured normal to original exposed surface.

**V-44 recession based on empirical large motor data.

Figure 70

Surface Recession of Motor Nozzle



Nozzle Surface Recession Profile, Motor 260-SL-2

Figure 71

147

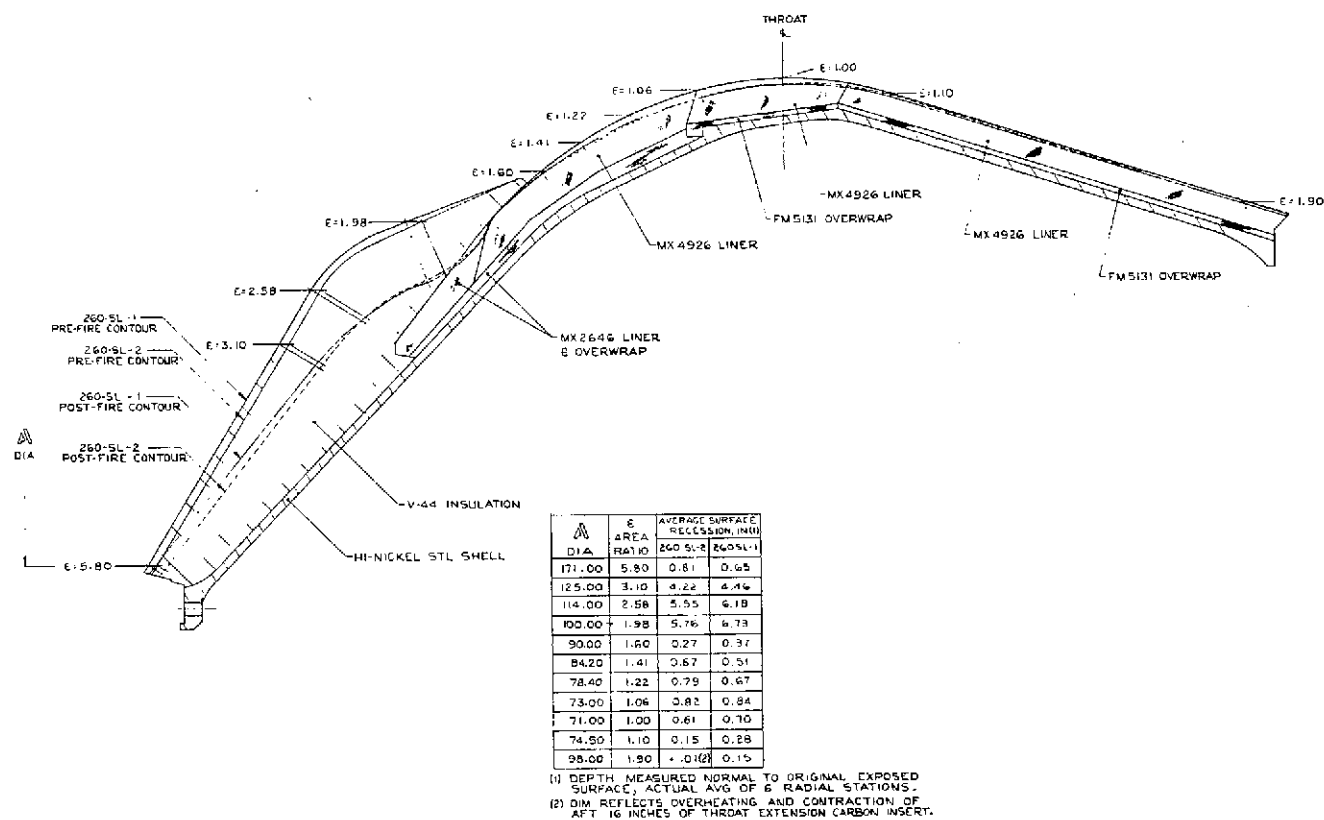
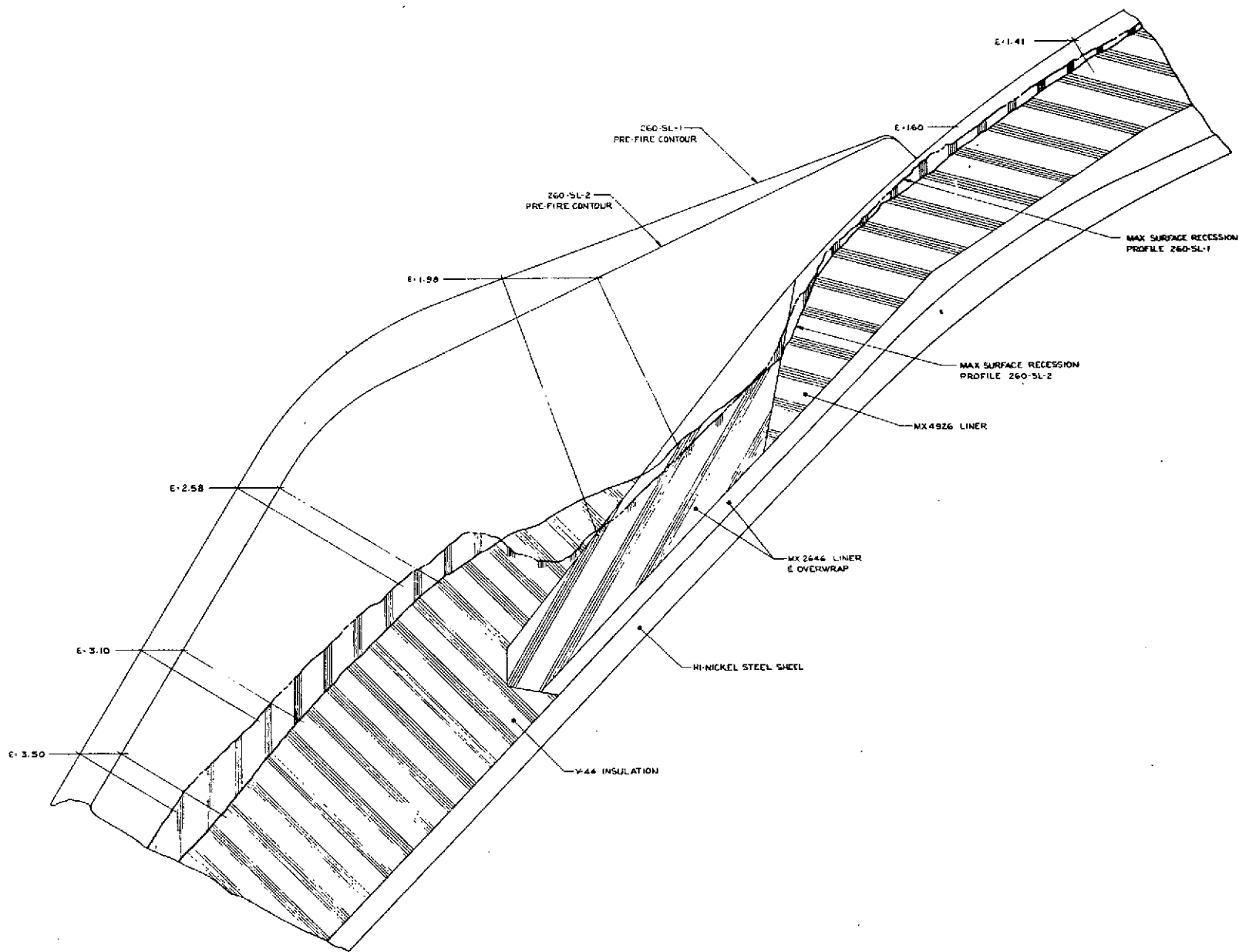
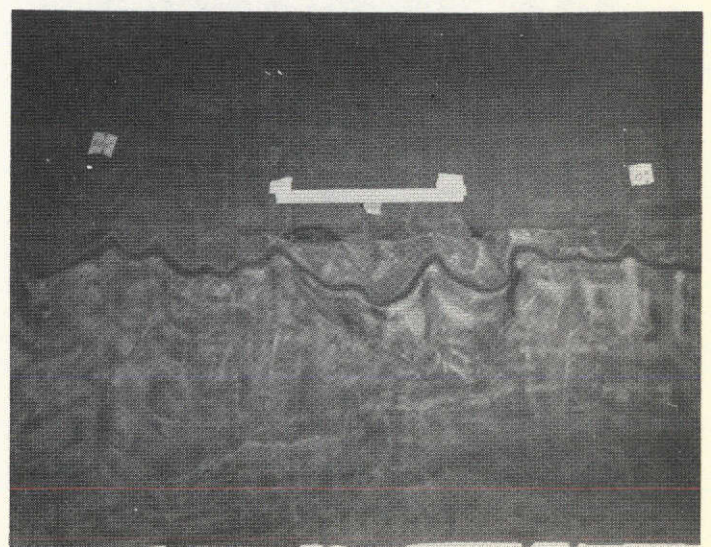
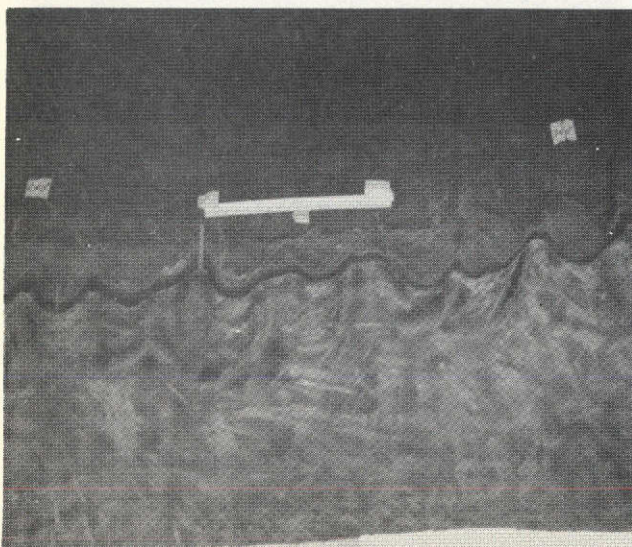
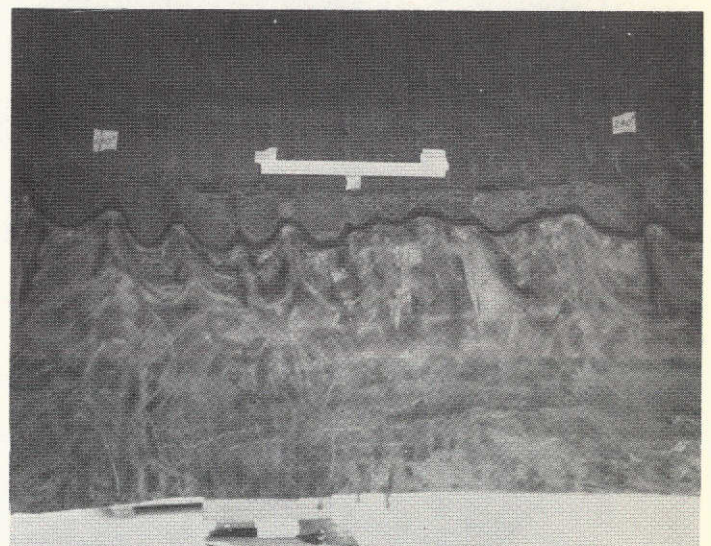
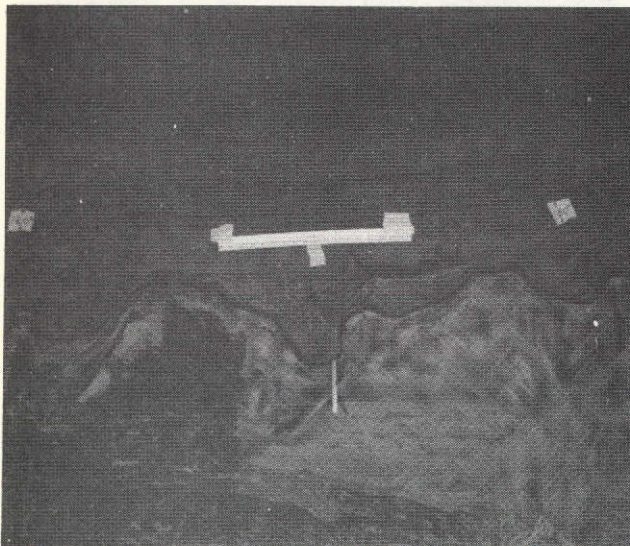
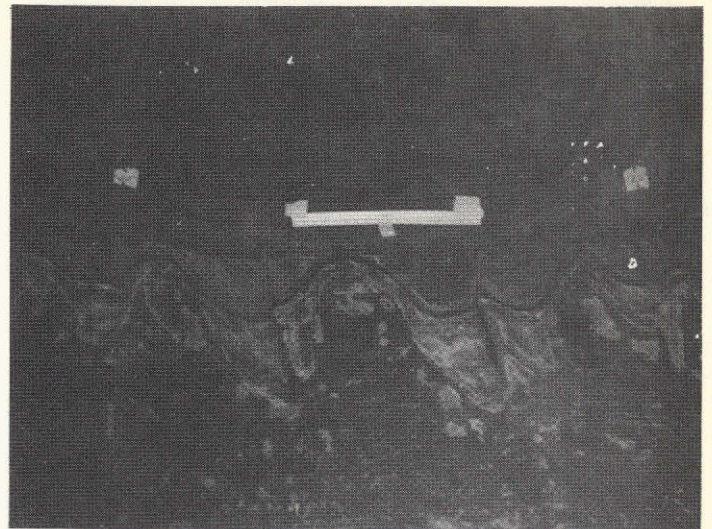
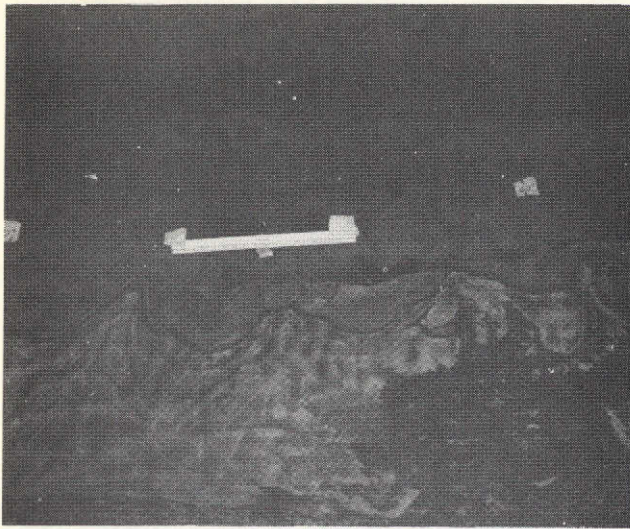


Figure 72

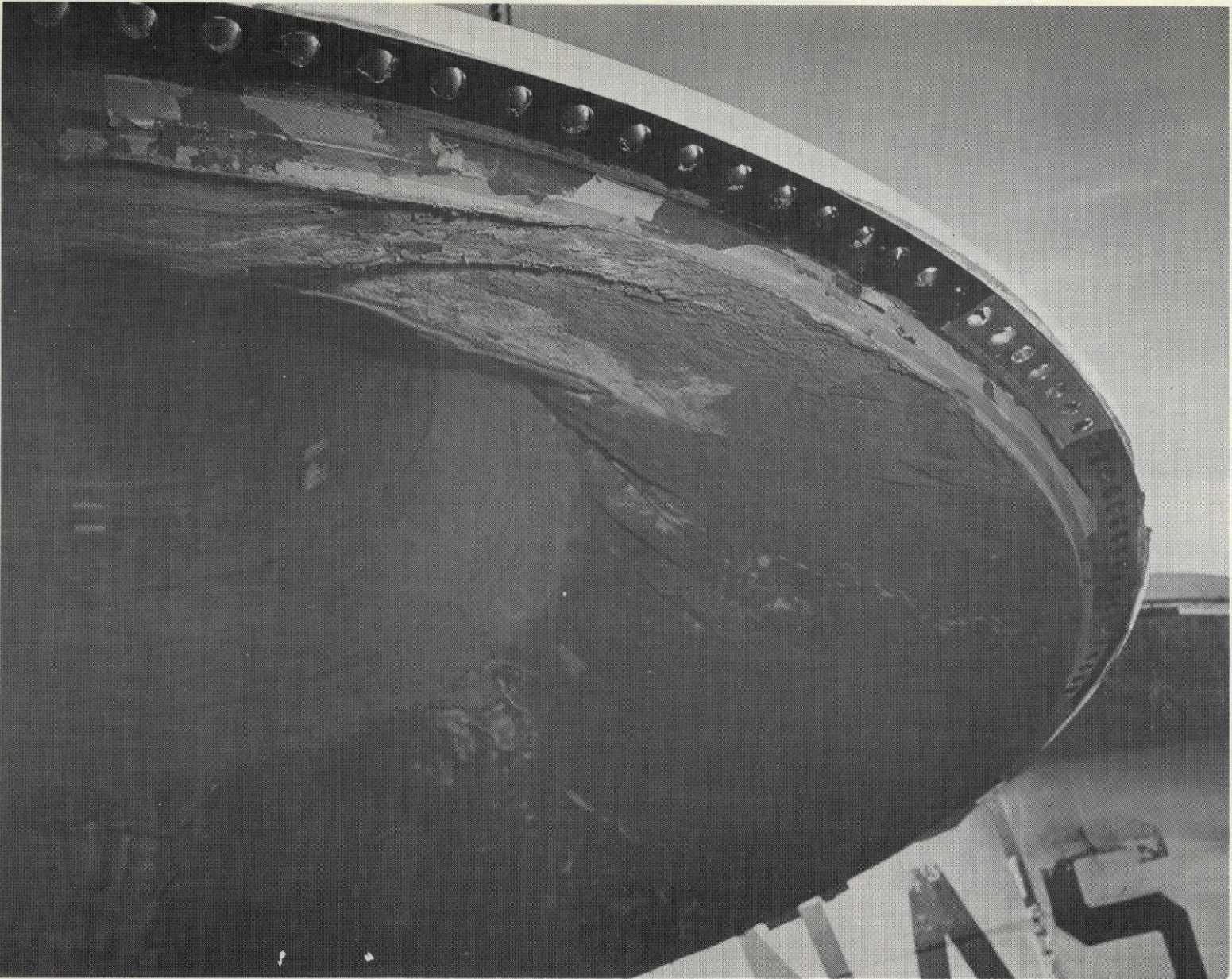


Nozzle Insulation Erosion Profile

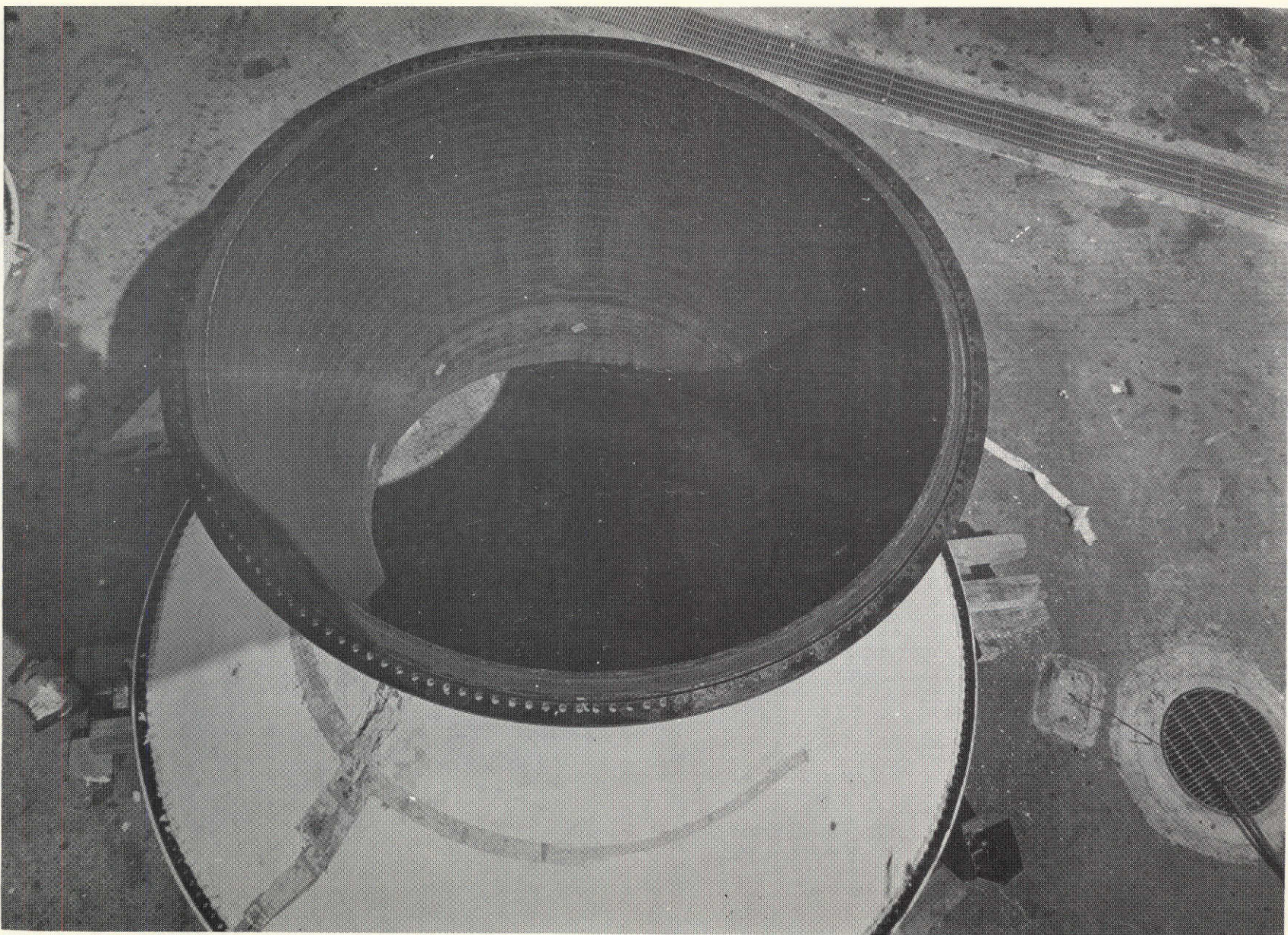


Nozzle Erosion Contour

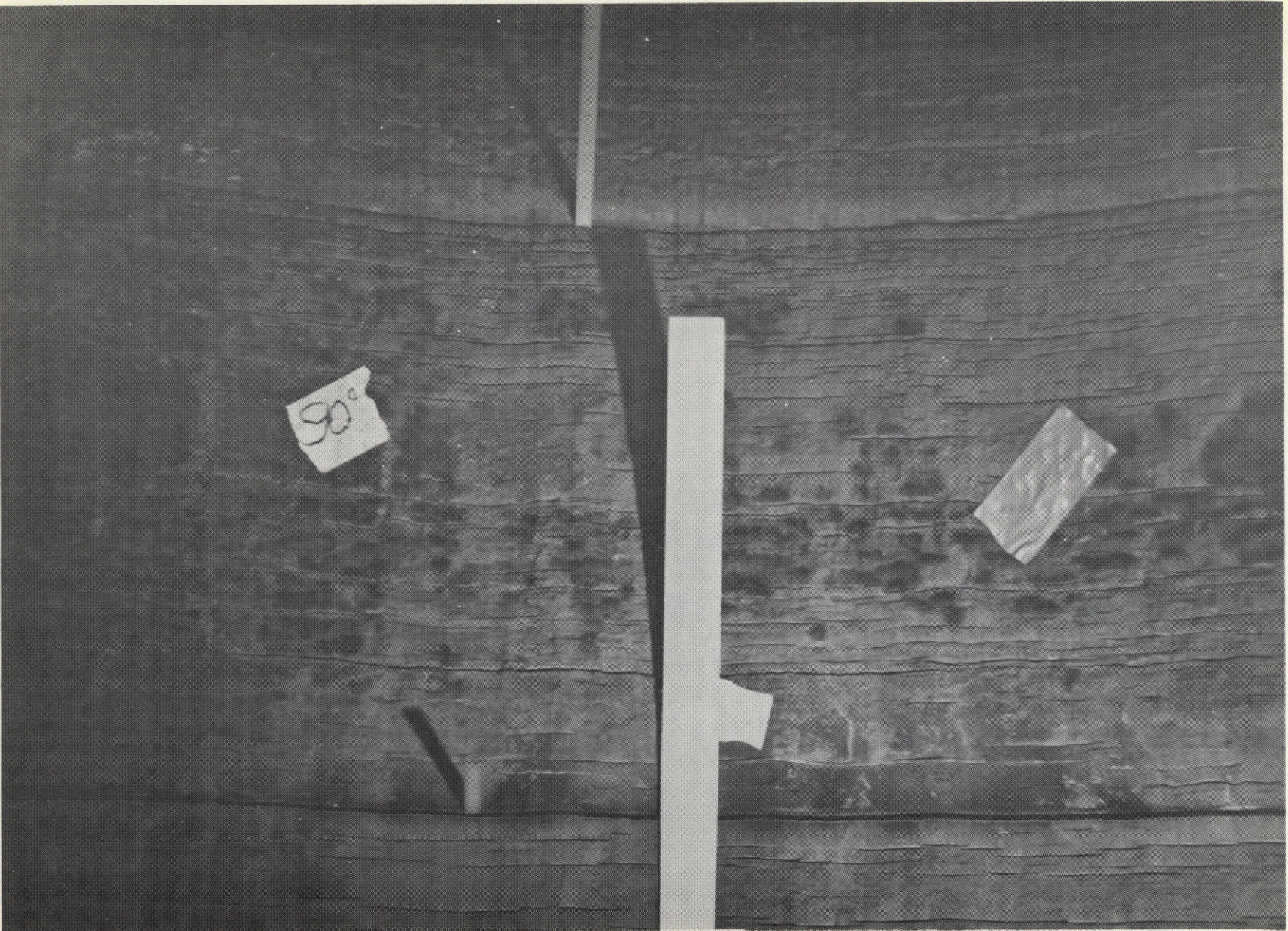
Figure 74



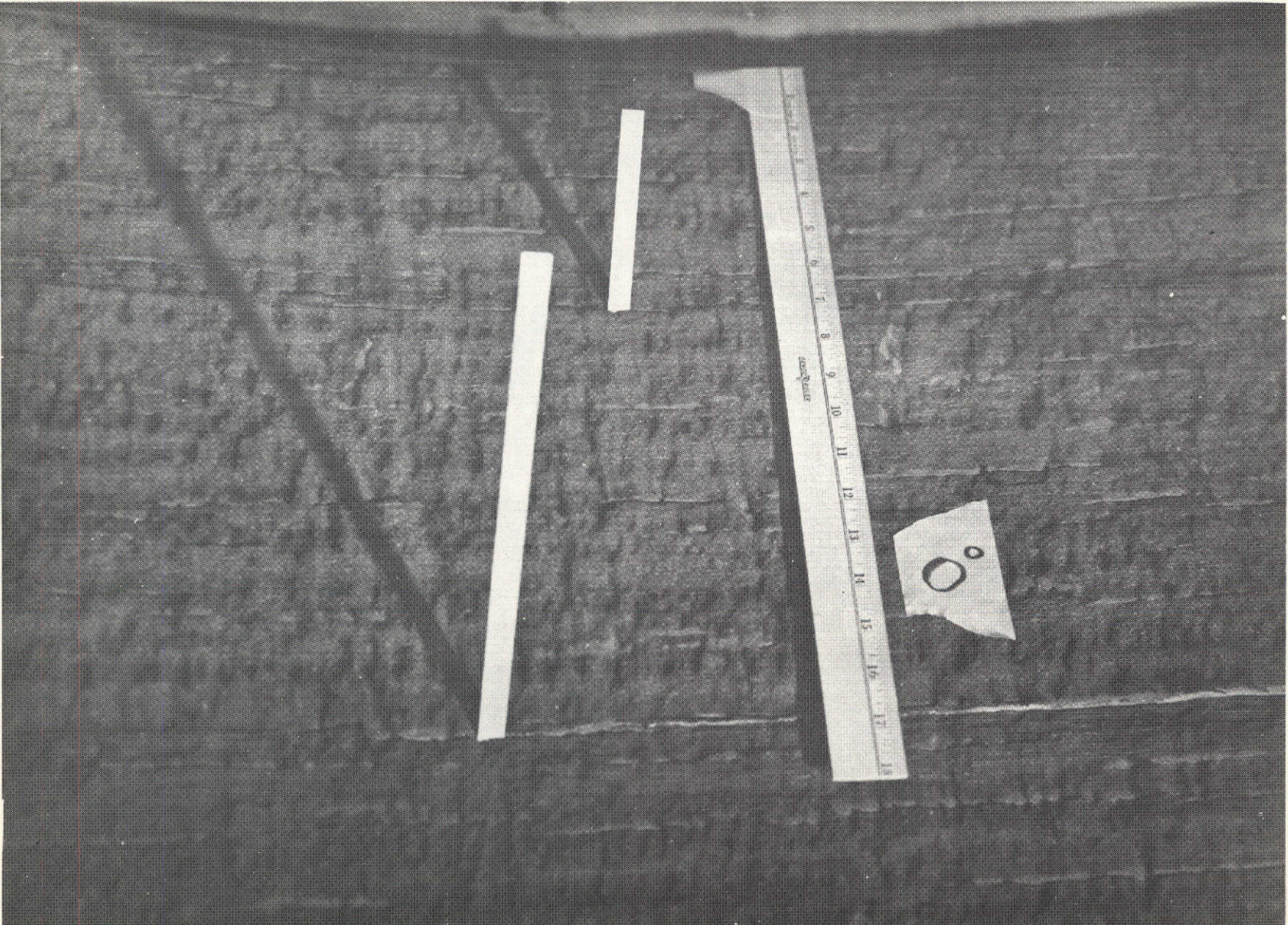
Posttest View of Nozzle Entrance Insert



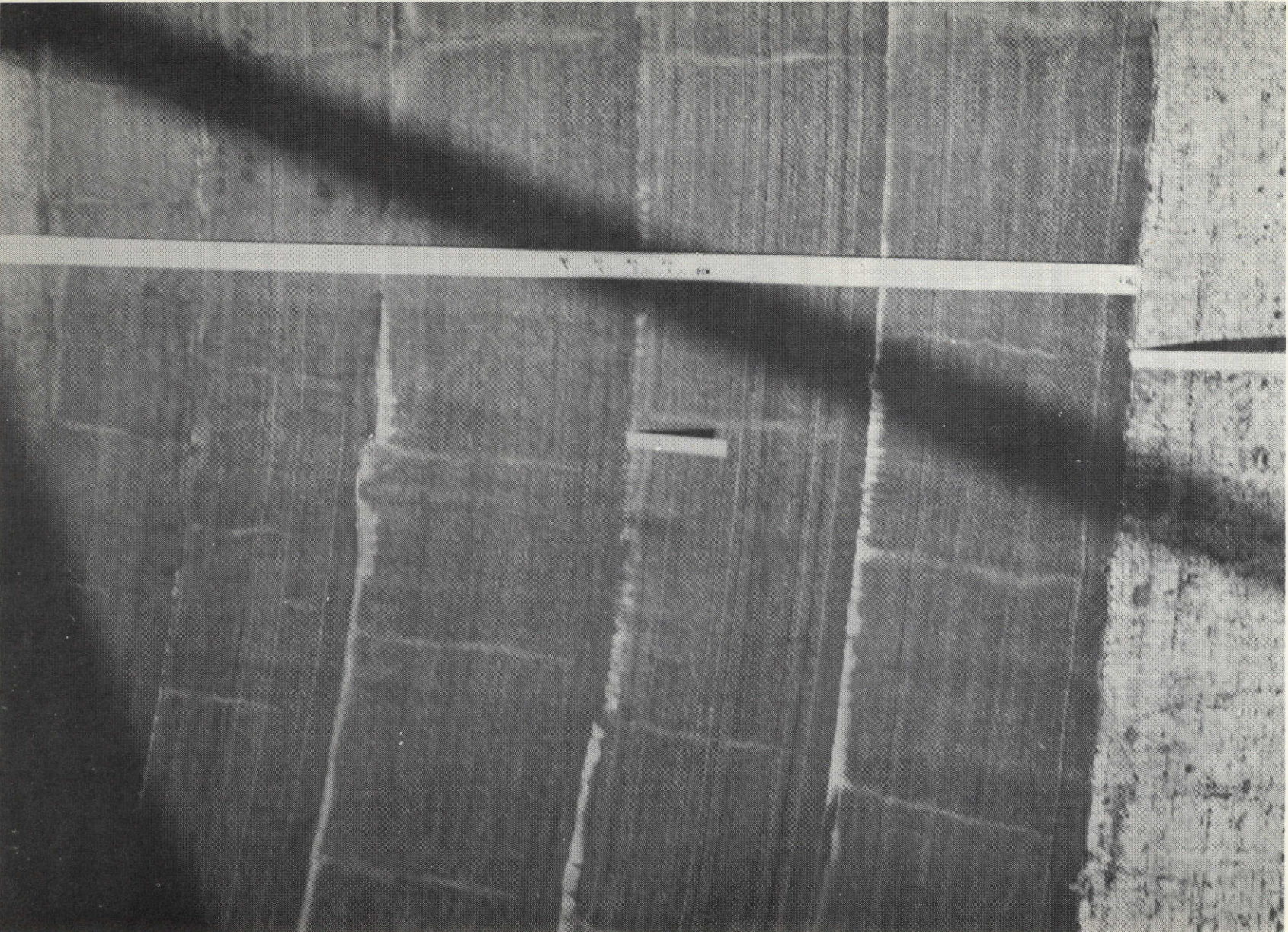
Posttest View of Nozzle Throat Insert



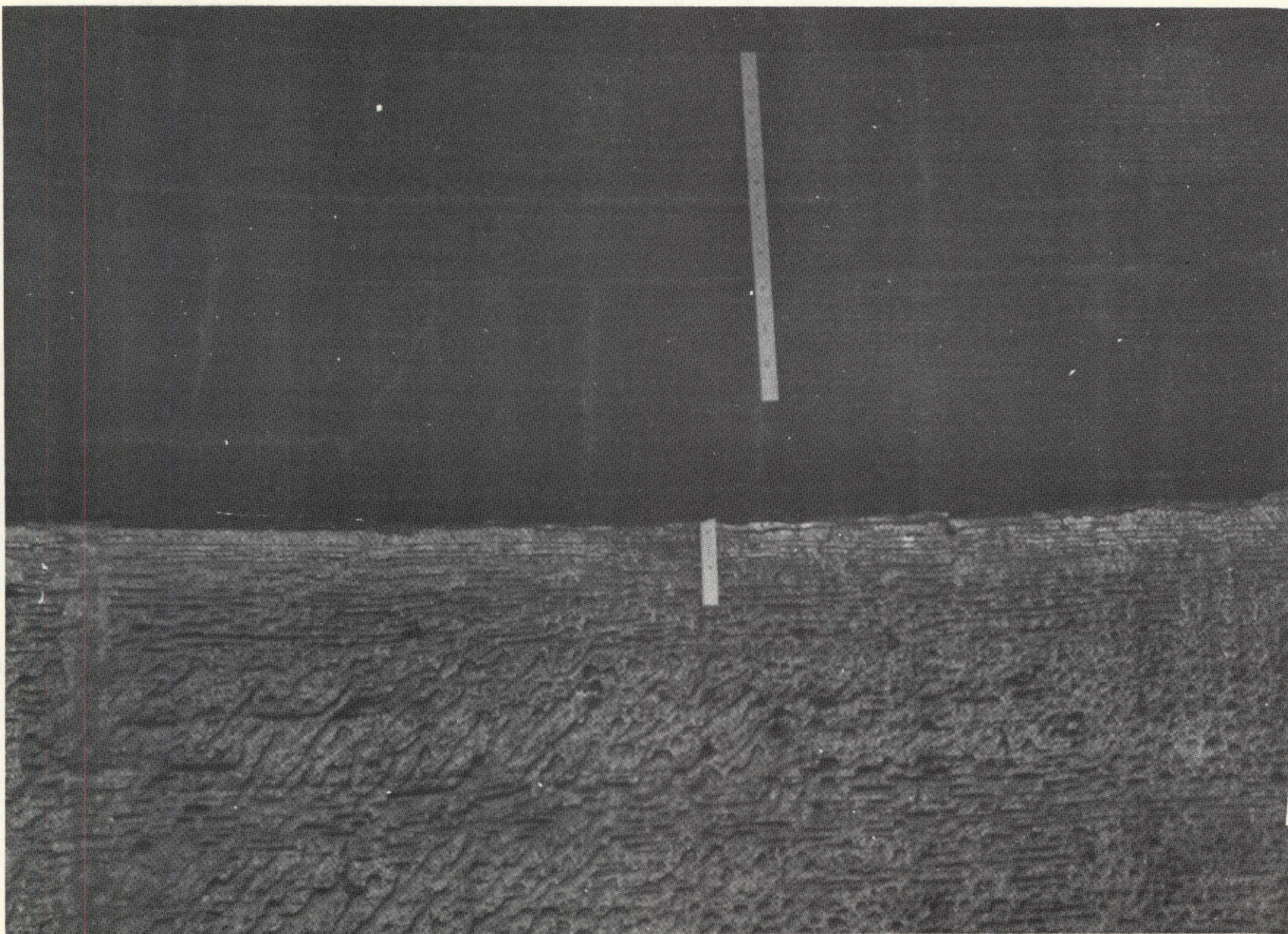
Posttest View of Nozzle Throat Insert Surface



Posttest View of Nozzle Throat Extension Insert



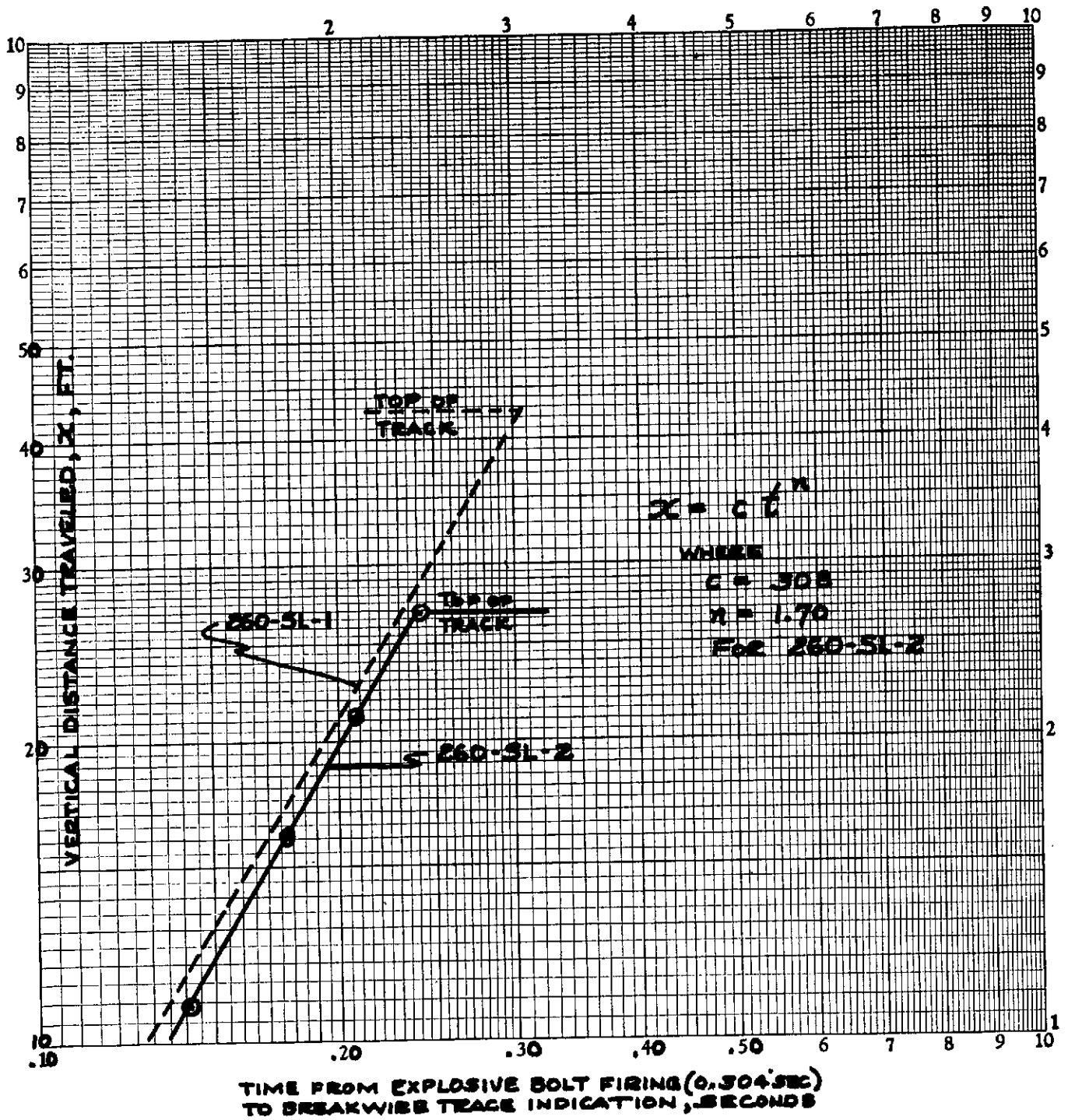
Posttest View of Exit Cone



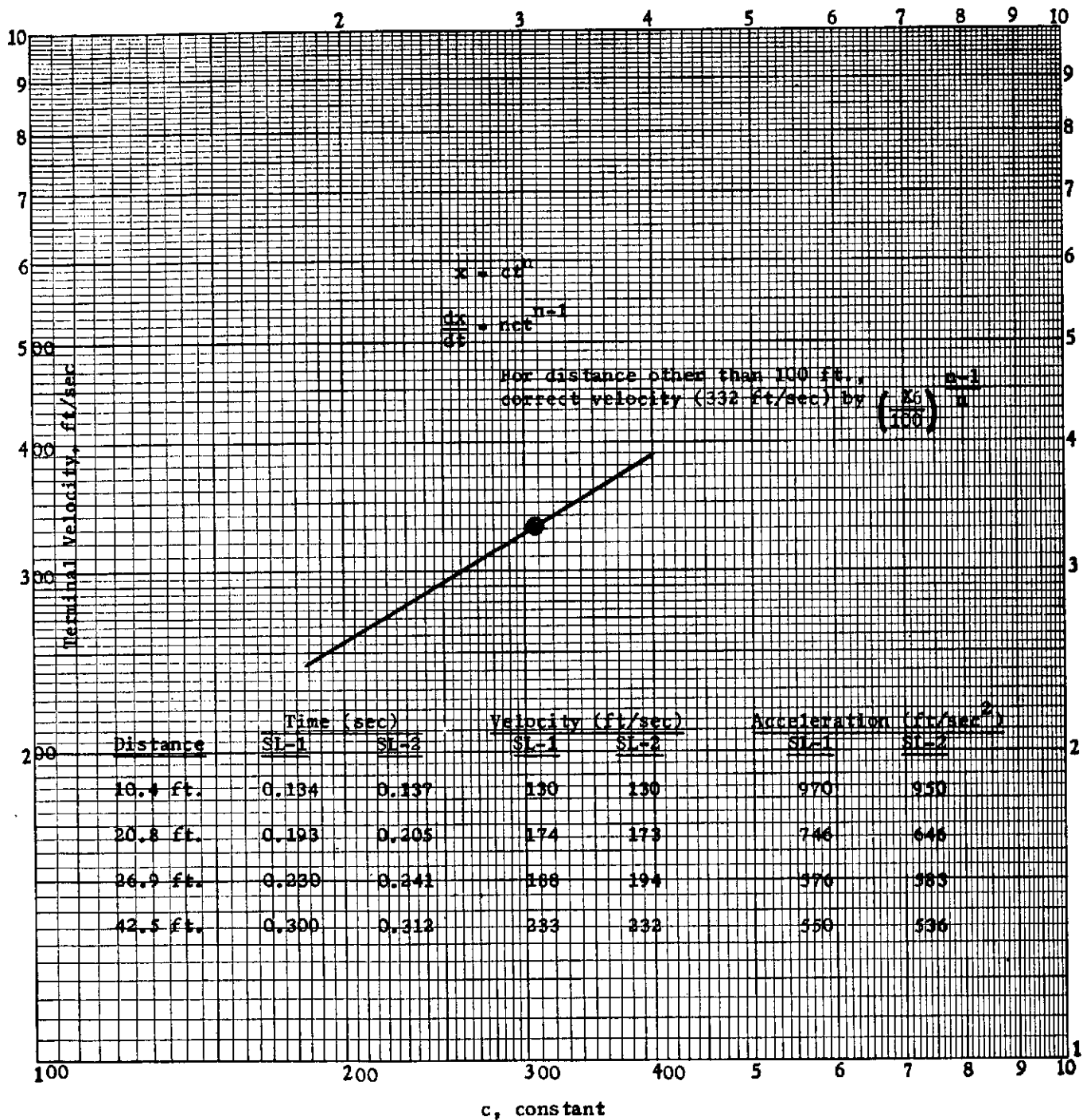
Posttest View of Exit-Cone Ablation Surface



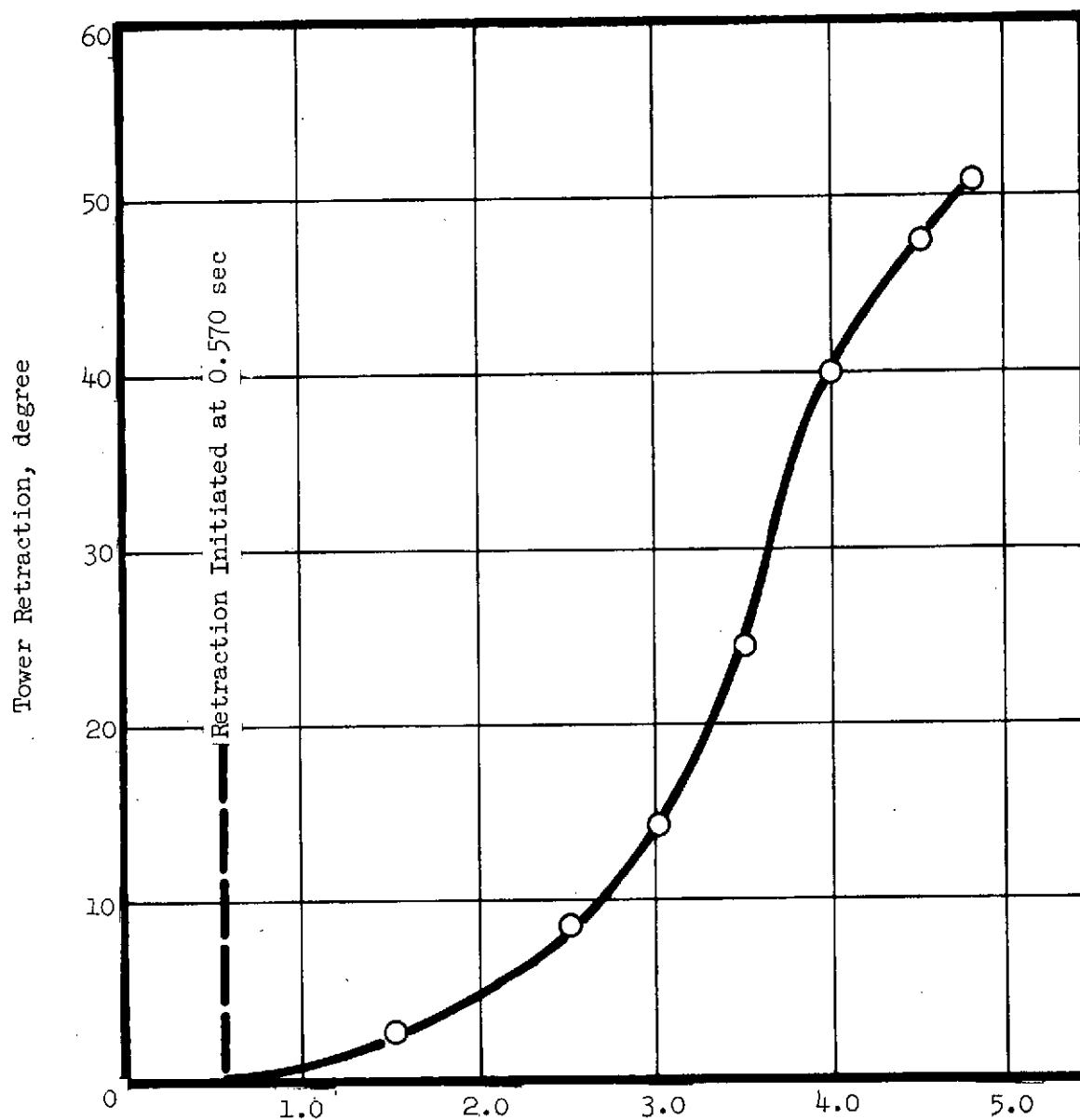
Posttest View of Exit-Cone Exterior



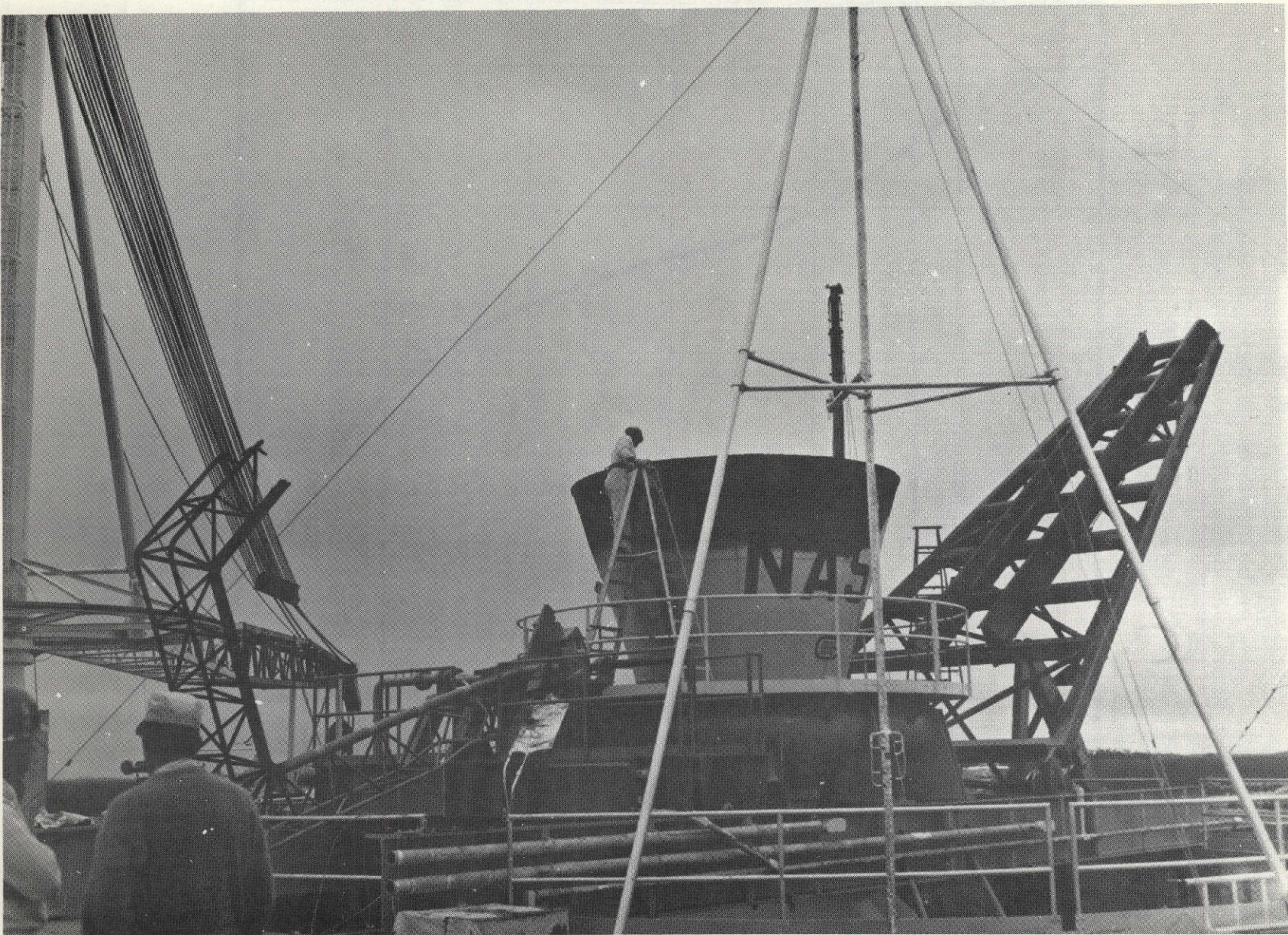
Vertical Distance vs Time for Ignition Motor and Support Fixture



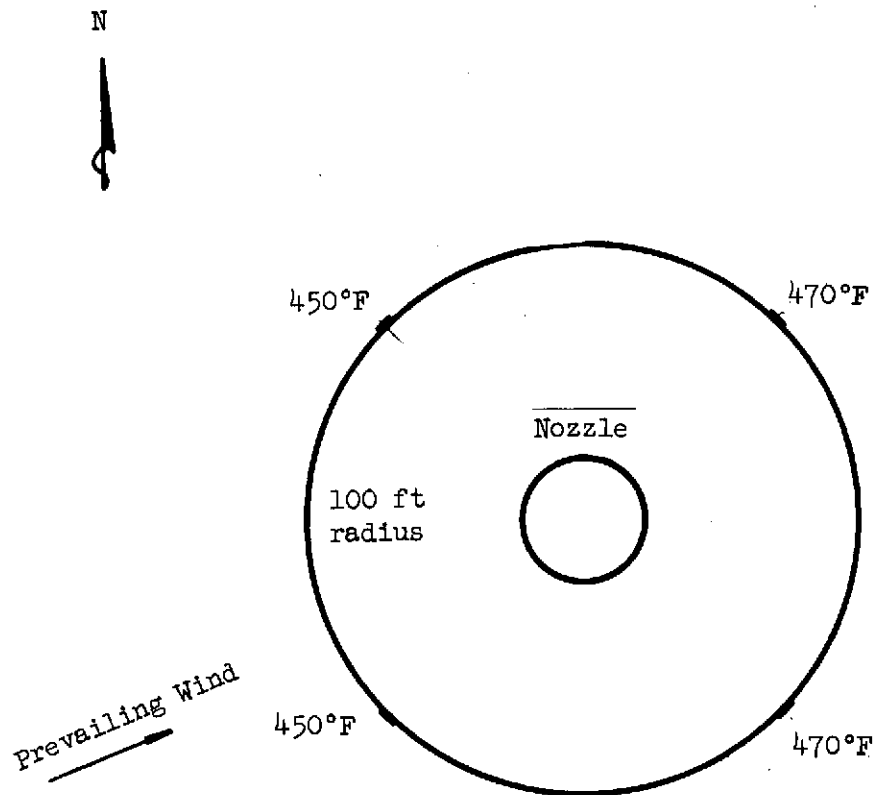
Terminal Velocity of Ignition Motor and Support Fixture at 100 ft



Tower Position-vs-Time Curve



Posttest View of Ignition Motor Track Assembly



Panels Located on Pad
Maximum indicated temperatures are noted on each panel

Location of Temperature Indication Paint Panels

Figure 86

APPENDIX

INSTRUMENTATION PLAN, MOTOR 260-SL-2
STATIC TEST

INSTRUMENTATION PLANMotor 260-SL-2 Static Test

<u>Function</u>	<u>Range</u>	<u>Recording Method (1)</u>	<u>Location and Purpose</u>
<u>I. Ballistic Evaluation</u>			
P _c 1	0-750 psig	R2; Bristol Ampex	Chamber pressure measured at forward cap
P _c 2	0-750 psig	R1; R2 Ampex	Chamber pressure measured at forward cap
P _c 3	0-750 psig	R3; Ampex	Chamber pressure measured at forward cap
F _y -1 _a	0-2.0 x 10 ⁶ lb	R2; R1 Ampex	Rocket motor axial thrust
F _y -1 _b	0-2.0 x 10 ⁶ lb	R2 Ampex	<u>Note:</u>
F _y -2 _a	0-2.0 x 10 ⁶ lb	R2; R1 Ampex	<u>Condition</u> <u>Approx. Load/Cell</u>
F _y -2 _b	0-2.0 x 10 ⁶ lb	R2 Ampex	1. Pretest 687,000 lb Zero
F _y -3 _a	0-2.0 x 10 ⁶ lb	R2; R1 Ampex	2. Max Load 1,700,000 lb
F _y -3 _b	0-2.0 x 10 ⁶ lb	R2 Ampex	3. Posttest 121,000 lb Zero
P _C -IM	0-1500 psig	R1; R2 Ampex	Igniter motor chamber pressure
P _i -IM	0-1500 psig	R2 Ampex	Igniter motor booster chamber pressure
<u>II. Chamber and Nozzle Heating</u>			
(T1) (2) T _{CF} -000-2.5	0-500°F	R5 (sampled)	Temperature of forward cap opposite silicone rubber step joint
(T2) T _{CF} -337.5-12.0	0-500°F	R5 (sampled)	Forward head temperature opposite Germax/V-61 joint surface

<u>Function</u>	<u>Range</u>	<u>Recording Method (1)</u>	<u>Location and Purpose</u>
(T3) T _{CF} -112.5-56.6	0-500°F	R5 (sampled)	Forward head temperature opposite V-61 joint at max. exposure
(T4) T _{CC} -000-595.0	0-500°F	R5 (sampled)	Chamber temperature opposite forward cylinder insulation at max. exposure
(T5) T _{CC} -270-595.0	0-500°F	R5 (sampled)	Chamber temperature opposite forward cylinder insulation at max. exposure
(T6) T _{CC} -000-350.0	0-500°F	R5 (sampled)	Chamber temperature opposite mid-chamber cylinder insulation at max. exposure
(T7) T _{CC} -270-350.0	0-500°F	R5 (sampled)	Same as (T6)
(T8) T _{CC} -000-114.0	0-500°F	R5 (sampled)	Chamber temperature opposite aft-cylinder insulation at max. exposure
(T9) T _{CC} -060-114.0	0-500°F	R5 (sampled)	Chamber temperature opposite aft-cylinder insulation at minimum exposure
(T10) T _{CC} -120-114.0	0-500°F	R5 (sampled)	Same as (T8)
(T11) T _{CC} -180-114.0	0-500°F	R5 (sampled)	Same as (T9)
(T12) T _{CC} -240-114.0	0-500°F	R5 (sampled)	Same as (T8)
(T13) T _{CC} -300-114.0	0-500°F	R5 (sampled)	Same as (T9)
(T14) T _{CA} -022.5-12.0	0-500°F	R5 (sampled)	Aft-head temperature opposite V-61 joint near edge of ray
(T15) T _{CA} -022.5-1.0	0-500°F	R5 (sampled)	Aft-head temperature opposite V-61 joint near edge of ray
(T16) T _{CA} -112.5-1.0	0-500°F	R5 (sampled)	Aft-head temperature opposite V-61 joint near center of ray

<u>Function</u>	<u>Range</u>	<u>Recording Method (1)</u>	<u>Location and Purpose</u>
(T17) T_{CA} -180-1.0	0-500°F	R5 (sampled)	Aft-head temperature center of star point
(T18) T_N -000-229.0	0-500°F	R5 (sampled)	Nozzle temperature opposite step joint at center of ray
(T19) T_N -090-229.0	0-500°F	R5 (sampled)	Nozzle temperature opposite step joint near edge of ray
(T20) T_N -000-200.0	0-500°F	R5 (sampled)	Nozzle temperature opposite point of maximum predicted insulation erosion
(T21) T_N -090-200.0	0-500°F	R5 (sampled)	Same as (T20)
(T22) T_N -180-200.0	0-500°F	R5 (sampled)	Same as (T20)
(T23) T_N -270-200.0	0-500°F	R5 (sampled)	Same as (T20)
(T24) T_N -000-177.0	0-500°F	R5 (sampled)	Nozzle temperature opposite throat insert forward joint
(T25) T_N -090-177.0	0-500°F	R5 (sampled)	Same as (T24)
(T26) T_N -000-163.0	0-500°F	R5 (sampled)	Nozzle temperature opposite throat insert aft joint
(T27) T_{NE} -090-163.0	0-500°F	R5 (sampled)	Same as (T26)
(T28) T_{NE} -000-117.0	0-500°F	R5 (sampled)	Exit cone attach flange temperature opposite nozzle/exit cone joint
(T29) T_{NE} -180-117.0	0-500°F	R5 (sampled)	Same as (T28)
(T30) T_{NE} -270-73.0	0-500°F	R5 (sampled)	Temperature of exit cone skin opposite graphite and silica interface
(T31) T_{NE} -270-72.0 (A)	0-500°F	R5 (sampled)	Ambient temperature adjacent to exit cone skin
(T32) T_{NE} -270-27.0	0-500°F	R5 (sampled)	Exit cone skin temperature adjacent to cork insulation

<u>Function</u>	<u>Range</u>	<u>Recording Method (1)</u>	<u>Location and Purpose</u>
(T33) T_{NE} -270-10.0 (A)	0-500°F	R5 (sampled)	Ambient temperature adjacent to exit cone skin
(T34) T_{NE} -270-1.0	0-500°F	R5 (sampled)	Temperature of exit cone aft flange adjacent to (S11) and under the V-61 insulation
(T35) Spare			
(T36) Spare			
<u>III. Motor Vibration and Shock</u>			
(G1) $(^2)G_{CAP}$ -y-090-2.5	+500 g	Ampex	Measure ignition shock and any oscillatory burning at the forward cap in longitudinal axis.
(G1A) G_{CAP} -y-090-2.5	+25 g	Ampex	Monitor steady-state vibration level at forward cap
(G2) G_{CF} -y-000-70.0	+200 g	Ampex	Measure ignition shock and any oscillatory burning on the forward head in the longitudinal axis.
(G3) G_{CC} -x-000-350.0	+10 g	Ampex	Monitor case vibration in radial axis at center of chamber
(G4) G_{CC} -x-000-95.0	+10 g	Ampex	Monitor case vibration in radial axis at aft end of chamber.
(G5) G_N -y-000-229.0	+50 g	Ampex	Determine vibration and shock at aft head and nozzle interface in longitudinal axis.
(G6) G_N -x-000-229.0	+50 g	Ampex	Determine vibration and shock at aft head and nozzle interface in radial axis.
(G7) G_N -x-000-168.5	+50 g	Ampex	Monitor vibration at nozzle throat section; detect any failures and define environment for future TVC systems.

<u>Function</u>	<u>Range</u>	<u>Recording Method (1)</u>	<u>Location and Purpose</u>
(G8) G_{NE} -y-000-117.25	± 100 g	Ampex	Monitor axial vibration at nozzle and exit cone flange; detect any failures and define environment for future TVC systems.
(G9) G_{NE} -x-000-117.25	± 100 g	Ampex	Same as (G8) except in a radial axis
(G10) G_{NE} -z-270-28.0	± 200 g	Ampex	Measure exit cone vibration during ignition transient.
(G11) G_{NE} -x-000-28.0	± 200 g	Ampex	Same as (G10)
<u>IV. Nozzle and Exit-Cone Strain</u>			
(S1) ⁽²⁾ S_N -A-000-208.5	-300 μ in./in.	R4	Measure the biaxial strain level on the nozzle shell, opposite location of maximum erosion and stress on the nozzle insulation.
(S2) S_N -T-000-208.5	2500 μ in./in.	R4	
(S3)* S_{CC} -A-000-203.0	1000 μ in./in.	R4	Measure the biaxial strain at the highest stressed location in the chamber (weld porosity)
(S4)* S_{CC} -T-000-203.0	5000 μ in./in.	R4	
(S5)* S_{CF} -A-000-11.0	5000 μ in./in.	R3	Measure the biaxial strain at the highest stressed location on the chamber forward head (contour deviation)
(S6)* S_{CF} -T-000-11.0	2500 μ in./in.	R3	
(S7)* S_{CF} -A-000-12.0	5000 μ in./in.	R3	Measure the biaxial strain adjacent to location (S5, S6) on opposite side of the weld.
(S8)* S_{CF} -T-000-12.0	2500 μ in./in.	R3	
(S9) S_{NE} -T-000-1.0	± 1000 μ in./in.	R3	Measure uniaxial tangential (hoop) strain at the exit plane. Determine the extent of asymmetrical loading (if any) due to exhaust gas impingement during igniter motor ejection.
(S10) S_{NE} -T-270-1.0	± 1000 μ in./in.	R3	
(S11) S_{NE} -T-090-1.0	± 1000 μ in./in.	R3	
(S12) S_{NE} -t-180-1.0	± 1000 μ in./in.	R3	

*More precise location will be provided by Department 5530 at installation.

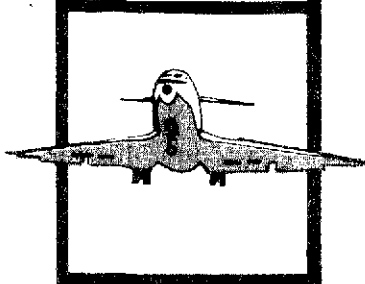
<u>Function</u>	<u>Range</u>	<u>Recording Method (1)</u>	<u>Location and Purpose</u>
(S13) S _{CC} -T-000-349.0	4000 <i>μ</i> in./in.	R4	Determine chamber growth in the axial and circumferential direction at the chamber mid-section.
(S14) S _{CC} -A-000-349.0	1030 <i>μ</i> in./in.	R4	
(S15) S _{FS} -A-030-633.0	-1000 <i>μ</i> in./in.	R4	Determine magnitude of non-symmetrical loading of forward skirt (if any) due to thrust axis misalignment.
(S16) S _{FS} -A-150-633.0	-1000 <i>μ</i> in./in.	R4	
(S17) S _{FS} -A-270-633.0	-1000 <i>μ</i> in./in.	R4	
V. <u>Event Sequence</u>			
E _{FS}	Trace	All	Fire-switch actuation, voltage
I _{FS}	Trace	R2	Fire-switch actuation, current
E _{CC}	Trace	R1	Capacitance bank charge volt.
I _{CC}	Trace	R1	Capacitance bank current
t _S RCA-1, -2	Trace	R1	Release controller actuation
E _{EBA}	Trace	R1, R2	Explosive bolt actuation
t _S TRA	Trace	R1	Tower release actuation
t _S TAM	Trace	R1	First motion, tower linkage
60 cps	Trace	All	Timing correlation
1000 cps	Trace	Ampex	Timing correlation
t _S LI-1, 3, 5	Trace	R3	Tower breakwire; 1 in.; 10.4 ft; and 20.7 ft sled travel.
t _S LI-2, 4, 6	Trace	R3	Tower breakwire; 5.0 ft; 15.0 ft; and 26.8 ft sled travel.
t _S TRC	Trace	R1	Tower breakwire; 26.8 ft sled travel (retraction command)

<u>Function</u>	<u>Range</u>	<u>Recording Method (1)</u>	<u>Location and Purpose</u>
E _{QVA} -CO ₂	Trace	R5	CO ₂ quench valve actuation
E _{QVA} -H ₂ O	Trace	R5	H ₂ O quench valve actuation
VI. <u>Position Indication (3)</u>			
L _T	0-60°	R4, Meter	Igniter tower movement
L _{QB}	0-120°	R4, Meter	Quench boom movement
L _{CA} -y-30°	0-1 in.	R4	Aft-closure deflection (monitor clearance between STE and motor).
L _{CA} -y-150°	0-1 in.	R4	
L _{CA} -y-270°	0-1 in.	R4	
VII. <u>STE and Facility Evaluation and Analysis Measurements (3)</u>			
P _{GN₂}	0-500 psig	R3	Accumulator pressure, tower retraction system
P _{RET}	0-5000 psig	R3	Hydraulic pressure, retract side of tower retract, system
P _{EXT}	0-5000 psig	R3	Hydraulic pressure, extend side of tower retract, system
P _{GNA₂} -QA	0-1500 psig	Meter	Nitrogen pressure to quench boom lock
P _{QA}	0-1500 psig	R1	Hydraulic pressure, quench actuation system
P _{CO₂}	0-1000 psig	Meter	CO ₂ quench media supply pressure
G _{MSF} -y	±100 g	Ampex	Acceleration of ignition motor support fixture, adjacent to forward head
G _T -z	±100 g	Ampex	Monitor vibration level of igniter tower at top; define any abnormal travel of igniter motor.
G _{TTR} -y	±50 g	Ampex	Define the dynamic response of the thrust take-out ring.

<u>Function</u>	<u>Range</u>	<u>Recording Method (1)</u>	<u>Location and Purpose</u>
T _B -90-(+ 10')	0-1000°F	R5 (sampled)	Ambient temperature at top edge of caisson
T _B -000-(+ 10')	0-1000°F	R5 (sampled)	Same as above
T _B -270-(+ 10')	0-1000°F	R5 (sampled)	Same as above
T _B -180-(+ 10')	0-1000°F	R5 (sampled)	Same as above
T _B -000-(-58)	0-250°F	R5 (sampled)	Ambient temperature at -58 ft (load cell) level
T _{QA} -1	0-2000°F	R5 (sampled)	Temperature measured on quench system components
T _{QAB} -1	0-2000°F	R5 (sampled)	Same as above
T _F -1	0-2000°F	R5 (sampled)	Temperature measured on the beam within the explosive bolt protective boxes at the top of the A-frames
T _T -270-15	0-2000°F	R5 (sampled)	Determine temperature at first beam above nozzle on igniter tower facing nozzle.
T _T -270-15A	0-2000°F	R5 (sampled)	Same except on rear of tower

NOTES:

- (1) R1 = Honeywell Visocorder. Recording speed: 40 in./sec; from T-7 sec until T+5 sec. 4.0 in./sec from T+5 sec until P_c = 0.
 R2 = CEC oscillograph. Recording speed: 10 in./sec from T-7 sec until P_c = 0.
 R3 = CEC oscillograph. Recording speed: 10 in./sec from T-7 until P_c = 0.
 R4 = CEC oscillograph. Recording speed: 10 in./sec from T-7 until P_c = 0.
 R5 = CEC oscillograph. Recording speed: 10.0 in./sec from T-7 sec until T+300 sec.
 Ampex = Ampex FR 1200 magnetic tape recorder. Recording speed: 60 in./sec.
- (2) (T1, G1, S1, etc.) = Code for locating parameter on Drawing No. 1126183, Instrumentation Layout, 260-SL-2 Static Test (Figure A1).
 Parameter designation (T_{CF}-000-2.5, etc.) per AGC-STD 3014.
- (3) Refer to Figure A2.

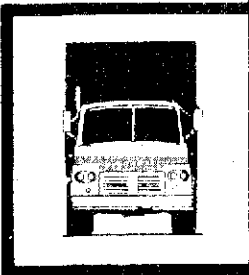
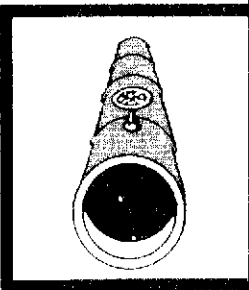
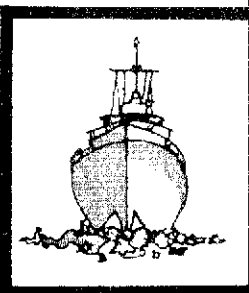
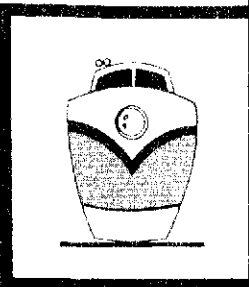


NATIONAL TRANSPORTATION SAFETY BOARD

WASHINGTON, D.C. 20594

AIRCRAFT ACCIDENT REPORT

**NORTHWEST AIRLINES, INC.,
BOEING 727-251, N274US,
NEAR THIELLS, NEW YORK
DECEMBER 1, 1974**



REPORT NUMBER: NTSB-AAR-75-13

UNITED STATES GOVERNMENT

TECHNICAL REPORT DOCUMENTATION PAGE

1. Report No. NTSB-AAR-75-B	2. Government Accession No.	3. Recipient's Catalog # FB 245 581	
4. Title and Subtitle Aircraft Accident Report - Northwest Airlines, Inc., Boeing 727-251, N274US, near Thiells, New York, December 1, 1974		5. Report Date August 13, 1975	
7. Author(s)		6. Performing Organization Code	
9. Performing Organization Name and Address National Transportation Safety Board Bureau of Aviation Safety Washington, D. C. 20594		8. Performing Organization Report No.	
12. Sponsoring Agency Name and Address NATIONAL TRANSPORTATION SAFETY BOARD Washington, D. C. 20594		10. Work Unit No. 1481-A	
		11. Contract or Grant No.	
		13. Type of Report and Period Covered Aircraft Accident Report December 1, 1974	
		14. Sponsoring Agency Code	
15. Supplementary Notes PRICES SUBJECT TO CHANGE			
16. Abstract About 1926 e.s.t. on December 1, 1974, Northwest Airlines Flight 6231, a Boeing 727-251, crashed about 3.2 nmi west of Thiells, New York. The accident occurred about 12 minutes after the flight had departed John F. Kennedy International Airport, Jamaica, New York, and while on a ferry flight to Buffalo, New York. Three crewmembers, the only persons aboard the aircraft, died in the crash. The aircraft was destroyed. The aircraft stalled at 24,800 feet m.s.l. and entered an uncontrolled spiralling descent into the ground. Throughout the stall and descent, the flightcrew did not recognize the actual condition of the aircraft and did not take the correct measures necessary to return the aircraft to level flight. Near 3,500 feet m.s.l., a large portion of the left horizontal stabilizer separated from the aircraft, which made control of the aircraft impossible. The National Transportation Safety Board determines that the probable cause of this accident was the loss of control of the aircraft because the flightcrew failed to recognize and correct the aircraft's high-angle-of-attack, low-speed stall and its descending spiral. The stall was precipitated by the flightcrew's improper reaction to erroneous airspeed and Mach indications which had resulted from a blockage of the pitot heads by atmospheric icing. Contrary to standard operational procedures, the flightcrew had not activated the pitot head heaters.			
17. Key Words Scheduled air carriers, pitot system errors; atmospheric icing ; stalls; attitude instrument flying.		18. Distribution Statement This document is available through the National Technical Information Service, Springfield, Virginia 22151	
19. Security Classification (of this report) UNCLASSIFIED	20. Security Classification (of this page) UNCLASSIFIED	21. No. of Pages 32	22. Price

TABLE OF CONTENTS

	<u>Page</u>
Synopsis	1
1. Investigation	1
1.1 History of the Flight	1
1.2 Injuries to Persons	2
1.3 Damage to Aircraft	2
1.4 Other Damage	2
1.5 Crew Information	2
1.6 Aircraft Information	3
1.7 Meteorological Information	4
1.8 Aids to Navigation	4
1.9 Communications	4
1.10 Aerodrome and Ground Facilities	5
1.11 Flight Recorders	5
1.12 Aircraft Wreckage	7
1.13 Medical and Pathological Information	8
1.14 Fire	8
1.15 Survival Aspects	9
1.16 Tests and Research	9
1.16.1 Pitot Head Examination and Icing Tests	9
1.16.2 Aircraft Performance Analysis	10
1.17 Other Information	11
1.17.1 Pretakeoff Checklist	11
1.17.2 Airspeed Measuring System	12
1.17.3 B-727 Stall Characteristics	13
2. Analysis and Conclusions	15
2.1 Analysis	15
2.2 Conclusions	19
(a) Findings	19
(b) Probable Cause	21
3. Recommendations	21
 Appendixes	
Appendix A - Investigation and Hearing	23
Appendix B - Crew Information	24
Appendix C - Aircraft Information	26
Appendix D - Recommendations A-75 25-27 to FAA	27

NATIONAL TRANSPORTATION SAFETY BOARD
WASHINGTON, D.C. 20594

AIRCRAFT ACCIDENT REPORT

Adopted August 13, 1975

NORTHWEST AIRLINES, INC.
BOEING 727-251, N274US
NEAR THIELLS, NEW YORK
DECEMBER 1, 1974

SYNOPSIS

About 1926 e.s.t. on December 1, 1974, Northwest Airlines Flight 6231, a Boeing 727-251, crashed about 3.2 nmi west of Thiells, New York. Flight 6231 was a ferry flight to Buffalo, New York. The accident occurred about 12 minutes after the flight had departed John F. Kennedy International Airport, Jamaica, New York. Three crewmembers, the only persons aboard the aircraft, died in the crash. The aircraft was destroyed.

The aircraft stalled at 24,800 feet m.s.l. and entered an uncontrolled, spiralling descent to the ground. Throughout the stall and descent the flightcrew did not recognize the actual condition of the aircraft and did not take the correct measures necessary to return the aircraft to level flight. Near 3,500 feet m.s.l., a large portion of the left horizontal stabilizer separated from the aircraft, which made control of the aircraft impossible.

The National Transportation Safety Board determines that the probable cause of this accident was the loss of control of the aircraft because the flightcrew failed to recognize and correct the aircraft's high-angle-of-attack, low-speed stall and its descending spiral. The stall was precipitated by the flightcrew's improper reaction to erroneous airspeed and Mach indications which had resulted from a blockage of the pitot heads by atmospheric icing. Contrary to standard operational procedures, the flightcrew had not activated the pitot head heaters.

1. INVESTIGATION

1.1 History of Flight

On December 1, 1974, Northwest Airlines, Inc., Flight 6231, a Boeing 727-251, N274US, was a ferry flight from John F. Kennedy International Airport (JFK), Jamaica, New York, to Buffalo, New York. Three crewmembers were the only persons aboard the aircraft.

Flight 6231 departed JFK about 1914 1/ on a standard instrument departure. After takeoff, Kennedy departure control cleared the flight to climb to 14,000 feet. 2/ At 1920:21, New York air route traffic control center (ZNY) assumed radar control of the flight, and at 1921:07, ZNY cleared the flight to climb to flight level 310. 3/

Flight 6231 proceeded without reported difficulty until 1924:42, when a crewmember transmitted, "Mayday, mayday ... " on ZNY frequency. The ZNY controller responded, "... go ahead," and the crewmember said, "Roger, we're out of control, descending through 20,000 feet."

After giving interim altitude clearances, at 1925:21, the ZNY controller asked Flight 6231 what their problem was, and a crewmember responded, "We're descending through 12, we're in a stall." The sound of an active radio transmitter was recorded at 1925:38. There were no further transmissions from Flight 6231.

At 1925:57, Flight 6231 crashed in a forest in the Harriman State Park, about 3.2 nmi west of Thiells, New York. No one witnessed the crash.

The accident occurred during hours of darkness.

The geographic coordinates of the accident site are 41° 12' 53" N. latitude and 74° 5' 40" W. longitude.

1.2 Injuries to Persons

<u>Injuries</u>	<u>Crew</u>	<u>Passengers</u>	<u>Other</u>
Fatal	3	0	0
Nonfatal	0	0	0
None	0	0	

1.4 Damage to Aircraft

The aircraft was destroyed.

1.4 Other Damage

Trees and bushes were either damaged or destroyed.

1.5 Crew Information

The crewmembers were qualified and certificated for the flight. The three crewmembers had off-duty periods of 15 hours 31 minutes during the 24-hour period preceding the flight. (See Appendix B.)

- 1/ All times herein are eastern standard, based on the 24-hour clock.
2/ All altitudes herein are mean sea level, unless otherwise indicated.
3/ An altitude of 31,000 feet which is maintained with an altimeter setting of 29.92 inches.

In October 1974, the first officer advanced from second officer in B-707 aircraft to first officer in B-727 aircraft; he had flown about 46 hours in the latter capacity.

1.6 Aircraft Information

N274US was owned and operated by Northwest Airlines, Inc. It was certificated and maintained in accordance with Federal Aviation Administration (FAA) regulations and requirements. (See Appendix C.)

N274US was loaded with 48,500 lbs. of Jet A fuel. The gross weight at takeoff was about 147,000 lbs. The weight and center of gravity (c.g.) were within prescribed limits. The aircraft was in compliance with all pertinent airworthiness directives.

In the Boeing 727 aircraft, the pitot-static instruments on the captain's panel, the pitot-static instruments on the first officer's panel, and the pitot-static instrumentation in the flight data recorder (FDR) are connected to separate pitot and static sources. The three pitot systems have no common elements and are completely independent. The three static systems are also independent except for manual selector valves in both the captain's and first officer's systems which provide for selection of the FDR static system as an alternate pressure source if either primary source malfunctions.

The first officer's pitot and static systems are connected to a Mach airspeed warning switch. The switch activates a warning horn when it senses a differential pressure which indicates that the aircraft's speed is exceeding V_{mo} or M_{mo} , ^{4/} depending on the aircraft's altitude. A redundant Mach airspeed warning system is incorporated in the FDR pitot and static systems.

The pitot head for the captain's pitot system is located on the left side of the aircraft's fuselage; the pitot heads for the first officer's system and the FDR system are located on the right side of the fuselage. Each of these heads incorporates a heating element and a small drain hole, for exhausting moisture, aft of the total pressure sensing inlet. The three static systems each have a static port located on either side of the fuselage. The left static port is connected to the right static port to offset sideslip effects by balancing the pressures within the systems. Each of the ports is equipped with a heating element.

In addition to the above systems, two independent pitot-static systems are connected to a mechanism in the aircraft's longitudinal control system. The force which the pilot must exert to move the elevator control surfaces varies as a function of the dynamic pressure measured by these systems. The two pitot heads for these systems are mounted one on each side of the vertical stabilizer, and their design is similar to the other pitot heads.

^{4/} Maximum operating limit speed or maximum operating limit Mach.

1.7 Meteorological Information

Northwest Airlines' meteorology department supplied the weather information for Flight 6231. This information included a synopsis of surface conditions, terminal forecasts, a tropopause and wind forecast for the 300-millibar level, appropriate surface observations, and turbulence plots. For the period 1700 to 2300, Northwest meteorologists forecasted moderate to heavy snowshowers from Lake Michigan to the Appalachian Mountains and moderate to heavy rainshowers and scattered thunderstorms east of the Appalachians.

Northwest's turbulence plot (TP) No. East 2 was in effect and available to the flightcrew on the day of the accident. TP East 2 was a triangular area defined by lines connecting Pittsburgh, Pennsylvania, New York City, New York, and Richmond, Virginia. Thunderstorm cells with maximum tops to 28,000 feet were located in this area.

SIGMET 5/ Delta 2, issued at 1755 and valid 1755 to 2200, predicted frequent moderate icing in clouds, locally severe in precipitation above the freezing level, which was at the surface in southwestern New York and which sloped to 6,000 feet eastward to the Atlantic coast.

The surface weather observations at Newburgh, New York, about 17 miles north of the accident site, were:

1900 - Estimated ceiling -- 2,500 feet broken, 5,000 feet overcast, visibility -- 12 miles, temperature -- 34°F., dew point -- 22°F., wind -- 070° at 14 kn, gusts -- 24 kn, altimeter setting -- 29.98 in.

2000 - Similar conditions to those reported at 1900 except that very light ice pellets were falling.

Another Northwest flight was on a similar route behind Flight 6231. The captain of that flight stated that he encountered icing and light turbulence in his climb. He was in instrument conditions from 1,500 feet to 23,000 feet, except for a few minutes between cloud layers at an intermediate altitude.

1.8 Aids to Navigation

There were no problems with navigational aids.

1.9 Communications

There were no problems with air-to-ground communications.

5/ A SIGMET is an advisory of weather severe enough to be potentially hazardous to all aircraft. It is broadcast on navigational and voice frequencies and by flight service stations. It is also transmitted on Service-A weather teletype circuits.

1.10 Aerodrome and Ground Facilities

Not applicable.

1.11 Flight Recorders

N274US was equipped with a Fairchild Model 5424 flight data recorder (FDR), serial No. 5146, and a Fairchild A-100 cockpit voice recorder (CVR), serial No. 1640. Both recorders sustained superficial mechanical damage, but the recording tapes were intact and undamaged. All of the FDR traces and the CVR channels were clearly recorded.

The readout of the FDR traces involved 11 minutes 54.6 seconds of flight, beginning 15 seconds before liftoff.

Pertinent portions of the CVR tape were transcribed, beginning with the flightcrew's execution of the pretakeoff checklist and ending with the sounds of impact. The following transcript was made of the flightcrew's activities between 1906:36 and 1906:51:

First Officer: Zero, zero and thirty-one, fifteen, fifteen blue.

Second Officer: Bug.

Second Officer: Pitot heat.

First Officer: Off and on.

Captain: One forty-two is the bug.

First Officer: Or ... do you want the engine heat on?

First Officer: Huh!

Sound of five clicks.

Air-to-ground communications, cockpit conversations, and other sounds recorded on the CVR were correlated to the FDR altitude, airspeed, heading, and vertical acceleration traces by matching the radio transmission time indications on both the CVR and FDR.

The FDR to CVR correlation showed that after takeoff, the aircraft climbed to 13,500 feet and remained at that altitude for about 50 seconds, during which time the airspeed 6/ increased from 264 kn to 304 kn. During that 50 seconds, the airspeed trace showed two aberrations in a 27-second period; each aberration was characterized by a sudden reduction in airspeed. These reductions were 40 kn and 140 kn and lasted for 7 and 5 seconds, respectively.

6/ All airspeeds are indicated airspeeds, unless otherwise noted.

The aircraft then began to climb 2,500 feet per minute while maintaining an airspeed of about 305 kn. As the altitude increased above 16,000 feet, the recorded airspeed began to increase. Subsequently, both the rate of climb and the rate of change in airspeed increased. About this same time, the first officer commented, "Do you realize we're going 340 kn and I'm climbing 5,000 feet a minute?"

The flightcrew discussed the implications of the high airspeed and high rate of climb. The second officer commented, "That's because we're light," after which the captain said, "It gives up real fast," and "I wish I had my shoulder harness on, it's going to give up pretty soon." The rate of climb eventually exceeded 6,500 feet per minute.

The sound of an overspeed warning horn was recorded as the altitude reached 23,000 feet. At that time, the recorded airspeed was 405 kn and the following conversation took place:

Captain: "Would you believe that #."

First Officer: "I believe it, I just can't do anything about it."

Captain: "No, just pull her back, let her climb."

This last comment was followed by the sound of a second overspeed warning horn.

The sound of the stall warning stick shaker was recorded intermittently less than 10 seconds after the onset of the overspeed warning. Five seconds later, vertical acceleration reduced to 0.8g, and the altitude leveled at 24,800 feet. The recorded airspeed was 420 kn.

The stall warning began again and continued while the first officer commented, "There's that Mach buffet, 7/ guess we'll have to pull it up." followed by the captain's command, "Pull it up," and the sound of the landing gear warning horn. The FDR readout shows the following:

Two seconds later (about 13 seconds after the aircraft arrived at 24,800 feet), the vertical acceleration trace again declined to 0.8g and the altitude trace began to descend at a rate of 15,000 feet per minute. The airspeed trace decreased simultaneously at a rate of 4 kn per second and the magnetic heading trace changed from 290° to 080° within 10 seconds, which indicated that the aircraft was turning rapidly to the right.

7/ A slight buffet that occurs when an aircraft exceeds its critical Mach number. The buffet is caused by the formation of a shock wave on the airfoil surfaces and a separation of airflow aft of the shock wave. The change from laminar flow to turbulent flow aft of the shock wave causes a high frequency vibration in the control surfaces which is described as "buffet" or "buzz."

As the aircraft continued to descend, the vertical acceleration trace increased to 1.5g. The aircraft's magnetic heading trace fluctuated, but moved basically to the right. About 10 seconds after the descent began, the "Mayday" was transmitted.

Thirty-three seconds later the crew reported, "We're descending through 12, we're in a stall." About 5 seconds after that transmission, the captain commanded, "Flaps two....," and a sound similar to movement of the flap handle was recorded. There was no apparent change in the rate of descent; however, the vertical acceleration trace increased immediately, with peaks to +3g. The recorded airspeed decreased to zero, and the sound of the stall warning became intermittent.

Five seconds after the captain's command for flaps, the first officer said, "Pull now ... pull, that's it." Ten seconds later, the peak values for vertical acceleration increased to +5g. The rate of descent decreased slightly; however, the altitude continued to decrease to 1,090 feet -- the elevation of the terrain at the accident site. The aircraft had descended from 24,800 feet in 83 seconds.

1.12 Aircraft Wreckage

The aircraft struck the ground in a slightly nosedown and right wing-down attitude in an area where the terrain sloped downward about 10°. The aircraft structure had disintegrated and ruptured and was distorted extensively. There was no evidence of a preexisting malfunction in any of the aircraft's systems.

Except for both elevator tips, the left horizontal stabilizer, and three pieces of light structure from the left stabilizer, the entire aircraft was located within an area 180 feet long and 100 feet wide. The above components were located between 375 feet and 4,200 feet from the main wreckage.

The horizontal stabilizer trim setting was 1.2 units of trim aircraft noseup. The landing gear and spoilers were retracted. The wing trailing edge flaps were extended to the 2° position, and the Nos. 2, 3, 6, and 7 leading edge slats were fully extended, which corresponded to a trailing edge flap selection of 2°.

The No. 1 and No. 3 engines were separated from their respective pylons. The No. 2 engine remained in its mounting in the empennage. The engines exhibited impact damage but little rotational damage. The speed servo cams in all three fuel control units were at or near their high speed detents.

The outboard section of the left horizontal stabilizer had separated between stations 50 and 60. The inboard section remained attached to the

vertical stabilizer. The left elevator between stations 78 and 223 remained attached to the separated section. The right horizontal stabilizer was attached to the vertical stabilizer except for the tip section from station 188 outboard. The right elevator, from station 188 inboard, remained attached to the horizontal stabilizer.

The three attitude indicators were damaged on impact. The indicators showed similar attitude information -- 20° nosedown, with the wings almost level.

The two pitot head heater switches were in the "off" position and the switches' toggle levers were bent aft. The damage to the switch levers and the debris deposited on them was that which would be expected if they had been in the "off" position at impact. A new switch with its toggle lever in the "off" position, when struck with a heavy object, exhibited internal damage similar to the damage found in the internal portions of the right pitot heater switch.

Four of the five pitot head heater circuit breakers were operable and were electrically closed. The auxillary pitot head heater circuit breaker was jammed into its mounting structure, and it was electrically open.

The left elevator pitot head was lying on the frozen ground; when retrieved, at least eight drops of water dripped from the pressure inlet port. After exposure to sunlight, more water drained from the port. The captain's pitot head was retrieved and cleared of frozen mud. The pressure inlet port was filled with dry wood fibers. After exposure to sunlight, wet wood fibers were removed from the interior of the inlet port, and moisture was present on the inner surface of the port. The copilot's pitot head and the auxillary pitot head were crushed and damaged severely; they could not be checked for water content. The right elevator pitot head remained attached to the vertical stabilizer. The head was in good condition and contained no water or ice.

The engine anti-ice switches for the Nos. 1 and 2 engines were in the "open" position. The switch for the No. 3 engine was in the "closed" position and the switch handle was bent aft. Tests of the bulb filaments of the engine anti-ice indicator lights showed that all three lights were on at impact.

1.13 Medical and Pathological Information

The three crewmembers were killed in the crash. Toxicological tests disclosed no evidence of carbon monoxide, hydrogen cyanide, alcohol, or drugs in any of the crewmembers.

1.14 Fire

There was no fire, either during flight or after impact.

1.15 Survival Aspects

The accident was not survivable.

1.16 Tests and Research

1.16.1 Pitot Head Examination and Icing Tests

A metallurgical examination of the separated heater conductor wire in the pitot head from the first officer's pitot system showed that the circumference of the wire was reduced before the wire broke. The metal in the wire had not melted, and there were no signs of electrical current arcing or shorting.

A pitot head of the same type that provided pitot pressure to the first officer's airspeed/Mach indicator was exposed to icing conditions in a wind tunnel. With the pitot heater inoperative, 1 to 2 inches of ice formed over the pressure inlet port. During the exposure, a thin film of water flowed into the pressure port, some of which flowed out of the drain hole.

Blockage of the drain hole by ice seemed to depend on the length of time required for ice to form and block the total pressure inlet port. The longer it took for ice to form and block the total pressure port, the more likely it became that the drain hole would be blocked by ice. Also, the greater the angle between the longitudinal axis of the pitot head and the relative wind, the greater the likelihood that the drain hole would become blocked with ice.

Constant altitude pressure measurements showed that when the total pressure inlet port was blocked by ice and the drain hole remained open, pressure changes occurred that would cause a reduction of indicated airspeed. However, when both the total pressure port and drain hole were blocked, the total pressure remained constant, which would cause indicated airspeed to remain fixed. Also, abrupt and small pressure fluctuations occurred shortly before either the pressure port or drain hole became blocked by ice.

In an effort to reproduce the apparent inconsistencies between the airspeed and altitude values on the FDR traces, tests were conducted with an airspeed indicator and an altimeter connected to vacuum and pressure sources. By altering the vacuum to the altimeter and to the airspeed indicator, the altitude trace could be reproduced. However, following ascent above 16,000 feet, the FDR airspeed and altitude values could be simultaneously duplicated only when the total pressure to the airspeed indicator was fixed at its FDR value for an altimeter reading of about 15,675 feet and an indicated airspeed of about 302 kn.

1.16.2 Aircraft Performance Analysis

Following the accident, the Safety Board requested that the aircraft manufacturer analyze the data from the CVR and FDR to determine: (1) The consistency of these data, particularly the airspeed and altitude values, with the theoretical performance of the aircraft; (2) the significance and possible reason for a simultaneous activation of the overspeed and stall warning systems; and (3) the body attitude of the aircraft during its final ascent and descent. The following are some results of the manufacturer's performance analysis:

The airspeed and altitude values which were recorded were consistent with the aircraft's predicted climb performance until the aircraft reached 16,000 feet. The simultaneous increases in both airspeed and rate of ascent which were recorded thereafter exceeded the theoretical performance capability of a B-727-200 series aircraft of the same weight as N274US. Consequently, the recorded airspeed values were suspected to be erroneous, and it appeared that they varied directly with the change in recorded altitude. The recorded airspeeds correlated within 5 percent with the theoretical airspeeds which would be expected if the pressure measured in the pitot system had remained constant after the aircraft's climb through 16,000 feet.

The indicated airspeed of the aircraft when the stick shaker was first activated was calculated to be 165 kn as compared to the 412 kn recorded by the FDR. The decrease in airspeed from 305 kn to 165 kn as the aircraft climbed from 16,000 feet to 24,000 feet (within 116 seconds) is within the aircraft's theoretical climb power performance. The aircraft's pitch attitude would have been about 30° noseup as stick shaker speed was approached. The stall warning stick shaker is activated by angle of attack instrumentation which is completely independent of, and therefore not affected by errors in, the aircraft's airspeed measuring systems.

Vertical acceleration reduced slightly as the aircraft leveled at 24,800 feet probably because the pilot relaxed the back pressure being applied to the control column. The stick shaker ceased momentarily; however, the aircraft continued to decelerate because of the drag induced by the high body attitude, and the stick shaker reactivated. Boeing personnel interpreted the sound of the landing gear warning horn on the CVR to indicate that the thrust levers had been retarded to idle. The second reduction in vertical acceleration -- to 0.8g which was coincident with a sudden descent and a rapid magnetic heading change -- was probably caused by an aerodynamic stall with a probable loss of lateral control.

Theoretical relationships of angle of attack, velocity, and drag were compared to the recorded rate of descent and load factor to determine the attitude of the aircraft after the stall. The comparison showed that the aircraft attained an angle of attack of 22°, or greater, during the

descent. Transient nosedown attitudes of more than 60° would have been required to achieve the measured descent rate with an angle of attack of 22° . The variations in load factors, which averaged about $+1.5g$, were attributed to variations in the aircraft's angle of bank.

The aircraft was probably exceeding 230 kn, with a nosedown attitude of about 50° as it descended below 11,000 feet, when the flaps were extended to 2° . The momentary cessation of the stick shaker indicated that the angle of attack had been reduced to less than 13° . The increase in vertical acceleration to $2.5g$ was attributed to the aircraft's being in a tight nosedown spiral with a bank angle between 70° and 80° .

With a normally operating elevator feel system, and a stabilizer trim setting of 1.2 units aircraft noseup, the pilot would have to exert a pull force of between 45 and 50 lbs. to achieve a $2.5g$ load factor at 5,000 feet and 250 kn. If, however, the elevator pitot system was blocked so that the system sensed a zero indicated airspeed, a pull force of less than 30 lbs. would have produced the same load factor. After the aircraft had descended through 5,000 feet, the load factor reached peak values of $+5g$.

The manufacturer's engineers stated that the aircraft's structural limits would have been exceeded at high angles of sideslip and load factors approaching $+5g$. They stated that a consequent failure of the elevator assemblies could have produced an aerodynamic flutter which could have, in turn, caused the elevator spar to fail and the left horizontal stabilizer to separate. With the aircraft at a stall angle of attack when the horizontal stabilizer separated, an uncontrollable noseup pitching moment would have been produced, which could have resulted in an angle of attack of 40° or more.

1.17 Other Information

1.17.1 Pretakeoff Checklist

Northwest Airlines' operational procedures require that the flight-crew make a pretakeoff check of certain items. The second officer is required to read the checklist items, and the first officer must check the items and respond to the second officer's challenge. Included on the checklist are:

Second Officer

Flaps
Marked Bug _____ K
Ice Protection
Pitot Heat
Pressurization

First Officer

15, 15 (25,25) Blue
(C, FO) Numbers Set
OFF (ON)
ON
(C, FO) Zero, _____ $^{\circ}$,
Normal Flags

Company pilots stated that the checklist is used only to check that the required action has already been performed; it is not used as a list of items to be accomplished. With regard to the activation of pitot head heaters, it was the first officer's duty to turn the two switches to the "on" position shortly after the engines had been started and to check the ammeter readings on the various heaters to confirm their proper operation. After checking these items, he was supposed to leave the pitot heater switches on and to check that they were on during the pretakeoff check.

1.17.2 Airspeed Measuring System

When an aircraft moves through an air mass, pressure is created ahead of the aircraft, which adds to the existing static pressure within the air mass. The added pressure, dynamic pressure, is directly proportional to the velocity of the aircraft. When a symmetrically shaped object, such as a pitot head, is placed into the moving airstream, the flow of air will separate around the nose of the object so that the local velocity at the nose is zero. At the zero velocity point, the airstream dynamic pressure is converted into an increase in the local static pressure. Thus, the pressure measured at the nose of the object is called total pressure, and it is equal to the sum of the dynamic pressure and the ambient static pressure.

In an aircraft airspeed measuring system, the total pressure is measured by the pitot head and is transmitted through the pitot system plumbing to one side of a differential pressure measuring instrument (airspeed indicator). The ambient static pressure is measured at static ports which are mounted in an area that is not significantly influenced by the moving airstream. The static pressure measured at these ports is transmitted to the opposite side of the differential pressure measuring instrument. In effect, the differential pressure instrument (whether it be an airspeed indicator gage, a flight data recorder pressure transmitter, or a component within an air data computer) subtracts the ambient static pressure measured by the static system from the total pressure measured by the pitot system. The resultant dynamic pressure is a direct measurement of indicated airspeed.

Since the ambient static pressure is a component part of total pressure, any change in static pressure would normally result in an equal change in both the pitot and static pressure systems. Therefore, a change in ambient static pressure, such as that encountered during a change in altitude, would normally have no effect on airspeed measurement. Only a change in dynamic pressure produced by a change in the aircraft's velocity would cause a change in the indicated airspeed. If, however, only one side of the airspeed indicator sensed a change in the ambient static pressure, an erroneous change in indicated airspeed would result, even though the actual dynamic pressure remained unchanged. Such a condition would occur if either the pitot or static system was blocked or was otherwise rendered insensitive to external pressure changes.

In the event of a blocked pitot or static system, the direction of the indicated airspeed error would depend on which of the systems was blocked and the direction of change in the ambient static pressure. Under conditions where the pressure in the static system increases with respect to the pressure in the pitot system, the indicated airspeed will read low erroneously. For the opposite condition, where the pressure in the static system decreases with respect to the pressure in the pitot system, the indicated airspeed will read high erroneously. The latter would exist if the pitot head was blocked so that a constant pressure was trapped in the pitot system while the aircraft was ascending. This is because the static system pressure would decrease and the resultant differential pressure would appear as an increase in dynamic pressure.

Indicated airspeed error may also occur when the pitot system becomes insensitive to changes in total pressure in such a manner that the system vents to an ambient static pressure source. The pressure measured by the pitot system will equalize with the pressure in the static system, and the dynamic pressure (indicated airspeed) will decrease to zero. The vent source in a pitot head which can produce this kind of error is the moisture drain hole which is located downstream from a blocked total pressure sensing inlet.

1.17.3 B-727 Stall Characteristics

During its type certification process, the B-727-200 series aircraft demonstrated stall characteristics which met the requirements of the Civil Air Regulations, parts 4b. 160-162. The significant requirements defined therein are: (1) That, at an angle of attack measurably greater than that of maximum lift, the inherent flight characteristics give a clear indication to the pilot that the aircraft is stalled -- typical indications are a nosedown pitch or a roll which cannot be readily arrested; (2) that recovery from the stall can be effected by normal recovery techniques starting as soon as the aircraft is stalled; (3) that there is no abnormal noseup pitching and that the longitudinal control force be positive, up to and including the stall; (4) that a safe recovery from a stall can be effected with the critical engine inoperative; and (5) that a clear and distinctive stall warning be apparent to the pilot at an airspeed at least 7 percent above the stalling airspeed.

The certification stall tests, conducted with the aircraft in all operating configurations and with the most adverse weight and c.g. conditions, demonstrated that as the aircraft was slowed and its wing angle of attack was increased, the buffet produced by airflow separation from the wing provided a natural warning of impending stall. With the landing flaps extended, however, the airspeed margin provided by the buffet warning was considered to be insufficient. Consequently, a stick shaker system was installed to provide an artificial warning for all configurations.

In the clean configuration, 8/ the stick shaker activated when the angle of attack reached 13° . When the aircraft was slowed further, natural buffeting occurred at an angle of attack between 16° and 18° . The buffet was described as "quite heavy" when the speed was reduced to within 2 to 3 kn of the speed associated with maximum lift. When the angle of attack for maximum lift (about 22°) was reached, there was a tendency for the nose to drop if the pilot relaxed pressure on the control column. Also, lateral stability was reduced noticeably, which increased the pilot's workload in maintaining wings-level flight.

During certification flight tests, the angle of attack was increased to 25° , after which recovery was effected by relaxing the pull force on the control column. With the use of engine thrust during recovery, the altitude lost was restricted to about 2,000 feet.

Up to the onset of stall buffet, the longitudinal control forces needed to effect stall entry increased as the angle of attack increased. At higher angles of attack, up to and beyond the angle for maximum lift, the pull force required to maintain a noseup pitching moment decreased. The forces did not reverse, however, and, with normal trim, a reduction in pull force resulted in a decreased angle of attack.

The B-727 longitudinal control system is capable of developing the noseup pitching moments needed to obtain angles of attack much higher than those associated with stall. For an aircraft having the same weight, c.g. location, and stabilizer trim setting as N274US, the manufacturer's analysis showed that an angle of attack of approximately 37° could be attained if a continuous pull force was exerted to hold the control column aft.

Like other aircraft which have horizontal stabilizers located near or on top of their vertical stabilizers, the B-727 does pass through a range of high angles of attack where longitudinal instability occurs. This instability causes the aircraft, when no control force is applied, to pitch to even higher angles of attack. Longitudinal instability is caused by degraded horizontal stabilizer effectiveness when the aircraft's attitude is such that the horizontal stabilizer is enveloped by the low-energy turbulent air in the wake from the wings. When these high angles of attack are reached, a push force on the control column is required to reduce the angle of attack. For a B-727 with an aft c.g. location and stabilizer trim in the cruise range, wind tunnel data show that a nosedown pitching moment will decrease the angle of attack and stall recovery can be attained by applying push forces to the control column.

A stick pusher is a device which will apply a force to move the control column forward when the angle of attack for maximum lift is exceeded. The usefulness of a stick pusher is controversial since it can effect primary control of the aircraft. However, a stick pusher is required on B-727 and other aircraft registered by the United Kingdom. That stick pusher is designed so that its action can be overpowered by a pull force of about 80 lbs. on the pilot's control column.

8/ Without landing gear, flaps, or spoilers extended.

2. ANALYSIS AND CONCLUSIONS

2.1 Analysis

The aircraft was certificated, equipped, and maintained in accordance with regulations and approved procedures. The aircraft weighed substantially less than its authorized maximum weight for takeoff.

Although the speed servo cams in all three engine fuel controllers were positioned for high engine revolutions per minute, the engines were producing very little thrust at impact as evidenced by the absence of significant rotational damage to the engines. Probably, the throttles had been advanced shortly before impact, but there was either insufficient time for the engines to accelerate, or acceleration was limited because airflow into the engine inlets had been distorted by the extreme angle of attack and probable sideslip.

The flightcrew was properly certificated and each crewmember had received the training and off-duty time prescribed by regulations. There was no evidence of medical or physiological problems that might have affected their performance.

The conversations recorded on the CVR revealed that, following ascent above 13,500 feet, the flightcrew became concerned and puzzled by the apparent performance of the aircraft because of the indicated airspeed and the indicated rate of ascent. The FDR airspeed and altitude traces provided investigators an insight regarding these conversations. The airspeed trace increased rapidly after the aircraft ascended above 16,000 feet while the rate of climb continued to increase and eventually reached a peak value of 6,500 feet per minute. The Boeing Company's analysis of the airspeed and rates of climb values that registered above 16,000 feet showed that these values were incompatible with the aircraft's performance capabilities.

Analysis showed that there was a direct relationship between the airspeed and altitude values. This relationship was based on the assumptions that (1) the total pressure measured by the FDR pitot system remained constant after the aircraft ascended above 16,000 feet, and (2) the pressure measured by the FDR static system varied according to the recorded altitude values. These assumptions were substantiated by the tests which determined that the FDR airspeed and altitude traces could be reproduced only if the total pressure to the airspeed indicator was held constant during ascent above 16,000 feet.

Although the pitot systems for the captain's and first officer's airspeed Mach indicators and the FDR airspeed instrumentation are three separate and completely independent systems, it is reasonable to conclude that all three systems were sensing nearly identical and erroneous total pressures. This can be concluded because the flightcrew made no reference to

any difference between the airspeed readings on the captain's and first officer's indicators, and the first officer's reference to "...going 340 kn ..." corresponded closely to the airspeed value recorded on the FDR at that time. Additionally, the near simultaneous activation of the overspeed warning systems tends to prove that the first officer's airspeed was close to the value recorded on the FDR when the aircraft neared its peak altitude.

The erroneously high airspeed indications were caused by a complete and nearly simultaneous blockage of all three pitot pressure systems. Moreover, since the only common elements among the systems were the design features of the pitot heads and the environment to which they were exposed, the Safety Board concludes that the pitot heads were blocked by ice which formed around the heads and closed the drain holes and the pressure inlet ports. The conclusion is supported by the airspeed aberrations that were recorded while the aircraft was flying level at 13,500 feet and by the moisture which was found in the pitot heads when they were recovered and examined. Additionally, it is known that icing conditions existed in the area through which Flight 6231 was flying, and it is unlikely that any other type of blockage or malfunction would simultaneously affect the three independent systems.

The formation of ice on the pitot heads should have been prevented by electrical heating elements which are activated by the pitot heater switches located in the cockpit. The Safety Board concludes that the heating elements were never activated because the pitot heater switches were not in the "on" position during the flight. This conclusion is substantiated by the position and condition of the switches in the wreckage, the internal damage to the right switch, and the lack of evidence that electrical current was present in the heater circuit to the pitot head in the first officer's pitot system at the time of impact.

The Safety Board was unable to determine why the pitot head heater switches were not placed in the "on" position before departure. It is clear that the flightcrew performed the pretakeoff checks required by Northwest's operational procedures. However, the proper checklist sequence was not followed, and it is possible that the first officer positioned the switches improperly because of an omission in the sequence and his inexperience as a B-727 copilot.

While reading the checklist, the second officer called "bug" and, before receiving a response from either the captain or first officer, he omitted the "ice protection" call and called "pitot heat." The first officer apparently responded to both the omitted call and the "pitot heat" call by saying, "off and on," but following the captain's response to the "bug" call, the first officer asked whether the engine heat was needed. The captain may or may not have responded with a nod or hand signal, but the sound of five clicks was recorded and the first officer returned to the task of setting his airspeed bug.

The five clicks may have been the movement of the pitot heater switches to the "off" position and the movement of the engine anti-ice switches to the "on" position -- a reversal of their normal positions. This assumption is supported by the position of the engine anti-ice and pitot heater switches in the wreckage, the condition of the lights associated with the engine anti-ice switches, and the lack of any reference during the flight to the need for engine anti-ice.

Because of the flightcrew's comments concerning aircraft performance and the absence of comments about possible instrument error or airspeed system icing, the Safety Board concludes that the flightcrew attributed the high airspeed and the high rate of climb to the aircraft's relatively low gross weight and to an encounter with unusual weather, which included strong updrafts. The flightcrew's analysis of the situation must have been strongly influenced by these factors and by the fact that both airspeed instruments were indicating essentially the same values. However, the aircraft's attitude as it neared the top of its ascent should have warned them that the aircraft's performance was abnormal because its nearly 30° noseup attitude was about 25° higher than the normal climb attitude, and at such a high noseup attitude it would have been impossible for the airspeed to continue to increase even if influenced by extreme updrafts. Because the use of attitude references is a fundamental of instrument flying, which is stressed in Northwest's flightcrew training program, the Safety Board concludes that the flightcrew improperly relied on airspeed indications as a means of determining aircraft performance.

Although the activation of the overspeed warning systems probably reinforced the flightcrew's belief that they were taking appropriate action, the operation of the stall warning stick shaker should have alerted them that the aircraft actually was approaching a stall. The first officer apparently misinterpreted the control column vibration produced by the stick shaker as Mach buffet because when the stick shaker began, he commented, "... there's that Mach buffet." The captain apparently agreed with this interpretation because he then commanded, "Pull it up." The almost simultaneous activation of the stall and the overspeed warning systems undoubtedly created some confusion; however, the differences between stall buffet and Mach buffet are substantial and the former should have been easily recognized. Again, though, it appears that the flightcrew relied almost exclusively on the airspeed indicators and their related warning systems to assess the aircraft's performance.

Even after the stall, as manifested by the rapid heading change (banked attitude) and the sudden descent, the flightcrew failed to recognize the problem for a number of seconds. They continued to exert back pressure on the control column which kept the aircraft at a high angle of attack. They probably were having difficulty with lateral control, and the aircraft entered into a spiralling descent to the right, during which the actual airspeed of the aircraft began to increase rapidly.

The erroneous airspeed indications, the steep nosedown attitude, and the proprioceptive sensations associated with the positive vertical acceleration forces undoubtedly contributed to confusion which prevented the flightcrew from recognizing the true condition of the aircraft. Additionally, it is probable that the nosedown and banked attitudes of the aircraft were so steep that the horizon references in the attitude instruments were nearly hidden. This would have made the lateral attitude of the aircraft difficult to determine. However, had the pilots concentrated more on the attitude indicators, and particularly the position of the "sky pointers", 9/ they probably could have returned the aircraft to level flight had they taken appropriate corrective action within 30 to 40 seconds after the stall.

Probably because of the low airspeed indications, the captain decided that the aircraft was in a stall. He transmitted: "We're descending through 12, we're in a stall," and he called for the flaps to be extended to 20° -- a proper step in the stall recovery procedure. However, the actual indicated airspeed at that time was probably in excess of 230 kn and increasing rapidly; consequently, although the stick shaker ceased operation momentarily, the extension of the flaps had little favorable effect.

Even after the pilots decided that the aircraft was stalled, the Safety Board believes that they continued to react primarily to the high rate of descent indications and proprioceptive sensations because they continued to exert a pull force on the control column. This is substantiated by the increasing vertical acceleration forces as the descent continued. However, because the wings were not leveled first, the aircraft continued to descend rapidly in a spiralling, accelerated stall.

Since the pitot heads for the elevator feel system were probably blocked by ice, the force required of the pilots to move the elevators would have been increased while the aircraft was above 16,000 feet. However, when the aircraft descended below that altitude, the force required would have been diminished. As the descent continued below 5,000 feet, the actual indicated airspeed probably exceeded 350 kn while the airspeed sensed by the elevator feel system was probably near zero. Consequently, conditions were created in which high vertical acceleration forces could be produced with relative ease. As evidenced by the FDR acceleration trace, high vertical acceleration forces were produced below 5,400 feet.

As the aircraft continued its descent through 3,500 feet, the high vertical acceleration forces induced were sufficient to cause the failure of the left horizontal stabilizer. Thereafter, the aircraft probably rolled to a near wings-level attitude, pitched up to an extremely high angle of attack, and continued to descend in an uncontrollable stall to the ground.

9/ A triangular index which is positioned above the movable horizon and which moves in the opposite direction from the aircraft's banked attitude to indicate the number of degrees of bank.

During the Safety Board's investigation, incidents involving possible pitot-static system icing were reviewed. Although none of these incidents resulted in a catastrophic accident, it became clear that pitot or static system icing during flight can and does occur. Also, the resultant effects on pressure-operated flight instruments can produce at least momentary confusion among the crewmembers.

While all of the flightcrews involved in these incidents reverted to attitude flying until the cause of the icing could be eliminated or instrument flight could be terminated, it was apparent from these incidents that some pilots who understood the basic principles of airspeed measurement failed to analyze the possible results of a blockage of the pitot or static systems. The pilots often failed to determine the proper reasons for an increasing airspeed indication; they attributed such indications to unusual weather phenomena.

Although unusual weather phenomena such as mountain waves, extreme turbulence, and vertical wind shear can produce significant airspeed deviations, these phenomena usually are of short duration and cause erratic or abruptly changing airspeed indications rather than steadily increasing, steadily decreasing, or fixed airspeed indications. Also, the aircraft's attitude during encounters with these phenomena is important in determining airspeed trends and possible sources of error. Consequently, the Safety Board believes that potential pitot-static system problems and attitude flying as a temporary remedy for these problems should be reemphasized in instrument flying training programs, and the Safety Board has made a recommendation to this effect to the Administrator, Federal Aviation Administration.

2.2 Conclusions

(a) Findings

1. All members of the flightcrew were properly certificated and were qualified for their respective duties.
2. The aircraft had been properly maintained and was airworthy for the flight; its gross weight and c.g. were within the prescribed limits.
3. There was no evidence of a system malfunction or failure or of a structural defect in the aircraft.
4. The flightcrew had adequate weather information for the flight.
5. The FDR vertical acceleration trace indicates that only light turbulence was encountered.

6. The weather conditions encountered during the flight were conducive to the formation of moderate airframe ice.
7. The aircraft accumulated sufficient ice during its flight to block completely the drain holes and total pressure inlet ports of the pitot heads; the static ports were not affected by the ice.
8. The pitot heads became blocked at an altitude of about 16,000 feet.
9. The ice formed on the pitot heads because the pitot head heater switches had not been turned on before Flight 6231 departed JFK.
10. The complete blockage of the pitot heads caused the cockpit airspeed indicators to read erroneously high as the aircraft climbed above 16,000 feet and the static pressure decreased.
11. The flightcrew reacted to the high airspeed indications by increasing the noseup attitude of the aircraft which increased the rate of climb. While this caused the indicated airspeed to increase more rapidly because the static pressure decreased more rapidly with the increased rate of climb, the actual airspeed was decreasing.
12. The airspeed overspeed warning and stall warning stick shaker operated simultaneously because of the blocked pitot heads and the high noseup attitude of the aircraft.
13. The flightcrew misconstrued the operation of the stall warning stick shaker as Mach buffet.
14. The flightcrew continued to increase the noseup attitude of the aircraft following the operation of the stall warning stick shaker.
15. The aircraft stalled at an altitude of 24,800 feet while in a noseup attitude of about 30°.
16. Following the stall, the aircraft entered into a right spiralling dive at a high rate of descent. Throughout the descent, the flightcrew reacted primarily to airspeed and rate of descent indications instead of attitude indications, and thus failed to initiate proper recovery techniques and procedures.

17. In an effort to recover the aircraft from a high rate of descent, the flightcrew exerted excessive pull forces on the control columns which induced high vertical acceleration forces and caused the left horizontal stabilizer to fail.

(b) Probable Cause

The National Transportation Safety Board determines that the probable cause of this accident was the loss of control of the aircraft because the flightcrew failed to recognize and correct the aircraft's high-angle-of-attack, low-speed stall and its descending spiral. The stall was precipitated by the flightcrew's improper reaction to erroneous airspeed and Mach indications which had resulted from a blockage of the pitot heads by atmospheric icing. Contrary to standard operational procedures, the flightcrew had not activated the pitot head heaters.

3. RECOMMENDATIONS

As a result of this accident, three recommendations were made to the Administrator, Federal Aviation Administration. (See Appendix D.)

BY THE NATIONAL TRANSPORTATION SAFETY BOARD

/s/ FRANCIS H. McADAMS
Member

/s/ LOUIS M. THAYER
Member

/s/ ISABEL A. BURGESS
Member

John H. Reed, Chairman, and William R. Haley, Member, did not participate in the adoption of this report.

August 13, 1975

APPENDIX A

Investigation and Hearing

1. Investigation

The National Transportation Safety Board was notified of the accident about 1935 on December 1, 1974. The Safety Board immediately dispatched an investigative team to the scene. The following morning the team established investigative groups for operations/witnesses, air traffic control, weather, structures, powerplants, systems, flight data recorder, maintenance records, and cockpit voice recorder.

Parties to the investigation were: The Federal Aviation Administration, Northwest Airlines, Inc., The Boeing Company, Air Line Pilots Association, International Association of Machinists and Aerospace Workers, and the Pratt and Whitney Division of the United Aircraft Corporation.

2. Hearing

A public hearing was held at Bear Mountain, New York, on February 12 and 13, 1975. All of the parties to the investigation except the Pratt and Whitney Aircraft Division were parties to the hearing.

Preceding page blank

APPENDIX B

Aircrew Information

Captain John B. Lagorio

Captain Lagorio, 35, was employed by Northwest Airlines on January 17, 1966. He held Airline Transport Pilot certificate No. 1496609 with airplane multiengine and single-engine land ratings, commercial privileges and a type rating in the B-727. He held Flight Engineer certificate No. 1682555 and a valid first-class medical certificate which was issued with no limitations on August 22, 1974.

Captain Lagorio had accumulated about 7,434 flight-hours, of which about 1,973 were in the B-727. In the 30-, 60-, and 90-day periods preceding the accident, he flew about 58, 122, and 185 hours, respectively, all in the B-727.

Captain Lagorio was advanced from first officer to captain on August 5, 1969. He completed his last general refresher training on January 15, 1974, and his last B-727 refresher training on November 15, 1974. He passed a proficiency flight check in the B-727 simulator on November 15, 1974.

First Officer Walter A. Zadra

First Officer Zadra, 32, was employed by Northwest Airlines on January 8, 1968. He held Commercial Pilot certificate No. 1624729 with airplane multiengine and single-engine land ratings, and an instrument rating. He held Flight Engineer certificate No. 1834609 and a valid first-class medical certificate which was issued with no limitations on July 9, 1974.

First Officer Zadra had flown about 1,550 hours as a pilot or first officer and about 3,152 hours as a second officer (flight engineer) of which about 1,244 hours were in the B-727. He upgraded from second officer in B-707 aircraft to first officer in B-727 aircraft on October 16, 1974, and he had flown about 46 hours in the latter capacity. In the 30-, 60-, and 90-days periods preceding the accident, he flew, respectively, about 46 hours as first officer in the B-727 and 23 and 76 hours as second officer in the B-707.

First Officer Zadra completed general refresher training on January 7, 1974, and he passed a first officer proficiency check in the B-727 on October 16, 1974.

Second Officer James F. Cox

Second Officer Cox, 33, was employed by Northwest Airlines on February 2, 1969. He held Commercial Pilot certificate No. 1643627 with multiengine land and instrument ratings. He held Flight Engineer (turbo-jet powered) certificate No. 1920999 and a first-class medical certificate which was issued with no limitations on March 1, 1974.

Second Officer Cox had acquired about 1,938 hours of flying time as a second officer with Northwest Airlines, including about 1,611 hours in B-727 aircraft. In the 30-, 60-, and 90-day periods preceding the accident, he flew about 45, 113 and 180 hours, respectively, all in B-727 aircraft.

Second Officer Cox completed general refresher training on January 10, 1974, and he passed a second officer proficiency check on April 10, 1974.

APPENDIX C

Aircraft Information

N274US was manufactured by The Boeing Company on December 2, 1969, and it was assigned serial No. 20295. It had accumulated about 10,289 hours of time in service.

N274US was powered by three Pratt and Whitney JT8D-7 engines. Pertinent engine data are as follows:

<u>Position</u>	<u>Serial No.</u>	<u>Total Time</u>	<u>Time Since Heavy Maintenance</u>
1	649153	18,641 hours	3,044 hours
2	654070	14,818 hours	2,234 hours
3	648988	17,612 hours	1,193 hours

All of the required maintenance inspections and checks on the aircraft had been performed in accordance with Northwest Airlines approved directives.

NATIONAL TRANSPORTATION SAFETY BOARD WASHINGTON, D.C.

APPENDIX D

ISSUED: March 20, 1975

Forwarded to:
Honorable Alexander P. Butterfield
Administrator
Federal Aviation Administration
Washington, D. C. 20591

SAFETY RECOMMENDATION(S)

A-75-25 thru -27

The National Transportation Safety Board is investigating the Northwest Airlines, Inc., Boeing 727, N274US, aircraft crash which occurred near Thielle, New York, on December 1, 1974. The Board's continuing investigation has revealed that ice blocked the pitot heads.

A preliminary review of the evidence in this accident suggests the possibility that the crew concentrated on air data instrumentation to the exclusion of aircraft attitude indications. The timely use of the attitude information may have prevented the stall and subsequent crash.

About 5 minutes before the rapid descent, the flight data recorder (FDR) recorded aberrations in the airspeed trace. These aberrations were caused by the closure of the ram air inlet and the drain hole of the pitot mast. These aberrations were verified by wind-tunnel icing tests of a pitot mast and pneumatic tests of an altimeter and airspeed system. These tests produced airspeed/altitude traces similar to those recorded on the FDR.

The Safety Board is aware of other incidents in which an aircraft encountered difficulties while flying in freezing precipitation because of a lack of pitot heat. In these incidents, the flightcrews recognized the problem and took corrective action.

Evidence in this case indicates that the pitot heater control switches were not on, although the heaters were capable of operation. The aircraft had been flying in clouds and freezing temperatures.

Recently, one air carrier reported that it is operating its pitot heater system continuously and the failure rate is minimal, i.e., one element failure per aircraft per year. Several other air carriers are actively considering the institution of a similar procedure, and they believe there would be no adverse affect on the life of the pitot heater elements.

APPENDIX D

Honorable Alexander P. Butterfield - 2 -

The National Transportation Safety Board believes that corrective action is necessary and recommends that the Federal Aviation Administration:

1. Issue an Operations Bulletin to all air carrier and general aviation inspectors to stress the need for pilots to use attitude information when questionable information is presented on instruments that are dependent on the air data system. The information in this Bulletin should be disseminated to all operators for incorporation into their operations procedures and training programs. (Class 1)
2. Issue an Airworthiness Directive to require that a warning system be installed on transport category aircraft which will indicate, by way of a warning light, when the flight instrument pitot heating system is not operating. The warning light should operate directly from the heater electrical current. (Class 2)
3. Amend the applicable Federal Air Regulations to require the pitot heating system to be on any time electrical power is applied to an aircraft. This should also be incorporated in the operator's operations manual. (Class 2)

Our staff is available to assist your personnel in this matter, if desired.

REED, Chairman, McADAMS, THAYER, BURGESS, AND HALEY, Members, concurred in the above recommendations.


By: John H. Reed
Chairman



THE SECRETARY OF TRANSPORTATION
WASHINGTON, D.C. 20590

March 13, 1975

Honorable John H. Reed
Chairman, National Transportation
Safety Board
800 Independence Avenue, S.W.
Washington, D. C. 20591

Dear Mr. Chairman:

This is to acknowledge receipt of your letter of March 12 enclosing a copy of a safety recommendation to the Federal Aviation Administrator concerning the Board's investigation of the Northwest Airlines, Inc., Boeing 727, N274US, aircraft crash which occurred near Thielle, New York, on December 1, 1974.

The recommendations are receiving attention by the Department's Assistant Secretary for Environment, Safety and Consumer Affairs, as well as other appropriate Departmental officials.

Sincerely,

A handwritten signature in cursive script, reading "William T. Coleman, Jr.".

William T. Coleman, Jr.

APPENDIX D

DEPARTMENT OF TRANSPORTATION
FEDERAL AVIATION ADMINISTRATION

WASHINGTON, D.C. 20590



OFFICE OF
THE ADMINISTRATOR

MAY 27 1975

Notation 1481

Honorable John H. Reed
Chairman, National Transportation Safety Board
800 Independence Avenue, S. W.
Washington, D. C. 20594

Dear Mr. Chairman:

This is in response to your letter of March 12 which transmitted NTSB Safety Recommendations A-75-25 thru 27.

Recommendation No. 1.

Issue an Operations Bulletin to all air carrier and general aviation inspectors to stress the need for pilots to use attitude information when questionable information is presented on instruments that are dependent on the air data system. The information in this Bulletin should be disseminated to all operators for incorporation into their operations procedures and training programs. (Class 1)

Comment.

Air Carrier Operations Alert Bulletin 75-3 dated February 13 covers this subject. A Part 135, Air Taxi Bulletin, is being prepared. We are also considering the issuance of an advisory circular on the subject.

Recommendation No. 2.

Issue an Airworthiness Directive to require that a warning system be installed on transport category aircraft which will indicate, by way of a warning light, when the flight instrument pitot heating system is not operating. The warning light should operate directly from the heater electrical current. (Class 2)

Comment.

We do not concur in this recommendation. Some current aircraft have cycling types of pitot heaters. These cycle on and off as controlled by thermostats or timers. Warning lights would flash on and off with

2

the cycling. We consider this as distracting and possibly detrimental to safety. Other aircraft in which the pitot heat is controlled directly by a simple on-off switch could be modified by adding a power relay and warning light. We do not consider this necessary or desirable. Operation of pitot heat is on cockpit checklists and is well covered in operations manuals and crew training. In addition, the effectiveness of additional warning lights among the many warning lights presently installed in the cockpit is of doubtful value.

Recommendation No. 3.

Amend the applicable Federal Air Regulations to require the pitot heating system to be on any time electrical power is applied to an aircraft. This should also be incorporated in the operator's operations manual. (Class 2)


Comment.

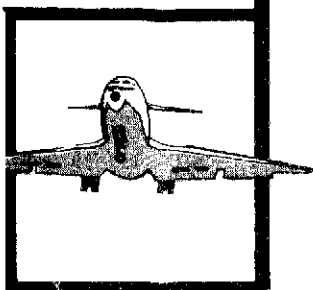
This recommendation is considered to apply to all types of aircraft in service and to future designs. We propose to delete from consideration those aircraft which are limited to VFR flight only since they are not required to have any deicing capabilities.

Retrofit on existing aircraft presents many problems and we do not consider the recommendation practical for general adoption. Some cyclic installations will not tolerate continuous heat and would have to be completely replaced. Continuous heat would be unsafe in many circumstances such as extended parking with electrical power on. As you mentioned, reliability would be reduced leading to more frequent unsafe conditions in flight. We do not consider retrofit of existing aircraft practical or feasible.

For new designs the recommendation may be feasible because the installations can be safe and reliable by design of interfacing electrical power systems, positioning of pitot tubes, and construction of pitot tubes. A regulatory project leading to a Notice of Proposed Rule Making and subsequently a rule requiring an appropriately designed pitot heating system is being established.

Sincerely,


James E. Dow
Acting Administrator



293

PB 245 581



NATIONAL TRANSPORTATION SAFETY BOARD

WASHINGTON, D.C. 20594

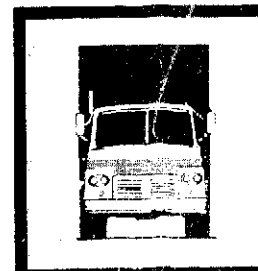
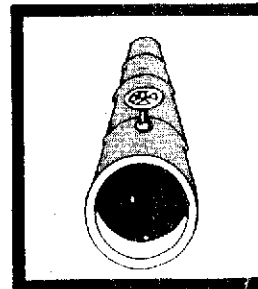
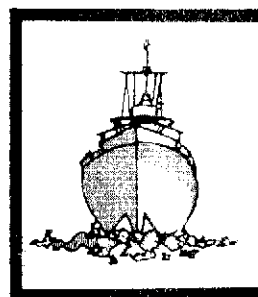
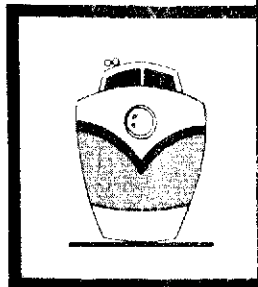
AIRCRAFT ACCIDENT REPORT

**NORTHWEST AIRLINES, INC.,
BOEING 727-251, N274US,
NEAR THIELLS, NEW YORK
DECEMBER 1, 1974**

Reproduced by
**NATIONAL TECHNICAL
INFORMATION SERVICE**
US Department of Commerce
Springfield, VA. 22151

REPORT NUMBER: NTSB-AAR-75-13

UNITED STATES GOVERNMENT



TECHNICAL REPORT DOCUMENTATION PAGE

1. Report No. NTSB-AAR-75-B		2. Government Accession No.		3. Recipient's Catalog No.	
4. Title and Subtitle Aircraft Accident Report - Northwest Airlines, Inc., Boeing 727-251, N274US, near Thiells, New York, December 1, 1974				5. Report Date August 13, 1975	
				6. Performing Organization Code	
7. Author(s)				8. Performing Organization Report No.	
9. Performing Organization Name and Address National Transportation Safety Board Bureau of Aviation Safety Washington, D. C. 20594				10. Work Unit No. 1481-A	
				11. Contract or Grant No.	
12. Sponsoring Agency Name and Address NATIONAL TRANSPORTATION SAFETY BOARD Washington, D. C. 20594				13. Type of Report and Period Covered Aircraft Accident Report December 1, 1974	
				14. Sponsoring Agency Code	
15. Supplementary Notes					
<p>16. Abstract</p> <p>About 1926 e.s.t. on December 1, 1974, Northwest Airlines Flight 6231, a Boeing 727-251, crashed about 3.2 nmi west of Thiells, New York. The accident occurred about 12 minutes after the flight had departed John F. Kennedy International Airport, Jamaica, New York, and while on a ferry flight to Buffalo, New York. Three crewmembers, the only persons aboard the aircraft, died in the crash. The aircraft was destroyed.</p> <p>The aircraft stalled at 24,800 feet m.s.l. and entered an uncontrolled spiralling descent into the ground. Throughout the stall and descent, the flightcrew did not recognize the actual condition of the aircraft and did not take the correct measures necessary to return the aircraft to level flight. Near 3,500 feet m.s.l., a large portion of the left horizontal stabilizer separated from the aircraft, which made control of the aircraft impossible.</p> <p>The National Transportation Safety Board determines that the probable cause of this accident was the loss of control of the aircraft because the flightcrew failed to recognize and correct the aircraft's high-angle-of-attack, low-speed stall and its descending spiral. The stall was precipitated by the flightcrew's improper reaction to erroneous airspeed and Mach indications which had resulted from a blockage of the pitot heads by atmospheric icing. Contrary to standard operational procedures, the flightcrew had not activated the pitot head heaters.</p>					
17. Key Words Scheduled air carriers, pitot system errors; atmospheric icing ; stalls; attitude instrument flying.				18. Distribution Statement This document is available through the National Technical Information Service, Springfield, Virginia 22151 PRICES SUBJECT TO CHANGE	
19. Security Classification (of this report) UNCLASSIFIED		20. Security Classification (of this page) UNCLASSIFIED		21. No. of Pages 32	
				22. Price \$3.75	

NTSB Form 1765.2 (Rev. 9/74)

Reproduced by
NATIONAL TECHNICAL
INFORMATION SERVICE
U.S. Department of Commerce
Springfield, VA. 22151

TABLE OF CONTENTS

	<u>Page</u>
Synopsis	1
1. Investigation	1
1.1 History of the Flight	1
1.2 Injuries to Persons	2
1.3 Damage to Aircraft	2
1.4 Other Damage	2
1.5 Crew Information	2
1.6 Aircraft Information	3
1.7 Meteorological Information	4
1.8 Aids to Navigation	4
1.9 Communications	4
1.10 Aerodrome and Ground Facilities	5
1.11 Flight Recorders	5
1.12 Aircraft Wreckage	7
1.13 Medical and Pathological Information	8
1.14 Fire	8
1.15 Survival Aspects	9
1.16 Tests and Research	9
1.16.1 Pitot Head Examination and Icing Tests	9
1.16.2 Aircraft Performance Analysis	10
1.17 Other Information	11
1.17.1 Pretakeoff Checklist	11
1.17.2 Airspeed Measuring System	12
1.17.3 B-727 Stall Characteristics	13
2. Analysis and Conclusions	15
2.1 Analysis	15
2.2 Conclusions	19
(a) Findings	19
(b) Probable Cause	21
3. Recommendations	21
 Appendixes	
Appendix A - Investigation and Hearing	23
Appendix B - Crew Information	24
Appendix C - Aircraft Information	26
Appendix D - Recommendations A-75 25-27 to FAA	27

NATIONAL TRANSPORTATION SAFETY BOARD
WASHINGTON, D.C. 20594

AIRCRAFT ACCIDENT REPORT

Adopted August 13, 1975

NORTHWEST AIRLINES, INC.
BOEING 727-251, N274US
NEAR THIELLS, NEW YORK
DECEMBER 1, 1974

SYNOPSIS

About 1926 e.s.t. on December 1, 1974, Northwest Airlines Flight 6231, a Boeing 727-251, crashed about 3.2 nmi west of Thiells, New York. Flight 6231 was a ferry flight to Buffalo, New York. The accident occurred about 12 minutes after the flight had departed John F. Kennedy International Airport, Jamaica, New York. Three crewmembers, the only persons aboard the aircraft, died in the crash. The aircraft was destroyed.

The aircraft stalled at 24,800 feet m.s.l. and entered an uncontrolled, spiralling descent to the ground. Throughout the stall and descent the flightcrew did not recognize the actual condition of the aircraft and did not take the correct measures necessary to return the aircraft to level flight. Near 3,500 feet m.s.l., a large portion of the left horizontal stabilizer separated from the aircraft, which made control of the aircraft impossible.

The National Transportation Safety Board determines that the probable cause of this accident was the loss of control of the aircraft because the flightcrew failed to recognize and correct the aircraft's high-angle-of-attack, low-speed stall and its descending spiral. The stall was precipitated by the flightcrew's improper reaction to erroneous airspeed and Mach indications which had resulted from a blockage of the pitot heads by atmospheric icing. Contrary to standard operational procedures, the flightcrew had not activated the pitot head heaters.

1. INVESTIGATION

1.1 History of Flight

On December 1, 1974, Northwest Airlines, Inc., Flight 6231, a Boeing 727-251, N274US, was a ferry flight from John F. Kennedy International Airport (JFK), Jamaica, New York, to Buffalo, New York. Three crewmembers were the only persons aboard the aircraft.

Flight 6231 departed JFK about 1914 1/ on a standard instrument departure. After takeoff, Kennedy departure control cleared the flight to climb to 14,000 feet. 2/ At 1920:21, New York air route traffic control center (ZNY) assumed radar control of the flight, and at 1921:07, ZNY cleared the flight to climb to flight level 310. 3/

Flight 6231 proceeded without reported difficulty until 1924:42, when a crewmember transmitted, "Mayday, mayday ... " on ZNY frequency. The ZNY controller responded, "... go ahead," and the crewmember said, "Roger, we're out of control, descending through 20,000 feet."

After giving interim altitude clearances, at 1925:21, the ZNY controller asked Flight 6231 what their problem was, and a crewmember responded, "We're descending through 12, we're in a stall." The sound of an active radio transmitter was recorded at 1925:38. There were no further transmissions from Flight 6231.

At 1925:57, Flight 6231 crashed in a forest in the Harriman State Park, about 3.2 nmi west of Thiells, New York. No one witnessed the crash.

The accident occurred during hours of darkness.

The geographic coordinates of the accident site are 41° 12' 53" N. latitude and 74° 5' 40" W. longitude.

1.2 Injuries to Persons

<u>Injuries</u>	<u>Crew</u>	<u>Passengers</u>	<u>Other</u>
Fatal	3	0	0
Nonfatal	0	0	0
None	0	0	

1.4 Damage to Aircraft

The aircraft was destroyed.

1.4 Other Damage

Trees and bushes were either damaged or destroyed.

1.5 Crew Information

The crewmembers were qualified and certificated for the flight. The three crewmembers had off-duty periods of 15 hours 31 minutes during the 24-hour period preceding the flight. (See Appendix B.)

- 1/ All times herein are eastern standard, based on the 24-hour clock.
2/ All altitudes herein are mean sea level, unless otherwise indicated.
3/ An altitude of 31,000 feet which is maintained with an altimeter setting of 29.92 inches.

In October 1974, the first officer advanced from second officer in B-707 aircraft to first officer in B-727 aircraft; he had flown about 46 hours in the latter capacity.

1.6 Aircraft Information

N274US was owned and operated by Northwest Airlines, Inc. It was certificated and maintained in accordance with Federal Aviation Administration (FAA) regulations and requirements. (See Appendix C.)

N274US was loaded with 48,500 lbs. of Jet A fuel. The gross weight at takeoff was about 147,000 lbs. The weight and center of gravity (c.g.) were within prescribed limits. The aircraft was in compliance with all pertinent airworthiness directives.

In the Boeing 727 aircraft, the pitot-static instruments on the captain's panel, the pitot-static instruments on the first officer's panel, and the pitot-static instrumentation in the flight data recorder (FDR) are connected to separate pitot and static sources. The three pitot systems have no common elements and are completely independent. The three static systems are also independent except for manual selector valves in both the captain's and first officer's systems which provide for selection of the FDR static system as an alternate pressure source if either primary source malfunctions.

The first officer's pitot and static systems are connected to a Mach airspeed warning switch. The switch activates a warning horn when it senses a differential pressure which indicates that the aircraft's speed is exceeding V_{mo} or M_{mo} , ^{4/} depending on the aircraft's altitude. A redundant Mach airspeed warning system is incorporated in the FDR pitot and static systems.

The pitot head for the captain's pitot system is located on the left side of the aircraft's fuselage; the pitot heads for the first officer's system and the FDR system are located on the right side of the fuselage. Each of these heads incorporates a heating element and a small drain hole, for exhausting moisture, aft of the total pressure sensing inlet. The three static systems each have a static port located on either side of the fuselage. The left static port is connected to the right static port to offset sideslip effects by balancing the pressures within the systems. Each of the ports is equipped with a heating element.

In addition to the above systems, two independent pitot-static systems are connected to a mechanism in the aircraft's longitudinal control system. The force which the pilot must exert to move the elevator control surfaces varies as a function of the dynamic pressure measured by these systems. The two pitot heads for these systems are mounted one on each side of the vertical stabilizer, and their design is similar to the other pitot heads.

^{4/} Maximum operating limit speed or maximum operating limit Mach.

1.7 Meteorological Information

Northwest Airlines' meteorology department supplied the weather information for Flight 6231. This information included a synopsis of surface conditions, terminal forecasts, a tropopause and wind forecast for the 300-millibar level, appropriate surface observations, and turbulence plots. For the period 1700 to 2300, Northwest meteorologists forecasted moderate to heavy snowshowers from Lake Michigan to the Appalachian Mountains and moderate to heavy rainshowers and scattered thunderstorms east of the Appalachians.

Northwest's turbulence plot (TP) No. East 2 was in effect and available to the flightcrew on the day of the accident. TP East 2 was a triangular area defined by lines connecting Pittsburgh, Pennsylvania, New York City, New York, and Richmond, Virginia. Thunderstorm cells with maximum tops to 28,000 feet were located in this area.

SIGMET 5/ Delta 2, issued at 1755 and valid 1755 to 2200, predicted frequent moderate icing in clouds, locally severe in precipitation above the freezing level, which was at the surface in southwestern New York and which sloped to 6,000 feet eastward to the Atlantic coast.

The surface weather observations at Newburgh, New York, about 17 miles north of the accident site, were:

1900 - Estimated ceiling -- 2,500 feet broken, 5,000 feet overcast, visibility -- 12 miles, temperature -- 34°F., dew point -- 22°F., wind -- 070° at 14 kn, gusts -- 24 kn, altimeter setting -- 29.98 in.

2000 - Similar conditions to those reported at 1900 except that very light ice pellets were falling.

Another Northwest flight was on a similar route behind Flight 6231. The captain of that flight stated that he encountered icing and light turbulence in his climb. He was in instrument conditions from 1,500 feet to 23,000 feet, except for a few minutes between cloud layers at an intermediate altitude.

1.8 Aids to Navigation

There were no problems with navigational aids.

1.9 Communications

There were no problems with air-to-ground communications.

5/ A SIGMET is an advisory of weather severe enough to be potentially hazardous to all aircraft. It is broadcast on navigational and voice frequencies and by flight service stations. It is also transmitted on voice-A weather teletype circuits.

1.10 Aerodrome and Ground Facilities

Not applicable.

1.11 Flight Recorders

N274US was equipped with a Fairchild Model 5424 flight data recorder (FDR), serial No. 5146, and a Fairchild A-100 cockpit voice recorder (CVR), serial No. 1640. Both recorders sustained superficial mechanical damage, but the recording tapes were intact and undamaged. All of the FDR traces and the CVR channels were clearly recorded.

The readout of the FDR traces involved 11 minutes 54.6 seconds of flight, beginning 15 seconds before liftoff.

Pertinent portions of the CVR tape were transcribed, beginning with the flightcrew's execution of the pretakeoff checklist and ending with the sounds of impact. The following transcript was made of the flightcrew's activities between 1906:36 and 1906:51:

First Officer: Zero, zero and thirty-one, fifteen, fifteen blue.

Second Officer: Bug.

Second Officer: Pitot heat.

First Officer: Off and on.

Captain: One forty-two is the bug.

First Officer: Or ... do you want the engine heat on?

First Officer: Huh!

Sound of five clicks.

Air-to-ground communications, cockpit conversations, and other sounds recorded on the CVR were correlated to the FDR altitude, airspeed, heading, and vertical acceleration traces by matching the radio transmission time indications on both the CVR and FDR.

The FDR to CVR correlation showed that after takeoff, the aircraft climbed to 13,500 feet and remained at that altitude for about 50 seconds, during which time the airspeed 6/ increased from 264 kn to 304 kn. During that 50 seconds, the airspeed trace showed two aberrations in a 27-second period; each aberration was characterized by a sudden reduction in airspeed. These reductions were 40 kn and 140 kn and lasted for 7 and 5 seconds, respectively.

6/ All airspeeds are indicated airspeeds, unless otherwise noted.

The aircraft then began to climb 2,500 feet per minute while maintaining an airspeed of about 305 kn. As the altitude increased above 16,000 feet, the recorded airspeed began to increase. Subsequently, both the rate of climb and the rate of change in airspeed increased. About this same time, the first officer commented, "Do you realize we're going 340 kn and I'm climbing 5,000 feet a minute?"

The flightcrew discussed the implications of the high airspeed and high rate of climb. The second officer commented, "That's because we're light," after which the captain said, "It gives up real fast," and "I wish I had my shoulder harness on, it's going to give up pretty soon." The rate of climb eventually exceeded 6,500 feet per minute.

The sound of an overspeed warning horn was recorded as the altitude reached 23,000 feet. At that time, the recorded airspeed was 405 kn and the following conversation took place:

Captain: "Would you believe that #."

First Officer: "I believe it, I just can't do anything about it."

Captain: "No, just pull her back, let her climb."

This last comment was followed by the sound of a second overspeed warning horn.

The sound of the stall warning stick shaker was recorded intermittently less than 10 seconds after the onset of the overspeed warning. Five seconds later, vertical acceleration reduced to 0.8g, and the altitude leveled at 24,800 feet. The recorded airspeed was 420 kn.

The stall warning began again and continued while the first officer commented, "There's that Mach buffet, 7/ guess we'll have to pull it up." followed by the captain's command, "Pull it up," and the sound of the landing gear warning horn. The FDR readout shows the following:

Two seconds later (about 13 seconds after the aircraft arrived at 24,800 feet), the vertical acceleration trace again declined to 0.8g and the altitude trace began to descend at a rate of 15,000 feet per minute. The airspeed trace decreased simultaneously at a rate of 4 kn per second and the magnetic heading trace changed from 290° to 080° within 10 seconds, which indicated that the aircraft was turning rapidly to the right.

7/ A slight buffet that occurs when an aircraft exceeds its critical Mach number. The buffet is caused by the formation of a shock wave on the airfoil surfaces and a separation of airflow aft of the shock wave. The change from laminar flow to turbulent flow aft of the shock wave causes a high frequency vibration in the control surfaces which is described as "buffet" or "buzz."

As the aircraft continued to descend, the vertical acceleration trace increased to 1.5g. The aircraft's magnetic heading trace fluctuated, but moved basically to the right. About 10 seconds after the descent began, the "Mayday" was transmitted.

Thirty-three seconds later the crew reported, "We're descending through 12, we're in a stall." About 5 seconds after that transmission, the captain commanded, "Flaps two....," and a sound similar to movement of the flap handle was recorded. There was no apparent change in the rate of descent; however, the vertical acceleration trace increased immediately, with peaks to +3g. The recorded airspeed decreased to zero, and the sound of the stall warning became intermittent.

Five seconds after the captain's command for flaps, the first officer said, "Pull now ... pull, that's it." Ten seconds later, the peak values for vertical acceleration increased to +5g. The rate of descent decreased slightly; however, the altitude continued to decrease to 1,090 feet -- the elevation of the terrain at the accident site. The aircraft had descended from 24,800 feet in 83 seconds.

1.12 Aircraft Wreckage

The aircraft struck the ground in a slightly nosedown and right wing-down attitude in an area where the terrain sloped downward about 10°. The aircraft structure had disintegrated and ruptured and was distorted extensively. There was no evidence of a preexisting malfunction in any of the aircraft's systems.

Except for both elevator tips, the left horizontal stabilizer, and three pieces of light structure from the left stabilizer, the entire aircraft was located within an area 180 feet long and 100 feet wide. The above components were located between 375 feet and 4,200 feet from the main wreckage.

The horizontal stabilizer trim setting was 1.2 units of trim aircraft noseup. The landing gear and spoilers were retracted. The wing trailing edge flaps were extended to the 2° position, and the Nos. 2, 3, 6, and 7 leading edge slats were fully extended, which corresponded to a trailing edge flap selection of 2°.

The No. 1 and No. 3 engines were separated from their respective pylons. The No. 2 engine remained in its mounting in the empennage. The engines exhibited impact damage but little rotational damage. The speed servo cams in all three fuel control units were at or near their high speed detents.

The outboard section of the left horizontal stabilizer had separated between stations 50 and 60. The inboard section remained attached to the

vertical stabilizer. The left elevator between stations 78 and 223 remained attached to the separated section. The right horizontal stabilizer was attached to the vertical stabilizer except for the tip section from station 188 outboard. The right elevator, from station 188 inboard, remained attached to the horizontal stabilizer.

The three attitude indicators were damaged on impact. The indicators showed similar attitude information -- 20° nosedown, with the wings almost level.

The two pitot head heater switches were in the "off" position and the switches' toggle levers were bent aft. The damage to the switch levers and the debris deposited on them was that which would be expected if they had been in the "off" position at impact. A new switch with its toggle lever in the "off" position, when struck with a heavy object, exhibited internal damage similar to the damage found in the internal portions of the right pitot heater switch.

Four of the five pitot head heater circuit breakers were operable and were electrically closed. The auxiliary pitot head heater circuit breaker was jammed into its mounting structure, and it was electrically open.

The left elevator pitot head was lying on the frozen ground; when retrieved, at least eight drops of water dripped from the pressure inlet port. After exposure to sunlight, more water drained from the port. The captain's pitot head was retrieved and cleared of frozen mud. The pressure inlet port was filled with dry wood fibers. After exposure to sunlight, wet wood fibers were removed from the interior of the inlet port, and moisture was present on the inner surface of the port. The copilot's pitot head and the auxiliary pitot head were crushed and damaged severely; they could not be checked for water content. The right elevator pitot head remained attached to the vertical stabilizer. The head was in good condition and contained no water or ice.

The engine anti-ice switches for the Nos. 1 and 2 engines were in the "open" position. The switch for the No. 3 engine was in the "closed" position and the switch handle was bent aft. Tests of the bulb filaments of the engine anti-ice indicator lights showed that all three lights were on at impact.

1.13 Medical and Pathological Information

The three crewmembers were killed in the crash. Toxicological tests disclosed no evidence of carbon monoxide, hydrogen cyanide, alcohol, or drugs in any of the crewmembers.

1.14 Fire

There was no fire, either during flight or after impact.

1.15 Survival Aspects

The accident was not survivable.

1.16 Tests and Research

1.16.1 Pitot Head Examination and Icing Tests

A metallurgical examination of the separated heater conductor wire in the pitot head from the first officer's pitot system showed that the circumference of the wire was reduced before the wire broke. The metal in the wire had not melted, and there were no signs of electrical current arcing or shorting.

A pitot head of the same type that provided pitot pressure to the first officer's airspeed/Mach indicator was exposed to icing conditions in a wind tunnel. With the pitot heater inoperative, 1 to 2 inches of ice formed over the pressure inlet port. During the exposure, a thin film of water flowed into the pressure port, some of which flowed out of the drain hole.

Blockage of the drain hole by ice seemed to depend on the length of time required for ice to form and block the total pressure inlet port. The longer it took for ice to form and block the total pressure port, the more likely it became that the drain hole would be blocked by ice. Also, the greater the angle between the longitudinal axis of the pitot head and the relative wind, the greater the likelihood that the drain hole would become blocked with ice.

Constant altitude pressure measurements showed that when the total pressure inlet port was blocked by ice and the drain hole remained open, pressure changes occurred that would cause a reduction of indicated airspeed. However, when both the total pressure port and drain hole were blocked, the total pressure remained constant, which would cause indicated airspeed to remain fixed. Also, abrupt and small pressure fluctuations occurred shortly before either the pressure port or drain hole became blocked by ice.

In an effort to reproduce the apparent inconsistencies between the airspeed and altitude values on the FDR traces, tests were conducted with an airspeed indicator and an altimeter connected to vacuum and pressure sources. By altering the vacuum to the altimeter and to the airspeed indicator, the altitude trace could be reproduced. However, following ascent above 16,000 feet, the FDR airspeed and altitude values could be simultaneously duplicated only when the total pressure to the airspeed indicator was fixed at its FDR value for an altimeter reading of about 15,675 feet and an indicated airspeed of about 302 kn.

1.16.2 Aircraft Performance Analysis

Following the accident, the Safety Board requested that the aircraft manufacturer analyze the data from the CVR and FDR to determine: (1) The consistency of these data, particularly the airspeed and altitude values, with the theoretical performance of the aircraft; (2) the significance and possible reason for a simultaneous activation of the overspeed and stall warning systems; and (3) the body attitude of the aircraft during its final ascent and descent. The following are some results of the manufacturer's performance analysis:

The airspeed and altitude values which were recorded were consistent with the aircraft's predicted climb performance until the aircraft reached 16,000 feet. The simultaneous increases in both airspeed and rate of ascent which were recorded thereafter exceeded the theoretical performance capability of a B-727-200 series aircraft of the same weight as N274US. Consequently, the recorded airspeed values were suspected to be erroneous, and it appeared that they varied directly with the change in recorded altitude. The recorded airspeeds correlated within 5 percent with the theoretical airspeeds which would be expected if the pressure measured in the pitot system had remained constant after the aircraft's climb through 16,000 feet.

The indicated airspeed of the aircraft when the stick shaker was first activated was calculated to be 165 kn as compared to the 412 kn recorded by the FDR. The decrease in airspeed from 305 kn to 165 kn as the aircraft climbed from 16,000 feet to 24,000 feet (within 116 seconds) is within the aircraft's theoretical climb power performance. The aircraft's pitch attitude would have been about 30° noseup as stick shaker speed was approached. The stall warning stick shaker is activated by angle of attack instrumentation which is completely independent of, and therefore not affected by errors in, the aircraft's airspeed measuring systems.

Vertical acceleration reduced slightly as the aircraft leveled at 24,800 feet probably because the pilot relaxed the back pressure being applied to the control column. The stick shaker ceased momentarily; however, the aircraft continued to decelerate because of the drag induced by the high body attitude, and the stick shaker reactivated. Boeing personnel interpreted the sound of the landing gear warning horn on the CVR to indicate that the thrust levers had been retarded to idle. The second reduction in vertical acceleration -- to 0.8g which was coincident with a sudden descent and a rapid magnetic heading change -- was probably caused by an aerodynamic stall with a probable loss of lateral control.

Theoretical relationships of angle of attack, velocity, and drag were compared to the recorded rate of descent and load factor to determine the attitude of the aircraft after the stall. The comparison showed that the aircraft attained an angle of attack of 22°, or greater, during the

descent. Transient nosedown attitudes of more than 60° would have been required to achieve the measured descent rate with an angle of attack of 22° . The variations in load factors, which averaged about $+1.5g$, were attributed to variations in the aircraft's angle of bank.

The aircraft was probably exceeding 230 kn, with a nosedown attitude of about 50° as it descended below 11,000 feet, when the flaps were extended to 2° . The momentary cessation of the stick shaker indicated that the angle of attack had been reduced to less than 13° . The increase in vertical acceleration to $2.5g$ was attributed to the aircraft's being in a tight nosedown spiral with a bank angle between 70° and 80° .

With a normally operating elevator feel system, and a stabilizer trim setting of 1.2 units aircraft noseup, the pilot would have to exert a pull force of between 45 and 50 lbs. to achieve a $2.5g$ load factor at 5,000 feet and 250 kn. If, however, the elevator pitot system was blocked so that the system sensed a zero indicated airspeed, a pull force of less than 30 lbs. would have produced the same load factor. After the aircraft had descended through 5,000 feet, the load factor reached peak values of $+5g$.

The manufacturer's engineers stated that the aircraft's structural limits would have been exceeded at high angles of sideslip and load factors approaching $+5g$. They stated that a consequent failure of the elevator assemblies could have produced an aerodynamic flutter which could have, in turn, caused the elevator spar to fail and the left horizontal stabilizer to separate. With the aircraft at a stall angle of attack when the horizontal stabilizer separated, an uncontrollable noseup pitching moment would have been produced, which could have resulted in an angle of attack of 40° or more.

1.17 Other Information

1.17.1 Pretakeoff Checklist

Northwest Airlines' operational procedures require that the flight-crew make a pretakeoff check of certain items. The second officer is required to read the checklist items, and the first officer must check the items and respond to the second officer's challenge. Included on the checklist are:

Second Officer

Flaps
Marked Bug _____ K
Ice Protection
Pitot Heat
Pressurization

First Officer

15, 15 (25,25) Blue
(C, FO) Numbers Set
OFF (ON)
ON
(C, FO) Zero, _____ $^{\circ}$,
Normal Flags

Company pilots stated that the checklist is used only to check that the required action has already been performed; it is not used as a list of items to be accomplished. With regard to the activation of pitot head heaters, it was the first officer's duty to turn the two switches to the "on" position shortly after the engines had been started and to check the ammeter readings on the various heaters to confirm their proper operation. After checking these items, he was supposed to leave the pitot heater switches on and to check that they were on during the pretakeoff check.

1.17.2 Airspeed Measuring System

When an aircraft moves through an air mass, pressure is created ahead of the aircraft, which adds to the existing static pressure within the air mass. The added pressure, dynamic pressure, is directly proportional to the velocity of the aircraft. When a symmetrically shaped object, such as a pitot head, is placed into the moving airstream, the flow of air will separate around the nose of the object so that the local velocity at the nose is zero. At the zero velocity point, the airstream dynamic pressure is converted into an increase in the local static pressure. Thus, the pressure measured at the nose of the object is called total pressure, and it is equal to the sum of the dynamic pressure and the ambient static pressure.

In an aircraft airspeed measuring system, the total pressure is measured by the pitot head and is transmitted through the pitot system plumbing to one side of a differential pressure measuring instrument (air-speed indicator). The ambient static pressure is measured at static ports which are mounted in an area that is not significantly influenced by the moving airstream. The static pressure measured at these ports is transmitted to the opposite side of the differential pressure measuring instrument. In effect, the differential pressure instrument (whether it be an airspeed indicator gage, a flight data recorder pressure transmitter, or a component within an air data computer) subtracts the ambient static pressure measured by the static system from the total pressure measured by the pitot system. The resultant dynamic pressure is a direct measurement of indicated airspeed.

Since the ambient static pressure is a component part of total pressure, any change in static pressure would normally result in an equal change in both the pitot and static pressure systems. Therefore, a change in ambient static pressure, such as that encountered during a change in altitude, would normally have no effect on airspeed measurement. Only a change in dynamic pressure produced by a change in the aircraft's velocity would cause a change in the indicated airspeed. If, however, only one side of the airspeed indicator sensed a change in the ambient static pressure, an erroneous change in indicated airspeed would result, even though the actual dynamic pressure remained unchanged. Such a condition would occur if either the pitot or static system was blocked or was otherwise rendered insensitive to external pressure changes.

In the event of a blocked pitot or static system, the direction of the indicated airspeed error would depend on which of the systems was blocked and the direction of change in the ambient static pressure. Under conditions where the pressure in the static system increases with respect to the pressure in the pitot system, the indicated airspeed will read low erroneously. For the opposite condition, where the pressure in the static system decreases with respect to the pressure in the pitot system, the indicated airspeed will read high erroneously. The latter would exist if the pitot head was blocked so that a constant pressure was trapped in the pitot system while the aircraft was ascending. This is because the static system pressure would decrease and the resultant differential pressure would appear as an increase in dynamic pressure.

Indicated airspeed error may also occur when the pitot system becomes insensitive to changes in total pressure in such a manner that the system vents to an ambient static pressure source. The pressure measured by the pitot system will equalize with the pressure in the static system, and the dynamic pressure (indicated airspeed) will decrease to zero. The vent source in a pitot head which can produce this kind of error is the moisture drain hole which is located downstream from a blocked total pressure sensing inlet.

1.17.3 B-727 Stall Characteristics

During its type certification process, the B-727-200 series aircraft demonstrated stall characteristics which met the requirements of the Civil Air Regulations, parts 4b. 160-162. The significant requirements defined therein are: (1) That, at an angle of attack measurably greater than that of maximum lift, the inherent flight characteristics give a clear indication to the pilot that the aircraft is stalled -- typical indications are a nosedown pitch or a roll which cannot be readily arrested; (2) that recovery from the stall can be effected by normal recovery techniques starting as soon as the aircraft is stalled; (3) that there is no abnormal noseup pitching and that the longitudinal control force be positive, up to and including the stall; (4) that a safe recovery from a stall can be effected with the critical engine inoperative; and (5) that a clear and distinctive stall warning be apparent to the pilot at an airspeed at least 7 percent above the stalling airspeed.

The certification stall tests, conducted with the aircraft in all operating configurations and with the most adverse weight and c.g. conditions, demonstrated that as the aircraft was slowed and its wing angle of attack was increased, the buffet produced by airflow separation from the wing provided a natural warning of impending stall. With the landing flaps extended, however, the airspeed margin provided by the buffet warning was considered to be insufficient. Consequently, a stick shaker system was installed to provide an artificial warning for all configurations.

In the clean configuration, 8/ the stick shaker activated when the angle of attack reached 13° . When the aircraft was slowed further, natural buffeting occurred at an angle of attack between 16° and 18° . The buffet was described as "quite heavy" when the speed was reduced to within 2 to 3 kn of the speed associated with maximum lift. When the angle of attack for maximum lift (about 22°) was reached, there was a tendency for the nose to drop if the pilot relaxed pressure on the control column. Also, lateral stability was reduced noticeably, which increased the pilot's workload in maintaining wings-level flight.

During certification flight tests, the angle of attack was increased to 25° , after which recovery was effected by relaxing the pull force on the control column. With the use of engine thrust during recovery, the altitude lost was restricted to about 2,000 feet.

Up to the onset of stall buffet, the longitudinal control forces needed to effect stall entry increased as the angle of attack increased. At higher angles of attack, up to and beyond the angle for maximum lift, the pull force required to maintain a noseup pitching moment decreased. The forces did not reverse, however, and, with normal trim, a reduction in pull force resulted in a decreased angle of attack.

The B-727 longitudinal control system is capable of developing the noseup pitching moments needed to obtain angles of attack much higher than those associated with stall. For an aircraft having the same weight, c.g. location, and stabilizer trim setting as N274US, the manufacturer's analysis showed that an angle of attack of approximately 37° could be attained if a continuous pull force was exerted to hold the control column aft.

Like other aircraft which have horizontal stabilizers located near or on top of their vertical stabilizers, the B-727 does pass through a range of high angles of attack where longitudinal instability occurs. This instability causes the aircraft, when no control force is applied, to pitch to even higher angles of attack. Longitudinal instability is caused by degraded horizontal stabilizer effectiveness when the aircraft's attitude is such that the horizontal stabilizer is enveloped by the low-energy turbulent air in the wake from the wings. When these high angles of attack are reached, a push force on the control column is required to reduce the angle of attack. For a B-727 with an aft c.g. location and stabilizer trim in the cruise range, wind tunnel data show that a nosedown pitching moment will decrease the angle of attack and stall recovery can be attained by applying push forces to the control column.

A stick pusher is a device which will apply a force to move the control column forward when the angle of attack for maximum lift is exceeded. The usefulness of a stick pusher is controversial since it can effect primary control of the aircraft. However, a stick pusher is required on B-727 and other aircraft registered by the United Kingdom. That stick pusher is designed so that its action can be overpowered by a pull force of about 80 lbs. on the pilot's control column.

8/ Without landing gear, flaps, or spoilers extended.

2. ANALYSIS AND CONCLUSIONS

2.1 Analysis

The aircraft was certificated, equipped, and maintained in accordance with regulations and approved procedures. The aircraft weighed substantially less than its authorized maximum weight for takeoff.

Although the speed servo cams in all three engine fuel controllers were positioned for high engine revolutions per minute, the engines were producing very little thrust at impact as evidenced by the absence of significant rotational damage to the engines. Probably, the throttles had been advanced shortly before impact, but there was either insufficient time for the engines to accelerate, or acceleration was limited because airflow into the engine inlets had been distorted by the extreme angle of attack and probable sideslip.

The flightcrew was properly certificated and each crewmember had received the training and off-duty time prescribed by regulations. There was no evidence of medical or physiological problems that might have affected their performance.

The conversations recorded on the CVR revealed that, following ascent above 13,500 feet, the flightcrew became concerned and puzzled by the apparent performance of the aircraft because of the indicated airspeed and the indicated rate of ascent. The FDR airspeed and altitude traces provided investigators an insight regarding these conversations. The airspeed trace increased rapidly after the aircraft ascended above 16,000 feet while the rate of climb continued to increase and eventually reached a peak value of 6,500 feet per minute. The Boeing Company's analysis of the airspeed and rates of climb values that registered above 16,000 feet showed that these values were incompatible with the aircraft's performance capabilities.

Analysis showed that there was a direct relationship between the airspeed and altitude values. This relationship was based on the assumptions that (1) the total pressure measured by the FDR pitot system remained constant after the aircraft ascended above 16,000 feet, and (2) the pressure measured by the FDR static system varied according to the recorded altitude values. These assumptions were substantiated by the tests which determined that the FDR airspeed and altitude traces could be reproduced only if the total pressure to the airspeed indicator was held constant during ascent above 16,000 feet.

Although the pitot systems for the captain's and first officer's airspeed Mach indicators and the FDR airspeed instrumentation are three separate and completely independent systems, it is reasonable to conclude that all three systems were sensing nearly identical and erroneous total pressures. This can be concluded because the flightcrew made no reference to

any difference between the airspeed readings on the captain's and first officer's indicators, and the first officer's reference to "...going 340 kn ..." corresponded closely to the airspeed value recorded on the FDR at that time. Additionally, the near simultaneous activation of the overspeed warning systems tends to prove that the first officer's airspeed was close to the value recorded on the FDR when the aircraft neared its peak altitude.

The erroneously high airspeed indications were caused by a complete and nearly simultaneous blockage of all three pitot pressure systems. Moreover, since the only common elements among the systems were the design features of the pitot heads and the environment to which they were exposed, the Safety Board concludes that the pitot heads were blocked by ice which formed around the heads and closed the drain holes and the pressure inlet ports. The conclusion is supported by the airspeed aberrations that were recorded while the aircraft was flying level at 13,500 feet and by the moisture which was found in the pitot heads when they were recovered and examined. Additionally, it is known that icing conditions existed in the area through which Flight 6231 was flying, and it is unlikely that any other type of blockage or malfunction would simultaneously affect the three independent systems.

The formation of ice on the pitot heads should have been prevented by electrical heating elements which are activated by the pitot heater switches located in the cockpit. The Safety Board concludes that the heating elements were never activated because the pitot heater switches were not in the "on" position during the flight. This conclusion is substantiated by the position and condition of the switches in the wreckage, the internal damage to the right switch, and the lack of evidence that electrical current was present in the heater circuit to the pitot head in the first officer's pitot system at the time of impact.

The Safety Board was unable to determine why the pitot head heater switches were not placed in the "on" position before departure. It is clear that the flightcrew performed the pretakeoff checks required by Northwest's operational procedures. However, the proper checklist sequence was not followed, and it is possible that the first officer positioned the switches improperly because of an omission in the sequence and his inexperience as a B-727 copilot.

While reading the checklist, the second officer called "bug" and, before receiving a response from either the captain or first officer, he omitted the "ice protection" call and called "pitot heat." The first officer apparently responded to both the omitted call and the "pitot heat" call by saying, "off and on," but following the captain's response to the "bug" call, the first officer asked whether the engine heat was needed. The captain may or may not have responded with a nod or hand signal, but the sound of five clicks was recorded and the first officer returned to the task of setting his airspeed bug.

The five clicks may have been the movement of the pitot heater switches to the "off" position and the movement of the engine anti-ice switches to the "on" position -- a reversal of their normal positions. This assumption is supported by the position of the engine anti-ice and pitot heater switches in the wreckage, the condition of the lights associated with the engine anti-ice switches, and the lack of any reference during the flight to the need for engine anti-ice.

Because of the flightcrew's comments concerning aircraft performance and the absence of comments about possible instrument error or airspeed system icing, the Safety Board concludes that the flightcrew attributed the high airspeed and the high rate of climb to the aircraft's relatively low gross weight and to an encounter with unusual weather, which included strong updrafts. The flightcrew's analysis of the situation must have been strongly influenced by these factors and by the fact that both airspeed instruments were indicating essentially the same values. However, the aircraft's attitude as it neared the top of its ascent should have warned them that the aircraft's performance was abnormal because its nearly 30° noseup attitude was about 25° higher than the normal climb attitude, and at such a high noseup attitude it would have been impossible for the airspeed to continue to increase even if influenced by extreme updrafts. Because the use of attitude references is a fundamental of instrument flying, which is stressed in Northwest's flightcrew training program, the Safety Board concludes that the flightcrew improperly relied on airspeed indications as a means of determining aircraft performance.

Although the activation of the overspeed warning systems probably reinforced the flightcrew's belief that they were taking appropriate action, the operation of the stall warning stick shaker should have alerted them that the aircraft actually was approaching a stall. The first officer apparently misinterpreted the control column vibration produced by the stick shaker as Mach buffet because when the stick shaker began, he commented, "... there's that Mach buffet." The captain apparently agreed with this interpretation because he then commanded, "Pull it up." The almost simultaneous activation of the stall and the overspeed warning systems undoubtedly created some confusion; however, the differences between stall buffet and Mach buffet are substantial and the former should have been easily recognized. Again, though, it appears that the flightcrew relied almost exclusively on the airspeed indicators and their related warning systems to assess the aircraft's performance.

Even after the stall, as manifested by the rapid heading change (banked attitude) and the sudden descent, the flightcrew failed to recognize the problem for a number of seconds. They continued to exert back pressure on the control column which kept the aircraft at a high angle of attack. They probably were having difficulty with lateral control, and the aircraft entered into a spiralling descent to the right, during which the actual airspeed of the aircraft began to increase rapidly.

The erroneous airspeed indications, the steep nosedown attitude, and the proprioceptive sensations associated with the positive vertical acceleration forces undoubtedly contributed to confusion which prevented the flightcrew from recognizing the true condition of the aircraft. Additionally, it is probable that the nosedown and banked attitudes of the aircraft were so steep that the horizon references in the attitude instruments were nearly hidden. This would have made the lateral attitude of the aircraft difficult to determine. However, had the pilots concentrated more on the attitude indicators, and particularly the position of the "sky pointers", 9/ they probably could have returned the aircraft to level flight had they taken appropriate corrective action within 30 to 40 seconds after the stall.

Probably because of the low airspeed indications, the captain decided that the aircraft was in a stall. He transmitted: "We're descending through 12, we're in a stall," and he called for the flaps to be extended to 20° -- a proper step in the stall recovery procedure. However, the actual indicated airspeed at that time was probably in excess of 230 kn and increasing rapidly; consequently, although the stick shaker ceased operation momentarily, the extension of the flaps had little favorable effect.

Even after the pilots decided that the aircraft was stalled, the Safety Board believes that they continued to react primarily to the high rate of descent indications and proprioceptive sensations because they continued to exert a pull force on the control column. This is substantiated by the increasing vertical acceleration forces as the descent continued. However, because the wings were not leveled first, the aircraft continued to descend rapidly in a spiralling, accelerated stall.

Since the pitot heads for the elevator feel system were probably blocked by ice, the force required of the pilots to move the elevators would have been increased while the aircraft was above 16,000 feet. However, when the aircraft descended below that altitude, the force required would have been diminished. As the descent continued below 5,000 feet, the actual indicated airspeed probably exceeded 350 kn while the airspeed sensed by the elevator feel system was probably near zero. Consequently, conditions were created in which high vertical acceleration forces could be produced with relative ease. As evidenced by the FDR acceleration trace, high vertical acceleration forces were produced below 5,400 feet.

As the aircraft continued its descent through 3,500 feet, the high vertical acceleration forces induced were sufficient to cause the failure of the left horizontal stabilizer. Thereafter, the aircraft probably rolled to a near wings-level attitude, pitched up to an extremely high angle of attack, and continued to descend in an uncontrollable stall to the ground.

9/ A triangular index which is positioned above the movable horizon and which moves in the opposite direction from the aircraft's banked attitude to indicate the number of degrees of bank.

During the Safety Board's investigation, incidents involving possible pitot-static system icing were reviewed. Although none of these incidents resulted in a catastrophic accident, it became clear that pitot or static system icing during flight can and does occur. Also, the resultant effects on pressure-operated flight instruments can produce at least momentary confusion among the crewmembers.

While all of the flightcrews involved in these incidents reverted to attitude flying until the cause of the icing could be eliminated or instrument flight could be terminated, it was apparent from these incidents that some pilots who understood the basic principles of airspeed measurement failed to analyze the possible results of a blockage of the pitot or static systems. The pilots often failed to determine the proper reasons for an increasing airspeed indication; they attributed such indications to unusual weather phenomena.

Although unusual weather phenomena such as mountain waves, extreme turbulence, and vertical wind shear can produce significant airspeed deviations, these phenomena usually are of short duration and cause erratic or abruptly changing airspeed indications rather steadily increasing, steadily decreasing, or fixed airspeed indications. Also, the aircraft's attitude during encounters with these phenomena is important in determining airspeed trends and possible sources of error. Consequently, the Safety Board believes that potential pitot-static system problems and attitude flying as a temporary remedy for these problems should be reemphasized in instrument flying training programs, and the Safety Board has made a recommendation to this effect to the Administrator, Federal Aviation Administration.

2.2 Conclusions

(a) Findings

1. All members of the flightcrew were properly certificated and were qualified for their respective duties.
2. The aircraft had been properly maintained and was airworthy for the flight; its gross weight and c.g. were within the prescribed limits.
3. There was no evidence of a system malfunction or failure or of a structural defect in the aircraft.
4. The flightcrew had adequate weather information for the flight.
5. The FDR vertical acceleration trace indicates that only light turbulence was encountered.

6. The weather conditions encountered during the flight were conducive to the formation of moderate airframe ice.
7. The aircraft accumulated sufficient ice during its flight to block completely the drain holes and total pressure inlet ports of the pitot heads; the static ports were not affected by the ice.
8. The pitot heads became blocked at an altitude of about 16,000 feet.
9. The ice formed on the pitot heads because the pitot head heater switches had not been turned on before Flight 6231 departed JFK.
10. The complete blockage of the pitot heads caused the cockpit airspeed indicators to read erroneously high as the aircraft climbed above 16,000 feet and the static pressure decreased.
11. The flightcrew reacted to the high airspeed indications by increasing the noseup attitude of the aircraft which increased the rate of climb. While this caused the indicated airspeed to increase more rapidly because the static pressure decreased more rapidly with the increased rate of climb, the actual airspeed was decreasing.
12. The airspeed overspeed warning and stall warning stick shaker operated simultaneously because of the blocked pitot heads and the high noseup attitude of the aircraft.
13. The flightcrew misconstrued the operation of the stall warning stick shaker as Mach buffet.
14. The flightcrew continued to increase the noseup attitude of the aircraft following the operation of the stall warning stick shaker.
15. The aircraft stalled at an altitude of 24,800 feet while in a noseup attitude of about 30°.
16. Following the stall, the aircraft entered into a right spiralling dive at a high rate of descent. Throughout the descent, the flightcrew reacted primarily to airspeed and rate of descent indications instead of attitude indications, and thus failed to initiate proper recovery techniques and procedures.

17. In an effort to recover the aircraft from a high rate of descent, the flightcrew exerted excessive pull forces on the control columns which induced high vertical acceleration forces and caused the left horizontal stabilizer to fail.

(b) Probable Cause

The National Transportation Safety Board determines that the probable cause of this accident was the loss of control of the aircraft because the flightcrew failed to recognize and correct the aircraft's high-angle-of-attack, low-speed stall and its descending spiral. The stall was precipitated by the flightcrew's improper reaction to erroneous airspeed and Mach indications which had resulted from a blockage of the pitot heads by atmospheric icing. Contrary to standard operational procedures, the flightcrew had not activated the pitot head heaters.

3. RECOMMENDATIONS

As a result of this accident, three recommendations were made to the Administrator, Federal Aviation Administration. (See Appendix D.)

BY THE NATIONAL TRANSPORTATION SAFETY BOARD

/s/ FRANCIS H. McADAMS
Member

/s/ LOUIS M. THAYER
Member

/s/ ISABEL A. BURGESS
Member

John H. Reed, Chairman, and William R. Haley, Member, did not participate in the adoption of this report.

August 13, 1975

APPENDIX A

Investigation and Hearing

1. Investigation

The National Transportation Safety Board was notified of the accident about 1935 on December 1, 1974. The Safety Board immediately dispatched an investigative team to the scene. The following morning the team established investigative groups for operations/witnesses, air traffic control, weather, structures, powerplants, systems, flight data recorder, maintenance records, and cockpit voice recorder.

Parties to the investigation were: The Federal Aviation Administration, Northwest Airlines, Inc., The Boeing Company, Air Line Pilots Association, International Association of Machinists and Aerospace Workers, and the Pratt and Whitney Division of the United Aircraft Corporation.

2. Hearing

A public hearing was held at Bear Mountain, New York, on February 12 and 13, 1975. All of the parties to the investigation except the Pratt and Whitney Aircraft Division were parties to the hearing.

Preceding page blank

APPENDIX B

Aircrew Information

Captain John B. Lagorio

Captain Lagorio, 35, was employed by Northwest Airlines on January 17, 1966. He held Airline Transport Pilot certificate No. 1496609 with airplane multiengine and single-engine land ratings, commercial privileges and a type rating in the B-727. He held Flight Engineer certificate No. 1682555 and a valid first-class medical certificate which was issued with no limitations on August 22, 1974.

Captain Lagorio had accumulated about 7,434 flight-hours, of which about 1,973 were in the B-727. In the 30-, 60-, and 90-day periods preceding the accident, he flew about 58, 122, and 185 hours, respectively, all in the B-727.

Captain Lagorio was advanced from first officer to captain on August 5, 1969. He completed his last general refresher training on January 15, 1974, and his last B-727 refresher training on November 15, 1974. He passed a proficiency flight check in the B-727 simulator on November 15, 1974.

First Officer Walter A. Zadra

First Officer Zadra, 32, was employed by Northwest Airlines on January 8, 1968. He held Commercial Pilot certificate No. 1624729 with airplane multiengine and single-engine land ratings, and an instrument rating. He held Flight Engineer certificate No. 1834609 and a valid first-class medical certificate which was issued with no limitations on July 9, 1974.

First Officer Zadra had flown about 1,550 hours as a pilot or first officer and about 3,152 hours as a second officer (flight engineer) of which about 1,244 hours were in the B-727. He upgraded from second officer in B-707 aircraft to first officer in B-727 aircraft on October 16, 1974, and he had flown about 46 hours in the latter capacity. In the 30-, 60-, and 90-days periods preceding the accident; he flew, respectively, about 46 hours as first officer in the B-727 and 23 and 76 hours as second officer in the B-707.

First Officer Zadra completed general refresher training on January 7, 1974, and he passed a first officer proficiency check in the B-727 on October 16, 1974.

Second Officer James F. Cox

Second Officer Cox, 33, was employed by Northwest Airlines on February 2, 1969. He held Commercial Pilot certificate No. 1643627 with multiengine land and instrument ratings. He held Flight Engineer (turbo-jet powered) certificate No. 1920999 and a first-class medical certificate which was issued with no limitations on March 1, 1974.

Second Officer Cox had acquired about 1,938 hours of flying time as a second officer with Northwest Airlines, including about 1,611 hours in B-727 aircraft. In the 30-, 60-, and 90-day periods preceding the accident, he flew about 45, 113 and 180 hours, respectively, all in B-727 aircraft.

Second Officer Cox completed general refresher training on January 10, 1974, and he passed a second officer proficiency check on April 10, 1974.

APPENDIX C

Aircraft Information

N274US was manufactured by The Boeing Company on December 2, 1969, and it was assigned serial No. 20295. It had accumulated about 10,289 hours of time in service.

N274US was powered by three Pratt and Whitney JT8D-7 engines. Pertinent engine data are as follows:

<u>Position</u>	<u>Serial No.</u>	<u>Total Time</u>	<u>Time Since Heavy Maintenance</u>
1	649153	18,641 hours	3,044 hours
2	654070	14,818 hours	2,234 hours
3	648988	17,612 hours	1,193 hours

All of the required maintenance inspections and checks on the aircraft had been performed in accordance with Northwest Airlines approved directives.

NATIONAL TRANSPORTATION SAFETY BOARD WASHINGTON, D.C.

APPENDIX D

ISSUED: March 20, 1975

Forwarded to:
Honorable Alexander P. Butterfield
Administrator
Federal Aviation Administration
Washington, D. C. 20591

SAFETY RECOMMENDATION(S)

A-75-25 thru -27

The National Transportation Safety Board is investigating the Northwest Airlines, Inc., Boeing 727, N274US, aircraft crash which occurred near Thielle, New York, on December 1, 1974. The Board's continuing investigation has revealed that ice blocked the pitot heads.

A preliminary review of the evidence in this accident suggests the possibility that the crew concentrated on air data instrumentation to the exclusion of aircraft attitude indications. The timely use of the attitude information may have prevented the stall and subsequent crash.

About 5 minutes before the rapid descent, the flight data recorder (FDR) recorded aberrations in the airspeed trace. These aberrations were caused by the closure of the ram air inlet and the drain hole of the pitot mast. These aberrations were verified by wind-tunnel icing tests of a pitot mast and pneumatic tests of an altimeter and airspeed system. These tests produced airspeed/altitude traces similar to those recorded on the FDR.

The Safety Board is aware of other incidents in which an aircraft encountered difficulties while flying in freezing precipitation because of a lack of pitot heat. In these incidents, the flightcrews recognized the problem and took corrective action.

Evidence in this case indicates that the pitot heater control switches were not on, although the heaters were capable of operation. The aircraft had been flying in clouds and freezing temperatures.

Recently, one air carrier reported that it is operating its pitot heater system continuously and the failure rate is minimal, i.e., one element failure per aircraft per year. Several other air carriers are actively considering the institution of a similar procedure, and they believe there would be no adverse affect on the life of the pitot heater elements.

APPENDIX D

Honorable Alexander P. Butterfield - 2 -

The National Transportation Safety Board believes that corrective action is necessary and recommends that the Federal Aviation Administration:

1. Issue an Operations Bulletin to all air carrier and general aviation inspectors to stress the need for pilots to use attitude information when questionable information is presented on instruments that are dependent on the air data system. The information in this Bulletin should be disseminated to all operators for incorporation into their operations procedures and training programs. (Class 1)
2. Issue an Airworthiness Directive to require that a warning system be installed on transport category aircraft which will indicate, by way of a warning light, when the flight instrument pitot heating system is not operating. The warning light should operate directly from the heater electrical current. (Class 2)
3. Amend the applicable Federal Air Regulations to require the pitot heating system to be on any time electrical power is applied to an aircraft. This should also be incorporated in the operator's operations manual. (Class 2)

Our staff is available to assist your personnel in this matter, if desired.

REED, Chairman, McADAMS, THAYER, BURGESS, AND HALEY, Members, concurred in the above recommendations.


By: John H. Reed
Chairman



THE SECRETARY OF TRANSPORTATION
WASHINGTON, D.C. 20590

March 13, 1975

Honorable John H. Reed
Chairman, National Transportation
Safety Board
800 Independence Avenue, S.W.
Washington, D. C. 20591

Dear Mr. Chairman:

This is to acknowledge receipt of your letter of March 12 enclosing a copy of a safety recommendation to the Federal Aviation Administrator concerning the Board's investigation of the Northwest Airlines, Inc., Boeing 727, N274US, aircraft crash which occurred near Thielle, New York, on December 1, 1974.

The recommendations are receiving attention by the Department's Assistant Secretary for Environment, Safety and Consumer Affairs, as well as other appropriate Departmental officials.

Sincerely,

A handwritten signature in dark ink, reading "William T. Coleman, Jr." in a cursive style.

William T. Coleman, Jr.

APPENDIX D

**DEPARTMENT OF TRANSPORTATION
FEDERAL AVIATION ADMINISTRATION**

WASHINGTON, D.C. 20590



OFFICE OF
THE ADMINISTRATOR

MAY 27 1975

Notation 1481

Honorable John H. Reed
Chairman, National Transportation Safety Board
800 Independence Avenue, S. W.
Washington, D. C. 20594

Dear Mr. Chairman:

This is in response to your letter of March 12 which transmitted NTSB Safety Recommendations A-75-25 thru 27.

Recommendation No. 1.

Issue an Operations Bulletin to all air carrier and general aviation inspectors to stress the need for pilots to use attitude information when questionable information is presented on instruments that are dependent on the air data system. The information in this Bulletin should be disseminated to all operators for incorporation into their operations procedures and training programs. (Class 1)

Comment.

Air Carrier Operations Alert Bulletin 75-3 dated February 13 covers this subject. A Part 135, Air Taxi Bulletin, is being prepared. We are also considering the issuance of an advisory circular on the subject.

Recommendation No. 2.

Issue an Airworthiness Directive to require that a warning system be installed on transport category aircraft which will indicate, by way of a warning light, when the flight instrument pitot heating system is not operating. The warning light should operate directly from the heater electrical current. (Class 2)

Comment.

We do not concur in this recommendation. Some current aircraft have cycling types of pitot heaters. These cycle on and off as controlled by thermostats or timers. Warning lights would flash on and off with

2

the cycling. We consider this as distracting and possibly detrimental to safety. Other aircraft in which the pitot heat is controlled directly by a simple on-off switch could be modified by adding a power relay and warning light. We do not consider this necessary or desirable. Operation of pitot heat is on cockpit checklists and is well covered in operations manuals and crew training. In addition, the effectiveness of additional warning lights among the many warning lights presently installed in the cockpit is of doubtful value.

Recommendation No. 3.

Amend the applicable Federal Air Regulations to require the pitot heating system to be on any time electrical power is applied to an aircraft. This should also be incorporated in the operator's operations manual. (Class 2)


Comment.

This recommendation is considered to apply to all types of aircraft in service and to future designs. We propose to delete from consideration those aircraft which are limited to VFR flight only since they are not required to have any deicing capabilities.

Retrofit on existing aircraft presents many problems and we do not consider the recommendation practical for general adoption. Some cyclic installations will not tolerate continuous heat and would have to be completely replaced. Continuous heat would be unsafe in many circumstances such as extended parking with electrical power on. As you mentioned, reliability would be reduced leading to more frequent unsafe conditions in flight. We do not consider retrofit of existing aircraft practical or feasible.

For new designs the recommendation may be feasible because the installations can be safe and reliable by design of interfacing electrical power systems, positioning of pitot tubes, and construction of pitot tubes. A regulatory project leading to a Notice of Proposed Rule Making and subsequently a rule requiring an appropriately designed pitot heating system is being established.

Sincerely,


James E. Dow
Acting Administrator